



Le rôle de la galanine dans le remodelage cardiaque

Andrei Timotin

► To cite this version:

| Andrei Timotin. Le rôle de la galanine dans le remodelage cardiaque. Médecine humaine et pathologie. Université Paul Sabatier - Toulouse III, 2017. Français. NNT : 2017TOU30166 . tel-01946607

HAL Id: tel-01946607

<https://theses.hal.science/tel-01946607>

Submitted on 6 Dec 2018

HAL is a multi-disciplinary open access archive for the deposit and dissemination of scientific research documents, whether they are published or not. The documents may come from teaching and research institutions in France or abroad, or from public or private research centers.

L'archive ouverte pluridisciplinaire **HAL**, est destinée au dépôt et à la diffusion de documents scientifiques de niveau recherche, publiés ou non, émanant des établissements d'enseignement et de recherche français ou étrangers, des laboratoires publics ou privés.



THÈSE

En vue de l'obtention du

DOCTORAT DE L'UNIVERSITÉ DE TOULOUSE

Délivré par :

Université Toulouse 3 Paul Sabatier (UT3 Paul Sabatier)

Présentée et soutenue par :
Andrei TIMOTIN

le jeudi 21 septembre 2017

Titre :

Le rôle de la Galanine dans le remodelage cardiaque

École doctorale et discipline ou spécialité :
ED BSB : Maladie métaboliques et cardiovasculaires

Unité de recherche :

INSERM U1048 - I2MC

Directeur/trice(s) de Thèse :

Dr. Oksana Kunduzova

Jury :

Dr. Stéphanie BARRERE-LEMAIRE - Rapporteur
Dr. Canan NEBIGIL-DESAUBRY - Rapporteur
Pr. Armand LATTES - Examinateur
Pr. Bernard FRANCES - Examinateur

«Le cœur est le commencement de la vie, car c'est par le cœur que le sang est distribué ... la source de toute action», William Harvey, 1673.

RESUME

La Galanine est un peptide ubiquitaire de 29 acides aminés chez les mammifères (30 chez l'homme) qui contrôle de nombreuses fonctions biologiques: (I) sécrétions endocrines (insuline, somatostatine, glucagon); (II) comportement (prise alimentaire, nociception, apprentissage, mémoire); (III) tonicité musculaire dans le tractus digestif. Ce peptide a particulièrement été étudié dans le système nerveux central où il joue un rôle dans l'évolution de certaines maladies neurodégénératives telles que les maladies de Parkinson et d'Alzheimer. La galanine agit en se fixant sur 3 récepteurs connus, GalR1-2-3 qui appartient à la grande famille des récepteurs couplés aux protéines G (GPCR). Bien que la Galanine et ses trois récepteurs soient fortement exprimés au niveau périphérique, leur rôle dans les effets périphériques et leur implication en pathologie ont été très peu étudié. L'objectif de mon travail de thèse a été d'identifier le rôle de la galanine dans le remodelage myocardique, qui constitue un déterminant majeur dans la progression de l'insuffisance cardiaque.

Dans un premier temps, nous avons démontré que la galanine possède des propriétés anti-apoptotiques et anti-oxydantes *in vitro* dans les cardiomyocytes. En effet, le traitement de cellules par la galanine entraîne une diminution de l'apoptose et de la production de radicaux libres oxygénés en réponse à l'hypoxie. En accord avec ces effets bénéfiques au niveau cellulaire, les études *in vivo* réalisées dans un modèle d'ischémie-reperfusion cardiaque, ont montré que le traitement à la galanine dans la phase précoce de reperfusion réduit l'apoptose et la nécrose myocardique. De plus, nous avons confirmé *in vivo* l'importance de la galanine dans la défense contre le stress oxydant associé aux lésions mitochondrielles post-ischémiques. Dans un deuxième temps, nous avons mis en évidence le rôle important de la galanine dans le contrôle de l'activité des fibroblastes cardiaques *in vitro*. Nous avons montré que la galanine inhibe des étapes clés d'activation de la cascade pro-fibrotique dans les fibroblastes cardiaques. Les propriétés anti-fibrotiques de la galanine ont également été confirmées *in vivo* dans un modèle de surcharge en pression par constriction aortique chez la souris. Dans ce modèle, nos résultats montrent que le traitement chronique à la galanine s'accompagne d'une amélioration de la fonction cardiaque.

Ces données nous ont permis de démontrer que la galanine joue un rôle clé dans le remodelage cardiaque et de proposer la galanine comme un candidat potentiel dans le traitement de l'insuffisance cardiaque.

ABSTRACT

Galanin is an ubiquitous 29 amino acid peptide in mammals (30 in humans) that controls many biological functions: (I) endocrine secretions (insulin, somatostatin, glucagon); (II) behavior control (food intake, nociception, learning, memory, pain); (III) muscle tonicity in the digestive tract. This peptide has been particularly studied in the central nervous system where it plays a role in the evolution of neurodegenerative diseases such as Parkinson's and Alzheimer's. Although Galanin and its three receptors (GalR1, GalR2, GalR3) are strongly expressed at the peripheral level, their role in peripheral effects and their involvement in the pathology have been poorly studied. The objective of my thesis work was to identify the role of galanin in myocardial remodeling, which is a major determinant in the progression of heart failure.

Firstly, we demonstrated that galanin has anti-apoptotic and anti-oxidant properties *in vitro* in cardiomyocytes. Indeed, the treatment of cells with galanin causes a dose-dependent decrease in apoptosis and reactive oxygen species in response to hypoxia. In line with these beneficial effects at the cellular level, using *in vivo* model of cardiac ischaemia-reperfusion we showed that galanin treatment reduces apoptosis and necrosis in the early phase of reperfusion. In addition, we confirmed *in vivo* the importance of galanin in the defense against oxidative stress associated with post-ischemic mitochondrial lesions. Secondly, we demonstrated the important role of galanin in controlling the activity of cardiac fibroblasts. Using *in vitro* models, we have shown that galanin inhibits activation of key steps of the profibrotic cascade in cardiac fibroblasts. The anti-fibrotic properties of galanin were also confirmed *in vivo* in a mouse model of pressure overload-induced heart failure. This observation is accompanied by an improvement of cardiac function.

These data reveal that galanin plays a key role in cardiac remodeling and suggest galanin as a potential candidate in the treatment of heart failure.

TABLE DE MATIERES

Résumé.....	3
Abstract.....	4
Table des matières.....	5
Abréviations.....	7
Index des figures.....	9
Index des tableaux.....	10
I. Insuffisance cardiaque - introduction.....	11
I.1 Définition.....	11
I.2 Epidémiologie, Etiologie.....	13
I.3 Physiopathologie.....	16
I.3.1 Physiologie cardiaque normale.....	16
I.3.2 La dysfonction ventriculaire.....	16
I.4 Le remodelage cardiaque.....	18
II. Le système Galaninergique.....	28
II.1 Les récepteurs de la Galanine.....	30
III.1.1 Le récepteur GalR1.....	32
III.1.2 Le récepteur GalR2.....	34
III.1.3 Le récepteur GalR3.....	36
II.2 Les agonistes et antagonistes de la Galanine.....	37
II.3 La Galanine et le système nerveux.....	41
II.4 La Galanine et le système neuroendocrine et endocrine.....	43
II.5 La Galanine et le cancer, l'inflammation et dans la peau.....	46
II.6 La Galanine et le système cardiovasculaire.....	50
III. Objectifs.....	52
IV. RESULTATS	
Manuscrit 1: Myocardial protection from ischemia/reperfusion injury by exogenous galanin fragment.....	53
Manuscrit 2: Cardioprotective properties of N-terminal galanin fragment (2-15) in experimental ischemia and reperfusion.....	66
V. Discussion et perspectives.....	80

VI.Conclusions.....	83
Bibliographie.....	84
ANNEXES.....	103
Manuscrit 1: Inhibition of PIKfyve prevents myocardial apoptosis and hypertrophy through activation of SIRT3 in obese mice.....	104
Manuscrit 2: Apelin-13 administration protects against ischaemia/reperfusion-mediated apoptosis through the FoxO1 pathway in high-fat diet-induced obesity.....	120
Manuscrit 3: Apelin regulates FoxO3 translocation to mediate cardioprotective responses to myocardial injury and obesity.....	134
Brevet.....	151

ABBREVIATIONS

AMPc: Adénosine monophosphate cyclique

ANP: Atrial Natriuretic Peptide

BNP: Brain Natriuretic Peptide

BSA: Bovine Serum Albumin

Col I: Collagène de type I

Col III: Collagène de type III

DMEM: Dulbecco's Modified Eagle Medium F12

EDTA: Éthylène Diamine Tétra-Acétique

eNOS: Oxyde nitrique synthase non couplée

FBS: Fetal Bovine Serum

FE: Fraction d'ejection

FR: Fraction de rétrécissement

GAPDH: GlycérAldéhyde-3-Phosphate DésHydrogénase

Gal1: Galanine receptor 1

Gal2: Galanine receptor 2

Gal3: Galanine receptor 3

GIRK: Courant potassique rectifiant activé par les protéines G

GPCR: Récepteurs couplés aux protéines G

GLUT4: Glucose transporter type 4

HBSS: Hanks' Balanced Salt Solution

HNSCC: Carcinome épidermoïde de la tête et du cou

IC: Insuffisance cardiaque

IL: Interleukine

IM: Infarctus dy myocarde

L-Glut: L-glutamine

MPO: Myéloperoxydase

PBS: Phosphate Buffered Saline

PFA: ParaFormAldehyde

PPVG: Paroi postérieure du ventricule gauche

PKA: Protéine kinase A

P/S: Pénicilline/Streptomycine

RTqPCR: Real Time quantitative Polymerase Chain Reaction

MCP-1: Monocyte Chemoattractant Protein-1

NAD(P)H: Nicotinamide adénine dinucléotide phosphate

NPY: Neuropeptide Y

TA: Température Ambiante

TAC: Transverse aortic constriction

TBS: Tris-Buffered Saline

TGF: Transforming Growth Factor β

TNBS: 2,4,6-Trinitrobenzenesulfonic acid

TUNEL: Terminal deoxynucleotidyl transferase-mediated biotinylated UTP Nick End

Labeling

SIV: Septum interventriculaire

SNC: Système Nerveux Central

SP: Substance P

SVF: Serum de Veau Fœtal

VIP: Vasoactive Intestinal Peptide

INDEX DES FIGURES

Figure 1. Les mecanismes impliqueés dans le remodelage cardiaque.....	20
Figure 2. Les différentes voies menant à une lésion cellulaire après ischémie.....	21
Figure 3. L'implication des derivés réactifs de l'oxygène mitocondriaux dans la l'apoptose.....	22
Figure 4. Les cibles cellulaires et subcellulaires potentielles du stress oxydatif affectant l'insuffisance cardiaque.....	23
Figure 5. Les mécanismes de remodelage cardiaque suite à l'hypertension artérielle chronique.....	26
Figure 6. L'organisation de la gêne de la preprogalanine.....	28
Figure 7. Exemple schématique des trois sous-types de récepteurs de la Galanine et de leurs mécanismes de transduction intracellulaire.....	30

INDEX DES TABLEAUX

Tableau 1. Diagnostic de l'insuffisance cardiaque selon la Société Européenne de Cardiologie.....	12
Tableau 2. Nombre et taux de décès par IC selon sexe et l'âge.....	14
Tableau 3. Les composants du processus de remodelage cardiaque.....	24
Tableau 4. Les ligands peptidiques de la Galanine.....	37
Tableau 5. Les ligands non-peptidiques de la Galanine.....	38
Tableau 6. Le phenotype KO de la Galanine et ses récepteurs.....	39

INTRODUCTION

L'insuffisance cardiaque (IC) est un syndrome de proportions épidémiques aggravé par une morbidité et une mortalité extrêmement élevées (Go *et al.*, 2014). Les perspectives pour ces patients sont médiocres, avec des taux de survie plus faible que pour le cancer de l'intestin, du sein ou de la prostate (Ambrosy *et al.*, 2014). Les demandes en matière de services de santé devraient augmenter de façon importante au cours de la prochaine décennie, car le nombre de patients avec IC augmente en raison du vieillissement de la population et des changements de style de vie.

Compte tenu de l'augmentation du fardeau de l'IC et malgré un effort considérable sur la recherche de traitements innovants, seulement quelques nouveaux traitements pharmacologiques ont été montrés efficaces contre l'IC dans les 10 dernières années (Zannad *et al.*, 2011).

La recherche continue est essentielle si nous voulons aborder les besoins non satisfaits en soins aux patients atteints d'IC. La recherche collaborative internationale axée sur les causes et le traitement de l'IC a le potentiel de bénéficier à des millions de personnes souffrant de cette maladie, afin de non seulement soulager les symptômes mais surtout la maladie en elle-même.

I.1 DEFINITION

L'IC se définit comme l'incapacité du cœur à répondre aux exigences de l'organisme et, plus précisément, l'échec du cœur à pomper le sang avec une efficacité normale. Lorsque cela se produit, le cœur est incapable de fournir un flux sanguin adéquat pour assurer le bon fonctionnement des organes tels que le cerveau, le foie et les reins (Braunwald, 2013). L'IC peut être due à une défaillance du ventricule droit ou gauche, ou des deux ventricules. Les symptômes cliniques peuvent inclure l'essoufflement (dyspnée), l'asthme cardiaque, la stase dans la circulation générale du corps (systémique) ou dans la circulation du foie (système veineux portal), le gonflement (œdème), la cyanose et l'élargissement du cœur (hypertrophie cardiaque) (Dickstein *et al.*, 2008).

Récemment, la Société Européenne de Cardiologie a publié un tableau d'aide au diagnostic de l'IC utilisant différents paramètres cliniques (Tableau 1). (Ponikowski *et al.*, 2016):

Evaluation	Diagnostique de l'insuffisance cardiaque	
	Supporter si présent	S'oppose si normal ou absent
Symptômes compatibles	++	++
Signes compatibles	+	+
Dysfonction cardiaque à l'échocardiographie	+++	+++
La réponse des symptômes ou signes au traitement	+++	++
ECG		
Normal		++
Anormal	++	+
Dysrythmie	+++	+
Laboratoire		
Augmentation BNP/NT-proBNP	+++	+
Réduit/normal BNPO/NT-proBNP	+	+++
Sodium sanguine diminué	+	+
Dysfonction rénale	+	+
Augmentation modérée de la troponine	+	+
Radiographie thoracique		
Congestion pulmonaire	+++	+
Diminution de l'effort physique	+++	++
Tests pulmonaires anormaux	+	+
Hémodynamique anormale au repos	+++	++

+ = petite importance; ++ = importance moyenne; +++ = grande importance

Tableau 1. Diagnostic de l'insuffisance cardiaque selon la Société Européenne de Cardiologie.

I.2 EPIDEMIOLOGIE, ETIOLOGIE

Les maladies cardiovasculaires ont été jusqu'en 2004 la première cause de mortalité en France (INSEE) (Saudubray *et al.*, 2005). A l'heure actuelle, elles restent encore la deuxième cause de mortalité derrière les pathologies néoplasiques. L'IC chronique est actuellement la seule pathologie cardiovasculaire dont l'incidence et la prévalence sont en augmentation du fait du vieillissement de la population, mais aussi d'une meilleure prise en charge des différentes cardiopathies et notamment les cardiopathies ischémiques. La prévalence de l'IC est évaluée en Europe de 2 à 3 % de la population générale, à plus de 10% chez les plus de 70 ans et même plus de 20% au-delà de 80 ans (McMurray JJV, Adamopoulos S, Anker SD, Auricchio A, Böhm M, Dickstein K, 2012). On estime à 1 million le nombre de patients insuffisants cardiaques en France soit une prévalence de 2,2%, ce qui représente 150 000 hospitalisations/an, pour un séjour moyen de 10,7 jours (Tuppin *et al.*, 2013). Ainsi, l'IC et ses complications représentent la première cause d'hospitalisation en France.

L'étude de la cohorte Framingham aux Etats Unis apporte des renseignements complémentaires: l'âge moyen du diagnostic d'IC est de 70 ans, l'incidence passe de 3% entre 50 et 59 ans, à 27% entre 80 et 89 ans chez l'homme (Oppenheimer, 2010). Cette cohorte montre que la survie à 5 ans, une fois le diagnostic d'IC chronique posé, est de 25% chez l'homme et de 38% chez la femme. L'IC chronique est toujours une des premières causes de décès d'origine cardiovasculaire (Tableau 2). En France, la mortalité attribuable à l'IC chronique est estimée à environ 54.8 cas/100000 (Gabet *et al.*, 2015). La mortalité intra hospitalière de l'IC aiguë est de 8,2% en 2009, et reste supérieure à celle de l'infarctus myocardique (IM) (Zuily *et al.*, 2010). Cependant, l'amélioration du traitement des symptômes de l'IC a permis d'améliorer le pronostic de l'IC au cours des vingt dernières années en Europe (Guha and McDonagh, 2013).

L'IC chronique dans les pays occidentaux est donc un problème majeur de santé publique. En France, on estime que les dépenses concernant l'IC chronique représentent environ 1.1 milliard d'euros (Tuppin *et al.*, 2013). Du fait du vieillissement de la population et de l'optimisation de la prise en charge des différentes cardiopathies, ces données risquent de s'aggraver, ce qui semble être confirmé par les dernières prévisions de la CNAM.

Nombre et taux de décès par IC selon le sexe et l'âge, 2011			
	Hommes	Femmes	Total
<i>Nombres de décès</i>			
Moins de 25 ans	116	84	200
24-44 ans	243	120	363
45-64 ans	2361	889	3250
65-84 ans	13714	10184	23898
85 ans et plus	14905	27356	42261
Total tous âges	31339	38633	69972
<i>Taux brut*</i>			
Moins de 25 ans	1.1	0.9	1.0
24-44 ans	2.9	1.4	2.1
45-64 ans	28.2	10.1	18.9
65-84 ans	336.4	194.7	256.8
85 ans et plus	2885.4	2275.2	2458.6
Total tous âges	99.4	115.1	107.5
Taux standardisé**	135.0	87.3	105.8

* - taux pour 100 000 habitants ; ** - taux standardisés sur l'âge de la population européenne s'Eurostat (IARC, 2010)

Tableau 2. Nombre et taux de décès par IC selon sexe et l'âge.

Les maladies qui peuvent conduire à une IC sont très différentes et leur détection est d'une grande importance, car cela permet de modifier l'approche diagnostique, thérapeutique et préventive, ainsi que le pronostic (Braunwald, 2013). Conformément aux principaux guides, il y a trois types de causes de l'IC: prédisposantes, déterminantes et précipitantes.

Les causes étiologiques prédisposantes comprennent des altérations structurelles, congénitales ou acquises, où il existe un trouble des vaisseaux périphériques, de la circulation coronarienne, péricardique, myocardique, endocardique ou des valves cardiaques. Cela a pour conséquence des altérations dans la physiologie normale du cœur (McMurray, 2000). La cause principale de l'IC sont les maladies coronariennes, qui sont responsables de plus de 50% des cas de l'IC aux États-Unis. L'IM est le facteur principal du développement des maladies coronariennes, avec un risque 10 fois plus élevé de développer une IC dans la première année qui suit l'infarctus, et jusqu'à 20 fois plus au cours des années suivantes (Kemp and Conte, 2012). La cardiomyopathie dilatée et les anomalies cardiaques congénitales sont d'autres étiologies prédisposantes moins fréquentes de l'IC.

Les causes déterminantes de l'IC sont celles qui modifient les mécanismes de régulation de la fonction ventriculaire (Oosterom-Calò *et al.*, 2012). Celles-ci peuvent être la surcharge hémodynamique, les défauts de remplissage ventriculaire, la dysynergie ventriculaire et les altérations de la fréquence cardiaque.

Les causes précipitantes de l'IC sont les facteurs qui provoquent une décompensation dans une situation stable chez les patients avec ou sans diagnostic antérieur de l'IC, mais avec une anomalie cardiaque structurelle sous-jacente. Ceux-ci sont divisés en causes cardiaques et extracardiaques. Les causes cardiaques sont des arythmies, l'apparition d'un nouveau dommage musculaire (le plus fréquent est l'infarctus aigu du myocarde) et les médicaments inotropes (antagonistes du calcium, bêta-bloquants, antiarythmiques, antidépresseurs tricycliques, adriamycine) (King, Kingery and Casey, 2012). Les causes extracardiaques sont les infections (principalement des voies respiratoires), les médicaments qui provoquent la rétention de sodium (en particulier les anti-inflammatoires non stéroïdiens qui sont très utilisés), l'arrêt du traitement, l'embolie pulmonaire, le stress physique ou psychologique, l'anémie ou la maladie intercurrente, la chirurgie et les habitudes toxiques, comme le tabagisme et l'alcoolisme (Roger, 2013).

I.3 PHYSIOPATHOLOGIE

I.3.1. Physiologie cardiaque normale

La fonction première du cœur est une fonction de pompe, permettant l'envoi du sang dans tout l'organisme. Chez l'homme, le débit cardiaque est typiquement de 4 à 8 l/min (Katz, 2011). Ce paramètre est affecté par différents facteurs comme la fréquence cardiaque, la contraction ventriculaire, l'intégrité de la paroi ventriculaire et la compétence valvulaire.

Le volume d'éjection systolique (VES) est la quantité de sang éjecté par le ventricule lors d'une contraction. Au repos, le volume d'éjection est de 60 à 100 ml par battement (Nadir, Beadle and Lim, 2014). Le VES est modulé par trois facteurs principaux: la précharge, qui est le volume qui existe dans le ventricule en fin de diastole; la postcharge correspond à la résistance contre laquelle le ventricule éjecte son contenu; et la contractilité, qui est l'état inotrope du cœur indépendamment de la précharge ou de la postcharge (Nyhan and Blanck, 2006).

Le cœur est un réseau complexe de tissus cellulaires et acellulaires qui est formé principalement de cardiomyocytes et des fibroblastes ainsi que des cellules endothéliales et immunitaires (Wilcken, 2015). Le cardiomyocyte différencié développe la tension en se raccourcissant. La matrice extracellulaire, majoritairement composée de collagènes de type I et III, fournit un réseau viscoélastique tolérant au stress qui couple les myocytes et maintient les relations spatiales entre les myofilaments et leur microcirculation capillaire (Tiyyagura and Pinney, 2006). Les fibroblastes peuvent administrer une force mécanique sur les cardiomyocytes par la contraction de l'unité collagénique qui forment la matrice extracellulaire (Goldsmith *et al.*, 2004).

I.3.2. La dysfonction ventriculaire

Différentes pathologies affectant le fonctionnement cardiaque peuvent conduire à des dysfonctions du ventricule gauche (VG) ou droit. Le dysfonctionnement du VG conduit à la diminution du débit cardiaque, ce qui entraîne une hypoperfusion globale, qui peut être à terme fatale (Yuzefpol'skaya, Weinberg and Kukin, 2010). La défaillance VG peut être divisée en deux catégories: le dysfonctionnement systolique ou diastolique. La systole correspond à la phase de contraction ventriculaire et d'éjection du sang par le ventricule gauche. A contrario,

la diastole correspond à la phase de relâchement du muscle cardiaque et de remplissage du ventricule (Schunkert *et al.*, 1998). Bien qu'il y ait beaucoup d'étiologies de l'IC, certaines tendent à affecter davantage la fonction systolique: 70% des patients atteints d'IC ont un dysfonctionnement systolique contre 30% avec un dysfonctionnement diastolique (McMurray, 2010). En outre, la plupart des patients souffrant de dysfonctionnement systolique présentent également un dysfonctionnement diastolique.

Il est toutefois important de noter que si les symptômes de l'IC systolique ou diastolique sont les mêmes, la fraction d'éjection (FE) du ventricule gauche peut les différencier. Si la FE est $< 40\%$ c'est un dysfonctionnement systolique, et si elle est $> 40\%$, c'est un dysfonctionnement diastolique (Chatterjee, 2012). On parle alors d'IC à fraction d'éjection préservée (Udelson, 2011).

La principale cause de dysfonction systolique du VG est la perte d'un myocarde fonctionnel due à une maladie ischémique et à un infarctus (Chatterjee and Massie, 2007). Une hypertension non contrôlée conduisant à un excès de la surcharge de pression est un autre facteur majeur (Genet *et al.*, 2016). La surcharge de volume en raison d'une'incompétence valvulaire et la défaillance de la contractilité cardiaque due aux cardiotoxines peuvent également y contribuer.

L'insuffisance ventriculaire droite reste assez peu étudier comme cause de l'IC, car dans la majorité des cas, c'est la conséquence de l'insuffisance cardiaque gauche (Serdahl, 2008). Comme le ventricule droit échoue, il y a une augmentation de la quantité de sang dans le ventricule qui conduit à une élévation de la pression de l'oreillette droite et une augmentation en conséquence de la pression dans le système de la veine cave qui altère le drainage veineux du corps. Cela entraîne une pression accrue dans le foie, le tractus gastro-intestinal et les extrémités avec l'apparition de signes cliniques: tels que la douleur abdominale, hépatomégalie, dyspnée et œdème périphérique (Krum and Abraham, 2009). D'autres causes de l'IC droite comprennent les cardiomyopathies arythmiques et la dysplasie ventriculaire droite.

I.4 REMODELAGE CARDIAQUE

Le terme «remodelage» a été utilisé pour la première fois en 1982 par Hockman et Buckey, dans un modèle d'infarctus myocardique (IM) (Hochman and Bulkley, 1982). Ce terme visait d'abord à caractériser le remplacement du myocarde endommagé après l'infarctus par du tissu cicatriciel. En 1990, Pfeffer et Braunwald ont publié une revue sur le remodelage cardiaque suite à l'IM, et le terme a été adopté pour caractériser les changements morphologiques importants après l'infarctus dans le ventricule gauche (Pfeffer and Braunwald, 1990). En 2000, le remodelage cardiaque est défini comme l'ensemble des changements moléculaires, cellulaires et interstitiels qui se manifestent cliniquement par un changement de taille, de forme et de fonction du cœur suite à un dommage cardiaque (Cohn, Ferrari and Sharpe, 2000).

Un cœur adulte sain consomme l'équivalent de 80kg d'ATP par jour pour assurer les fonctions normales de contraction. La très grande majorité de cette énergie (80%) est produite par l'oxydation des acides gras, le reste provenant de la glycolyse et d'autres métabolites (Doenst, Nguyen and Abel, 2013). Le remodelage du ventricule gauche induit par le stress pathologique se caractérise d'abord par une altération de cette balance énergétique en faveur de la consommation du glucose. Cela entraîne rapidement un déficit en ATP qui induit à son tour des dégâts cellulaires importants, des défauts de contraction des cardiomyocytes et qui conduit, à terme, à une perte massive de cardiomyocytes par apoptose et au développement de la fibrose cardiaque (Gajarsa and Kloner, 2011).

Le remodelage cardiaque peut être physiologique (adaptatif) ou pathologique (Klabunde, 2004). Le remodelage cardiaque physiologique peut être induit par l'entraînement physique, la grossesse ou la croissance postnatale du cœur de la naissance à l'âge adulte (Quattrini and Pelliccia, 2012). Le remodelage du ventricule gauche induit par des stimuli physiologiques conduit à une fonction VG préservée ou même améliorée, une diminution de la fibrose cardiaque, une angiogenèse accrue, un stress oxydant myocardique réduit et une diminution du dysfonctionnement mitochondrial, ce qui réduit la mort cellulaire par apoptose et/ou nécrose des cardiomyocytes (Burchfield, Xie and Hill, 2013).

Le remodelage pathologique peut se produire après un IM comme initialement décrit (Hochman and Bulkley, 1982), une augmentation de la postcharge (sténose aortique, hypertension), une maladie inflammatoire cardiaque (myocardite), une cardiomyopathie

idiopathique dilatée ou une surcharge de volume (régurgitation valvulaire) (Cohn, Ferrari and Sharpe, 2000).

La phase précoce de remodelage cardiaque est caractérisée par la dégradation du collagène intermyocytaire par les sérine protéases et activation des métalloprotéines de la matrice (MMPs) libérées principalement par les cellules immunitaires infiltrées (neutrophiles, macrophages et monocytes); la dilatation précoce du ventricule suite à l'infarctus; l'augmentation du stress pariétal suivi par une hypertrophie du ventricule, qui stimule à son tour la libération de l'angiotensine II afin d'augmenter la performance cardiaque (Cleutjens *et al.*, 1995). La réponse adaptative concerne la partie du myocarde sain. L'expansion de l'infarctus provoque la déformation de la zone frontalière du myocarde, qui modifie la loi de Frank/Starling¹ et augmente le raccourcissement des cardiomyocytes (Lew *et al.*, 1985). Les perturbations de la circulation hémodynamique déclenchent l'activation du système sympathique adrénnergique, qui stimule la synthèse des catécholamines par les surrénales, l'activation du système rénine-angiotensin-aldostérone et la stimulation de la production des peptides natriurétiques: Atrial Natriuretic Peptide (ANP) et Brain Natriuretic Peptide (BNP) (Opie *et al.*, 2006) (Figure 1). L'augmentation du rythme cardiaque et de la stimulation sympathique, entraîne une hyperkinésie du myocarde non infarci et une compensation temporaire de la fonction cardiaque. De plus, les peptides natriurétiques réduisent le volume intravasculaire et la résistance vasculaire systémique, normalisent le remplissage ventriculaire et améliorent la fonction de la pompe (Sutton and Sharpe, 2000).

Le remodelage cardiaque peut également être considéré comme un processus compensatoire, apparaissant suite à une hypertrophie et une dilatation du tissu non ischémique après IM ou comme une réponse cardiaque inadaptée à une hypertrophie secondaire à une hypertension systémique de longue durée. Le processus de remodelage lui-même peut devenir auto-inductif, entraînant une progression de la dysfonction ventriculaire et l'induction de l'apoptose (Konstam *et al.*, 2011). Cependant, le stimulus inducteur, comme l'ischémie ou la myocardite, peut continuer à être actif et conduire à une perte de tissu supplémentaire et à un remodelage progressif. Cette progression peut conduire à une série de réactions neurohormonales et hémodynamiques manifestées par un élargissement de la paroi, une

¹ La loi de Frank-Starling (décrite en 1895 par Otto Frank) stipule que l'énergie créée par un ventricule cardiaque pour éjecter le sang est corrélée au volume télediastolique. Ainsi, plus le volume télediastolique s'accroît et plus la force d'éjection du sang sera importante. Selon cette loi, la force de contraction du muscle cardiaque augmente en même temps que le ventricule cardiaque s'emplit de sang.

hypertrophie et une dilatation ventriculaire. Ces caractéristiques du remodelage cardiaque vont aboutir finalement à l'apparition clinique de l'IC (Gaballa and Goldman, 2002). En revanche, plusieurs études indiquent que la modification du processus de remodelage peut limiter l'apparition de l'IC dans un certain nombre de pathologies (Gjesdal, Bluemke and Lima, 2011; Azevedo *et al.*, 2016).

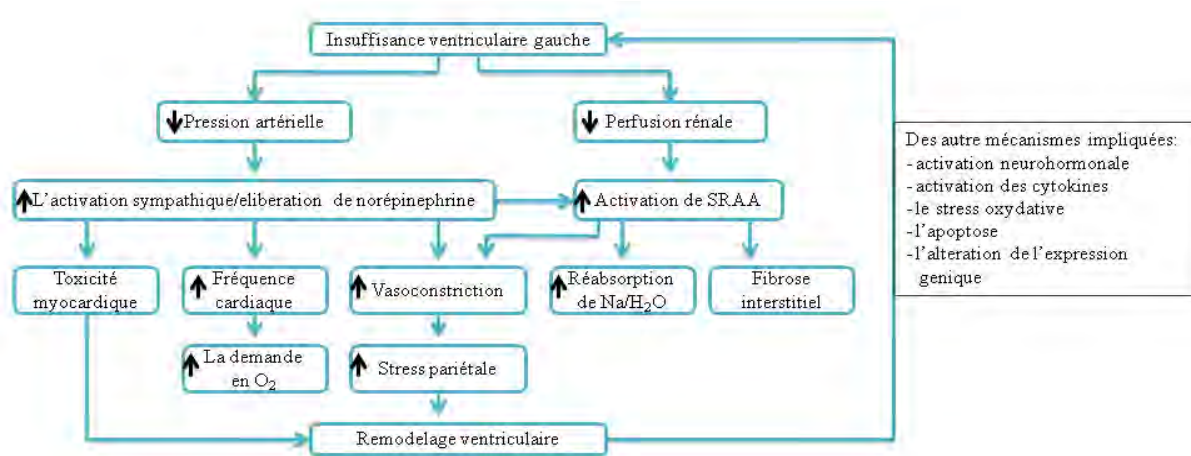


Figure 1. Les mecanismes impliqueés dans le remodelage cardiaque

Un apport constant d'oxygène est indispensable pour la viabilité et la fonction myocardique. Cependant, l'oxygène est également au centre de la génération d'espèces réactives d'oxygène (ROS). Les ROS peuvent exercer des effets potentiellement bénéfiques ou préjudiciables qui contribuent au dysfonctionnement cardiaque et à la mort cellulaires. Au cours des dernières décennies, les études cliniques et expérimentales ont fourni des preuves substantielles que le stress oxydatif, défini comme une production excédentaire de ROS par rapport à la défense antioxydante reste un élément crucial dans le développement de l'IC (Grieve and Shah, 2003; Sheeran and Pepe, 2006; Sugamura, Keaney and Jr., 2011). Les sources cellulaires de la génération de ROS dans le cœur comprennent les myocytes cardiaques, les cellules endothéliales et les neutrophiles. Dans les myocytes cardiaques, les ROS peuvent être produits par plusieurs sources, y compris les mitochondries, la nicotinamide adénine dinucléotide phosphate (NAD(P)H) oxydase, la xanthine oxydase et l'oxyde nitrique synthase non couplée (eNOS) (Taverne *et al.*, 2013) (Figure 2).

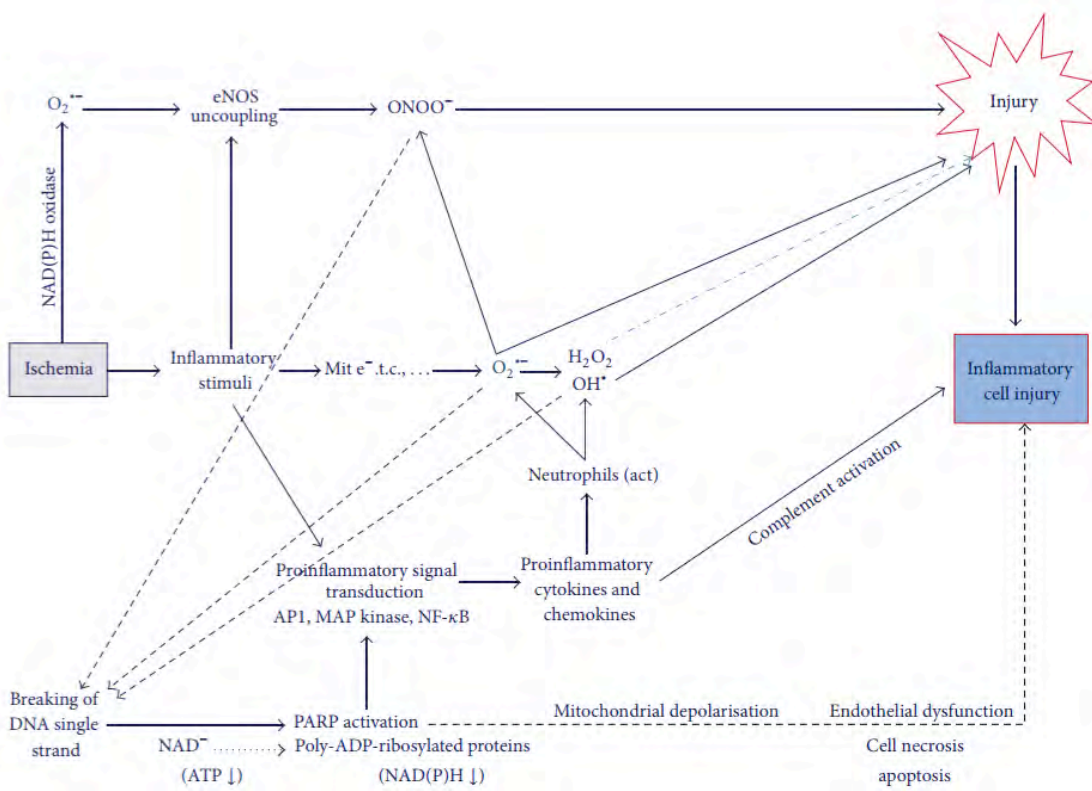


Figure 2. Les différentes voies menant à une lésion cellulaire après l'ischémie.

La production excessives des ROS provoque un dysfonctionnement cellulaire, la peroxydation des protéines et des lipides et des dommages à l'ADN et peuvent entraîner des lésions myocardique irréversibles, tels que la morte cellulaire, impliqués dans l'apparition des pathologies cardio-vasculaires (Circu and Aw, 2010). L'implication du stress oxydatif émerge de plus en plus dans la pathophysiologie du remodelage cardiaque responsable du développement et de la progression de l'IC (Tsutsui, Kinugawa and Matsushima, 2011). Plus précisément, les ROS peuvent affecter directement la fonction contractile en modifiant les protéines centrales ayant un rôle cruciale dans le couplage excitation-contraction. Ils stimulent également la prolifération des fibroblastes cardiaques et activent les métalloprotéinases matricielles (MMP), conduisant au remodelage de la matrice extracellulaire (Kameda, 2003). Ces événements cellulaires sont impliqués dans le développement et la progression du remodelage. En outre, les ROS activent des kinases et des facteurs de transcription qui sont à l'origine de l'apoptose (Figure 3).

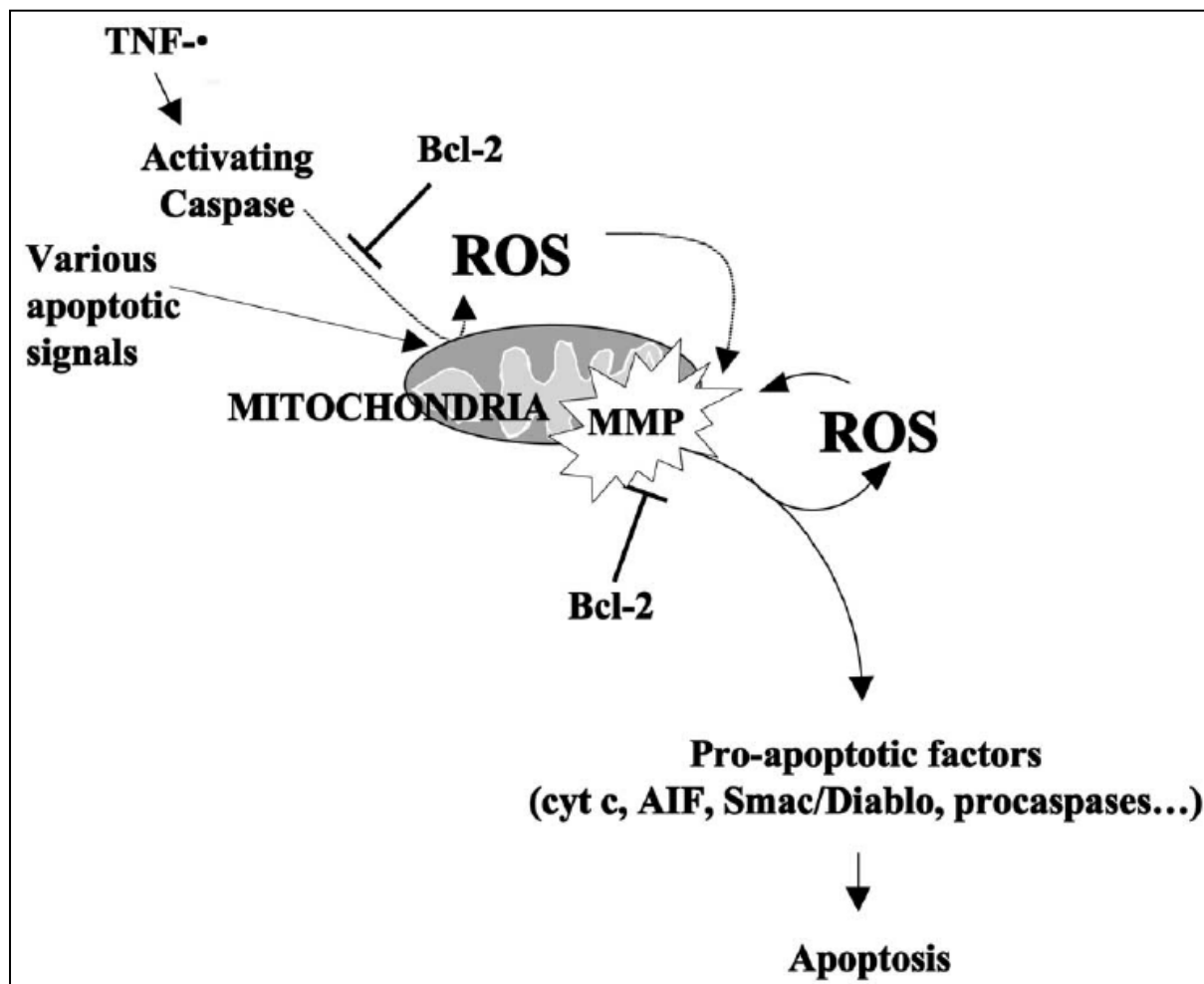


Figure 3. L'implication des dérivés réactifs de l'oxygène mitochondriaux dans l'apoptose (Fleury C, Mignotte B, Vayssiére JL.. Mitochondrial reactive oxygen species in cell death signaling. Biochimie 84: 131-141).

L'apoptose est impliquée dans la disparition aiguë ou chronique de cardiomyocytes dans l'infarctus du myocarde, la cardiopathie ischémique, les lésions de réperfusion, diverses formes de cardiomyopathie et le développement de l'IC aiguë et chronique (Kang and Izumo, 2003). L'apoptose est différente de la nécrose, dans laquelle la lyse cellulaire produit une réponse inflammatoire environnante. De plus il existe des changements biochimiques et morphologiques qui caractérisent l'apoptose: la ségrégation de la chromatine à la périphérie de l'enveloppe nucléaire, la condensation du cytoplasme et la formation d'invaginations des membranes plasmiques et nucléaires (Kerr, 1971). Contrairement à l'apoptose, la nécrose est considérée comme une mort cellulaire non coordonnée et est caractérisée par une modification de la perméabilité membranaire entraînant une dilatation du cytoplasme et des organites; la

cellule se gorge d'eau. Les études sur les animaux et les humains ont démontré que l'apoptose est présente dans la zone bordante de l'infarctus du myocarde, confirmant le rôle important de l'apoptose dans la perte tissulaire du myocarde dans la phase aiguë d'IM (Olivetii et all., 2005). Des études complémentaires montrant que l'apoptose est également détectée, plusieurs mois plus tard, suggèrent que l'apoptose peut également jouer un rôle dans le remodelage et dans le développement ultérieur de l'IC (Takemura et all., 1998). L'apoptose est un processus biologique réglementé qui régule l'équilibre entre les signaux cellulaires pro-mort et pro-survie (Figure 4).

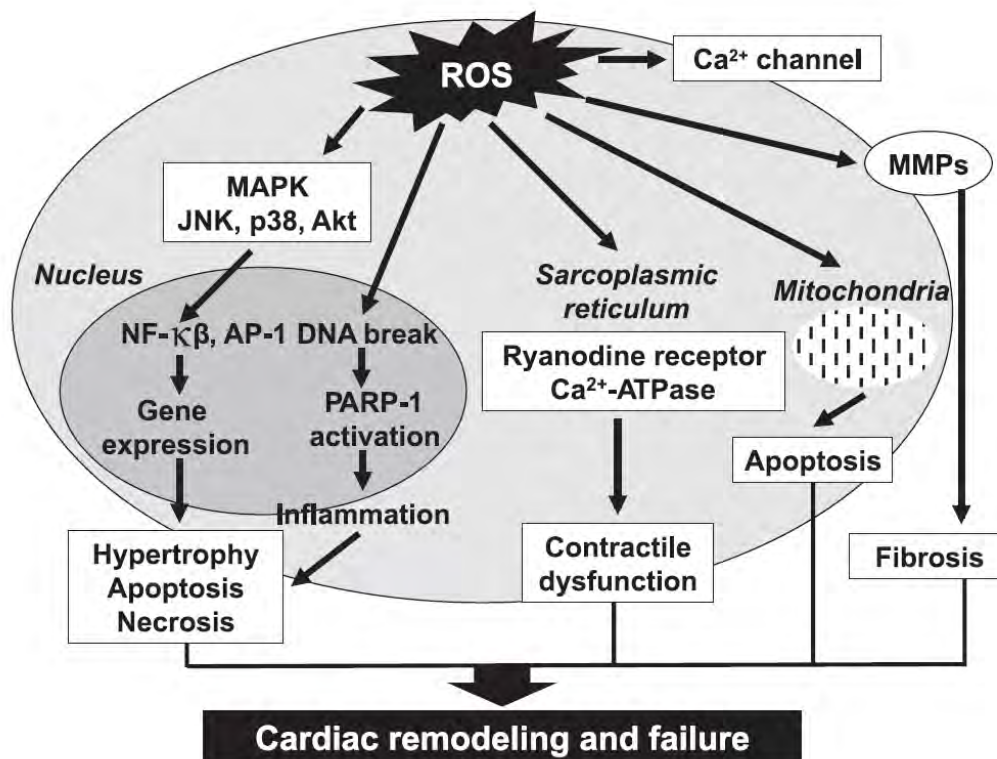


Figure 4. Les cibles cellulaires et subcellulaires potentielles du stress oxydatif affectant l'insuffisance cardiaque. reproduced from (Tsutsui, Kinugawa and Matsushima, 2011)

La famille de protéines Bcl-2 est une composante clé du processus apoptotique de la mort cellulaire. La famille Bcl-2 est composée d'antagonistes de la mort (Bcl-2, Bcl-xL) et d'agonistes (Bax, Bak), qui fonctionnent principalement pour protéger ou altérer l'intégrité de la membrane mitochondriale pour permettre la libération de protéines pro-apoptotiques. Il a

été suggéré que le myocyte cardiaque pourrait également utiliser une voie apoptotique alternative qui active les caspases en aval des "récepteurs de la mort" (ex.: Fas, récepteur du facteur de nécrose tumorale (TNF) et caspase-8 (Saraste, 1999; Filippatos *et al.*, 2004)).

Il convient de souligner que le processus de remodelage ventriculaire affecte la biologie du cardiomyocytes et l'ensemble des cellules myocytaires et non-myocytaires, ainsi que la géométrie et l'architecture de la chambre du ventricule gauche (Tableau 3).

Les composants du processus de remodelage cardiaque

- Les modifications de la biologie du cardiomyocyte
 - Le couplage excitation-contraction
 - L'expression génique de la chaîne lourde de la myosine
 - La désensibilisation β-adrénergique
 - L'hypertrophie avec la perte des myofilaments
 - Les protéines cytosquelettiques
- Les changements dans le myocarde
 - La mort des myocytes
 - La nécrose
 - L'apoptose
 - Les modifications de la matrice extracellulaire
 - La dégradation de la matrice
 - Le remplacement fibrotique
- Les modifications de la géométrie de la chambre ventriculaire gauche
 - Conformation sphérique
 - Amincissement pariétal
 - Insuffisance de la valve mitrale

Tableau 3. Les composants du processus de remodelage cardiaque

L'infarctus aigu du myocarde est une cause majeure de décès et d'invalidité dans le monde entier. Une grande partie de cette morbidité et mortalité est la conséquence du remodelage cardiaque qui se produit après l'infarctus (M. G. Sutton and Sharpe, 2000). Bien que ce remodelage soit souvent associé à des événements qui se produisent dans les semaines et les mois qui suivent, les conséquences sont directement liées à la taille initiale de l'infarctus.

Le stress cardiaque prolongé entraîne une fibrose cardiaque et une hypertrophie des cardiomyocytes, fréquemment observées dans l'IC – et constitue un caractère commun

de nombreuses maladies CV en phase finale (Segura, Frazier and Buja, 2014). L'étude Framingham a révélé que chez les patients suivis pendant une période de 20 ans, 91% des cas d'IC interviennent suite à une hypertension artérielle (Oppenheimer, 2010). L'importance de l'hypertrophie secondaire suite à l'hypertension de longue date et les changements anatomiques associés à l'hypertrophie ont été signalés pour la première fois par Linzbach (Linzbach, 1960). Il a montré la relation entre la pression artérielle et la longueur et l'épaississement des cardiomyocytes.

Les études expérimentales et cliniques démontrent que l'hypertension artérielle est associée aux changements structurels cardiaques défavorables, tels que l'élargissement de l'oreillette gauche, l'hypertrophie du VG et la fibrose myocardique, mais également à des changements de la performance incluant le dysfonctionnement systolique et diastolique du VG (Cohn, Ferrari and Sharpe, 2000). Dans ces conditions l'activation des fibroblastes cardiaques entraînent un excès de production du collagène I et III, ce qui conduit à la formation d'une véritable cicatrice qui permet de stabiliser les forces de distension et de prévenir une déformation supplémentaire (Anversa *et al.*, 1986). L'hypertrophie des myocytes est initiée par l'activation neurohormonale, l'étirement myocardique, l'activation du système rénine-angiotensine (SRAA) et les facteurs paracrine/autocrine (Olivetti *et al.*, 1991). La prévention et la réversion de l'hypertrophie VG sont associées à une amélioration de la fonction cardiaque et à la diminution du risque de complication cardiovasculaire. La prévention de l'hypertrophie ventriculaire devrait être une priorité chez les sujets atteints de l'hypertension artérielle.

Le développement de l'hypertrophie cardiaque est influencée par des facteurs hémodynamiques, tels que l'augmentation du stress pariétal, et des autres facteurs, tels que le génotype altéré, les cardiomyocytes, la matrice cellulaire, l'apoptose, les vaisseaux sanguins, le système neurohormonal et les cytokines (Kenchaiah and Pfeffer, 2004) (Figure 5).

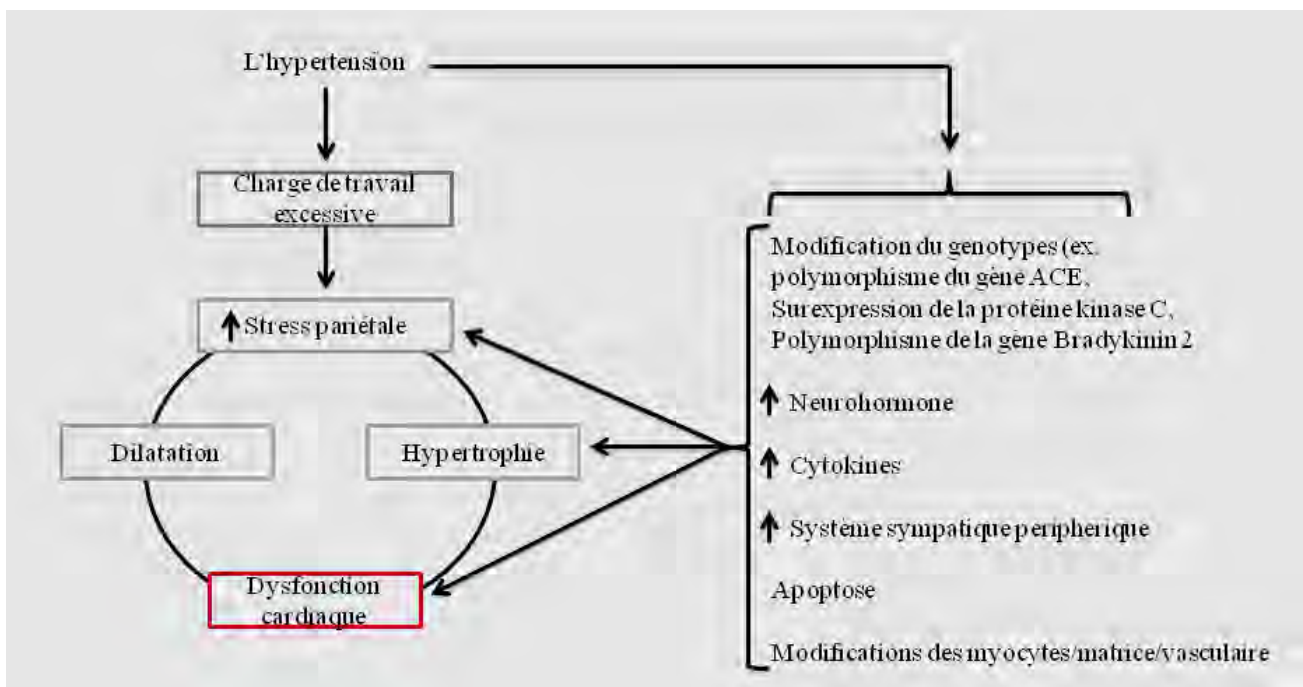


Figure 5. Les mécanismes de remodelage cardiaque suite à l'hypertension artérielle chronique (*modifié depuis Kenchaiah and Pfeffer, 2004*).

En plus de la croissance des myocytes, le tissu interstitiel participe également au remodelage cardiaque induit par la surcharge de pression par l'activation et la prolifération des fibroblastes et le dépôt en excès des types de collagène extracellulaire. Au cours de l'hypertension, la matrice extracellulaire se développe en raison de la fibrose réactive et réparatrice. L'épaississement de la matrice extracellulaire autour des cardiomyocytes est également susceptible de diminuer l'approvisionnement énergétique des cardiomyocytes. Dans un même temps, la charge de travail du muscle cardiaque augmente en réponse à l'hypertension systémique. Ce déséquilibre entraîne la mort cellulaire, probablement à la fois par la nécrose et l'apoptose. Les fibroblastes environnants synthétisent une nouvelle matrice visant à remplacer les cellules endommagées qui forment des cicatrices en fonction de la taille de la lésion. Ce processus s'appelle la fibrose réparatrice. À l'heure actuelle, l'élément déclencheur n'est pas clairement identifié.

L'inflammation joue un rôle important dans le remodelage cardiaque et spécialement l'inflammation périvasculaire. Des études récentes ont suggéré que le stress hémodynamique artériel pourrait activer les communications pro-inflammatoires autour de la paroi artérielle. Premièrement, l'augmentation de la pression artérielle est impliquée dans l'activation du

signal conduisant à l'induction de l'activation de la Monocyte Chemoattractant Protein-1 (MCP-1) dans la paroi aortique hypertendue, ce qui suggère une régulation positive de MCP-1 par contrainte mécanique de la paroi artérielle. Deuxièmement, la production des ROS et l'induction de cytokines inflammatoires et de facteurs de croissance, tels que le TGF- β et l'angiotensine II, ont été montrés dans la paroi artérielle hypertensive (Sprague and Khalil, 2009).

II. LE SYSTEME GALANINERGIQUE

La Galanine a été identifiée pour la première fois dans des extraits intestinaux porcins en 1978 par le Professeur Viktor Mutt et ses collègues de l'Institut Karolinska, en Suède, en utilisant une technique de dosage chimique qui détecte les peptides selon leurs structures d'alanine amide C-terminales. La galanine a été ainsi nommée car elle présente un résidu de glycine en N-terminal et une alanine en C-terminal (Hökfelt and Tatemoto, 2008). La structure de la galanine a été résolue en 1983 par la même équipe (Tatemoto *et al.*, 1983) et l'ADNc de la galanine a été cloné pour la première fois à partir de l'hypophyse de rat en 1987 (Vrontakis *et al.*, 1987).

La galanine est un neuropeptide constitué de 29/30 acides aminés provenant de l'hydrolyse d'un polypeptide plus longue. Ce neuropeptide est exprimé dans l'ensemble du cerveau et plus précisément au niveau des noyaux paraventriculaires (PVN) de l'hypothalamus (Merchenthaler, López and Negro-Vilar, 1993) et dans le système périphérique (Tatemoto *et al.*, 1983). Les acides aminés N-terminaux de 1 à 15 sont hautement conservés. La galanine humaine présente la particularité d'avoir 30 acides aminés sans amidation à son extrémité N-terminale (Evans and Shine, 1991). Le précurseur peptidique de la galanine, la "pré-progalanine" est codé par un gène à copie unique, situé sur le chromosome 11q13.3-q13.5 et est organisé en 6 exons couvrant environ 6 kb d'ADN génomique, en fonction de l'espèce (Kofler *et al.*, 1996). (Figure 6)

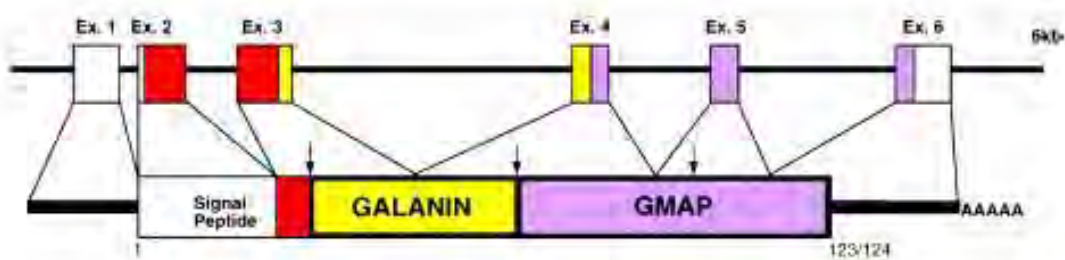


Figure 6. L'organisation du gène de la préprogalanine (*modifié du Liu *et al.*, 1996*).

La galanine et ses récepteurs sont impliqués dans le contrôle de la sécrétion de certaines hormones hypophysaires (Melander, Staines and Rökaeus, 1986), ainsi que dans la

régulation de la sécrétion d'autres neuropeptides, comme la vasopressine, la cholecystokinine et le neuropeptide Y (Meister *et al.*, 1990). Outre ses effets au niveau du SNC, la galanine a aussi des effets périphériques propres. En concordance avec sa distribution dans les nerfs, la galanine exerce de multiples effets biologiques, parmi lesquels, la contraction des muscles lisses intestinaux, l'inhibition de la sécrétion de la somatostatine et de l'insuline (Lindskog and Ahren, 1987), et la diminution du taux de glucagon et de l'hormone de croissance. En effet, la sécrétion de la galanine modifie la motilité gastro-intestinale à la fois par l'augmentation et la diminution de la libération de substances neuro-humorales (rôle de neuromodulateur). Certaines actions de la galanine peuvent être médiées par l'activation directe du/de ces récepteur/s situés sur les cellules musculaires lisses (rôle de neurotransmetteur) (Ahrén *et al.*, 1986). Des nombreuses données indiquent également un rôle de la galanine dans l'immunité innée, l'inflammation et le cancer (Lang *et al.*, 2001).

II.1 LES RECEPTEURS DE LA GALANINE

La Galanine joue un rôle important dans la régulation de nombreux processus physiologiques et physiopathologiques par sa liaison à trois récepteurs couplés aux protéines G: le galanine récepteur 1 (GalR1), le galanine récepteur 2 (GalR2) et le galanine récepteur 3 (GalR3). Ces récepteurs déclenchent plusieurs voies de signalisation, y compris la stimulation de la phospholipase C, pour GalR2, ou l'activation de l'adenylate cyclase, conduisant à la diminution de l'AMPc, pour les 3 récepteurs (Figure 7). Les récepteurs à la galanine sont extrêmement bien conservés entre les espèces mais peu conservés entre eux (Howard, Peng and Hyde, 1997; Iismaa *et al.*, 1998; Kolakowski *et al.*, 1998).

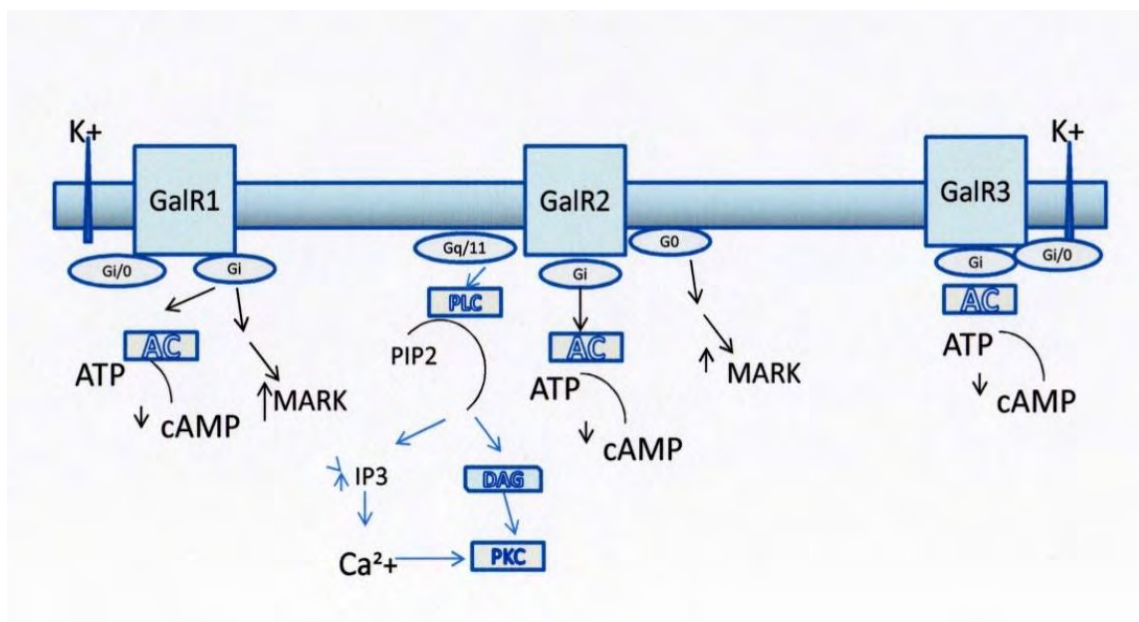


Figure 7. Exemple schématique des trois sous-types de récepteurs de la Galanine et de leurs mécanismes de transduction intracellulaire (Maria-Elena Lautatzis and Maria Vrontakis (2011). *Profile of Galanin in Embryonic Stem Cells and Tissues, Embryonic Stem Cells - Basic Biology to Bioengineering, Prof. Michael Kallos (Ed.), InTech, DOI: 10.5772/23771. Available from: <https://www.intechopen.com/books/embryonic-stem-cells-basic-biology-to-bioengineering/profile-of-galanin-in-embryonic-stem-cells-and-tissues>*).

La distribution des récepteurs à la galanine est également spécifique aux tissus. La présence de GalR1 a été montrée dans l'hypothalamus, l'hippocampe ventral, le thalamus, l'amygdale, le tronc cérébral et la moelle épinière. GalR2 est fortement exprimé dans plusieurs régions du cerveau, en particulier dans l'hypothalamus, l'hippocampe, l'hypophyse antérieure et aussi dans l'amygdale et les régions du cortex. Enfin, GalR3 montre l'expression la plus élevée dans la zone préoptique/hypothalamique et l'hypophyse.

Les trois sous-types des récepteurs ont une plus grande affinité pour la partie N-terminale conservée de la galanine que pour d'autres composés testés. Il est clair que la synthèse de nouveaux ligands sélectifs pour les sous-types de récepteurs est nécessaire pour caractériser finement les profils pharmacologiques des récepteurs.

II.1.1 LE RECEPTEUR GALR1

Le récepteur GalR1 est le sous-type de récepteur le plus abondant dans les tissus adultes. Il est associé à la sous-famille des protéines Gi, qui conduit à l'inhibition de la synthèse d'AMPc par l'adénylate cyclase.

Les ADNc codant pour des homologues d'espèces humaines et de rat du récepteur GalR1 ont été clonés et caractérisés pour la première fois en 1995. Le profil de l'expression de l'ARNm du récepteur GalR1 de rat dans les tissus périphériques et les régions du système nerveux central est en corrélation générale avec la plupart des sites où la galanine marquée à l'iode 125 se lie et où des effets fonctionnels de la galanine ont été observés. En utilisant l'analyse par Northern Blot, Parker et al. ont détecté l'expression de l'ARNm du récepteur GalR1 dans le cerveau, la moelle épinière et l'intestin grêle, mais pas dans l'hypophyse antérieure, la rate, l'estomac, le gros intestin, la glande surrénale, le foie, le poumon, le rein ou le cœur (Parker *et al.*, 1995). Les récepteurs GalR1 humains et de rat partagent les mêmes sites de consensus pour la N-glycosylation et pour la phosphorylation intracellulaire à l'exception de la présence de deux sites de phosphorylation supplémentaires dans le domaine C-terminal du GalR1 humain. Le gène codant pour le récepteur GalR1 humain est localisé sur le chromosome 18q23 (Nicholl *et al.*, 1995). L'homologue GalR1 de souris a été clone et localisé sur le chromosome 18E4 (Jacoby *et al.*, 1997), en position identique à celle du gène humain. Des études pharmacologiques ont démontré que la surexpression de GALR1 humain ou de rat dans des lignées cellulaires inhibe la production d'AMPc stimulée par la forskoline d'une manière sensible à la toxine de pertusis (PTX) (E Habert-Ortoli *et al.*, 1994; Parker *et al.*, 1995; Smith *et al.*, 1997; Wang *et al.*, 1998).

L'expression ectopique du récepteur GalR1 réduit ainsi la concentration d'AMPc (Estelle Habert-Ortoli *et al.*, 1994; Burgevin *et al.*, 1995; Parker *et al.*, 1995), ouvre les courant potassique rectifiant activé par les protéines G (GIRK), et stimule l'activité des MAP kinase (Wang *et al.*, 1998) d'une manière sensible à la toxine de pertusis; ceci est cohérent avec un couplage aux protéines G de type Gi /o.

Chez le rat, l'ARNm de GalR1 hypothalamique est plus élevé chez les femelles que chez les mâles et varie selon le cycle oestral (Faure-Virelizier *et al.*, 1998). Dans une autre étude, il a été montré que l'expression de l'ARNm de GALR1 dans les ganglions de la racine dorsale du rat diminue après une inflammation ou une lésion du nerf périphérique (Xu *et al.*,

1996). Cependant, l'ARNm GALR1 de rat n'a pas été détecté dans le noyau du nerf facial avant ou après une lésion expérimentale du nerf facial (Burazin and Gundlach, 1998). Dans d'autres travaux, l'ARNm de GalR1 est retrouvé en grande quantité dans les noyaux hypothalamiques de rat, soit injectés avec du 2-déoxy-D-glucose (un anti-métabolite de glucose), ou du mercaptoacétate de sodium (un anti-métabolite d'acide gras), qui stimulent l'alimentation (Gorbatyuk and Hökfelt, 1998). À l'inverse, l'ARNm de GalR1 est diminué lors de la lactation et suite à une hypophysectomie (Landry, Aman and Hökfelt, 1998).

II.1.2 LE RECEPTEUR GALR2

L'ADNc du récepteur GalR2 a été isolé première fois chez le rat et il est composé par une région codante interrompue par un intron juste après le 3ème domaine transmembranaire (TM) (Smith *et al.*, 1997). L'épissage de l'intron a restauré le cadre de lecture ouvert pour révéler la structure d'un GPCR contenant 372 acides aminés, y compris trois sites consensus pour la N-glycosylation dans la partie extracellulaire et plusieurs sites de phosphorylation de la partie intracellulaire distincts de ceux présent dans GalR1. Le récepteur GALR2 humain contient 387 acides aminés, soit 15 de plus que le récepteur GalR2 de rat dans sa partie C-terminale, avec seulement 85% d'homologie avec ce récepteur. Le gène codant pour le récepteur GalR2 humain est localisé sur le chromosome 17q25.3 (Fathi *et al.*, 1997); son homologue chez la souris a été cloné et localisé sur le chromosome 11 (Kolakowski *et al.*, 1998; Pang *et al.*, 1998). Fait intéressant, le chromosome contenant le gène codant pour le récepteur GalR2 chez l'homme est associé à deux maladies humaines: l'amyotrophie névralgique héréditaire et le syndrome de Russel-Silver, caractérisées en partie par une petite stature ou nanisme et un faible poids à la naissance, respectivement, en plus de défauts de développement (Fathi *et al.*, 1998). Cependant à l'heure actuelle, l'implication potentielle du gène GalR2 dans ces maladies n'est pas connu.

L'ARNm codant pour le récepteur GalR2 de rat est largement distribué dans presque tous les tissus, y compris le cerveau et des tissus périphériques tels que le canal déférent, la prostate, l'utérus, l'ovaire, l'estomac, le gros intestin, les ganglions de la racine dorsale et les cellules dérivées du pancréas (Fathi *et al.*, 1997; Howard, Peng and Hyde, 1997; Smith *et al.*, 1997; Sten Shi *et al.*, 1997; O'Donnell *et al.*, 1999). Dans l'hypophyse antérieure de rat, l'ARNm de GalR2 a été détecté par hybridation *in situ* et par RT-PCR, cette dernière technique soutenant l'absence d'ARNm de GalR1 dans ce tissu (Fathi *et al.*, 1997). Ainsi, le récepteur GalR2 pourrait servir de médiateur de la galanine sur la sécrétion d'hormones hypophysaires chez le rat. De plus, le récepteur GalR2 humain a été détecté par RT-PCR dans plusieurs tissus centraux et périphériques, y compris l'hippocampe, l'amygdale, l'hypophyse, le cœur et l'intestin grêle, mais contrairement au GalR2 de rat, il est apparemment absent de l'hypothalamus (Fathi *et al.*, 1998).

Les récepteurs GalR1 et GalR2 de rat partagent des profils pharmacologiques similaires dans le sens qu'ils possèdent une affinité élevée pour la galanine et la partie N-

terminale de la galanine, mais aussi pour des peptides chimériques (Smith *et al.*, 1997; Kolakowski *et al.*, 1998).

L'activation de GalR2 conduit à la stimulation de multiples événements intracellulaires. La voie de signalisation principale implique la phospholipase C. En effet, GalR2 hydrolyse le phosphatidylinositol(4,5)-bis-phosphate générant de l'inositol phosphate IP₃ qui contrôle la mobilisation intracellulaire de Ca²⁺ et l'activation du canal Ca²⁺ chlore-dépendant (Smith *et al.*, 1997; Fathi *et al.*, 1998; Wang *et al.*, 1998).

De plus, GalR2 inhibe également l'accumulation d'AMPc selon les types cellulaires et son couplage à la protéine G (Fathi *et al.*, 1998; Wang *et al.*, 1998). Par exemple, les groupes de Smith et Wang, ont observé une stimulation de l'accumulation d'IP₃ dans des cellules d'ovaire de hamster chinois (CHO), transfectées de façon stable avec le récepteur GalR2 de rat, mais seule l'équipe de Wang montre que GalR2 peut également médier une diminution faible de l'AMPc après stimulation par la forskoline, vraisemblablement par une voie Gi/o (Smith *et al.*, 1997; Wang *et al.*, 1998). En utilisant les cellules HEK293 comme hôte, Fathi et collaborateurs ont rapporté que la transfection stable du récepteur GalR2 humain entraîne une augmentation de l'accumulation d'IP₃ et une mobilisation de Ca²⁺ ainsi qu'une diminution de l'AMPc (seule la dernière est bloquée par la toxine pertussique), alors que la transfection stable de GalR2 de rat conduit à la régulation galanine-dépendante de l'IP₃ et du Ca²⁺, mais pas de l'AMPc (Fathi *et al.*, 1997, 1998). Enfin, le récepteur GalR2 de rat stimule les MAP kinases dans les cellules CHO; cet effet est bloqué par la toxine pertussique, ou par une déplétion (par siRNA) ou une inhibition (indolylmaleimide) de la protéine kinase C, mais pas par l'expression du peptide C-terminal compatible avec une signalisation médiée par Go (Wang *et al.*, 1998).

La présence d'ARNm GalR2 dans de nombreux tissus chez le rat suggère son rôle modulateur dans de nombreuses fonctions physiologiques tel que la libération de prolactine, la lactation, la libération d'hormone de croissance, l'alimentation, l'émotion, la mémoire, le nociception, la croissance cellulaire, la régénération nerveuse, la fonction des îlots pancréatiques, le tonus cardiovasculaire, le métabolisme périphérique et la reproduction.

II.1.3 LE RECEPTEUR GALR3

Le récepteur GalR3 a été d'abord cloné chez le rat (Smith *et al.*, 1998). L'ADNc du récepteur GalR3 de rat code pour une protéine de 370 résidus, avec une similarité en acides aminés avec les récepteurs GalR1 et GalR2 de rat, respectivement de 36% et 55%. Il existe 83 acides aminés conservés dans les trois sous-types de récepteurs de la galanine de rat, ce qui donne une homologie pour les acides aminés de ~ 23%.

Le récepteur humain GalR3 a été cloné à partir d'une banque génomique humaine basée sur une similarité structurelle avec GalR1 et GalR2 humain. D'ailleurs la présence d'un intron au même endroit (après le TM3) que celui décrit pour GalR2 confirme la similitude observé pour la structure des récepteurs (Smith *et al.*, 1998). La protéine humaine de la GalR3 contient 368 acides aminés et a 90% de homologie avec le GalR3 de rat. Les récepteurs GalR3 de rat et humain contiennent un seul site de consensus pour la N-glycosylation et de multiples sites de consensus intracellulaires de phosphorylation, notamment un pour la PKC dans la partie C-terminale. Le géne du récepteur GalR3 humain est localisé sur le chromosome 22q12.2-13.1 (Kolakowski *et al.*, 1998). Le géne codant pour le récepteur GalR3 de la souris a été cloné et est localisé sur le chromosome 15 (Bailey and Crawley, 2009).

Les premières analyses par transfert d'ARN (Northern Blot) ont détecté la présence de transcrits de GalR3 dans le cœur, la rate et les testicules (Wang *et al.*, 1997). À l'aide de méthodes plus sensibles, Smith et ses collaborateurs ont détecté une expression majoritaire de transcrits de GalR3 de rat dans l'hypothalamus et l'hypophyse; ils ont également trouvé GalR3 réparti dans certaines régions du SNC du rat comme l'ampoule olfactive, le cortex cérébral, la médulla oblongata, le noyau caudé, le cervelet et la moelle épinière, mais pas dans l'hippocampe ou la substance noire (Smith *et al.*, 1998). Les transcrits du GalR3 de rat ont également été détectés dans les tissus périphériques, y compris le foie, le rein, l'estomac, les testicules, le cortex surrénal, le poumon, la glande surrénale, la rate et le pancréas, mais pas dans le cœur, l'utérus, le canal déférent, le plexus choroïde ou les ganglions dorsaux.

La localisation de l'ARNm du GalR3 dans des régions telles que le noyau caudé, l'hypothalamus, l'hypophyse, la moelle épinière, le pancréas, le foie, le rein, l'estomac et la glande surrénale suggère que GalR3 pourrait être impliqué dans la modulation de l'émotion, la régulation de l'alimentation, la libération d'hormones hypophysaires, la nociception et le métabolisme.

II.2 LES AGONISTES ET ANTAGONISTES DE LA GALANINE

L'extrémité N-terminale de la galanine est fortement conservée entre différentes espèces et les 15 premiers acides aminés sont suffisants pour la liaison de l'agoniste à son récepteur dans le cerveau et dans la moelle épinière chez le rat (Fisone *et al.*, 1989; Xu *et al.*, 1990). Le clonage moléculaire de sous-types de récepteurs à la galanine a permis de concevoir et de cribler de nombreux agonistes et antagonistes spécifiques de chaque sous-type afin d'étudier les bases moléculaires des actions de la galanine et de développer des composés thérapeutiques potentiels. Dans le tableau 4 sont présentées les caractéristiques générales des principaux agonistes et antagonistes peptidiques de la galanine.

Les peptides de la galanine mentionnés dans le tableau 4 et les différents ligands peptidiques chimères décrits dans la littérature, agissent tous comme des agonistes complets *in vitro*, spécifiquement dans des lignées cellulaires. C'est seulement *in vivo* que ces peptides agissent comme des antagonistes, bien que ce ne soit pas une observation générale faite dans tous les laboratoires. Par exemple, le peptide chimère, M35 (galanine (1-3) -bradykinine (2-9) amide), est un ligand du récepteur à la galanine de haute affinité qui agit comme antagoniste dans de nombreux modèles expérimentaux tels que le réflexe fléchisseur chez le rat (Xu *et al.*, 1997). Cependant, en l'absence de galanine endogène dans le modèle de souris invalidées pour la gène de la galanine, M35 a un effet agoniste, améliorant de manière significative l'excroissance des neurones des ganglions dorsaux adultes cultivés. Cependant, en présence de galanine, son activité agonistique est masquée et elle agit comme antagoniste (Mahoney *et al.*, 2003). D'ailleurs Fang et ses collaborateurs ont montré que l'administration intracérébrale chez le rat de l'agoniste M617 diminue considérablement l'insulinémie à jeun et la concentration de glucose, *via* l'activation du transporteur du glucose GLUT4 (Fang *et al.*, 2014).

Le ligand peptidique	La séquence	Spécificité de récepteur	L'activité	L'espèce
Galanine humaine (1-30)	GWTLNSAGYLLGPHAV GNHRSFSDKNGLTS	-	Agoniste	-
Galanine rat/souris (1-29)	GWTLNSAGYLLGPHAID NHRSFSDKHGLT	-	Agoniste	-
Galanine porc (1-29)	GWTLNSAGYLLGPHAID NHRSFHDKYGLA	-	Agoniste	-
Galanine (2-11) (AR-MI1896)	WTLNSAGYLL	GalR2/GalR3 ^{1,2}	Agoniste ¹	rat
C7 = galanin (1-13)-spantide	GWTLNSAGYLLGPRPKP QQWFPLL	-	Antagoniste ³	rat
M15 = galantide = galanine (1-13)-substance P(5-11)	GWTLNSAGYLLGPQQFF GLM	-	Antagoniste ⁴	rat
M32 = galanine (1-13)-neuropeptide Y (25-36) amide	GWTLNSAGYLLGPRHYI NLITRQRY	-	Antagoniste ⁵	rat
M35 = galanine (1-13)-bradykinine (2-9) amide	GWTLNSAGYLLGPPPGF SPFR	-	Antagoniste ⁶	rat
M40 = galanine (1-13)-Pro-Pro-(Ala-Leu) ₂ Ala amide	GWTLNSAGYLLGPALALA	-	Antagoniste ^{3,7}	rat
M617 = galanine (1-13)-G1,14-bradykinine (2-9) amide	GWTLNSAGYLLGPQPGF SPFR	GalR1>GalR2	Agoniste ^{8,9}	rat
M871 = galanine (2-13)-Glu-His-(Pro) ₃ (Ala-Leu) ₂ Ala amide	WTLNSAGYLLGPEHPPP ALALA	GalR2 ^{10,11}	Antagoniste ⁹	rat
M1160	RGRGNWLNSAGYLLGP VLPPP ALALA	GalR2 ¹²	Agoniste ¹²	souris
J18	RGRGNWTLSAGYLLG PkkK(eNH-C(O) _k stearic acid)	GalR2>GalR3>GalR1	Agoniste ¹²	souris
Gal-B2 (NAX 5055)	(Sar)WTLNSAGYLLGPKK K _{palmitoyl} K	GalR1>GalR2 ¹³	Agoniste ¹⁴	souris
[N-Me, des-Sar]Gal-B2	N-Me(Sar)WTLNSAGYLLGP KKK _{palmitoyl} K	GalR2>GalR1 ¹³	Agoniste ¹⁵	souris
Gal-S2	(Sar)WTLNSAGYLLGPXK KXX	- ¹³	Agoniste ¹⁶	souris
GALP humaine (1-60)	APAHRGRGGWTLNSAG YLLGPVLHLP QMGDQDGKRETALEILD LWKAIDGL PYSHPPQPS	- ¹⁷	Agoniste ¹⁸	souris
GALP humaine (3-32)	AHRGRGGWTLNSAGYL LGPVLHLPQMGDQ	- ^{17,13}	Agoniste ¹⁸	souris

Tableau 4. Les ligands peptidiques de la Galanine.

¹Liu et al. (2001), ²Lu et al. (2005), ³Crawley et al. (1993), ⁴Bartfai et al. (1991), ⁵Xu et al. (1995), ⁶Wiesenfeld-Hallin et al. (1992), ⁷Leibowitz and Kim (1992), ⁸Lundstrom et al. (2005), ⁹Jimenez-Andrade et al. (2006), ¹⁰Sollenberg et al. (2006), ¹¹Sollenberg et al. (2010), ¹²Saar et al. (2013), ¹³Non testé pour GalR3; X = (S)-2-4-pentenyl)alanine, ¹⁴Bulaj et al. (2008), ¹⁵Robertson et al. (2010), ¹⁶Green et al. (2013), ¹⁷Lang et al. (2005), ¹⁸Schmidhuber et al. (2007).

Des études ont été réalisées pour délimiter les fonctions des sous-types individuels des récepteurs à la galanine en utilisant des ligands non peptidiques (Tableau 5).

Le ligand nonpeptidique	Structure	Ligné cellulaire	Spécificité du récepteur	L'activité
SPIROCOUMARONE	Sch202596	Human Bowes melanoma cells ¹	GalR1, GalR3 ²	antagoniste
RWJ-57408	(2,3-dihydro-2-(4methylphenyl)-1,4-dithiepine 1,1,4,4-tetroxide)	Human Bowes melanoma cells ³ , Neurones myentériques de rat cultivés ⁴	-	antagoniste
GALNON	[7-((9-fluorenyl-methoxycarbonyl)cyclohexyl alanyllysyl)amino-4-methylcoumarin]	Human Bowes melanoma cells, Cellules d'ovaire de hamster ⁵	- ⁶	agoniste ⁷
GALMIC		Souris, rat	GalR1 ^{8,9}	agoniste
SNAP37889	1-Phenyl-3-[[3(trifluoromethyl)phenyl]iminoo]-1H-indol-2-one	Souris, rat, porc	GalR3 ¹⁰	antagoniste ¹⁰
SNAP398299	1-[3-(2-(Pyrrolidin-1-yl)ethoxy)phenyl]-3-(3-trifluoromethyl)phenylimino)indolin-2-one	Rat	GalR3 ¹⁰	antagoniste ¹⁰
CYM2503	(9H-Fluoren-9-yl)methyl((S)-1(((S)-6(tertbutoxycarbonyl)amino-1-((4-methyl-2-oxo-1,2-dihydroquinolin-7-yl)amino)-1-oxohexan-2-yl)amino))-3-cyclohexyl-1-oxopropan-2-yl carbamate	Souris, rat	GalR2 ^{11,12}	agoniste ^{11,12}

Tableau 5. Les ligands non-peptidiques de la Galanine.

¹Chu et al. (1997), ²Lang et al. (2001), ³Scott et al. (2000), ⁴Anselmi et al. (2009), ⁵Bartfai et al. (2009), ⁶Interactions avec des autres récepteurs, ⁷Saar et al. (2002), ⁸Bartfai et al. (2004), ⁹Non testé sur GalR3, ¹⁰Swanson et al. (2005), ¹¹Lu et al. (2010), ¹²Modulateur allostérique positif de la galanine endogène.

Le développement de souris KO pour la Galanine et pour ses récepteurs a permis d'identifier les phénotypes spécifiques liés à cette inactivation génique (tableau 6).

Knockout	Le phenotype
Galanine	<p>Réduit l'allodynie mécanique après une blessure nerveuse (Kerr <i>et al.</i>, 2000; Holmes <i>et al.</i>, 2003).</p> <p>Augmentation de l'apoptose dans le DRG au jour 3-4 postnatal avec réduction du nombre de petits neurones peptidergiques. Diminution de la régénération in vivo et in vitro (Holmes <i>et al.</i>, 2000; Sachs <i>et al.</i>, 2007)</p> <p>Perte d'un tiers des neurones cholinergiques dans le cerveau antérieur basal (O'Meara <i>et al.</i>, 2000).</p> <p>Perte de la mémoire spatiale chez les souris âgées (O'Meara <i>et al.</i>, 2000; Massey <i>et al.</i>, 2003).</p> <p>Augmentation de la mort des cellules de l'hippocampe in vivo et in vitro (Elliot-Hunt <i>et al.</i>, 2004, 2011).</p> <p>Augmentation des crises épileptiques induites (Mazarati <i>et al.</i>, 2000).</p> <p>Augmentation de la sécrétion des glandes sudoripares suite à la stimulation thermique (Vilches <i>et al.</i>, 2012).</p> <p>Diminution de l'orexine et de la mélanine dans l'hypothalamus (Karatyev <i>et al.</i>, 2010).</p>
GalR1	<p>Sensibilité accrue à la chaleur et intacte au froid. Augmentation de la durée de l'analgésie pour une douleur neurogène (Blakeman <i>et al.</i>, 2003).</p> <p>Augmentation du comportement lors du sevrage aux opiacés (Holmes <i>et al.</i>, 2012).</p> <p>Apparition de crises d'épilepsie spontanées et taux plasmatiques réduits d'IGF-1. (Jacoby <i>et al.</i>, 2002).</p> <p>Intolérance légère au glucose après l'alimentation et perte de l'élimination du glucose. Augmentation de l'apport alimentaire pendant un régime riche en matières grasses (Zorrilla <i>et al.</i>, 2007).</p> <p>Augmentation de la mort des cellules de l'hippocampe in vivo après traitement au glutamate (Elliot-Hunt <i>et al.</i>, 2011).</p> <p>Niveaux réduits d'ERK et AKT après injection de glutamate <i>in vivo</i> (Elliot-Hunt <i>et al.</i>, 2007).</p>
GalR2	<p>Phénotype dépressif persistant (Lu <i>et al.</i>, 2008).</p> <p>Augmentation du comportement anxieux (Bailey <i>et al.</i>, 2007).</p>
GalR3	Phénotype d'anxiété mais pas de comportement de type dépressif (Brunner <i>et al.</i> , 2014).

Tableau 6. Le phenotype des souris KO pour la Galanine et pour ses récepteurs.

II.3 LA GALANINE ET LE SYSTEME NERVEUX

La galanine régule de nombreuses fonctions physiologiques dans le système nerveux de mammifère adulte, y compris la régulation de l'excitation et du sommeil (Sherin *et al.*, 1998; Steininger *et al.*, 2001), l'homéostasie énergétique et osmotique (Gundlach, 2002; Lawrence and Fraley, 2011), la reproduction (Richter, 1999; Gundlach, 2002), la nociception (Liu and Hökfelt, 2002) et la cognition (McDONALD *et al.*, 1998; Wrenn and Crawley, 2001; Barreda-Gómez *et al.*, 2015). En utilisant une combinaison d'agonistes et d'antagonistes sélectifs sur des modèles de souris transgéniques (WYNICK *et al.*, 1998; Elliott-Hunt *et al.*, 2007; Kerr *et al.*, 2015; Lang *et al.*, 2015) il a montré que le récepteur GalR2 était impliqué dans la transmission de l'influx nerveux dans la moelle épinière (Liu and Hökfelt, 2002) et dans l'hippocampe (Mazarati, 2004). En effet, GalR2 module la croissance des neurites dans le ganglion de la racine dorsale (Mahoney *et al.*, 2003) et de l'hippocampe (Elliott-Hunt *et al.*, 2004, 2007), et contrôle la survie neuronale et la neurogenèse dans l'hippocampe suite à une lésion (Elliott-Hunt *et al.*, 2004; Mazarati, 2004; Pirondi *et al.*, 2005).

Des recherches approfondies ont été faites pour examiner la fonction du système galaninénergique dans le traitement de la douleur dans le système nerveux intact et dans des modèles de neuropathie et de douleur inflammatoire afin de définir son implication dans la régénération axonale et la neurite prolifération des neurones sensoriels. Une récente étude d'hybridation *in situ* chez des rats naïfs a montré la présence de neurones positifs pour l'ARNm de GalR1 dans la lame I-III ainsi que dans des couches plus profondes, y compris la corne ventrale, la zone X et le noyau latéral de la colonne vertébrale (Xu *et al.*, 1998).

Différents travaux montrent que la galanine montre à la fois un effet analgésique et hyperalgesique. L'action relative ou anti-nociceptive de la galanine semble dépendre de l'état aigu ou chronique du stimulus nociceptif, de sa nature (thermique, mécanique ou chimique) et de la concentration de galanine disponible pour agir sur les nerfs afférents nociceptifs (Kerr *et al.*, 2000; Liu and Hokfelt, 2000; Liu *et al.*, 2001; Flatters, Fox and Dickenson, 2003). Des études électrophysiologiques révèlent que la galanine réduit l'hyperexcitabilité de la colonne vertébrale et que les antagonistes des récepteurs à la galanine induisent une allodynie chez les rats naïfs. Le rôle de la galanine dans le nociception aigu a été évalué chez des souris transgéniques. Les souris adulte galanine-KO ont une plus grande sensibilité aux douleurs

mécaniques et thermiques aiguës, tandis que les souris qui surexpriment la galanine ont une réponse réduite à la chaleur nociceptive aiguë (Lang *et al.*, 2015).

Dans les affections chroniques de la douleur telles que la douleur neuropathique, l'expression de la galanine est nettement augmentée dans les voies nociceptives dans le ganglion de la racine dorsale et la moelle épinière. L'effet analgésique de la galanine dépend de sa concentration. De fortes doses de galanine exogène atténuent les comportements neuropathiques suite à une lésion du nerf périphérique (Hao, 1999; Liu *et al.*, 2001), tandis que de faibles doses d'agonistes des récepteurs GalR1/GalR2 (AR-M1896 ou AR-M961) administrées par perfusion intrathécale augmentent la sensibilité à la douleur thermique et mécanique (Liu *et al.*, 2001; Flatters, Fox and Dickenson, 2002). La sensibilité à la douleur est également augmentée lorsque la galanine est administrée de manière chronique par infusion intrathécale (Kerr *et al.*, 2000).

Il a été démontré que la galanine agit comme un facteur de survie et de croissance pour différents types de neurones périphériques et du système nerveux central, y compris les neurones sensoriels du ganglion de la racine dorsale (Mahoney *et al.*, 2003; Lang *et al.*, 2015), les neurones cholinergiques du cerveau antérieur basal (O'Meara *et al.*, 2000) et les neurones de l'hippocampe (Elliott-Hunt *et al.*, 2004, 2007). Ces effets ont été observés à la fois dans des modèles *in vitro* et *in vivo* et sont censés se produire dans les systèmes nerveux adultes et en développement. La galanine est également impliquée dans le contrôle de la neurogénèse (la prolifération, la différenciation et/ou la migration des cellules souches neurales) dans le cerveau sain et blessé (Shen, Larm and Gundlach, 2003; Elliott-Hunt *et al.*, 2004; Mazarati, 2004).

II.4 LA GALANINE ET LE SYSTEME NEUROENDOCRINE ET ENDOCRINE

La galanine exerce également son action dans le cerveau et les tissus périphériques impliqués dans les circuits complexes contrôlant le métabolisme, l'appétit et l'obésité (Lang *et al.*, 2015).

Une augmentation aiguë de la concentration en galanine dans le système nerveux central peut augmenter l'apport alimentaire et la consommation de matières grasses chez les mammifères (Adams *et al.*, 2008). En effet, l'injection de la galanine dans le système nerveux central, particulièrement dans le noyau paraventriculaire de l'hypothalamus, stimule l'apport alimentaire chez les rats (Gundlach, 2002).

Contrairement à l'administration aiguë de galanine, une augmentation du taux de galanine dans le SNC pour un temps relativement long peut entraîner une hyperphagie et un gain de poids. En outre, l'administration chronique de la galanine par des pompes mini-osmotiques dans le ventricule latéral des souris knock-out pour la Galanine a inversé partiellement le phénotype d'évitement des graisses (Adams *et al.*, 2008). Ces résultats suggèrent que la production de la galanine hypothalamique favorise la suralimentation et le gain de poids lorsque les aliments, en particulier les graisses alimentaires, sont abondants. Les données de la littérature montrent que l'augmentation de la consommation alimentaire induite par la galanine au niveau du SNC est médiaée par le récepteur GalR1 (Zorrilla *et al.*, 2007; Zhang *et al.*, 2016).

À l'exception de l'augmentation de l'apport alimentaire par la stimulation du SNC par la galanine, la galanine circulante peut moduler l'appétit et le contrôle du poids chez les animaux. L'injection intraveineuse de galanine diminue la synthèse de la leptine et la sécrétion dans le tissu adipeux viscéral des rats, qui est impliqué dans la régulation de l'alimentation et l'équilibre énergétique des animaux (Jureus *et al.*, 2000). Afin d'étudier les effets périphériques de la galanine des souris transgéniques homozygotes mâles galanine (Gal-Tg) ont été utilisées. Dans ce modèle, l'augmentation de la galanine circulante contribue au développement de l'obésité et du métabolisme lipidique, entraînant une augmentation du poids corporel, de l'adiposité viscérale, du cholestérol sérique total et des triglycérides sériques totaux, mais sans incidence sur l'apport alimentaire par rapport au groupe control (Poritsanos *et al.*, 2009). Il semble exister une association de plusieurs voies de signalisation médiées par la galanine dans l'activation de l'adipogénèse à la suppression concomitante de la

thermogenèse dans les tissus adipeux dans un modèle de souris soumise à un régime à haute teneur en graisse (Kim and Park, 2010).

L'augmentation chronique du taux de galanine dans le sang induit l'installation de l'obésité et modifie le métabolisme lipidique (Poritsanos *et al.*, 2009) et peut donc contribuer au développement de troubles métaboliques conduisant au diabète de type 2. Legakis et Fang, ont montré que le niveau plasmatique de galanine est augmenté significativement chez les patients atteint de diabète de type 2 et chez les femmes atteintes de diabète gestationnel (Fang *et al.*, 2013). En outre, la Galanine a récemment été proposée comme biomarqueur potentiel pour la prédition du diabète gestationnel (Zhang *et al.*, 2014).

Diverses études démontrent l'existence d'une relation entre les taux de galanine et de glucose. Les études fonctionnelles ont montré que la perfusion intraveineuse de galanine provoque une hyperglycémie légère mais statistiquement significative chez le chien. Celle-ci produit une diminution transitoire du niveau basal d'insuline et des réponses à l'insuline après stimulation par du glucose ou à l'arginine chez le chien (McDonald *et al.*, 1985; McDonald *et al.*, 1986). Une corrélation positive entre les taux de la galanine et les taux de glucose dans le sang a été observée chez les enfants atteints de diabète de type 1 (Celi *et al.*, 2005), chez des patients atteint de diabète de type 2 (Legakis, Mantzouridis and Mountokalakis, 2005) et chez des femmes atteintes de diabète gestationnel (Fang *et al.*, 2013; Nergiz *et al.*, 2014; Zhang *et al.*, 2014). Chez les patients atteints de diabète de type 1 ou de type 2, les taux plasmatiques de galanine ont également été corrélés positivement avec l'hémoglobine glyquée, qui est fréquemment utilisée comme marqueur pour guider le traitement du diabète (Celi *et al.*, 2005). Plusieurs études indiquent que la galanine pourrait réguler la libération d'insuline. En effet, l'administration de galanine diminue les taux plasmatiques d'insuline dans diverses espèces, y compris les rats et les porcs (McDonald *et al.*, 1985; Lindskog *et al.*, 1990; Manabe *et al.*, 2003). Cependant, des résultats contradictoires ont été rapportés chez l'homme, et bien que des taux d'insuline diminués aient été détectés après une infusion de galanine dans une étude (Bauer *et al.*, 1989), d'autres études n'ont observé aucun effet de l'administration de la galanine sur la sécrétion basale d'insuline plasmatique (Gilbey *et al.*, 1989; Ahrén, 1990). Il est probable que la galanine inhibe la libération d'insuline induite par le glucose par des terminaux nerveux sympathiques qui innervent les îlots pancréatiques (Kashimura *et al.*, 1994).

La galanine inhibe directement la sécrétion d'insuline stimulée par le glucose à partir de tissus pancréatiques isolés de plusieurs espèces (Lindskog *et al.*, 1990; Flynn and White, 2015). Les souris hyperinsulinémiques, génétiquement obèses, présentent une teneur réduite en galanine pancréatique (Dunning and Ahrén, 1992). Fait intéressant, les rats diabétiques ont également montré une réduction significative des cellules des îlots pancréatiques exprimant la galanine (Adeghate and Ponery, 2001). Les données de plusieurs études suggèrent que la galanine réduit la résistance à l'insuline en augmentant le transporteur de glucose GLUT4 présent dans les cellules du muscle squelettique et les adipocytes de rats diabétiques de type 2 et de rats sains. Enfin il a été montré que l'exercice diminué la résistance à l'insuline et les niveaux élevés de galanine plasmatique chez les rats (Jiang *et al.*, 2009; Guo *et al.*, 2011; He *et al.*, 2011).

L'activation de la voie Akt2 est nécessaire pour promouvoir les effets de la galanine sur la translocation de GLUT4 à la membrane plasmique et l'absorption ultérieure de glucose dans les adipocytes d'animaux diabétiques. En outre, l'injection de galanine augmente la phosphorylation d'Akt2 et d'AS160 stimulée par l'insuline, mais réduit la phosphorylation de FoxO1 et GSK-3 β concomitante avec une augmentation de l'absorption de glucose dans les adipocytes (Zhu *et al.*, 2017).

II.5 LA GALANINE DANS LE CANCER, L'INFLAMMATION ET DANS LA PEAU

L'expression du neuropeptide Galanine a été détectée dans une variété de tumeurs et les niveaux d'expression se sont révélés en corrélation avec le niveau de différenciation ou l'agressivité tumorale (Rauch and Kofler, 2010).

La première description de récepteurs à la galanine a été faite dans une tumeur de cellules pancréatiques de hamster et dans une lignée cellulaire d'insulinome de rat (Lagny-Pourmir *et al.*, no date; Amiranoff *et al.*, 1987). Chez l'homme, les récepteurs à la galanine ont été décrit pour la première fois dans les tumeurs hypophysaires (Hulting *et al.*, 1993) et ont ensuite été identifiées dans le phéochromocytome (Berger *et al.*, 2005), le neuroblastome (Tuechler *et al.*, 1998), le gliome (Berger *et al.*, 2003), le carcinome de la prostate (Berger *et al.*, 2005), le carcinome du colon (Stevenson *et al.*, 2012; Nagayoshi *et al.*, 2014) et le carcinome épidermoïde de la tête et du cou (HNSCC) (Misawa *et al.*, 2008).

Les études *in vivo* d'Iishi et al. ont révélé que l'administration prolongée de la galanine diminue considérablement l'incidence des cancers gastriques chez les rats Wistar, suggérant pour la galanine un rôle inhibiteur de la carcinogenèse gastrique qui pourrait être lié à la suppression de la prolifération des cellules épithéliales antrales. Cependant, ces effets médiés par la galanine semblent être spécifiques de la tumeur et du type cellulaire cellule, car le galanine est également considéré comme un agent mitogène dans le cancer du poumon à petites cellules (Sethi and Rozengurt, 1991). Dans des expériences de culture cellulaire sur des lignées de cellules tumorales, la galanine a montré des effets favorisant ou inhibant la croissance. L'activation de GalR1 est généralement anti-proliférative, alors que l'activation de GalR2 peut avoir des effets pro-ou anti-prolifératifs.

En 1994, GalR1 a été cloné à partir de la lignée cellulaire humaine de mélanome de Bowes (E Habert-Ortolie *et al.*, 1994) et est le récepteur de la galanine le plus clairement exprimé dans le méningiome humain, le glioblastome (Berger *et al.*, 2003) et le neuroblastome (Berger *et al.*, 2002). De plus, l'expression élevée de GalR1 est associée à une malignité accrue (Perel *et al.*, 2002b). Une augmentation de l'expression de GalR1 a également été observée dans les adénomes hypophysaires humains par rapport aux niveaux dans les hypophyses humaines normales (Tofighi *et al.*, 2012), ce qui suggère des propriétés favorisant le cancer pour GalR1, au moins dans ces tumeurs. En outre, l'activation de GalR1 induit l'arrêt du cycle cellulaire et supprime la prolifération des lignées cellulaires HNSCC

(Henson *et al.*, 2005; Kanazawa *et al.*, 2007; Misawa *et al.*, 2008). Les effets antiprolifératifs via la signalisation GalR1 ont également été observés dans des cellules de neuroblastome humain SH-SY5Y transfectées avec GalR1 (Berger *et al.*, 2004).

En revanche, la présence de GalR2 est moins fréquente dans le gliome humain (Berger *et al.*, 2003), le neuroblastome (Tuechler *et al.*, 1998) et les adénomes hypophysaires humains (Tofighi *et al.*, 2012). Dans une étude récente, dans les cellules de neuroblastome humain SH-SY5Y transfectées avec GalR2, l'activation du récepteur sur le traitement par la galanine inhibe complètement la prolifération cellulaire et l'apoptose (Berger *et al.*, 2004). Les récepteurs à la galanine présentent des propriétés de signalisation mitogènes par exemple via la voie de MAP kinases, ce qui joue un rôle important dans la prolifération cellulaire (Seger and Krebs, 1995; Hammond *et al.*, 1996; Seufferlein and Rozengurt, 1996; Wittau *et al.*, 2000). L'expression ectopique de GalR2 inhibe la prolifération cellulaire et induit une apoptose dans des cellules HNSCC mutée pour p53 suggérant que GalR2 peut être une cible possible pour le traitement par HNSCC (Kanazawa *et al.*, 2009). Banerjee *et al.*, ont démontré que GalR2 stimule l'angiogenèse tumorale et induit les voies de signalisation ERK et PI3K / AKT via rap1 pour favoriser la croissance et la survie dans les cellules HNSCC et la progression tumorale *in vivo* (Banerjee *et al.*, 2011).

L'activité biologique de récepteur GalR3 est le moins étudiée. L'expression du récepteur GalR3 a été démontrée dans la lignée cellulaire humaine de HNSCC (Henson *et al.*, 2005), dans les cellules de mélanomes humaines de Bowes (Lang *et al.*, 2001), dans le scellules phéochromocytomes PC12 de rat et dans les lignées cellulaires de neuroblastome de rat B104 (Cheng and Yuan, 2007). Dans les tumeurs l'expression du récepteur GalR3 a été détectée dans le neuroblastome (Berger *et al.*, 2002; Perel *et al.*, 2002a) et dans le gliome (Berger *et al.*, 2003). Une augmentation d'expression du récepteur GalR3 a été trouvée dans les lignées humaine tumorales HNSCC par rapport au tissu sain (Sugimoto *et al.*, 2009). Enfin, une étude de Tofighi et ses collaborateurs montre une expression augmentée du récepteur GalR3 dans les adénomes d'hypophyse humaine, mais qui n'est pas retrouvée dans l'hypophyse post-mortem (Tofighi *et al.*, 2012). Ces données suggèrent le rôle potentiel de GalR3 dans la biologie du cancer, mais des investigations supplémentaires sont nécessaires afin de décortiquer le mécanisme.

Par des méthodes d'immunohistochimie et hybridisation *in situ* une augmentation de la synthèse de la Galanine a été démontrée dans l'inflammation de la peau, tant dans les

macrophages que dans l'épithélium, mais absente dans l'épithélium normal (Ji *et al.*, 1995). Il est intéressant de noter que les souris adultes portant une mutation de perte de fonction dans le gène de la galanine (souris knock-out galanine) montrent des réponses inflammatoires neurogéniques anormales au niveau de la peau, probablement dues à des déficits neurologiques lors du développement (Schmidhuber *et al.*, 2008). La galanine semble agir comme un régulateur de la production de cytokines proinflammatoires, puisque l'administration de galanine provoque une augmentation de la production de TNF-a, IL-1-a et IL-8 dans les kératinocytes humains, même sans stimulation inflammatoire antérieure (Dalloz *et al.*, 2006). De même, l'injection intracérébroventriculaire de la galanine dans des rats Sprague Dawley a stimulé la production d'IL-1a et d'IL-1b dans les macrophages et/ou la microglie dans certaines zones du cerveau (Man and Lawrence, 2008).

En outre, les souris knock-out galanine présentent une pancréatite aiguë induite par la céruleine moins sévère par rapport aux souris sauvage, qui est exacerbée par l'administration de galanine (Bhandari *et al.*, 2011). Bien que les trois récepteurs de la galanine soient exprimés dans le pancréas de souris, une étude récente suggère un rôle majeur pour GALR3 dans la médiation des effets de la galanine dans la pancréatite aiguë. En effet, l'antagoniste spécifique de GalR3, SNAP-37889, réduit l'activité de la myéloperoxydase pancréatique, les dommages aux acinus pancréatiques et l'hyperamylasémie dans la pancréatite aiguë induite par la céruleine chez la souris (Barreto *et al.*, 2011).

Similaire aux vaisseaux cutanés, où la galanine a une activité vasoconstrictrice (Schmidhuber *et al.*, 2007), celle-ci réduit le flux sanguin à travers le pancréas, ce qui est un facteur contribuant à la nécrose pancréatique dans la pancréatite aiguë (Brooke-Smith *et al.*, 2008). Par contre, dans un modèle de rat de colite aiguë expérimental induite par le 2,4,6-Trinitrobenzenesulfonic acid (TNBS), l'administration de galanine réduit considérablement les dommages macroscopiques à la muqueuse colique et l'activité de la myéloperoxydase (MPO) (Talero *et al.*, 2006). Les effets anti-inflammatoires de la galanine ont également été observés dans la colite chronique induite par le TNBS (Talero *et al.*, 2007). Cependant, la réduction de l'accumulation de neutrophiles, reflétée par une activité MPO réduite chez les souris KO galanine ne se limite pas exclusivement à la pancréatite aiguë et semble être un phénomène plus général de l'inflammation, car elle a également été observée avec des réponses inflammatoires de la peau (Schmidhuber *et al.*, 2008). Le traitement par la galanine entraîne également une réduction significative de la diarrhée chez les rats atteints de colite

aiguë induite par le TNBS (Talero *et al.*, 2006). Ces derniers résultats sont en désaccord avec l'étude du Benya et al., dans lequel l'administration de la galanine conduit à une sécrétion de fluide accrue dans la colite induite par le dextran sulfate de sodium chez les souris (Benya *et al.*, 2000).

En conclusion, la galanine et ses récepteurs sont des cibles thérapeutiques potentielles pour le traitement de la pancréatite aiguë et d'autres troubles inflammatoires si les actions pléiotropes de la galanine à différents niveaux de l'inflammation peuvent être prises en compte et exploitées avec succès.

II.6 LA GALANINE ET LE SYSTEME CARDIOVASCULAIRE

Après plus d'une trentaine années d'études, il ne fait aucun doute que la galanine est impliquée dans la modulation de l'activité cardiaque par le système nerveux central. En effet, une injection intracisternale de galanine induit une faible hypotension associée à une légère tachycardie, qu'il est possible de bloquer par l'antagoniste de la galanine M40 chez le rat (Díaz-Cabiale *et al.*, 2005). Une étude récente a démontré que la galanine exogène appliquée à la médulla ventrolatérale rostrale réduit l'activité cardiovasculaire sympathique, produisant un effet hypotenseur (Abbott and Pilowsky, 2009). Chez les souris anesthésiées, la galanine administrée par voie intraveineuse atténue la capacité du nerf vague à ralentir le cœur en fonction de la dose utilisée. L'effet inhibiteur de la galanine n'est pas été modifié dans des souris galanine KO mais est absent chez les souris GalR1 KO (Smith-White, Iismaa and Potter, 2003), suggérant l'activation du récepteur GalR1 par la galanine.

L'injection périphérique de la galanine inhibe la libération d'acétylcholine à partir des neurones parasympathiques cardiaques dans une grande variété d'espèces (Parsons *et al.*, 1989; Revington, Potter and McCloskey, 1990; Ulman *et al.*, 1993; Mahns and Courtice, 1996; Smith-White, Iismaa and Potter, 2003) et est suivi par une augmentation de la fréquence cardiaque et une diminution de l'intervalle de temps lors de la prise du pouls.

Selon une étude récente, les taux plasmatiques de galanine sont significativement diminués chez les patients obèses atteints d'hypertension par rapport au groupe témoin obèse, tandis que les taux de galanine sont significativement augmentés dans les témoins obèses par rapport aux témoins maigres. Dans les deux groupes d'obésité, les taux de galanine sont corrélés de façon négative à la pression artérielle diastolique et sont corrélés de façon positive aux niveaux d'insuline et de triglycérides, mais pas à la fréquence cardiaque (Fang *et al.*, 2017). De plus, chez les rats hypertendus induits par la coarctation de l'aorte, les niveaux d'expression de l'ARNm de la galanine sont diminués dans le noyau du tractus solitaire et le noyau paraventriculaire hypothalamique (Coelho *et al.*, 2004). Enfin, il existe des dimérisations entre les récepteurs à la galanine et les récepteur à l'alpha-2 noradrénergique, à la sérotonine de type 1A (5-HT1A), au neuropéptide Y (NPY) et à l'angiotensine 1 (AT1) dans les zones centrales de contrôle cardiovasculaire (Díaz-Cabiale *et al.*, 2000, 2005, 2010).

De plus, la galanine joue un rôle important dans l'homéostasie du métabolisme du glucose. En effet, la galanine endogène agit comme un régulateur métabolique via ses

récepteurs au niveau du SNC et présente un effet bénéfique sur l'expression de GLUT4 dans le muscle cardiaque chez les rats diabétiques type 2 (Fang *et al.*, 2014).

La combinaison des dommages aux axones et de la production de cytokines inflammatoires suite à une ischémie-reperfusion pourrait modifier la production de neuropeptides dans les neurones sympathiques innervant le cœur. La galanine peut jouer un rôle important dans le remodelage cardiaque et neuronal ainsi que dans la régénération après ischémie-reperfusion (Habecker *et al.*, 2005). D'ailleurs, une lésion ischémique myocardique peut réguler l'expression de la galanine et accélérer le transporteur de glucose 1 et la translocation GLUT4 sur le sarcolemme, entraînant une augmentation de l'absorption du glucose et de la glycolyse pendant l'ischémie (Jiang *et al.*, 2009; He *et al.*, 2011). De plus, la galanine protège le muscle cardiaque contre les perturbations contractiles induites par l'hypoxie (KOCIC, 1998). Habecker et ses collègues ont montré une augmentation du taux de galanine dans le ventricule gauche en dessous de la ligature de l'artère coronaire du cœur, mais qui n'est pas retrouvée de manière significative dans les oreillettes ou la base du cœur au-dessus de la ligature (Habecker *et al.*, 2005). L'accumulation de la galanine spécifiquement dans le VG endommagé est compatible avec les rapports précédents selon lesquels la galanine est transporté à la régénération des terminaisons nerveuses après les dommages aux axones (Shadiack and Zigmond, 1998).

IV. OBJECTIFS

L'objectif de ma thèse a été de déterminer le rôle de la Galanine dans les processus du remodelage cardiaque par des approches *in vitro*, *in vivo* et *ex vivo*. Une première partie de mon étude concerne la description de l'effet de la galanine sur le remodelage cellulaire et tissulaire du myocarde dans une phase précoce (modèle d'ischemie reperfusion cardiaque).

Dans une seconde partie, je me suis intéressé à l'étude du rôle du système galaninergique dans la phase tardive du remodelage cardiaque (modèle de la constriction aortique transverse -TAC) par des approches *in vitro* et *in vivo*.

Les résultats obtenu seront décrites dans le chapitre «Résultats» de cette thèse.

V. RESULTATS

Article 1: Myocardial protection from ischemia/reperfusion injury by exogenous galanin fragment

AVANT PROPOS

Nos travaux ont permis de mettre en évidence une activité cardioprotectrice de la Galanine. De plus, nous avons démontré que le récepteur GalR2 est majoritairement exprimé dans les cardiomyoblastes et le tissu cardiaque. Récemment il a été démontré que le fragment Gal2-11 (G1) possède une spécificité pour le récepteur GalR2 (ref), donc, nous avons décidé d'étudier l'effet de G1 dans le remodelage cellulaire et tissulaire du myocarde. Pour cela nous avons choisi des approches *in vitro* (lignées cellulaires H9C2), *ex vivo* (cœur isolé de rat) et *in vivo* (I/R cardiaque). Ces études ont été réalisées en collaboration avec l'équipe de Dr. Pisarenko Oleg (l'Institut de Cardiologie de Moscou, Russie), qui ont synthétisé le fragment et réalisé les expériences *in vivo* et *ex-vivo*.

Nos résultats ont permis de montrer que le peptide G1 joue un rôle important dans le rétablissement du statut cardio-métabolique en réponse à l'hypoxie et à l'ischémie / réperfusion myocardique. La réalisation de cette étude a mis en évidence que la préservation du métabolisme énergétique du myocarde par G1 est associée avec la prévention des lésions myocardiques et une amélioration de la fonction cardiaque.

Ces résultats ont été publiés dans le journal Oncotarget (2017).

Myocardial protection from ischemia/reperfusion injury by exogenous galanin fragment

Andrei Timotin^{1,2}, Oleg Pisarenko³, Maria Sidorova³, Irina Studneva³, Valentin Shulzhenko³, Marina Palkeeva³, Larisa Serebryakova³, Aleksander Molokoedov³, Oksana Veselova³, Mathieu Cinato^{1,2}, Helene Tronchere^{1,2}, Frederic Boal^{1,2,*}, Oksana Kunduzova^{1,2,*}

¹National Institute of Health and Medical Research (INSERM), Toulouse, Cedex 4, France

²University of Toulouse, UPS, Institute of Metabolic and Cardiovascular Diseases, Toulouse, France

³Russian Cardiology Research-and-Production Complex, Moscow, Russian Federation, Russia

*These authors have contributed equally to this work

Correspondence to: Oksana Kunduzova, email: Oxana.Koundouzova@inserm.fr

Keywords: galanin (2-11), heart, ischemia and reperfusion, energy metabolism, ROS production

Received: November 02, 2016

Accepted: January 09, 2017

Published: February 03, 2017

ABSTRACT

Background and purpose: Galanin is a multifunctional neuropeptide with pleiotropic roles. The present study was designed to evaluate the potential effects of galanin (2-11) (G1) on functional and metabolic abnormalities in response to myocardial ischemia-reperfusion (I/R) injury.

Experimental approach: Peptide G1 was synthesized by the 9-fluorenylmethoxycarbonyl (Fmoc)-based solid-phase method. The chemical structure was identified by ¹H-NMR spectroscopy and mass spectrometry. Experiments were conducted using a rat model of I/R injury *in vivo*, isolated perfused rat hearts *ex vivo* and cultured rat cardiomyoblast H9C2 cells *in vitro*. Cardiac function, infarct size, myocardial energy metabolism, hemodynamic parameters, plasma levels of creatine kinase-MB (CK-MB) and lactate dehydrogenase (LDH) were measured in order to evaluate the effects of G1 on myocardial I/R injury.

Key results: Treatment with G1 increased cell viability in a dose-dependent manner, inhibited cell apoptosis and excessive mitochondrial reactive oxygen species (ROS) production in response to oxidative stress in H9C2 cells. Pre- or postischemic infusion of G1 enhanced functional and metabolic recovery during reperfusion of the ischemic isolated rat heart. Administration of G1 at the onset of reperfusion significantly reduced infarct size and plasma levels of CK-MB and LDH in rats subjected to myocardial I/R injury.

Conclusions and implications: These data provide the first evidence for cardioprotective activity of galanin G1 against myocardial I/R injury. Therefore, peptide G1 may represent a promising treatment strategy for ischemic heart disease.

INTRODUCTION

Galanin is a highly conserved 29-(30 in human) amino acid neuropeptide with multiple biological functions. Galanin modulates the release and secretion of many neurotransmitters and hormones in the central nervous system and periphery, such as acetylcholine, gastrin, insulin, dopamine, somatotropin and prolactin. Central

administration of galanin stimulates feeding behavior and energy balance that impact body weight regulation [1]. Galanin is involved in central cardiovascular regulation, which affects the blood pressure and the heart rate [2]. Administration of galanin into the rostral ventrolateral medulla produces a weak hypotension and tachycardia effect by reducing the sympathetic vasomotor tone in rats [3], which may be blocked by the intracerebroventricular

injection of galanin antagonist M40 [4]. Recent studies suggest that galanin and its fragment play a major role in the regulation of metabolic homeostasis in cardiac muscle and galanin is an important hormone relative to diabetic heart [4]. The endogenous galanin, acting through its central receptor, has an important attribute to glucose transporter 4 (GLUT4) regulation, leading to enhanced insulin sensitivity and glucose uptake in cardiac muscle of type 2 diabetic rats [5]. In response to ischemia-reperfusion, galanin may stimulate sensory nerve regeneration and promote the regrowth of cardiac sensory nerves [6, 7]. Furthermore, galanin protects the heart muscle against hypoxia-induced contractile disturbances to improve inotropic action [8]. Although galanin and its fragments are involved in central cardiovascular regulation, the therapeutic potential of galanin-receptor ligands for coronary heart disease remains unexplored.

Galanin is involved in the regulation of physiological processes in peripheral organ systems via neuronal mechanisms and direct receptor mediated cellular effects. Currently three types of galanin receptors (GalR1, GalR2, and GalR3) have been identified by molecular cloning and characterized pharmacologically in various species [9]. They are members of the G-protein coupled receptor superfamily, but have differences in their functional coupling and signaling activities. All subtypes of galanin receptors are distributed in the hypothalamus, paraventricular nucleus, hippocampus, amygdale, peripheral nervous system and other tissues, including the heart [10]. The N-terminal end of galanin is highly conserved between different species, and the first 15 amino acid residues were found to be responsible for agonistic receptor binding [11]. The C-terminal region (amino acid residue 17-29) varies in most species and has a weak receptor affinity [11]. All three galanin receptor subtypes couple to $G_{i/o}$ and inhibit adenylyl cyclase causing a decrease of the activity of the cAMP response element binding protein (pCREB). The activated pCREB may inhibit the Rab GTPase-activating protein (AS160), a substrate of Akt and GLUT4 translocation, thus promoting insulin resistance [11, 12]. GalR2 receptor signals through several classes of G-proteins and stimulates multiple intracellular pathways. Signaling via $G_q/11$ activates phospholipase C (PLC) and protein kinase C (PKC) [13]. Activation of PLC leads to an increase in the hydrolysis of phosphatidylinositol (4,5) bis-phosphate (PI(4,5)P₂) and promotes Ca²⁺ release from the endoplasmic reticulum [14], suggesting that galanin signaling via GalR2 receptor may modulate multiple cell death mechanisms in the failing heart. In spite of a variety of potential galanin receptor ligands developed to elucidate the specific roles of galaninergic system, very few agonists have high selectivity towards GalR2 receptor. One of them is a short N-terminal galanin fragment (2-11, G1) with no appreciable activation of GalR1 receptor [15]. The ability of this peptide to act as a non-GalR1 receptor agonist has provided evidence for the strong anti-kindling activities

of G1. In fact, the action of G1 could be identified as anti-epileptogenic, as judged by the complete prevention of both full motor seizures and of a post-kindling increase of hippocampal excitability [16]. However, the peripheral action of this peptide remains poorly understood. No data regarding the role of G1 in cardiac cells and cardiovascular diseases is available so far.

In the present study we have evaluated the effects of G1 on myocardial I/R injury in various experimental models including cardiomyoblasts, perfused isolated heart and the heart *in situ*.

RESULTS

The effects of G1 on H9C2 cell survival in response to stress

To determine whether G1 affects cell survival in response to oxidative stress, we examined the dose-dependent effects of the peptide on H₂O₂-induced loss of cardiomyoblast viability measured by ATP concentration. As shown in Figure 1, cell exposure to 400 μ M H₂O₂ for 4 hours led to a significant reduction of the cell viability compared to control. Dose-response studies revealed that at the dose of 50 and 250 nM G1 was able to prevent H₂O₂-induced decrease of cell survival. Next, we examined by terminal deoxynucleotidyltransferase dUTP nick end labeling (TUNEL) assay whether G1 affects apoptotic cell death in response to hypoxic stress. Because 50 nM of G1 produced approximately a 20% increase in cardiomyoblast viability, we used this concentration in subsequent experiments. As shown in Figure 2, the exposure of H9C2 cells to hypoxia caused a significant increase in the number of TUNEL-positive cells as compared to normoxia. However, the treatment of cells with 50 nM G1 significantly reduced hypoxia-induced apoptosis (Figure 2A-2B).

The effects of G1 on hypoxia-induced mitochondrial ROS production in H9C2 cells

The excessive generation of ROS and impaired cellular metabolism are closely linked to cell death and myocardial damage [17]. To determine whether G1 could affect ROS generation in response to hypoxia, we examined the effects of G1 on mitochondrial superoxide (O₂⁻) production using the MitoSOX Red fluorescent probe. As shown in Figure 3A-3B, cell exposure to hypoxic stress caused a significant increase in O₂⁻ production as compared to normoxia. Importantly, treatment of H9C2 cells with 50 nM G1 markedly prevented hypoxia-induced O₂⁻ formation (Figure 3A-3B).

The cardioprotective potential of exogenous G1 in isolated rat hearts after I/R injury

To study the functional role of galanin fragment in the failing heart, we evaluated the effects of G1 on

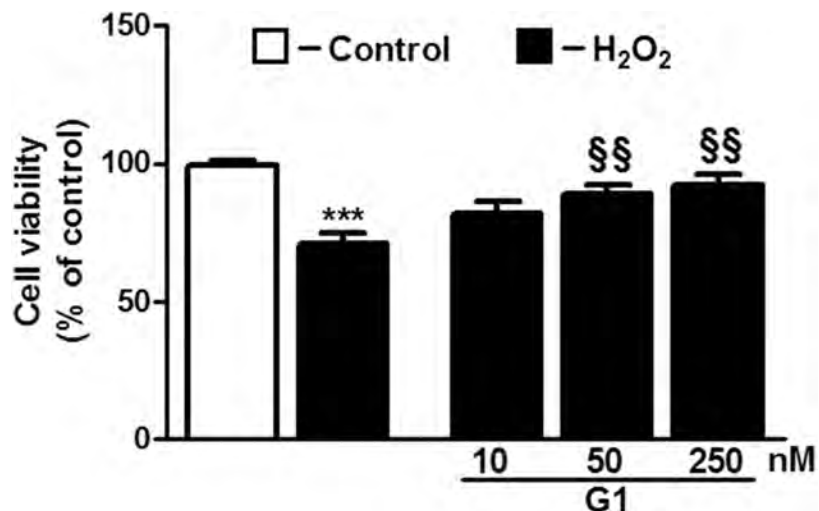


Figure 1: Dose-dependent effect of G1 on cell survival in response to oxidative stress. Treatment of cardiomyoblasts with G1 prevents H₂O₂-induced decrease of cell viability in a dose-dependent manner. The H9C2 were pretreated with G1 (10, 50, 250 nM) for 20 min and then exposed to 400 μM H₂O₂ for 4h. Values are the means ± SEM for three experiments. ***P < 0.001, vs control; §§P < 0.01, vs H₂O₂ treatment.

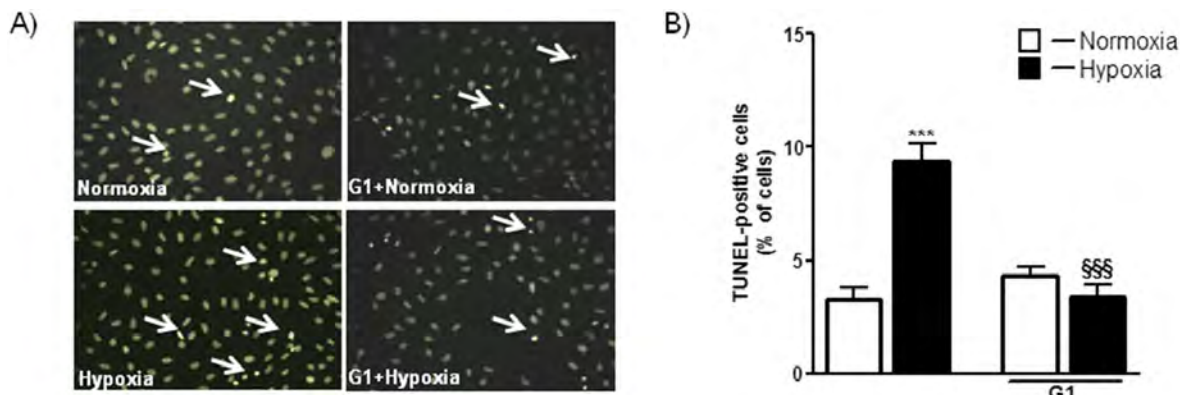


Figure 2: Effect of G1 on hypoxia-induced cell apoptosis. A. Representative fluorescence images of H9C2 cells pretreated with 50 nM G1 for 20 min and then exposed to normoxia or hypoxia (1% O₂) followed by reoxygenation. Apoptosis was measured by TUNEL assay in H9C2 cells after 16h of hypoxia followed by 4h of reoxygenation. B. Quantitative analysis of TUNEL-positive cells in H9C2 cells. Values are the means ± SEM from three experiments. ***P < 0.001, vs normoxia; §§§P < 0.001, vs hypoxia.

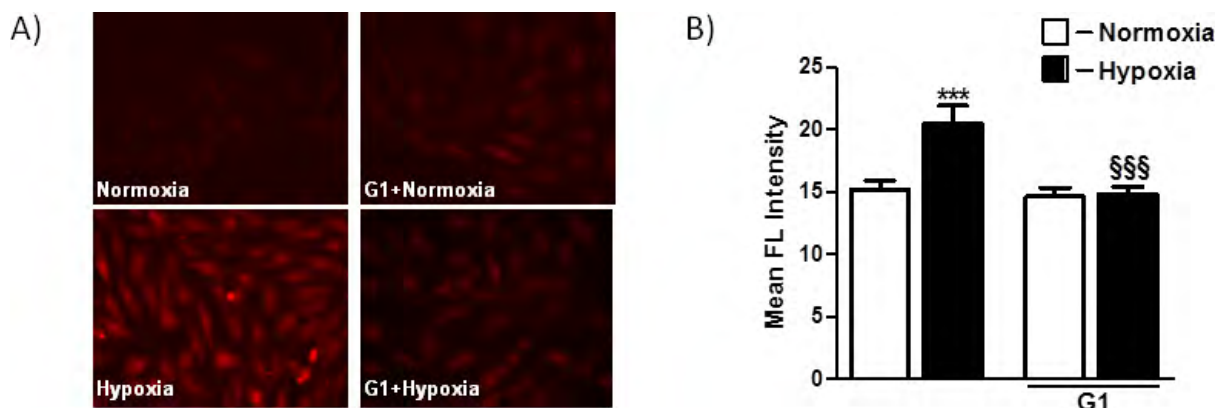


Figure 3: Effect of G1 on hypoxia-induced mitochondrial O₂⁻ production. A. Representative fluorescence images of H9C2 cells pretreated with G1 peptide. Mitochondrial O₂⁻ formation was assessed by MitoSOX Red in H9C2 cells exposed to 16h hypoxia followed by 4h of reoxygenation. B. Quantitative analysis of mitochondrial O₂⁻ production in H9C2 cells exposed to normoxia or hypoxia/reoxygenation. Values are the means ± SEM from three experiments. ***P < 0.001 vs normoxia; §§§P < 0.001 vs hypoxia.

the recovery of perfused hearts subjected to I/R injury (Figure 4A). Infusion of peptide G1 before global ischemia or at onset of reperfusion enhanced recovery of cardiac function during reperfusion compared with control. A dose-dependent effect of G1 on recovery of cardiac output (CO) by the end of reperfusion is shown on Figure 4B. The significant increase in CO recovery was observed after pre- or postischemic infusion of 80 μ M G1 as compared with the control. The differences in CO recovery between the experimental and control groups became more pronounced with an increase in G1 concentration in Krebs-Henseleit bicarbonate buffer (KHB). The maximal response to G1 was observed at the concentration of 240 μ M; at a higher concentration a dose-effect curve reached a plateau. Within the range of 80 - 280 μ M, CO recovery was more effective when peptide infusion was performed after ischemia. A similar dose-dependent effects were obtained for recovery of the left ventricular (LV) developed pressure (LVDp) \times heart rate (HR) product (Figure 4C).

Cardiac function indices were compared at the end of reperfusion for preischemic (G1-I) and postischemic (G1-R) infusion of the optimal G1 concentration (240 μ M) in Table 1. In addition to recovery of CO, recovery of aortic output and stroke volume was also significantly higher in the G1-R group compared to the G1-I group. An augmented restoration of the LVDp \times HR product in both G1 groups was due to better recovery of HR and LVDp comparing with control. A significant increase in LVDp was caused by a marked reduction of LV diastolic

pressure during reperfusion. Both G1 groups exhibited an increase in coronary flow with concomitant reduction in coronary resistance in comparison with control. Data in Table 1 show that recovery of cardiac function was more effective after G1 administration at the onset of reperfusion.

Myocardial energy status is a critical aspect of cardiac function. We next evaluated the effects of exogenous G1 on the energy metabolism in isolated hearts in response to I/R. The control group exhibited poor recovery of energy metabolism at the end of reperfusion. A dramatic decrease in myocardial ATP to 31% of the initial content was accompanied by a reduction of adenine nucleotide pool (Σ AN) and adenylate energy charge (AEC) by 45 and 33%, respectively, as compared to steady state values (Figure 5A-5B). Myocardial phosphocreatine (PCr) recovery was about 52% of the initial value, total creatine pool (Σ Cr) was significantly reduced by 15%, while myocardial lactate content was almost 5 times higher than steady state value (Figure 5C-5D). Pre- or postischemic infusion of G1 significantly enhanced restoration of ATP, Σ AN and increased AEC in reperfused hearts compared with control. These effects were combined with a significant increase in PCr recovery, better preservation of Σ Cr and a substantial reduction in myocardial lactate content. Recovery of metabolic state in the G1-R group was more effective than in the G1-I group. G1 infusion after ischemia improved preservation of ATP, Σ AN and PCr, and reduced lactate accumulation in myocardial tissue at the end of reperfusion in comparison with effects

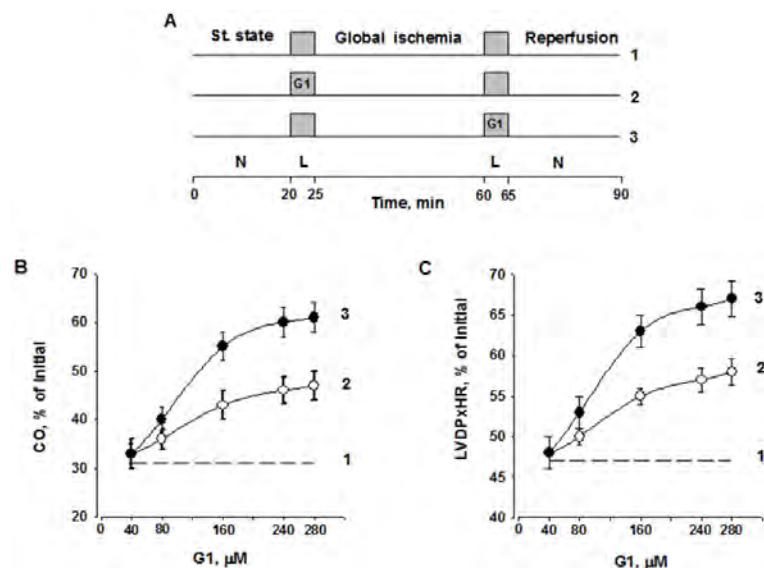


Figure 4: Dose-dependent effect of G1 infusion on functional recovery of isolated rat heart at the end of reperfusion. A. Study design including three groups: 1 - Control; 2 - G1 infusion before ischemia; 3 - G1 infusion after ischemia; L - a 5-min Langendorff perfusion at a flow rate of 4 ml/min before or after ischemia; N - a working perfusion according to a method of Neely. **B.** Effects of peptide G1 on cardiac output (CO) recovery at the end of reperfusion. **C.** Effects of peptide G1 on the contractile function intensity index (left ventricular developed pressure (LVDp) \times heart rate (HR)) recovery at the end of reperfusion. The values are expressed as means \pm SEM from 8 experiments.

Table 1: Effect of infusion of 240 μ M G1 before (G1-I) and after global ischemia (G1-R) on recovery of isolated rat hearts at the end of reperfusion

	Steady state	Control	G1-R	G1-I	Vehicle
Coronary flow, ml/min	17 \pm 2	13 \pm 1 ^a	16 \pm 1 ^b	14 \pm 1	13 \pm 1 ^a
Perfusion pressure, mmHg	62 \pm 4	58 \pm 1	60 \pm 1	59 \pm 1	58 \pm 1
Coronary resistance, mmHg/ml	3.62 \pm 0.03	4.46 \pm 0.07 ^a	3.95 \pm 0.10 ^{abc}	4.20 \pm 0.13 ^a	4.45 \pm 0.13 ^a
LV systolic pressure, mmHg	98 \pm 3	69 \pm 1 ^a	85 \pm 2 ^{abc}	76 \pm 3 ^{ab}	69 \pm 2 ^a
LV diastolic pressure, mmHg	-3 \pm 1	10 \pm 1 ^a	3 \pm 1 ^{abc}	6 \pm 1 ^{ab}	10 \pm 1 ^{ac}
LV developed pressure, mm Hg	101 \pm 1	59 \pm 2 ^a	82 \pm 3 ^{ac}	70 \pm 4 ^{ab}	59 \pm 3 ^a
Heart rate, beat/min	301 \pm 2	238 \pm 3 ^a	272 \pm 5 ^{abc}	254 \pm 6 ^{ab}	238 \pm 5 ^a
LVDP x HR, mmHg/min	30380 \pm 373	14186 \pm 525 ^a	22318 \pm 1270 ^{abc}	17812 \pm 1309 ^{ab}	14052 \pm 969 ^{ac}
Aortic output, ml/min	26 \pm 3	0 \pm 1 ^a	14 \pm 1 ^{abc}	7 \pm 1 ^{ab}	0 \pm 1 ^{ac}
Cardiac output, ml	43 \pm 2	13 \pm 1 ^a	29 \pm 2 ^{abc}	21 \pm 2 ^{ab}	13 \pm 1 ^{ac}
Stroke volume, μl	144 \pm 1	54 \pm 4 ^a	106 \pm 6 ^{abc}	81 \pm 8 ^{ab}	53 \pm 5 ^{ac}

The hearts were perfused as indicated in Materials and methods. Data are the mean \pm SEM for 10 experiments. ^a p<0.05 vs. steady state; ^b p<0.05 vs. control and vehicle; ^c p<0.05 vs. G1-I.

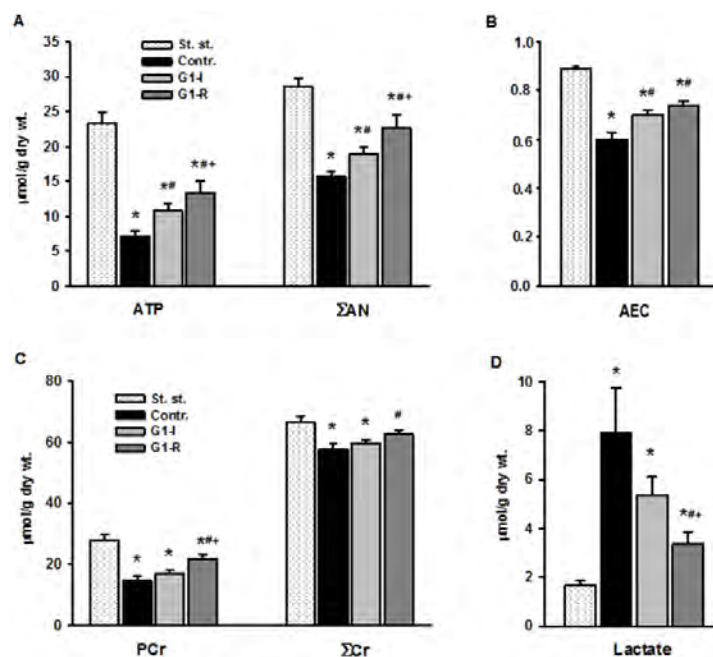


Figure 5: Effects of G1 infusion on metabolic state of isolated rat heart at the end of reperfusion. St. - steady state; Contr. - control; G1-I - peptide infusion at the dose of 240 μ M before ischemia; G1-R - peptide infusion at the dose of 240 μ M after ischemia. **A.** Pre- or postischemic infusion of G1 improved recovery of myocardial ATP and adenine nucleotide pool (Σ AN) = (ATP+ADP+AMP) and **B.** adenylate energy charge (AEC) = (ATP+0.5ADP)/ Σ AN at the end of reperfusion. **C.** Infusion of G1 increased recovery of myocardial phosphocreatine (PCr), total creatine (Σ Cr) = (PCr+Cr) and **D.** reduced myocardial lactate accumulation. Values are the means \pm SEM from 8 experiments. *P < 0.05 vs. steady state; #P < 0.05 vs control, +P < 0.05 vs G1-I.

Table 2: Effects of G1 administration on systemic hemodynamic variables in anesthetized rats *in vivo*

Group	Steady state	LAD reperfusion	
		1-2 min	60 min
SAP, mm Hg			
Control	86 ± 3	85 ± 2	86 ± 3
G1-0.4	82 ± 2	63 ± 2 ^{a b}	81 ± 4
G1-0.7	84 ± 2	64 ± 2 ^{a b}	83 ± 2
G1-1.3	89 ± 3	69 ± 3 ^{a b}	87 ± 2
HR, beats /min			
Control	334 ± 5	331 ± 4	332 ± 4
G1-0.4	338 ± 6	314 ± 7 ^{a b}	337 ± 7
G1-0.7	329 ± 5	306 ± 6 ^{a b}	330 ± 5
G1-1.3	332 ± 4	246 ± 4 ^{a b c d}	327 ± 6

G1 was administrated by i.v. bolus injection at the onset of reperfusion at doses of 0.4; 0.7 or 1.3 $\mu\text{mol/kg}$ (groups G1-0.4, G1-0.7 or G1-1.3, respectively). An equal volume of saline was injected in control. Values are expressed as mean ± SEM for 12 experiments. Significant difference ($P < 0.05$) from: ^a steady state; ^b control; ^c G1-0.4; ^d G1-0.7.

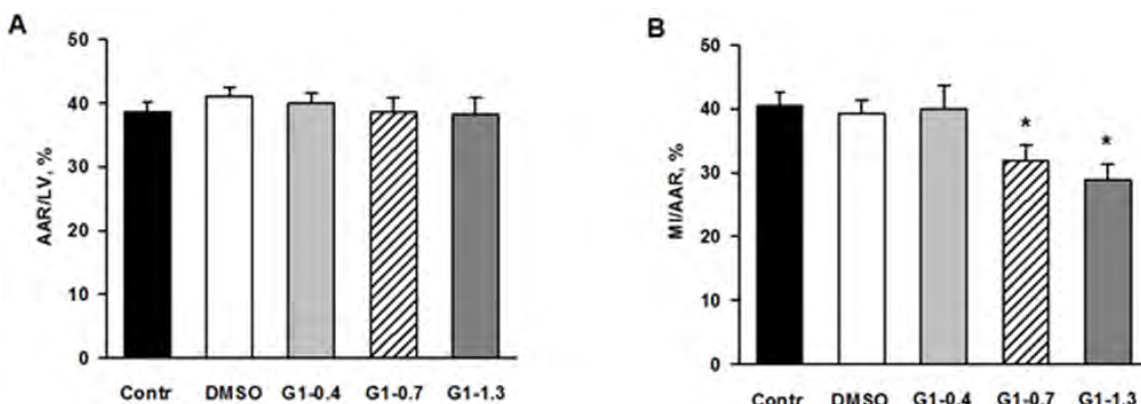


Figure 6: Effects of G1 on myocardial infarct size and area at risk in rats *in vivo*. Dose-dependent effects of peptide G1 on **A.** area at risk (AAR) and **B.** myocardial infarct size. AAR was expressed as percentage of the left ventricular weight (AAR/LV, %) and myocardial infarct size (MI) was expressed as percentage of the AAR (MI/AAR, %). Control - i.v. bolus injection of 0.5 ml of saline; DMSO - i.v. bolus injection of 0.5% DMSO in saline; G1- i.v. bolus injection of peptide G1 at dose of 0.4, 0.7 or 1.3 $\mu\text{mol/kg}$. Values are the means ± SEM from 8 experiments. * $P < 0.05$ vs control.

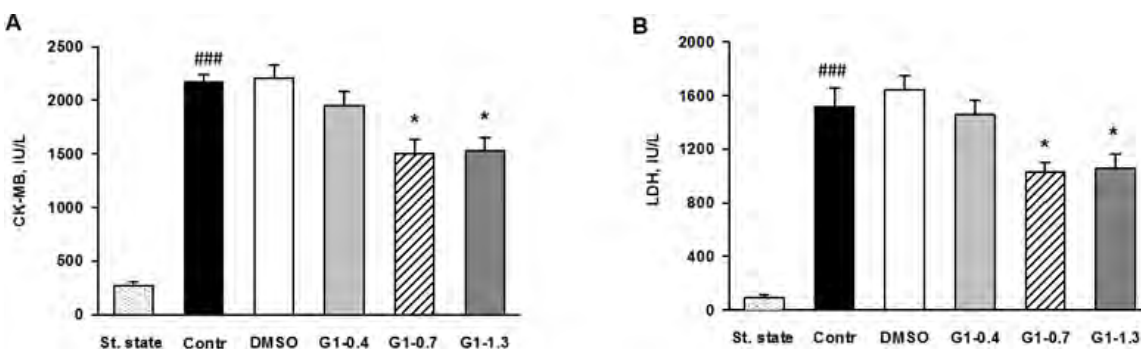


Figure 7: Effects of G1 on plasma level of necrosis markers in rats *in vivo*. Dose-dependent effects of peptide G1 on **A.** activity of creatine kinase-MB (CK-MB) and **B.** lactate dehydrogenase (LDH) in blood plasma. St. state - steady state; Control - i.v. bolus injection of 0.5 ml of saline; DMSO - i.v. bolus injection of 0.5% DMSO in saline; G1- i.v. bolus injection of peptide G1 at dose of 0.4, 0.7 or 1.3 $\mu\text{mol/kg}$. Values are the means ± SEM from 8 experiments. * $P < 0.05$ vs Control; *** $P < 0.001$ vs St. state.

of preischemic peptide infusion. Thus, the experiments on perfused rat hearts clearly demonstrated metabolic and functional advantages of postischemic infusion with G1 over its administration prior to ischemia.

The cardioprotective effects of exogenous G1 in anesthetized rats *in vivo*

In the steady state, there were no differences in the systolic arterial pressure (SAP) or HR between the groups (Table 2). Bolus injection of saline after the period of left anterior descending (LAD) coronary artery occlusion did not affect SAP and HR during reperfusion in control. Treatment with G1 at a dose of 0.4, 0.7 or 1.3 $\mu\text{mol}/\text{kg}$ resulted in a fall in SAP (on average by 23 \pm 4% of the initial value at the second min of reperfusion). By the end of reperfusion, SAP recovered to near baseline (98 \pm 4%). A slight decrease in HR on average by 7 \pm 1% from baseline was observed in groups G1-0.4 and G1-0.7 at the first minute of reperfusion. It was accompanied by complete restoration of HR by the end of reperfusion. Similar hemodynamic changes were observed when G1 was administrated at a dose of 0.4 and 0.7 $\mu\text{mol}/\text{kg}$ in sham-operated animals. In the G1-1.3 group, HR reduced to 73 \pm 6% of the initial value at the first min of reperfusion and returned to baseline by the end of reperfusion. G1 administration at dose of 2.0 or 2.7 $\mu\text{mol}/\text{kg}$ caused a pronounced bradycardia up to 200 and 100 beats/min, respectively and was accompanied by a sharp drop in SAP by 50 and 80%, respectively, followed by gain of bradycardia.

We evaluated effects of G1 administration at doses of 0.4; 0.7 and 1.3 $\mu\text{mol}/\text{kg}$ on myocardial infarct size and cell membrane damage. The percentage ratios of area at risk to LV weight (AAR/LV, %) were similar among G1-0.4, G1-0.7 and G1-1.3 groups and did not differ significantly from the values in control and the vehicle group (Figure 6A). Treatment with G1 at a dose of 0.4 $\mu\text{mol}/\text{kg}$ or the vehicle alone did not affect the percentage ratio of myocardial infarction/area at risk (MI/AAR, %) compare with control and the vehicle group. Administration of G1 at a dose of 0.7 or 1.3 $\mu\text{mol}/\text{kg}$ significantly reduced the percentage ratio of MI/AAR (on average by 25% compared with the value in control) thus indicating limitation of infarct size (Figure 6B). In addition, we analyzed the effects of G1 on plasma level of myocardial damage markers. In the steady state, plasma CK-MB and LDH activity of 270.1 \pm 24.2 and 90.3 \pm 15.5 IU/l were respectively observed (Figure 7A-7B). The activity of CK-MB and LDH in blood plasma increased by 8 and 16 times, respectively, by the end of reperfusion in the control animals. Administration of G1 at dose of 0.4 $\mu\text{mol}/\text{kg}$ did not significantly affect the activity of both enzymes compared with control. Treatment with G1 at the dose of 0.7 or 1.3 $\mu\text{mol}/\text{kg}$ reduced the CK-MB and LDH activity compared with the control group suggesting less damage to cell membranes.

DISCUSSION

Galaninergic system has been implicated in diverse higher order physiological functions including cognition, feeding, nociception, mood regulation, and neuroendocrine modulation [18]. The peripheral functional properties of galanin and its receptors have not yet been fully elucidated. One major limitation to delineate the pathophysiological role of galaninergic system is the lack of receptor subtype specific ligands. Numerous studies within the galaninergic system have mainly been focusing on the GalR1 subtype, which therefore is the best-characterized among the three receptors. However, an intense interest has lately been addressed towards the other two receptors, GalR2 and GalR3. The increased attention for GalR2 coincides with the introduction of the GalR2 selective ligand G1, which has lower affinity for GalR3 but does not affect GalR1 [19, 20]. In the present study, we provide the first direct evidence that G1 has potent *in vitro* and *in vivo* cardioprotective activities against I/R-induced myocardial injury. Our data revealed that G1 prevents apoptotic cell death and mitochondrial ROS production under hypoxic stress in cardiomyoblasts. Furthermore, exogenous G1 attenuated cardiac damage, reduced infarct size and improved cardiac function in rat myocardial I/R injury suggesting the potential therapeutic value of G1 in heart diseases.

Compelling evidence has implicated a role for galanin and G1 in neuroprotection. For example, galanin knockout mice show a higher loss of pyramidal neurons in the hippocampus than wild-type mice after peripheral injection of kainic acid, and galanin or galanin (2-11) counteracts cell death induced by glutamate in hippocampal cultures [21, 22]. Our work demonstrates that exogenous G1 improves metabolic recovery of isolated rat heart subjected to I/R injury and cardiomyoblast survival after hypoxia and reoxygenation suggesting that galaninergic system may play an important role in metabolic remodeling of the heart in response to stress. Clinical studies and animal models demonstrate that abnormalities in cardiac energy metabolism are characteristic features of various heart diseases [23, 24]. The present results showing that the pre- or postischemic administrations of G1 improve recovery of myocardial energy status in response to I/R damage suggest that peptide G1 is an important regulator of cardiac metabolism in the failing myocardium. The ability of G1 to preserve energy state of postischemic myocardium may be related to enhanced uptake and utilization of glucose. At the metabolic level, administration of galanin antagonist M35 to diabetic rats reduces insulin sensitivity, decreases GLUT4 content [25], and reduces GLUT4 mRNA expression in the membrane of myocytes and adipocytes [26, 27]. Alterations in glucose utilization in the heart may be a metabolic indicator of progressing chronic heart failure. Indeed, in patients with diabetes and

coronary artery disease, the loss of GLUT4 content in the heart takes place simultaneously with the development of severe heart failure and ischemic cardiomyopathy [28, 29]. Importantly, we show that improvement of myocardial energy metabolism by peptide G1 was associated with the preservation of contractile function in isolated rat heart after I/R injury. In addition, the exogenous administration of peptide G1 at the onset of reperfusion reduced infarct size and plasma levels of necrosis markers in rats subjected to I/R suggesting a beneficial role for peptide G1 in limiting myocardial ischemic injury. This is the first demonstration of a cardioprotective activity of peptide G1. Compared to the more selective synthetic GalR2 agonists M1153 and M1145 [12, 30], the main advantages of G1 are better solubility, the simplicity of chemical structure and the fact that this peptide is a fragment of natural galanin.

Recent findings indicate that changes in mitochondrial ROS production could be relevant in cardiovascular pathophysiology, as such alterations may have an impact on cellular fate decisions [24]. Excessive ROS generation in mitochondria may provoke a state of oxidative stress, associated with pathophysiological progression in heart ischemic diseases. The intracellular changes during ischemia, including accumulation of H⁺ and Ca²⁺ as well as the disruption of mitochondrial membrane potential, lead to the formation of ROS [31]. Furthermore, ROS accumulation directly activates the pathways of stress response, subsequently resulting in activation of apoptosis [32]. The primary ROS generated by mitochondria, as a result of mono-electronic reduction of O₂, is superoxide anion O₂⁻, the precursor of most ROS and a mediator in oxidative chain reactions [33]. In the present study, our results revealed that G1 prevents mitochondrial O₂⁻ formation in living cardiomyoblasts and apoptosis in response to hypoxic stress. These findings suggest that G1 may control oxidative stress status and activation of apoptotic cell death pathways in cardiac cells. One of the principal results of our study is that G1-dependent increased cardiomyoblast survival in response to hypoxic stress was associated with reduced generation of mitochondrial O₂⁻, a mediator in oxidative chain reactions. This association may be related to an increase in enzymatic antioxidant capacity induced by the peptide or to their direct antioxidant actions. Indeed, we have previously demonstrated that some endogenous peptides such as apelin, may exhibit powerful antioxidant properties [34, 35]. Further studies are required to define the potential mechanisms of how G1 inhibits mitochondrial ROS production and cell apoptosis and to identify the precise role of GalR2/GalR3 interactions in these processes.

In conclusion, our data provide the first evidence that the peptide G1 reduces I/R-associated cardiac dysfunction and myocardial damage. These beneficial effects are accompanied by substantial improvement of

myocardial energy state and cell membrane integrity. In addition, we report that in cardiomyoblasts, G1 regulates mitochondrial ROS production and apoptosis in response to hypoxic stress. Taken together, these data collectively indicate that peptide G1 may be a promising new agent for cardioprotection against I/R injury.

MATERIALS AND METHODS

Galanin peptides

The peptide utilized in this study was rat galanin fragment G1 (Supplementary Table 1). Peptide G1 was synthesized by solid-phase method on Rink-amide-resin (Nova BioChem, Switzerland). The synthesis was carried out in automatic mode with Fmoc-(9-fluorenylmethoxycarbonyl)-technology on a peptide synthesizer Tribute-UV (Protein Technologies, Inc., USA). Fmoc amino acids (Nova BioChem, Switzerland) were coupled as 1-hydroxybenzotriazole esters. The peptide was cleaved from the resin using a solution of 95% trifluoroacetic acid, 2.5% triisopropylsilane and 2.5% H₂O for 2 h. The crude product of solid-phase synthesis was purified by preparative reverse-phase HPLC with 98% homogeneity. The synthesized G1 has correct mass-spectrometric ($m/z = 1137.3 [M+H]^+$) and ¹H-NMR characteristics.

Analytical HPLC was performed on a Gilson (France) system using 4.6×250 mm Kromasil-100 5 μm C18 columns (Sweden). Preparative HPLC was performed on a Knauer (Germany) system using Eurosphere octadecylsilyl columns (20 × 250 mm, 10 μm) (Knauer, Germany). Acetonitrile (Panreac, Spain) was used for HPLC. The mass spectra were recorded on a VISION 2000 mass spectrometer (Termobioanalysis corp., Finnigan, United States) with matrix assisted laser desorption ionization time-of-flight (MALDI-TOF) method. ¹H-NMR was performed on WH-500 Bruker 500 MHz (Germany) in DMSO-d6 at 300 K, peptide concentration was 2-3 mg/ml, chemical shifts in ¹H-NMR spectra were measured relative to an internal standard tetramethylsilane.

Reagents

Enzymes and chemicals for *in vivo* experiments were purchased from Sigma Chemical Co. (St Louis, MO USA). Solutions were prepared using deionized water (Millipore Corp. Bedford, MA, USA).

Animals

Male Wistar rats weighing 300 to 340 g were housed in cages in groups of three, maintained at 20–30°C with a natural light-dark cycle. All animals had free access to standard pelleted diet (Aller Petfood, St. Petersburg,

Russia) and tap water. The care and use of the animals were conducted in accordance with the European Convention for the Protection of Vertebrate Animals Used for Experimental and other Scientific Purposes (No 123 of 18 March 1986).

Isolated perfused rat hearts

The isolated heart provides a highly reproducible preparation that can be studied in a time-dependent manner. It allows a broad spectrum of biochemical, physiological, morphological and pharmacological indices to be measured, permitting detailed analysis of ventricular mechanics, metabolism and coronary vascular responses. In principle, two different isolated heart models exist: 1) the isolated heart according to Langendorff (1895), in which hearts are supplied with coronary flow through retrograde perfusion and 2) the working, fluid-ejecting heart, in which hearts are perfused via the left atrium and eject fluid through the left ventricle into the aorta thus perfusing their own coronaries. The present study is designed with a combination of features from both the Langendorff (non-working) and the Neely (working) systems. The working heart performs pressure-volume work, an important distinction from its Langendorff counterpart, which performs energetically less demanding isovolumetric contractions.

Briefly, rats were heparinized (1600 IU/kg body weight, intraperitoneally (i.p.)) and anaesthetized with urethane (1.3 g/kg body weight, i.p.). Hearts were perfused with KHB containing (in mM): NaCl 118, KCl 4.7, CaCl₂ 3.0, Na₂EDTA 0.5, KH₂PO₄ 1.2, MgSO₄ 1.2, NaHCO₃ 25.0 and glucose 11.0. It was oxygenated with a mixture of 95% O₂ and 5% CO₂; pH was 7.4±0.1 at 37°C. KHB was passed through a 5 µm Millipore filter (Bedford, MA, USA) before use. A needle was inserted into the LV cavity to register LV pressure via a Gould Statham P50 transducer, SP 1405 monitor and a Gould Brush SP 2010 recorder (Gould, Oxnard, Ca, USA). The contractile function intensity index was calculated as the LVDP×HR, where LVDP is the difference between LV systolic and LV end-diastolic pressure. Cardiac pump function was assessed by CO, the sum of aortic output and coronary flow as previously described [34].

The steady state values of cardiac function were recorded after preliminary 20-min perfusion in working mode according to a modified method of Neely under constant left atrium pressure and aortic pressure of 20 and 100 cm H₂O, respectively. After the steady state period, the control hearts were perfused in Langendorff mode for 5 min at a constant flow rate of 4 ml/min, and then they were subjected to 35-min normothermic global ischemia followed by 5-min Langendorff perfusion with subsequent 30-min working reperfusion by Neely method (Figure 4A).

In order to provide a successful G1 transport to cardiomyocyte membranes of ischemic heart we had to profoundly increase G1 concentration in KHB compared to cell experiments. Thus, in the G1-I group, 5-min Langendorff perfusion with KHB containing 40, 80, 160, 240 or 280 µM G1 was applied before global ischemia. Further procedure was the same as for the control group. The hearts of the G1-R group were perfused for 5 min with KHB containing 40, 80, 160, 240 or 280 µM G1 in Langendorff mode after global ischemia. Other experimental stages were the same as in control. The final concentration of dimethyl sulfoxide (DMSO) in KHB with peptide G1 was 0.2%. In a separate series of experiments, it was found that 5-min infusion of KHB containing 0.2% DMSO did not affect the recovery of cardiac function after ischemia.

Analysis of metabolites

After preliminary working perfusion (steady state) and at the end of reperfusion, the hearts were freeze-clamped in liquid nitrogen for metabolite analysis. Frozen isolated perfused hearts were quickly homogenized in cooled 6% HClO₄ (10 ml/g) using an Ultra-Turrax T-25 homogenizer (IKA-Labortechnik, Staufen, Germany), and the homogenates were centrifuged at 2800×g for 10 min at 4°C. The supernatants were then neutralized with 5M K₂CO₃ to pH 7.40, and the extracts were centrifuged after cooling to remove KClO₄ precipitate. Tissue dry weights were determined by weighing a portion of the pellets after extraction with 6% HClO₄ and drying overnight at 110°C. Concentrations of ATP, ADP, AMP, PCr, creatine (Cr) and lactate in neutralized tissue extracts were determined by enzymatic methods [36].

In vivo rat model of I/R injury

Rats were anesthetized with 20% urethane (120 mg/kg, i.p.) and artificially ventilated with a KTR-5 animal respirator (Hugo Sacks Electronik) with a volume of 2–3 ml at a rate of 70–75 breaths/min. Further preparation of animals was performed as described earlier [37]. Arterial blood pressure was recorded with a pressure transducer (Statham p23Db, Oxnard, USA) using a polygraph Biograph-4 (St. Petersburg, Russia). The mean arterial pressure, heart rate and standard lead II ECG were recorded on a computer using a LabVIEW 7.1 data acquisition system (National Instruments, USA).

After 30-min stabilization of hemodynamic parameters (steady state), LAD coronary artery was occluded for 40 min to simulate regional ischemia; the duration of subsequent reperfusion was 1 h. In the experimental series, G1 was administrated by i.v. bolus injection at the onset of reperfusion at doses of 0.4; 0.7; 1.3; 2.0 or 2.7 µmol/kg (groups G1-0.4; G1-0.7; G1-1.3; G1-2.0 or G1-2.7, respectively). An equal volume

of saline (0.5 ml) was injected in the control series of experiments. The influence of a vehicle, 0.5% DMSO, on myocardial infarct size was studied in a separate series of experiments. Additionally, effects of i.v. G1 administration on hemodynamic data were evaluated. At the end of experiments, LAD coronary artery was occluded and 2 ml of 2% Evans Blue (Sigma, USA) solution was injected through the jugular vein to distinguish the myocardial non-ischemic area from the AAR.

Determination of myocardial infarct size

After staining with Evans Blue, the heart was excised and the LV was frozen. A frozen LV was transversely cut into 1.5 mm thick slices which were incubated in 0.1 M sodium phosphate buffer pH 7.4, containing 1% 2,3,5-triphenyl-tetrazolium chloride (TTC, Sigma, USA) 10 min at 37°C. The slices were fixed in 10% formalin for 5 min. Then they were placed between two transparent glasses and captured using a scanner at 600 d.p.i. resolution; the saved images were analyzed by computerized planimetry using Imagecal software. The slices were then weighed for determination of LV weight. The AAR was expressed as a percentage of LV weight; MI was expressed as a percentage of the AAR in each group.

Determination of necrosis markers

At the end of the steady state and reperfusion, blood samples were collected for plasma separation. Plasma LDH activity was determined enzymatically with pyruvate as substrate by using standard kits from BioSystems S.A. (Barcelona, Spain). Plasma CK-MB activity was assessed by an immunoinhibition method using standard kits from BioSystems S.A. (Barcelona, Spain) from the rate of nicotinamide adenine dinucleotide phosphate formation by means of the hexokinase and glucose-6-phosphate dehydrogenase coupled reactions.

Cell culture and treatments

Rat ventricular myocardial H9C2 cells were obtained from American Type Culture Collection (Manassas, VA, USA). H9C2 cells at passages 18 to 24 were seeded in 24 or 96-well cell culture plates with Dulbecco's Modified Eagle Medium (Invitrogen, Cergy-Pontoise, France) containing 10% Fetal Bovine Serum (Invitrogen, Cergy Pontoise, France), 100U mL⁻¹ penicillin and 100µg mL⁻¹ streptomycin at 37°C in a humidified atmosphere of 5% CO₂ and were used at less than 80% of confluence.

Measurement of mitochondrial O₂⁻ production

The mitochondrial levels of ROS were determined in H9C2 cells subjected to hypoxia (1% O₂, 5% CO₂) for 16h followed by 4h of reoxygenation (95% O₂, 5% CO₂) using

mitochondrial superoxide indicator (MitoSOX™ red, Life Technologies). Before hypoxia the H9C2 were pretreated with G1 analogue for 20 min. After reoxygenation, cells were washed once with phosphate-buffered saline (PBS) and incubated in 1µM MitoSOX red for 30 min at 37°C followed by three washes with PBS. The fluorescence was then measured at the excitation wavelength of 510 nM and emission wavelength of 580 nM.

Evaluation of apoptosis

The apoptosis level was assessed using the TUNEL system according to manufacturer's instructions (Promega, Madison, WI, USA) as described previously [38]. TUNEL is a general method to detect nuclear DNA fragmentation during apoptosis. TUNEL technique relies on the use of endogenous enzymes that allow the incorporation of labeled nucleotides into the 3'-hydroxyl (3'OH) recessed termini of DNA breaks. The added value in this approach resides in the possibility of evaluating both morphological and staining features in the same sample.

ATP measurement

ATP was measured with the CellTiter-Glo® Luminescent Cell Viability Assay from Promega (Madison, WI). H9C2 cells were seeded at a density of 2 x 10⁵ cells/ml with 100µl per well in a white 96-well plate and allowed to grow for 24h. Before addition of 400µM of H₂O₂ for 4h, H9C2 cells were pretreated for 20min with G1 at the different doses (10, 50 and 250 nM). The cells were equilibrated at room temperature for 30 min and, followed by addition of the CellTiter-Glo® reagents, per manufactured instructions. The luminescence was read after a 10 min incubation of the reagents on the INFINITE F500 on luminescence module (TECAN, Switzerland, Mennedorf) and expressed as mean percentage of control group.

Statistical analysis

Data are presented as means ± SEM. Results were analyzed by one-way ANOVA followed by Bonferroni multiple range test post-hoc analysis for calculation differences between more than two groups. Comparisons between two groups involved use of the Student's unpaired t-test. All statistical analyses were performed using SigmaPlot version 12 (Systat Software Inc, San Jose, CA). A *p* < 0.05 was defined as significant.

ACKNOWLEDGMENTS

This work was supported by grants from the National Institute of Health and Medical Research (INSERM), Région Midi-Pyrénées, ERASMUS

MUNDUS MEDEA project and The Russian Foundation for Basic Research (grant No. 14-04-00012a).

CONFLICTS OF INTEREST

The authors declare no conflicts of interest.

Author contributions

A.T., O.P. and O.K. conceived and designed the study. O.P., I.S., L.S., V.S. and O.V. performed *in vivo* experiments. A.T. and O.K. performed *in vitro* experiments. V.S. and L.S. performed microsurgery procedures on rats. M.S., M.P. and A.M. synthesized and purified the galanin analogue. F.B., A.T., O.P. and O.K. analyzed the data and wrote the paper. H.T., F.B. and M.C. contributed to tools and discussion.

REFERENCES

1. Fang, P.H., M. Yu, Y.P. Ma, J. Li, Y.M. Sui, M.Y. Shi. Central nervous system regulation of food intake and energy expenditure: role of galanin-mediated feeding behavior. *Neurosci Bull*, 2011. 27: p. 407-412.
2. Diaz-Cabiale, Z., C. Parrado, M. Narvaez, C. Millon, A. Puigcerver, K. Fuxe, J.A. Narvaez. Neurochemical modulation of central cardiovascular control: the integrative role of galanin. *EXS*, 2010. 102: p. 113-131.
3. Abbott, S.B., P.M. Pilowsky. Galanin microinjection into rostral ventrolateral medulla of the rat is hypotensive and attenuates sympathetic chemoreflex. *Am J Physiol Regul Integr Comp Physiol*, 2009. 296: p. R1019-1026.
4. Chen, A., M. Li, L. Song, Y. Zhang, Z. Luo, W. Zhang, Y. Chen, B. He. Effects of the Galanin Receptor Antagonist M40 on Cardiac Function and Remodeling in Rats with Heart Failure. *Cardiovasc Ther*, 2015. 33: p. 288-293.
5. He, B., M. Shi, L. Zhang, G. Li, L. Zhang, H. Shao, J. Li, P. Fang, Y. Ma, Q. Shi, Y. Sui. Beneficial effect of galanin on insulin sensitivity in muscle of type 2 diabetic rats. *Physiol Behav*, 2011. 103: p. 284-289.
6. Elliott-Hunt, C.R., F.E. Holmes, D.M. Hartley, S. Perez, E.J. Mufson, D. Wynick. Endogenous galanin protects mouse hippocampal neurons against amyloid toxicity *in vitro* via activation of galanin receptor-2. *J Alzheimers Dis*, 2011. 25: p. 455-462.
7. Habecker, B.A., K.R. Gritman, B.D. Willison, D.M. Van Winkle. Myocardial infarction stimulates galanin expression in cardiac sympathetic neurons. *Neuropeptides*, 2005. 39: p. 89-95.
8. Kocic, I. The influence of the neuropeptide galanin on the contractility and the effective refractory period of guinea-pig heart papillary muscle under normoxic and hypoxic conditions. *J Pharm Pharmacol*, 1998. 50: p. 1361-1364.
9. Lautatzis, M.-E., M. Vrontakis. Profile of Galanin in Embryonic Stem Cells and Tissues. *Embryonic Stem Cells - Basic Biology to Bioengineering*. 2011.
10. Floren, A., T. Land, U. Langel. Galanin receptor subtypes and ligand binding. *Neuropeptides*, 2000. 34: p. 331-337.
11. Lang, R., A.L. Gundlach, B. Kofler. The galanin peptide family: receptor pharmacology, pleiotropic biological actions, and implications in health and disease. *Pharmacol Ther*, 2007. 115: p. 177-207.
12. Langel, U. Galanin receptor ligands. *Springerplus*, 2015. 4: p. L18.
13. Pang, L., T. Hashemi, H.J. Lee, M. Maguire, M.P. Graziano, M. Bayne, B. Hawes, G. Wong, S. Wang. The mouse GalR2 galanin receptor: genomic organization, cDNA cloning, and functional characterization. *J Neurochem*, 1998. 71: p. 2252-2259.
14. Brown, E.M., R.J. MacLeod. Extracellular calcium sensing and extracellular calcium signaling. *Physiol Rev*, 2001. 81: p. 239-297.
15. Webling, K., J. Runesson, A. Lang, I. Saar, B. Kofler, U. Langel. Ala5-galanin (2-11) is a GAL2R specific galanin analogue. *Neuropeptides*, 2016.
16. Mazarati, A., L. Lundstrom, U. Sollenberg, D. Shin, U. Langel, R. Sankar. Regulation of kindling epileptogenesis by hippocampal galanin type 1 and type 2 receptors: The effects of subtype-selective agonists and the role of G-protein-mediated signaling. *J Pharmacol Exp Ther*, 2006. 318: p. 700-708.
17. Zhou, T., C.C. Chuang, L. Zuo. Molecular Characterization of Reactive Oxygen Species in Myocardial Ischemia-Reperfusion Injury. *Biomed Res Int*, 2015. 2015: p. 864946.
18. Gundlach, A.L., T.C. Burazin, J.A. Larm. Distribution, regulation and role of hypothalamic galanin systems: renewed interest in a pleiotropic peptide family. *Clin Exp Pharmacol Physiol*, 2001. 28: p. 100-105.
19. Liu, H.X., P. Brumovsky, R. Schmidt, W. Brown, K. Payza, L. Hodzic, C. Pou, C. Godbout, T. Hokfelt. Receptor subtype-specific pronociceptive and analgesic actions of galanin in the spinal cord: selective actions via GalR1 and GalR2 receptors. *Proc Natl Acad Sci U S A*, 2001. 98: p. 9960-9964.
20. Lu, X., L. Lundstrom, T. Bartfai. Galanin (2-11) binds to GalR3 in transfected cell lines: limitations for pharmacological definition of receptor subtypes. *Neuropeptides*, 2005. 39: p. 165-167.
21. Elliott-Hunt, C.R., B. Marsh, A. Bacon, R. Pope, P. Vanderplank, D. Wynick. Galanin acts as a neuroprotective factor to the hippocampus. *Proc Natl Acad Sci U S A*, 2004. 101: p. 5105-5110.
22. Pirondi, S., M. Fernandez, R. Schmidt, T. Hokfelt, L. Giardino, L. Calza. The galanin-R2 agonist AR-M1896 reduces glutamate toxicity in primary neural hippocampal cells. *J Neurochem*, 2005. 95: p. 821-833.

23. Neubauer, S. The failing heart--an engine out of fuel. *N Engl J Med*, 2007. 356: p. 1140-1151.
24. Parra, V., H. Verdejo, A. del Campo, C. Pennanen, J. Kuzmicic, M. Iglewski, J.A. Hill, B.A. Rothermel, S. Lavandero. The complex interplay between mitochondrial dynamics and cardiac metabolism. *J Bioenerg Biomembr*, 2011. 43: p. 47-51.
25. Fang, P., J. Sun, X. Wang, Z. Zhang, P. Bo, M. Shi. Galanin participates in the functional regulation of the diabetic heart. *Life Sci*, 2013. 92: p. 628-632.
26. Leto, D., A.R. Saltiel. Regulation of glucose transport by insulin: traffic control of GLUT4. *Nat Rev Mol Cell Biol*, 2012. 13: p. 383-396.
27. Guo, L., M. Shi, L. Zhang, G. Li, L. Zhang, H. Shao, P. Fang, Y. Ma, J. Li, Q. Shi, Y. Sui. Galanin antagonist increases insulin resistance by reducing glucose transporter 4 effect in adipocytes of rats. *Gen Comp Endocrinol*, 2011. 173: p. 159-163.
28. Adachi, H., T. Ohno, M. Oguri, S. Oshima, K. Taniguchi. Effect of insulin sensitivity on severity of heart failure. *Diabetes Res Clin Pract*, 2007. 77: p. S258-262.
29. Doehner, W., D. Gathercole, M. Cicoira, A. Krack, A.J. Coats, P.G. Camici, S.D. Anker. Reduced glucose transporter GLUT4 in skeletal muscle predicts insulin resistance in non-diabetic chronic heart failure patients independently of body composition. *Int J Cardiol*, 2010. 138: p. 19-24.
30. Saar, I., J. Runesson, I. McNamara, J. Jary, J.K. Robinson, U. Langel. Novel galanin receptor subtype specific ligands in feeding regulation. *Neurochem Int*, 2011. 58: p. 714-720.
31. Feissner, R.F., J. Skalska, W.E. Gaum, S.S. Sheu. Crosstalk signaling between mitochondrial Ca²⁺ and ROS. *Front Biosci (Landmark Ed)*, 2009. 14: p. 1197-1218.
32. Simon, H.U., A. Haj-Yehia, F. Levi-Schaffer. Role of reactive oxygen species (ROS) in apoptosis induction. *Apoptosis*, 2000. 5: p. 415-418.
33. Turrens, J.F. Mitochondrial formation of reactive oxygen species. *J Physiol*, 2003. 552: p. 335-344.
34. Pisarenko, O.I., V.Z. Lankin, G.G. Konovalova, L.I. Serebryakova, V.S. Shulzhenko, A.A. Timoshin, O.V. Tskitishvili, Y.A. Pelogeykina, I.M. Studneva. Apelin-12 and its structural analog enhance antioxidant defense in experimental myocardial ischemia and reperfusion. *Mol Cell Biochem*, 2014. 391: p. 241-250.
35. Foussal, C., O. Lairez, D. Calise, A. Pathak, C. Guilbeau-Frugier, P. Valet, A. Parini, O. Kunduzova. Activation of catalase by apelin prevents oxidative stress-linked cardiac hypertrophy. *FEBS Lett*, 2010. 584: p. 2363-2370.
36. Bergmeyer, H.U. Methods of enzymatic analysis. Academic Press, 1974: p. 1464-1467; 1772-1776; 1777-1781; 2127-2131.
37. Pisarenko, O.I., V.S. Shulzhenko, I.M. Studneva, L.I. Serebryakova, Y.A. Pelogeykina, O.M. Veselova. Signaling pathways of a structural analogue of apelin-12 involved in myocardial protection against ischemia/reperfusion injury. *Peptides*, 2015. 73: p. 67-76.
38. Pchejetski, D., C. Foussal, C. Alfarano, O. Lairez, D. Calise, C. Guilbeau-Frugier, S. Schaak, M.H. Seguelas, E. Wanecq, P. Valet, A. Parini, O. Kunduzova. Apelin prevents cardiac fibroblast activation and collagen production through inhibition of sphingosine kinase 1. *Eur Heart J*, 2012. 33: p. 2360-2369.

Article 2: Cardioprotective properties of N-terminal galanin fragment (2-15) in experimental ischemia and reperfusion

AVANT PROPOS

Plus récemment, en collaboration avec l'équipe de Dr. Pisarenko Oleg de l'Institut de Cardiologie de Moscou, Russie, nous avons « designé » et synthétisé un nouveau peptide court dérivé de l'extrémité N-terminale de la Galanine, le Gal 2-15 (G3) et nous avons décidé d'étudier l'implication de ce peptide dans le processus de remodelage cardiaque suite à une I/R myocardique.

Par des approches *in vivo*, *ex vivo* et *in vitro* nous avons montré que le peptide G3 joue un rôle majeur dans le contrôle du remodelage cardiaque au niveau cellulaire et tissulaire dans un contexte physiopathologique. Les résultats de cette étude ont mis en évidence que le G3 est capable de préserver le statut énergétique du myocarde et d'améliorer la récupération cardiaque post-ischémique. De plus le traitement par G3 contrôle la production de ROS au niveau de la mitochondrie et prévient les lésions myocardiques au cours de l'I/R cardiaque.

Ces résultats ont été publiés dans le journal Oncotarget (2017).

Cardioprotective properties of N-terminal galanin fragment (2-15) in experimental ischemia/reperfusion injury

Oleg Pisarenko^{1,*}, Andrei Timotin^{2,3,*}, Maria Sidorova¹, Irina Studneva¹, Valentin Shulzhenko¹, Marina Palkeeva¹, Larisa Serebryakova¹, Aleksander Molokoedov¹, Oksana Veselova¹, Mathieu Cinato^{2,3}, Frederic Boal^{2,3}, Helene Tronchere^{2,3} and Oksana Kunduzova^{2,3,*}

¹Russian Cardiology Research and Production Complex, Moscow, Russian Federation

²National Institute of Health and Medical Research (INSERM) U1048, Toulouse, France

³University of Toulouse, UPS, Institute of Metabolic and Cardiovascular Diseases, Toulouse, France

*These authors have contributed equally to this work

Correspondence to: Oksana Kunduzova, email: Oxana.Koundouzova@inserm.fr

Keywords: galanin (2-15); apoptosis; cardiac injury; energy metabolism; oxidative stress

Received: August 02, 2017

Accepted: September 04, 2017

Published: October 05, 2017

Copyright: Pisarenko et al. This is an open-access article distributed under the terms of the Creative Commons Attribution License 3.0 (CC BY 3.0), which permits unrestricted use, distribution, and reproduction in any medium, provided the original author and source are credited.

ABSTRACT

Background and purpose: Galanin is an endogenous peptide involved in diverse physiological functions in the central nervous system including central cardiovascular regulation. The present study was designed to evaluate the potential effects of the short N-terminal galanin fragment 2-15 (G) on cardiac ischemia/reperfusion (I/R) injury.

Experimental Approach: Peptide G was synthesized by the automatic solid phase method and identified by ¹H-NMR spectroscopy and mass spectrometry. Experiments were performed on cultured rat cardiomyoblast (H9C2) cells, isolated perfused working rat hearts and anaesthetized open-chest rats.

Key Results: Cell viability increased significantly after treatment with 10 and 50 nM of G peptide. In hypoxia and reoxygenation conditions, exposure of H9C2 cells to G peptide decreased cell apoptosis and mitochondrial reactive oxygen species (ROS) production. Postischemic infusion of G peptide reduced cell membrane damage and improved functional recovery in isolated hearts during reperfusion. These effects were accompanied by enhanced restoration of myocardial metabolic state. Treatment with G peptide at the onset of reperfusion induced minor changes in hemodynamic variables but significantly reduced infarct size and plasma levels of necrosis markers.

Conclusion and implications: These findings suggest that G peptide is effective in mitigating cardiac I/R injury, thereby providing a rationale for promising tool for the treatment of cardiovascular diseases.

INTRODUCTION

Galanin, a 29/30 amino acid neuropeptide, is widely distributed throughout the central and peripheral nervous system as well as endocrine system, preferentially in brain, hypothalamus, pituitary, and other tissues including the heart. Galaninergic system is involved in multiple

regulatory functions, including central cardiovascular control [1]. The N-terminal fragments of galanin are crucial for its biological activity and the first 15 amino acids are conserved in most species [2], while the C-terminal region (residues 17-29) varies among species and lacks receptor affinity [2]. To date, three galanin receptors (GalR1, GalR2 and GalR3), members of the

GPCR superfamily, have been identified by molecular cloning and pharmacologically characterized [3].

GalR1 and GalR3 activate the intracellular effectors through pertussis toxin (PTX) sensitive Gi/o proteins, which results in the inhibition of adenylyl cyclase activity and a decrease in cAMP in the cytosol that leads to the opening of G protein gated inwardly-rectifying potassium (GIRK) channels [4, 5]. Additionally, GalR1 activation stimulates MAPK activity in a PKC-independent manner by coupling with a G_i-type G-protein via G $\beta\gamma$ subunits [6]. GalR2 triggers PLC activity via G $\alpha_{q/11}$ -proteins, leading to IP3-mediated opening of Ca²⁺-dependent channels and release of Ca²⁺ into the cytoplasm from intracellular stores [7]. GalR2 is also able to activate MAPK through PKC and G α_o -proteins dependent mechanism leading to the downstream PI3K-dependent phosphorylation of Akt resulting in suppression of caspase-3 and caspase-9 activity [8]. GalR2 activation also inhibits forskolin stimulated cAMP production in a PTX-sensitive manner, suggesting the activation of G $\alpha_i\alpha_o$ -proteins [8]. Thus, activation of all galanin receptors can inhibit the formation of the transcription factor cAMP regulatory element binding protein (CREB) [8]. Noteworthy, the activated CREB may inhibit the Rab GTPase-activating protein (AS160), a substrate of Akt and glucose transporter 4 (GLUT4) translocation, thus promoting insulin resistance [9]. The differences in the functional coupling and subsequent signaling activities contribute to the diversity of galanin physiological effects. Although the galanin signaling has been characterized in neuronal cells, carcinoma cells and rat gastrointestinal tract [10], the role of GalR-mediated signaling pathways in the heart is poorly explored.

The cardiovascular effects of galanin and its fragments are complex. These peptides are involved in central cardiovascular control affecting arterial pressure and heart rate (HR). Administration of galanin into the rostral ventrolateral medulla produced a hypotensive effect by reducing the sympathetic vasomotor tone in rats [10]. Intracisternal injections of galanin or its fragments (1–15) and (1–16) produce a transient pressor response followed by a decrease in mean arterial pressure (MAP) which is accompanied by tachycardia in rats [10]. It has been demonstrated that cardiovascular action of galanin occurs by interactions of its receptors with α_2 -adrenergic receptors and angiotensin II receptor type 1 and neuropeptide Y1 receptor subtypes [1]. Infusion of human galanin into male volunteers increased resting HR by decreasing vagal tone and stimulated the release of growth hormone (GH) [11], thus indicating that this peptide is able to modulate GH secretion and vagal control of the heart. Galanin may have a direct action on cardiomyocytes, since all three galanin receptor subtypes are expressed in the heart [5, 12]. However, the available data on the effects of galanin peptides on cardiac function are scanty. In isolated guinea pig papillary muscle galanin exerted a positive inotropic action and prolonged effective

refractory period [13]. These effects may be associated with galanin-induced activation of inwardly rectifying K⁺ channels, in cardiac myocytes [14]. Under hypoxic conditions, galanin may protect the cardiac muscle against contractile disturbances through activation of ATP-sensitive K⁺ channels [13, 14]. The ability of galanin to gate ATP-sensitive K⁺ channels and hyperpolarize membrane potential was also demonstrated in the insulinoma cell line RINm5F [15]. Galanin mRNA levels in cardiac sympathetic neurons and myocardial galanin content are increased one week after cardiac ischemia and reperfusion in rats [16]. The increase in galanin content specifically in the damaged left ventricle is consistent with studies showing that the peptide is transported to regenerating nerve endings after axon damage [16, 17]. In addition, galanin stimulates sensory nerve regeneration and may promote the re-growth of cardiac sensory nerves following ischemia-reperfusion [18, 19]. These observations suggest that galaninergic system plays an important role in the pathophysiology of many diseases at the level of central cardiovascular regulation. However, the peripheral function of galanin and its fragments remains to be determined.

Therefore, we aimed to investigate the effects of G peptide on *in vitro* in H9C2 cardiomyoblast cell line subjected to hypoxia/reoxygenation (H/R), *ex vivo* in isolated perfused rat hearts and *in vivo* in a rat model of I/R injury.

RESULTS

The effects of G on H9C2 cell survival in response to stress

To determine whether G affects cell viability, we examined the dose-dependent effects of the peptide on H₂O₂-induced loss of ATP in H9C2 cells. As shown in Figure 1, cell exposure to 400 μ M H₂O₂ for 4 hours led to a significant reduction of the cell viability compared to control. Dose-response studies revealed that G at the dose of 10 and 50 nM was able to prevent H₂O₂-induced decrease of ATP levels. Next, we examined by TUNEL assay whether G affects apoptotic cell death in response to hypoxic stress. Because 50 nM of G produced approximately a 20 % increase in cardiomyoblast viability, we used this concentration in subsequent experiments. As shown in Figure 2, the exposure of H9C2 cells to hypoxia caused an increase in the number of TUNEL-positive cells as compared to normoxia. However, the treatment of cells with 50 nM G significantly reduced hypoxia-induced apoptosis (Figure 2).

The effects of G on hypoxia-induced mitochondrial ROS production in H9C2 cells

The excessive generation of ROS and impaired cellular metabolism are closely linked to cell death and myocardial

damage [20]. To determine whether G could affect ROS generation, we examined the effects of G on mitochondrial superoxide (O_2^-) production using the MitoSOX Red fluorescent probe. As shown in Figure 3A, 3B, cell exposure to hypoxic stress caused a significant increase in O_2^- production as compared to normoxia. Importantly, treatment of H9C2 cells with 50 nM G markedly prevented hypoxia-induced O_2^- formation (Figure 3).

Effects of exogenous G in isolated rat heart subjected to I/R injury

Infusion of peptide G after global ischemia enhanced recovery of cardiac function during reperfusion

compared with control. A concentration-dependent effect of G on recovery of CO at the end of reperfusion is shown on Figure 4A. The maximal response to G infusion was observed at the concentration of 225 μ M; at higher peptide concentrations CO recovery reduced. A similar effect was obtained for recovery of the index of contractile function intensity expressed as LVDP \times HR product (Figure 4B). Comparison of the main cardiac function indices for 225 μ M G infusion and control is shown in Table 1. In addition to enhanced recovery of CO and LVDP \times HR product, the recovery of LV systolic pressure, aortic output and stroke volume was also significantly higher whereas LV diastolic pressure and coronary resistance were markedly reduced in the G group compared with these

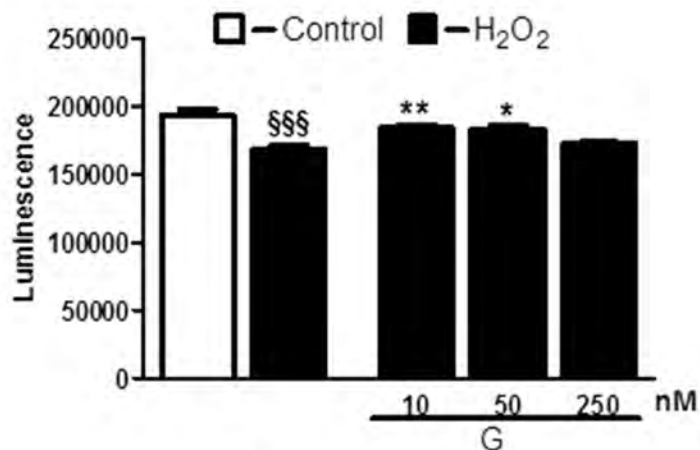


Figure 1: Dose-dependent effect of G on cell viability in response to oxidative stress. Treatment of cardiomyoblasts with G prevents H₂O₂-induced decrease of cell viability in a dose-dependent manner. The H9C2 were pretreated with G (10, 50, 250 nM) for 20 min and then exposed to 400 μ M H₂O₂ for 4 h. Values are the means \pm SEM for three experiments. *P < 0.05 vs H₂O₂ treatment; **P < 0.01 vs H₂O₂ treatment; §§§P < 0.001, vs control.

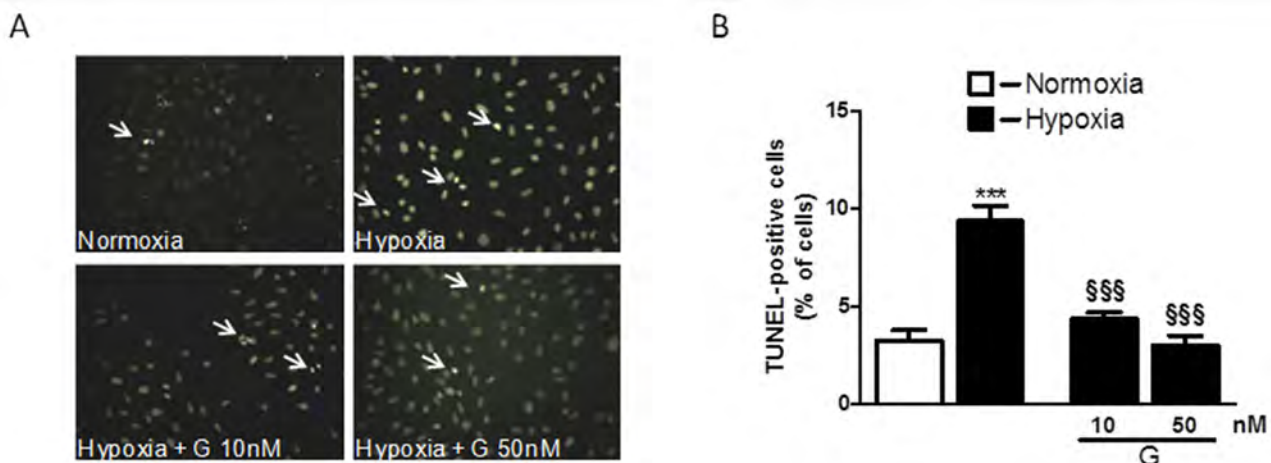


Figure 2: Effect of G on hypoxia-induced cell apoptosis. (A) Representative fluorescence images of H9C2 cells pretreated with 50 nM G for 20 min and then exposed to normoxia or hypoxia-reoxygenation. Apoptosis was measured by TUNEL assay in H9C2 cells after 16 h of hypoxia followed by 3 h of reoxygenation. (B) Quantitative analysis of TUNEL-positive cells in H9C2 cells. The arrows indicate apoptotic cells. Values are the means \pm SEM from three experiments. ***P < 0.001, vs normoxia (C); §§§P < 0.001, vs hypoxia (H).

indices in control. Thus, administration of the optimal concentration of peptide G at the onset of reperfusion caused a pronounced reduction of I/R injury.

We evaluated the effects of 225 μ M G infusion on the energy state of reperfused hearts and LDH leakage during early reperfusion. The hearts of the control group exhibited a poor restoration of high-energy phosphates, significant decrease in the total creatine (Σ Cr) and lactate accumulation in myocardial tissue at the end of reperfusion compared with the steady state (Figure 5). Postischemic G infusion significantly enhanced restoration of ATP, Σ AN and increased adenylate energy charge (AEC) in reperfused hearts compared with control. These effects were combined with a significant increase in PCr recovery, better preservation of Σ Cr and a substantial reduction in myocardial lactate content. LDH leakage in the perfuse before ischemia did not differ significantly between the studied groups (Figure 6A). In control, the release of LDH at early reperfusion increased by more than two-fold compared with the value before ischemia. G infusion significantly decreased LDH leakage compared with control, thus suggesting fewer defects of the sarcolemma. *In vivo* studies on activity of necrosis marker showed that plasma level of CK-MB and LDH increased by 8 and 20 times respectively, at the end of reperfusion in the control animals (Figure 6B, 6C). Administration of G at dose of 0.35 or 2.10 μ mol/kg did not significantly reduce the activity of both enzymes compared with control. However, treatment with G at dose of 0.7 or 1.4 μ mol/kg reduced the CK-MB and LDH activity (on average 1.6 and 1.5-times respectively, compared to the values in the control group). Decrease in the plasma activity of both necrosis markers

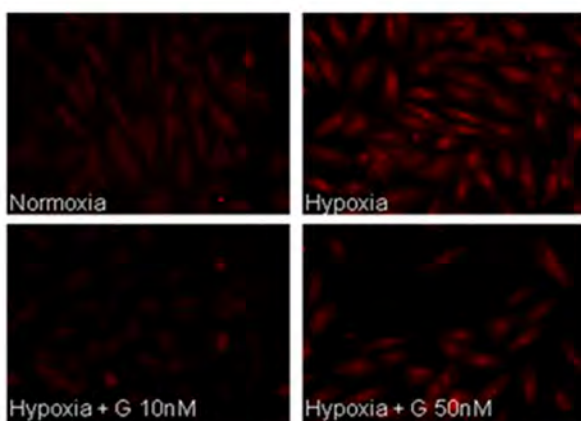
in the group G-1.4 is shown in Figure 6B, 6C. These experiments demonstrated a direct cardioprotective action of exogenous peptide G on the heart after ischemia and reperfusion.

Effects of G administration in rats with myocardial regional ischemia and reperfusion

Changes in hemodynamic variables in rats treated with increasing doses of peptide G are shown in Table 2. Mean systolic arterial pressure (SAP) and heart rate (HR) did not differ significantly between studied groups in the steady state. Bolus injection of saline after the period of LAD coronary artery occlusion did not affect SAP and HR during reperfusion in control. Postischemic administration of any dose of peptide G resulted in a transient rise in SAP followed by its decrease (on average by 10 \pm 1 and 26 \pm 3% of the initial value at the first minutes of reperfusion). By the end of reperfusion, SAP recovered to near baseline (94 \pm 3%). A decrease in HR was observed in all G-treated groups at the first minute of reperfusion (on average by 10 \pm 1% from baseline). Further reperfusion resulted in HR restoration in the groups G-0.35 and G-2.10. In the other two groups, HR decreased on average by 18 \pm 2% of the steady state value. By the end of reperfusion, HR did not differ from baseline values in all G-treated groups.

The percentage ratios of AAR/LV did not differ significantly in all studied groups. AAR/LV in the control group and the mean AAR/LV value in G-treated groups were 39.6 \pm 0.7 and 40.8 \pm 1.0%, respect. Peptide G administration at a dose of 0.35 μ mol/kg did not affect the percentage ratio of MI/AAR compared with control (40.8 \pm 1.3 and

A



B

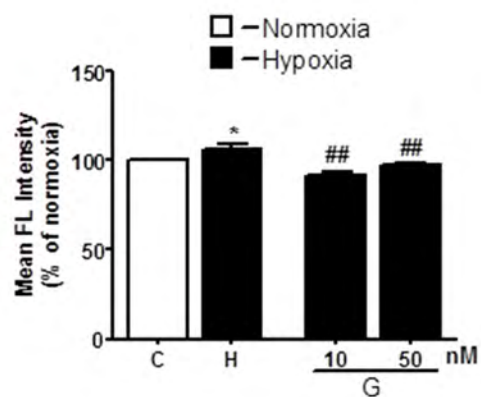


Figure 3: Effect of G on hypoxia-induced mitochondrial O_2^- production. (A) Representative fluorescence images of H9C2 cells pretreated with G peptide. Mitochondrial O_2^- formation was assessed by MitoSOX RED in H9C2 cells exposed to 16h hypoxia followed by 3h of reoxygenation. (B) Quantitative analysis of O_2^- production in H9C2 cells exposed to normoxia or hypoxia-reoxygenation. Values are the means \pm SEM from three experiments. * $P < 0.05$ vs normoxia; ## $P < 0.01$ vs hypoxia.

$40.7 \pm 2.1\%$, respectively) (Figure 7). Administration of the peptide at dose of 0.7 and 1.4 $\mu\text{mol/kg}$ significantly reduced the percentage ratio of MI/AAR (on average by $22 \pm 1\%$ compared with the value in control), thus indicating limitation of infarct size. Infarct size did not significantly differ from control in the group G-2.10.

The results of *in vivo* study showed that i.v. administration of peptide G slightly affected systemic hemodynamic parameters but significantly reduced

irreversible myocardial damage induced by LAD coronary artery occlusion followed by reperfusion.

DISCUSSION

Galanin is involved in regulating numerous of pathological and physiological processes, through interactions with three G-protein-coupled receptors, GalR1-3. Over the past decade, it was shown that both

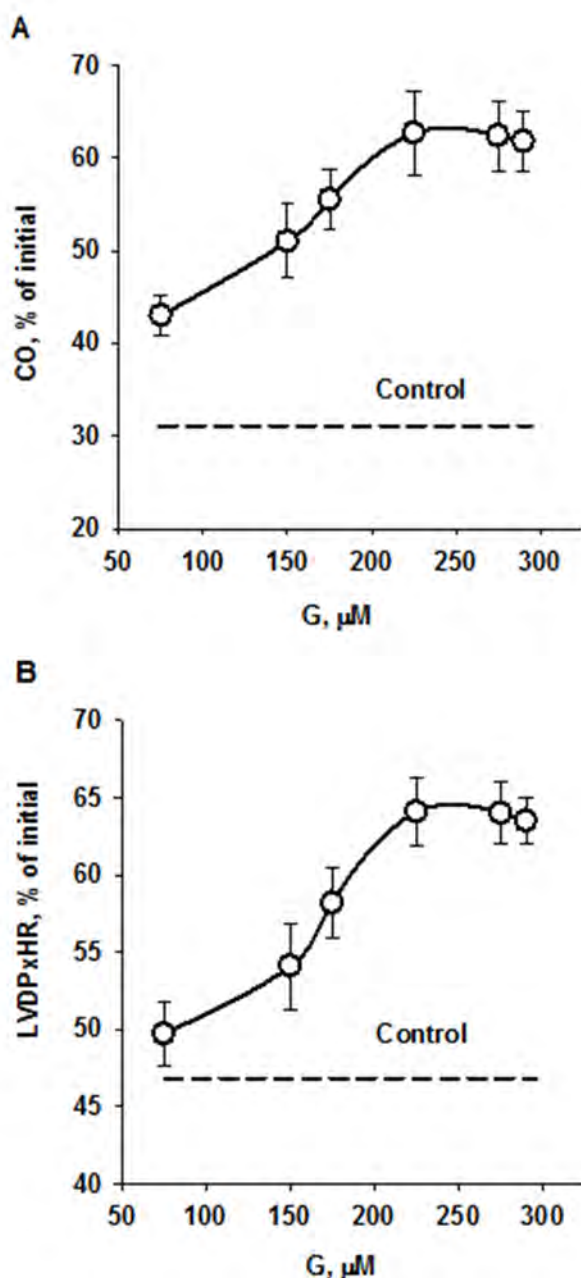


Figure 4: Effects of peptide G concentrations in KHB on recovery of cardiac output (A) and the index of contractile function intensity (B) at the end of reperfusion. Values are means \pm SEM from 8 experiments and are expressed in percentage of the initial value. CO, cardiac output; LVDP \times HR, the index of contractile function intensity. The dotted lines show recovery of the indices in control.

Table 1: Effect of infusion of 225 μ M G after global ischemia on recovery of isolated rat hearts at the end of reperfusion

	Steady state	Control	G
Coronary flow, ml/min	17 \pm 2	13 \pm 1 ^a	15 \pm 1
Perfusion pressure, mmHg	62 \pm 3	58 \pm 1	61 \pm 1
Coronary resistance, mmHg/ml	3.65 \pm 0.03	4.46 \pm 0.07 ^a	4.06 \pm 0.10 ^{ab}
LV systolic pressure, mmHg	98 \pm 3	69 \pm 1 ^a	85 \pm 2 ^{ab}
LV diastolic pressure, mmHg	-3 \pm 1	10 \pm 1 ^a	5 \pm 1 ^{ab}
LV developed pressure, mm Hg	101 \pm 1	59 \pm 2 ^a	80 \pm 3 ^{ab}
Heart rate, beat/min	302 \pm 2	240 \pm 3 ^a	245 \pm 3 ^a
LVDP x HR, mmHg/min	30380 \pm 373	14186 \pm 525 ^a	19474 \pm 643 ^{ab}
Aortic output, ml/min	26 \pm 3	0 \pm 1 ^a	12 \pm 1 ^{ab}
Cardiac output, ml	43 \pm 2	13 \pm 1 ^a	27 \pm 2 ^{ab}
Stroke volume, μ l	142 \pm 1	54 \pm 4 ^a	110 \pm 4 ^{ab}

The hearts were perfused as indicated in Materials and methods. Data are the mean \pm SEM for 8 experiments. ^a P<0.05 vs. steady state; ^b P<0.05 vs. control.

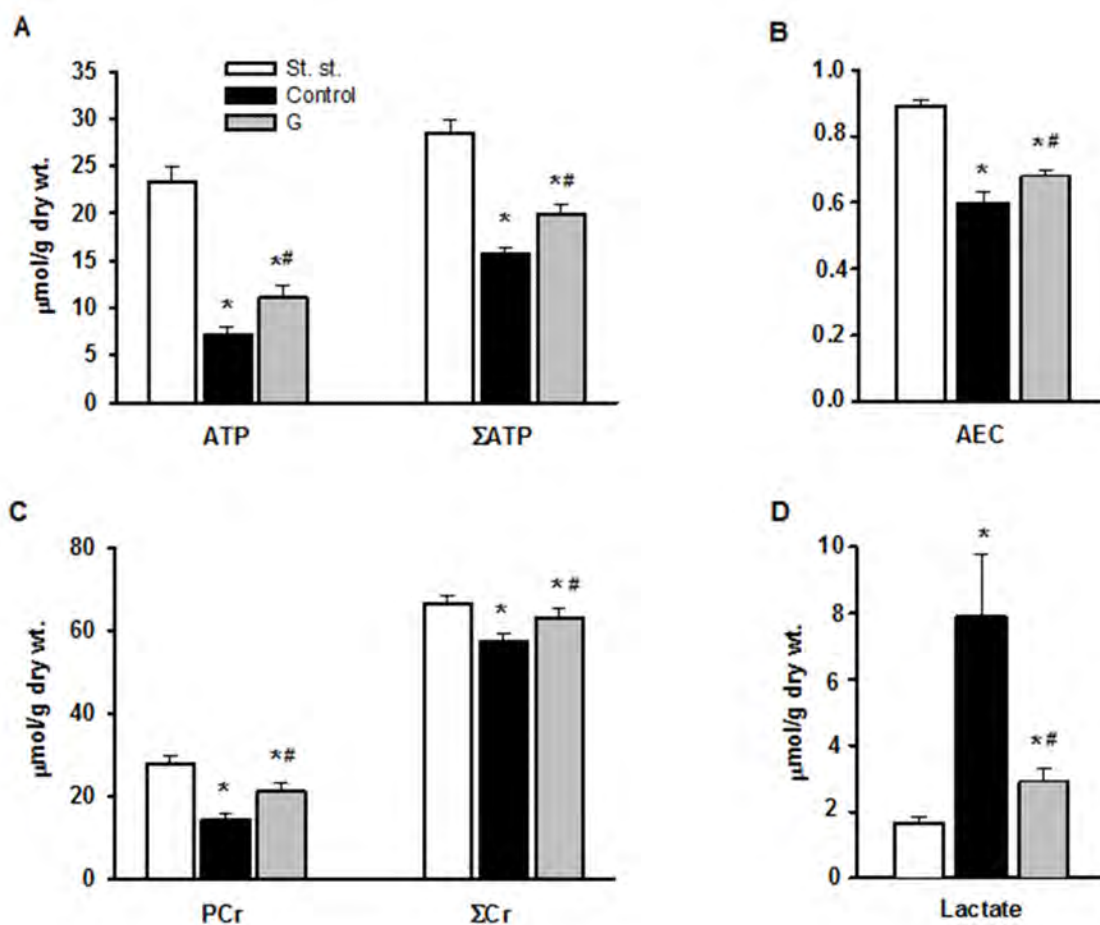


Figure 5: Effect of G infusion on energy state of isolated rat heart at the end of reperfusion. St. st. - steady state; G - 5-min infusion of 225 μ M G after ischemia. (A) Myocardial contents of ATP and Σ AN=ATP+ADP+AMP. (B) Adenylate energy charge (AEC) = (ATP+0.5ADP)/ Σ AN. (C) Myocardial contents of PCr and total creatine Σ Cr=PCr+Cr. (D) Myocardial content of lactate. Values are the means \pm SEM from 8 experiments. *P < 0.05 vs. steady state; **P < 0.05 vs. control.

agonists and antagonists for galanin receptor subtypes can be used as putative therapeutics targets for the treatment of various human diseases. These compounds exhibit an antidepressant and anxiolytic efficacy in animal models, have adhesive and antidepressant properties and may be also useful as potential regulators of feeding behavior and agents for the treatment of Alzheimer's disease [21]. In addition to the complete peptide, several truncated galanin fragments are also biologically active [12]. In the current study, we provide the first *in vitro*, *ex vivo* and *in vivo* evidence that short galanin fragment G reduces I/R-induced injury in the heart. Using live-cell model we show that G prevents mitochondrial ROS production in response to stress. Several lines of evidence suggest that excessive ROS generation in mitochondria may provoke a state of

oxidative stress, associated with pathophysiological progression in heart ischemic diseases [22]. In addition, in cardiomyoblasts exposed to hypoxia, G is able to reduce apoptotic cardiac cell death suggesting that G may control activation of apoptotic cell death pathways and oxidative stress during stressful conditions. These effects may be related to an increase in enzymatic antioxidant capacity induced by the peptide or the antioxidant action. Indeed, we have previously demonstrated that some endogenous peptides such as apelin, may exhibit powerful antioxidant properties [23, 24]. Signaling via GalR1-3 receptors triggers multiple intracellular routes that mimic postconditioning. Unfortunately, the non-selectivity of galanin (2-15) to GalR1-3 receptors excludes more specific suggestions. Undoubtedly, reduction in mitochondrial ROS formation

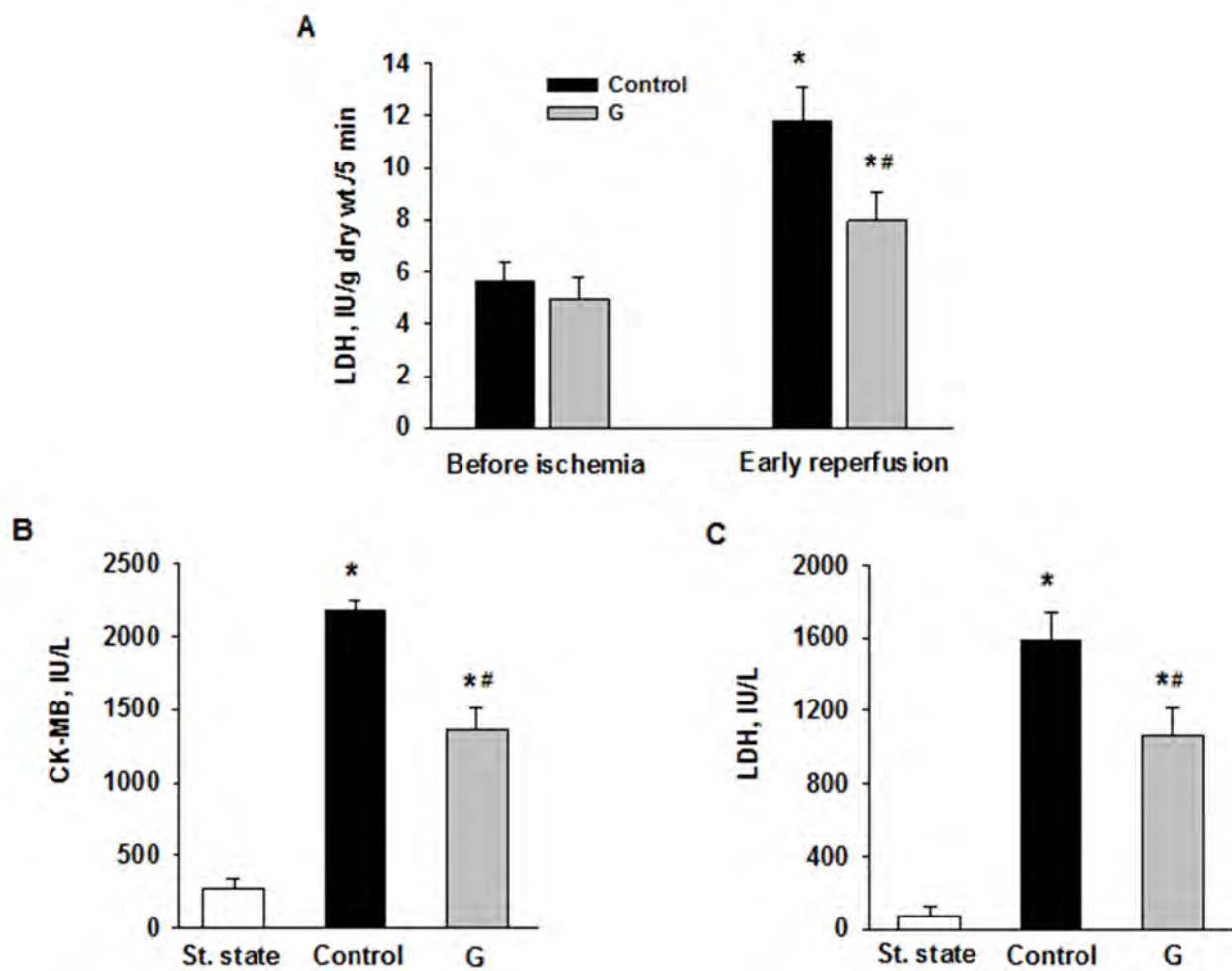


Figure 6: Effects of G administration on necrosis markers in *ex vivo* and *in vivo* models of myocardial I/R injury. (A) LDH release in myocardial effluent from isolated perfused rat heart. Control - postischemic infusion of KHB; G - postischemic infusion of KHB with 225 μ M G. Values are the means \pm SEM of 8 experiments and are expressed in IU/g dry wt. for 5-min Langendorff perfusion before or after global ischemia (early reperfusion). * p<0.05 vs. the value before ischemia; # p<0.05 vs. the value in control. Activities of LDH (B) and CK-MB (C) in blood plasma in rats *in vivo*. St. state - steady state; Control – i.v. administration of saline at the onset of reperfusion; G - i.v. administration of peptide G (1.4 μ mol/kg) at the onset of reperfusion. Values are the means \pm SEM for 8 experiments.* P<0.05 vs. steady state; # P<0.05 vs. control.

Table 2: Effects of i.v. G administration on hemodynamic variables in anesthetized rats *in vivo*

Group	Steady state	LAD reperfusion		
		1-2 min	2-3 min	60 min
SAP, mm Hg				
Control	90 ± 4	88 ± 2	87 ± 2	86 ± 3
G-0.35	86 ± 2	97 ± 3 ^{ab}	73 ± 2 ^{ab}	82 ± 4
G-0.70	87 ± 2	94 ± 2 ^{ab}	71 ± 2 ^{ab}	80 ± 2
G-1.40	89 ± 3	97 ± 3 ^b	76 ± 3 ^{ab}	85 ± 2
G-2.10	85 ± 3	94 ± 3	72 ± 3 ^{ab}	81 ± 3
HR, beats /min				
Control	321 ± 12	315 ± 8	313 ± 8	308 ± 5
G-0.35	312 ± 11	290 ± 7	308 ± 7	296 ± 7
G-0.70	328 ± 9	295 ± 10 ^a	287 ± 9 ^{ab}	302 ± 6
G-1.40	314 ± 10	274 ± 7 ^{ab}	261 ± 7 ^{ab}	292 ± 6
G-2.10	319 ± 12	297 ± 8	328 ± 9	299 ± 9

Peptide G was administrated by i.v. bolus injection at the onset of reperfusion at doses of 0.35, 0.70, 1.40 or 2.10 μmol/kg (groups G-0.35, G-0.70, G-1.40 or G-2.10, respect.). An equal volume of saline was injected in control. Values are expressed as mean ± SEM for 8 experiments. Significant difference ($P < 0.05$) from: ^a steady state; ^b control.

may be one of the operative mechanisms contributing to less cell damage. In addition, galanin-induced cardioprotection is associated with a reduction in infarct size after acute reperfusion. This finding implies the activation of survival kinase pathways that prevents opening of the mPTP. But the functional involvement of these mechanisms can be confirmed only by using

inhibitors of signaling cascades and antioxidants. Exploration of the nature of cardioprotective properties of galanin deserves further expanded research.

A short-term postischemic G infusion caused the concentration-dependent recovery of cardiac function during reperfusion of isolated rat heart. Noteworthy, the optimal peptide concentration effectively restored metabolic state

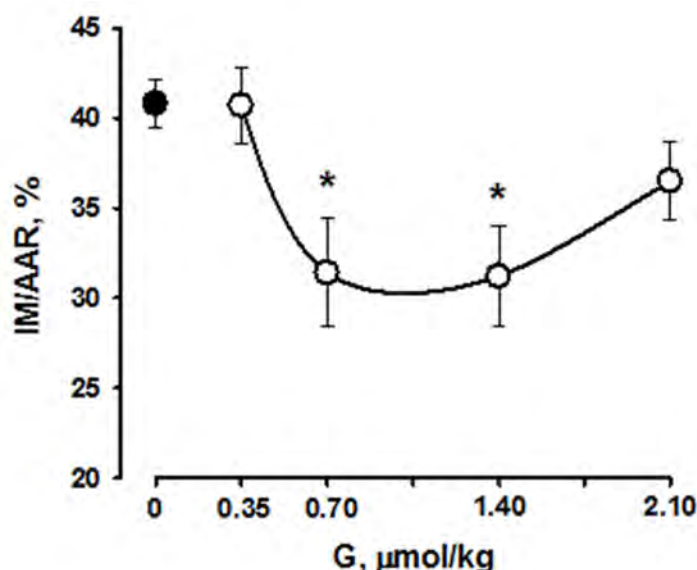


Figure 7: Effects of intravenous G administration on myocardial infarct size (MI/AAR, %) in rats *in vivo*. Black circle corresponds to myocardial infarction in control. Values are means ± SEM from 8 experiments. * $P < 0.05$ vs. control.

of reperfused heart and reduced cell membrane damage. Intravenous injection of G at the onset of reperfusion also exerted the dose-dependent limitation of myocardial infarct size in rats along with the concomitant decrease in activity of necrosis markers in blood plasma. These data suggest, for the first time, that peptide G may act as postconditioning agent effectively reducing reperfusion injury.

Galaninergic system plays an important role in determining the status of cardiovascular system in pathological states. Our findings identify G peptide as a potent protective agent in mitigating metabolic disturbance in the heart. Importantly, the preservation of metabolic status of the myocardium after I/R stress was associated with reduction in infarct size and improvement of cardiac function. Our previous study has demonstrated that galanin fragment (2-11) has a role in regulating biological activity of cardiac cells under stress conditions [20]. At the same time, it is not possible to evaluate the contribution of GalR1, GalR2 and GalR3 receptors to G effects based on the obtained results. Indeed, several of the physiological effects modulated by galanin may be mediated via both GalR2 and GalR3 subtypes activation. GalR2 couples to PLC mediated via $G_{q/11}$ and hence activates the MAPK pathways (ERK) and Akt leading to inhibition of caspase-3 and caspase-9, thus reducing apoptotic cell death [4, 6, 8, 20, 25]. Additionally, PLC activation increases inositol phosphate hydrolysis, mediating the release of Ca^{2+} into the cytoplasm from intracellular stores and opening Ca^{2+} -dependent chloride channels [4, 7, 20]. Signaling via GalR3 coupled to a Gi/o-type G-protein stimulates PTX-sensitive opening of GIRK channels [4, 5, 26]. Lastly, GalR2 and GalR3 activation inhibits the phosphorylation of CREB [4, 6, 27], which leads to GLUT4 translocation from intracellular membrane compartments to plasma membranes to enhance glucose uptake [28, 29]. All these mechanisms are implicated in recovery of cardiac function and reduction of irreversible cardiomyocyte damage in the heart subjected to I/R injury. Therefore, further studies are required to identify the precise role of these receptors in cardioprotective activity of G peptide.

The involvement of galaninergic signaling in a variety of physiological and pathological functions amplify interest in investigation of agonist and antagonists of GalR1-3 receptors for the correction of cardiac disturbances in ischemic heart disease and heart failure. Recently it was shown that the GalR1 antagonist M40 attenuated remodeling and improved cardiac function in a rat model of HF [30]. The beneficial effects of M40 are attributed to suppression of the inhibitory action on the vagal nerve induced by galanin in HF and improvement of the balance of the autonomic nervous system and cardiac function. These data suggest that GalR1 antagonist may be a potential therapeutic agent for HF. On the other hand, our recent studies demonstrate that galanin fragment (2-11) can enhance metabolic and functional tolerance to I/R stress [20]. Although the deletion of the Gly¹

residue results in loss of affinity for GalR1 [31], further delineation of cardioprotective mechanisms against I/R injury requires the development of selective agonists.

In conclusion, by combining *in vitro*, *ex vivo* and *in vivo* approaches, we show that G peptide is effective in mitigating myocardial I/R injury. These data provide the first evidence that G treatment after ischemia improved recovery of cardiac function and reduced infarct size. The preservation of cardiac function by the G was accompanied by restoration of myocardial energy state and cell membrane integrity. In addition, G attenuates mitochondrial ROS production and apoptosis in cardiomyoblasts in response to hypoxic stress. Taken together, these results indicate that peptide G may be a promising tool for the treatment of myocardial I/R damage.

MATERIALS AND METHODS

Galanin (2-15)

Galanin fragment (2-15) H-Trp-Thr-Leu-Asn-Ser-Ala-Gly-Tyr-Leu-Leu-Gly-Pro-His-Ala-OH (G) was synthesized by solid-phase method on a Tribute-UV peptide synthesizer (Protein Technologies Inc., USA) according to standard protocol for condensation of Fmoc-amino acids using *O*-(benzotriazole-1-yl)-1,1,3,3-tetramethyluronium tetrafluoroborate (TBTU). Amino acid side chain functional groups were blocked with the acid labile protecting groups: tert-butoxycarbonyl (Boc) at indole moiety of Trp; tert-butyl (But) at hydroxyl groups of Ser, Thr and Tyr; trityl (Trt) at imidazole ring of His; and at carboxamide function of Asn. Fmoc-Ala-Wang resin (capacity 0.64 mmol/g) was used as the starting material. All amino acids were coupled as active derivatives in a 4-fold excess with the use of the TBTU with addition of N-methylmorpholine coupling method. Cleavage of the Fmoc group was carried out with 25% 4-methylpiperidine in *N,N*-dimethylformamide. After synthesis had been completed, side chain deprotection and cleavage of peptide from a solid support were performed by treatment with a solution containing 90% TFA, 2.5% water, 5% dithiothreitol and 2.5% triisobutylsilane for 1.5 h at 20 °C. The peptide was precipitated with dry diethyl ether. Crude peptide was purified by HPLC. Preparative HPLC was performed on a Knauer (Germany) system using Eurosphere C18 column (20 × 250mm, 10 μm particle size) (Knauer, Germany). The elution was achieved with a linear gradient of acetonitrile (B) in aqueous 0.1% TFA (A) at a flow rate of 10 ml/min with UV detection at 220 nm. Purity of the peptide (96.6%) was checked by an analytical HPLC with Luna 100 C18 (2) column (4.6×250 mm, 5 μm particle size) with linear gradient of acetonitrile in aqueous 0.1% TFA. Peptide structure was confirmed by both ¹H-NMR and mass spectrometry techniques. ¹H-NMR spectra were obtained using a WM-500 spectrometer (Bruker, Germany). Mass-spectrometry

data were obtained using an Ultrafex MALDI TOF/TOF (Bruker Daltonics, Germany) instrument.

Reagents

Fmoc-protected amino acids derivatives were purchased from Novabiochem and Bachem (Switzerland). Chemicals for peptide synthesis were from Fluka (Switzerland). Enzymes and chemicals were purchased from Sigma Chemical Co. (St Louis, MO USA). Solutions were prepared using deionized water (Millipore Corp. Bedford, MA, USA).

Animals

Male Wistar rats weighing 300 to 340 g were housed in cages in groups of three, maintained at 20–30°C with a natural light-dark cycle. All animals had free access to standard pelleted diet (Aller Petfood, St. Petersburg, Russia) and tap water. They were purchased in the Pushchino Nursery for laboratory animals, Russian Academy of Sciences. The care and use of the animals were conducted in accordance with the European Convention for the Protection of Vertebrate Animals Used for Experimental and other Scientific Purposes (No 123 of 18 March 1986).

Isolated perfused rat hearts

Rats were heparinized by intraperitoneal injection (1600 IU/kg body weight) and anaesthetized with urethane (i.p., 1.3 g/kg body weight). Hearts were perfused with Krebs-Henseleit buffer (KHB) supplied with 11 mM glucose. A needle was inserted into the left ventricular (LV) cavity to register LV pressure via a Gould Statham P50 transducer, SP 1405 monitor and a Gould Brush SP 2010 recorder (Gould, Oxnard, Ca, USA). The contractile function intensity index was calculated as the LV developed pressure-heart rate product (LVDP×HR), where LVDP is the difference between LV systolic and LV end-diastolic pressure. Cardiac pump function was assessed by cardiac output (CO), the sum of aortic output and coronary flow [20].

The steady state values of cardiac function were recorded after preliminary 20-min perfusion in working mode according to a modified method of Neely under constant left atrium pressure and aortic pressure of 20 and 100 cm H₂O, respectively. After the steady state period, the control hearts were perfused with KHB in Langendorff mode for 5 min at a constant flow rate of 4 ml/min, and then they were subjected to 35-min normothermic global ischemia followed by 5-min Langendorff reperfusion in the same mode with subsequent 25-min working reperfusion by Neely method. In the G group, 5-min Langendorff reperfusion at a constant flow rate of 4 ml/min with KHB containing 75, 150, 175, 225, 275

or 290 μM G was applied after global ischemia. Other experimental stages were the same as in control. After preliminary working perfusion (steady state) and at the end of reperfusion, the hearts were freeze-clamped in liquid nitrogen for metabolite analysis. The myocardial effluent was collected in ice-cold tubes during both periods of Langendorff perfusion for assessment of LDH activity.

Analysis of metabolites

Frozen tissue of the left ventricle (LV) of the heart was quickly homogenized in cooled 6% HClO₄ (10 ml/g) using an Ultra-Turrax T-25 homogenizer (IKA-Labortechnik, Staufen, Germany), and the homogenates were centrifuged at 2800×g for 10 min at 4°C. The supernatants were then neutralized with 5 M K₂CO₃ to pH 7.40, and the extracts were centrifuged after cooling to remove KClO₄ precipitate. Tissue dry weights were determined by weighing a portion of the pellets after extraction with 6% HClO₄ and drying overnight at 110°C. Concentrations of ATP, ADP, AMP, phosphocreatine (PCr), creatine (Cr) and lactate in neutralized tissue extracts were determined by enzymatic methods [20].

Anesthetized rats *in vivo*

Rats were anesthetized with 20% urethane (120 mg/kg body wt i.p.) and artificially ventilated with a KTR-5 animal respirator (Hugo Sacks Electronik) with a volume of 2–3 ml at a rate of 70–75 breaths/min. Further preparation of animals was performed as described earlier [27]. Arterial blood pressure was recorded with a pressure transducer (Statham p23Db, Oxnard, USA) using a polygraph Biograph-4 (St. Petersburg, Russia). The mean arterial pressure, HR and standard lead II ECG were recorded on a computer using a LabVIEW 7.1 data acquisition system (National Instruments, USA) [20].

In control, after 30-min stabilization of hemodynamic parameters (steady state), LAD coronary artery was occluded for 40 min to simulate regional ischemia; the duration of subsequent reperfusion was 1 h. Prior to intravenous administration, G was dissolved in saline. In the experimental series, G was administrated by i.v. bolus injection at the onset of reperfusion at doses of 0.35, 0.70, 1.40 and 2.1 μmol/kg (groups G-0.35, G-0.7, G-1.4 and G-2.1, respect.) An equal volume of saline (0.5 ml) was injected in control. At the end of experiments, LAD coronary artery was reoccluded and 2 ml of 2% Evans Blue (Sigma, USA) solution was injected through the jugular vein to distinguish the myocardial non-ischemic area from the area at risk (AAR).

Determination of myocardial infarct size

After staining with Evans Blue, the heart was excised and the LV was frozen. A frozen LV was transversely cut into 1.5 mm thick slices which were

incubated in 0.1 M sodium phosphate buffer pH 7.40, containing 1% 2,3,5-triphenyl-tetrazolium chloride (TTC, Sigma, USA) 10 min at 37°C. The slices were fixed in 10% formalin for 5 min. Then they were placed between two transparent glasses and captured on both sides using a scanner at 600 d.p.i. resolution; the saved images were analyzed by computerized planimetry using Imagecal software. The slices were then weighed for determination of LV weight. The AAR was expressed as a percentage of LV weight, myocardial infarction (MI) was expressed as a percentage of the AAR in each group [20].

Determination of necrosis markers

At the end of the steady state and reperfusion, blood samples were collected for plasma separation. Plasma LDH activity was determined enzymatically with pyruvate as substrate by using standard kits from BioSystems S.A. (Barcelona, Spain). Plasma CK-MB activity was assessed by an immunoinhibition method using standard kits from BioSystems S.A. (Barcelona, Spain) from the rate of NADPH formation in the hexokinase and glucose-6-phosphate dehydrogenase coupled reactions.

Cell culture and treatments

Rat ventricular myocardial H9C2 cells were obtained from American Type Culture Collection (Manassas, VA, USA). H9C2 cells at passages 18 to 24 were seeded in 24 or 96-well cell culture plates with Dulbecco's Modified Eagle Medium (Invitrogen, Cergy-Pontoise, France) containing 10% Fetal Bovine Serum (Invitrogen, Cergy Pontoise, France), 100U mL⁻¹ penicillin and 100µg mL⁻¹ streptomycin at 37°C in a humidified atmosphere of 5% CO₂ and were used at less than 80% of confluence.

Measurement of mitochondrial O₂⁻ production

The mitochondrial levels of ROS were determined in H9C2 cells subjected to hypoxia (1% O₂, 5% CO₂, 94% N₂) for 16h followed by 4h of reoxygenation (95% O₂, 5% CO₂) using mitochondrial superoxide indicator (MitoSOX™ red, Life Technologies). Before hypoxia the H9C2 were pretreated with G for 20 min. After reoxygenation, cells were washed once with PBS and incubated in 1µM MitoSOX red for 30 min at 37°C followed by three washes with PBS. The fluorescence was then measured at the excitation wavelength of 510 nM and emission wavelength of 580 nM.

Evaluation of apoptosis

The apoptosis level was assessed using the TUNEL system according to manufacturer's instructions (Promega, Madison, WI, USA) as described previously [22]. TUNEL is a general method to detect nuclear DNA fragmentation during apoptosis. TUNEL technique

relies on the use of endogenous enzymes that allow the incorporation of labeled nucleotides into the 3'-hydroxyl (3'OH) recessed termini of DNA breaks. The added value in this approach resides in the possibility of evaluating both morphological and staining features in the same sample.

ATP measurement

ATP was measured with the CellTiter-Glo® Luminescent Cell Viability Assay from Promega (Madison, WI). H9C2 cells were seeded at a density of 2 x 10⁵ cells/ml with 100 µl per well in a white 96-well plate and allowed to grow for 24 h. Before addition of 400 µM of H₂O₂ for 4 h, H9C2 cells were pretreated for 20 min with G at the different doses (10, 50 and 250 nM). The cells were equilibrated at room temperature for 30 min and, followed by addition of the CellTiter-Glo® reagents, per manufactured instructions. The luminescence was read after a 10 min incubation of the reagents on the INFINITE F500 on luminescence module (TECAN, Switzerland, Mennedorf) and expressed as mean percentage of control group.

Statistical analysis

Data are presented as means ± SEM. Results were analyzed by one-way ANOVA followed by Bonferroni multiple range test post-hoc analysis for calculation differences between more than two groups. Comparisons between two groups involved use of the Student's unpaired t-test. All statistical analyses were performed using SigmaPlot version 12 (Systat Software Inc, San Jose, CA). P < 0.05 was defined as significant. The data and statistical analysis complied with the recommendations on experimental design and analysis in pharmacology [23].

Nomenclature of targets and ligands

Key protein targets and ligands in this article are hyperlinked to corresponding entries in <http://www.guidetopharmacology.org>, the common portal for data from the IUPHAR/BPS.

Abbreviations

- AAR – area at risk
- AEC – adenylate energy charge
- Boc – tert-butoxycarbonyl
- BUT – tert-butyl
- CK-MB – creatine kinase-MB
- CO – cardiac output
- ΣCr – total creatine
- Cr – creatine
- CREB – cAMP responsive element
- G – galanin fragment (2-15)

GAL – galanin
 GalR – galanin receptor (1, 2, 3)
 GH – growth hormone
 GIRK – gated inwardly-rectifying potassium
 GLUT4 – glucose transporter 4
¹H-NMR – proton nuclear magnetic resonance
 HF – heart failure
 H/R – hypoxia/reoxygenation
 HR – heart rate
 I/R – ischemia/reperfusion
 KHB – Krebs-Henseleit buffer
 LAD – left anterior descending artery
 LV – left ventricular
 LVDP – left ventricular developed pressure
 MAP – mean arterial pressure
 MI – myocardial infarction
 PCr – phosphocreatine
 PTX – pertussis toxin
 SAP – systolic arterial pressure
 TBTU – *O*-(benzotriazole-1-yl)-1,1,3,3-tetramethyluronium tetrafluoroborate
 TFA – trifluoroacetic acid
 TTC – 2,3,5-triphenyl-tetrazolium chloride

Author contributions

A.T., O.P. and O.K. conceived and designed the study. O.P., I.S., L.S., V.S. and O.V. performed *in vivo* experiments. A.T. and O.K. performed *in vitro* experiments. V.S. and L.S. performed microsurgery procedures on rats. M.S., M.P. and A.M. synthesized and purified the galanin analogue. A.T., O.P. and O.K. analyzed the data and wrote the paper. H.T., F.B. and M.C. contributed to tools and discussion.

CONFLICTS OF INTEREST

None.

FUNDING

This work was supported by grants from the National Institute of Health and Medical Research (INSERM), Région Midi-Pyrénées, ERASMUS MUNDUS MEDÉA project and The Russian Foundation for Basic Research (grant No. 15-04-00359a).

REFERENCES

- Díaz-Cabiale Z, Parrado C, Narváez M, Millón C, Puigcerver A, Fuxé K, Narváez JA. Neurochemical modulation of central cardiovascular control: the integrative role of galanin. EXS. 2010; 102: 113–31.
- Kakuyama H, Kuwahara A, Mochizuki T, Hoshino M, Yanaihara N. Role of N-terminal active sites of galanin in neurally evoked circular muscle contractions in the guinea-pig ileum. Eur J Pharmacol. 1997; 329: 85–91.
- Branchek TA, Smith KE, Gerald C, Walker MW. Galanin receptor subtypes. Trends Pharmacol Sci. 2000; 21: 109–17.
- Wang S, Hashemi T, Fried S, Clemmons AL, Hawes BE. Differential intracellular signaling of the GalR1 and GalR2 galanin receptor subtypes. Biochemistry. 1998; 37: 6711–7. <https://doi.org/10.1021/bi9728405>.
- Kolakowski LF, O'Neill GP, Howard AD, Broussard SR, Sullivan KA, Feighner SD, Sawzdargo M, Nguyen T, Kargman S, Shiao LL, Hreniuk DL, Tan CP, Evans J, et al. Molecular characterization and expression of cloned human galanin receptors GALR2 and GALR3. J Neurochem. 1998; 71: 2239–51.
- Kim A, Park T. Diet-induced obesity regulates the galanin-mediated signaling cascade in the adipose tissue of mice. Mol Nutr Food Res. 2010; 54: 1361–70. <https://doi.org/10.1002/mnfr.200900317>.
- Smith KE, Forray C, Walker MW, Jones KA, Tamm JA, Bard J, Branchek TA, Linemeyer DL, Gerald C. Expression cloning of a rat hypothalamic galanin receptor coupled to phosphoinositide turnover. J Biol Chem. 1997; 272: 24612–6.
- Elliott-Hunt CR, Pope RJ, Vanderplank P, Wynick D. Activation of the galanin receptor 2 (GalR2) protects the hippocampus from neuronal damage. J Neurochem. 2007; 100: 780–9. <https://doi.org/10.1111/j.1471-4159.2006.04239.x>.
- Langel Ü. Galanin receptor ligands. Springerplus. 2015; 4: L18. <https://doi.org/10.1186/2193-1801-4-S1-L18>.
- Henson BS, Neubig RR, Jang I, Ogawa T, Zhang Z, Carey TE, D'Silva NJ. Galanin receptor 1 has anti-proliferative effects in oral squamous cell carcinoma. J Biol Chem. 2005; 280: 22564–71. <https://doi.org/10.1074/jbc.M414589200>.
- Carey DG, Iismaa TP, Ho KY, Rajkovic IA, Kelly J, Kraegen EW, Ferguson J, Inglis AS, Shine J, Chisholm DJ. Potent effects of human galanin in man: growth hormone secretion and vagal blockade. J Clin Endocrinol Metab. 1993; 77: 90–3. <https://doi.org/10.1210/jcem.77.1.7686918>.
- Wang S, He C, Hashemi T, Bayne M. Cloning and expressional characterization of a novel galanin receptor. Identification of different pharmacophores within galanin for the three galanin receptor subtypes. J Biol Chem. 1997; 272: 31949–52.
- Kocic I. The influence of the neuropeptide galanin on the contractility and the effective refractory period of guinea-pig heart papillary muscle under normoxic and hypoxic conditions. J Pharm Pharmacol. 1998; 50: 1361–4.
- Parsons RL, Merriam LA. Galanin activates an inwardly rectifying potassium conductance in mudpuppy atrial myocytes. Pflugers Arch. 1993; 422: 410–2.
- Dunne MJ, Bullett MJ, Li GD, Wollheim CB, Petersen OH. Galanin activates nucleotide-dependent K⁺ channels in insulin-secreting cells via a pertussis toxin-sensitive G-protein. EMBO J. 1989; 8: 413–20.

16. Ewert TJ, Gritman KR, Bader M, Habecker BA. Post-infarct cardiac sympathetic hyperactivity regulates galanin expression. *Neurosci Lett.* 2008; 436: 163–6. <https://doi.org/10.1016/j.neulet.2008.03.012>.
17. Alston EN, Parrish DC, Hasan W, Tharp K, Pahlmeyer L, Habecker BA. Cardiac ischemia-reperfusion regulates sympathetic neuropeptide expression through gp130-dependent and independent mechanisms. *Neuropeptides.* 2011; 45: 33–42. <https://doi.org/10.1016/j.npep.2010.10.002>.
18. Mahoney SA, Hosking R, Farrant S, Holmes FE, Jacoby AS, Shine J, Iismaa TP, Scott MK, Schmidt R, Wynick D. The second galanin receptor GalR2 plays a key role in neurite outgrowth from adult sensory neurons. *J Neurosci.* 2003; 23: 416–21.
19. Suarez V, Guntinas-Lichius O, Streppel M, Ingorkova S, Grosheva M, Neiss WF, Angelov DN, Klimaschewski L. The axotomy-induced neuropeptides galanin and pituitary adenylate cyclase-activating peptide promote axonal sprouting of primary afferent and cranial motor neurones. *Eur J Neurosci.* 2006; 24: 1555–64. <https://doi.org/10.1111/j.1460-9568.2006.05029.x>.
20. Timotin A, Pisarenko O, Sidorova M, Studneva I, Shulzhenko V, Palkeeva M, Serebryakova L, Molokoedov A, Veselova O, Cinato M, Tronchere H, Boal F, Kunduzova O. Myocardial protection from ischemia/reperfusion injury by exogenous galanin fragment. *Oncotarget.* 2017; 8: 21241–52. <https://doi.org/10.18632/oncotarget.15071>.
21. Lang R, Gundlach AL, Kofler B. The galanin peptide family: receptor pharmacology, pleiotropic biological actions, and implications in health and disease. *Pharmacol Ther.* 2007; 115: 177–207. <https://doi.org/10.1016/j.pharmthera.2007.05.009>.
22. Gao L, Laude K, Cai H. Mitochondrial pathophysiology, reactive oxygen species, and cardiovascular diseases. *Vet Clin North Am Small Anim Pract.* 2008; 38: 137–55. <https://doi.org/10.1016/j.cvsm.2007.10.004>.
23. Foussal C, Lairez O, Calise D, Pathak A, Guilbeau-Frugier C, Valet P, Parini A, Kunduzova O. Activation of catalase by apelin prevents oxidative stress-linked cardiac hypertrophy. *FEBS Lett.* 2010; 584: 2363–70. <https://doi.org/10.1016/j.febslet.2010.04.025>.
24. Pisarenko OI, Lankin VZ, Konovalova GG, Serebryakova LI, Shulzhenko VS, Timoshin AA, Tskitishvili OV, Pelogeykina YA, Studneva IM. Apelin-12 and its structural analog enhance antioxidant defense in experimental myocardial ischemia and reperfusion. *Mol Cell Biochem.* 2014; 391: 241–50. <https://doi.org/10.1007/s11010-014-2008-4>.
25. Borowsky B, Walker MW, Huang LY, Jones KA, Smith KE, Bard J, Branchek TA, Gerald C. Cloning and characterization of the human galanin GALR2 receptor. *Peptides.* 1998; 19: 1771–81.
26. Smith KE, Walker MW, Artymyshyn R, Bard J, Borowsky B, Tamm JA, Yao WJ, Vaysse PJ, Branchek TA, Gerald C, Jones KA. Cloned human and rat galanin GALR3 receptors. Pharmacology and activation of G-protein inwardly rectifying K⁺ channels. *J Biol Chem.* 1998; 273: 23321–6.
27. Badie-Mahdavi H, Lu X, Behrens MM, Bartfai T. Role of galanin receptor 1 and galanin receptor 2 activation in synaptic plasticity associated with 3',5'-cyclic AMP response element-binding protein phosphorylation in the dentate gyrus: studies with a galanin receptor 2 agonist and galanin receptor 1 knockout mice. *Neuroscience.* 2005; 133: 591–604. <https://doi.org/10.1016/j.neuroscience.2005.02.042>.
28. He B, Shi M, Zhang L, Li G, Zhang L, Shao H, Li J, Fang P, Ma Y, Shi Q, Sui Y. Beneficial effect of galanin on insulin sensitivity in muscle of type 2 diabetic rats. *Physiol Behav.* 2011; 103: 284–9. <https://doi.org/10.1016/j.physbeh.2011.02.023>.
29. Fang P, Sun J, Wang X, Zhang Z, Bo P, Shi M. Galanin participates in the functional regulation of the diabetic heart. *Life Sci.* 2013; 92: 628–32. <https://doi.org/10.1016/j.lfs.2013.01.024>.
30. Chen A, Li M, Song L, Zhang Y, Luo Z, Zhang W, Chen Y, He B. Effects of the galanin receptor antagonist M40 on cardiac function and remodeling in rats with heart failure. *Cardiovasc Ther.* 2015; 33: 288–93. <https://doi.org/10.1111/1755-5922.12144>.
31. Liu HX, Brumovsky P, Schmidt R, Brown W, Payza K, Hodzic L, Pou C, Godbout C, Hökfelt T. Receptor subtype-specific pronociceptive and analgesic actions of galanin in the spinal cord: selective actions via GalR1 and GalR2 receptors. *Proc Natl Acad Sci U S A.* 2001; 98: 9960–4. <https://doi.org/10.1073/pnas.161293598>.

VI. DISCUSSIONS ET PERSPECTIVES

Le remodelage cardiaque est considéré comme un déterminant clé de la phase clinique de l'insuffisance cardiaque. Défini comme une expression du génome qui entraîne des changements moléculaires, cellulaires et interstitiels, le remodelage cardiaque est influencé par la charge hémodynamique et l'activation neurohormonale. Au niveau cellulaire le remodelage se traduit par l'hypertrophie des myocytes, la nécrose, l'apoptose et l'activation des fibroblastes.

Certains peptides jouent un rôle crucial dans le contrôle du remodelage cardiaque. Nous avons récemment démontré qu'une altération de l'expression de l'apeline, un nouveau peptide vasoactif, associée à une réponse cellulaire spécifique, participait à la mise en place d'un remodelage cardiométabolique (Pisarenko *et al.*, 2015). Lors de ce travail de thèse, nous avons pu montrer que la galanine, un peptide de 29 acides aminés, pourrait jouer un rôle dans le remodelage du myocarde.

Le système galaninergique est mis en jeu dans le contrôle du comportement, l'alimentation, la nociception, et la modulation neuroendocrine. Les propriétés fonctionnelles périphériques de la galanine et de ses récepteurs n'ont pas encore été entièrement élucidées. Dans le système cardiovasculaire le rôle de la galanine reste peu étudié. Au niveau central l'injection de galanine réduit l'activité cardiovasculaire sympathique produisant une légère hypotension et une tachycardie (Díaz-Cabiale *et al.*, 2005; Abbott and Pilowsky, 2009). Habecker *et al.* ont montré une augmentation du taux de galanine dans le ventricule gauche en dessous de la ligature de l'artère coronaire (Habecker *et al.*, 2005). L'accumulation de galanine spécifiquement dans le ventricule gauche endommagé est compatible avec les rapports précédents montrant que la galanine est transportée à la régénération des terminaisons nerveuses après les dommages aux axones. Plusieurs études ont démontré que la galanine peut réduire la transmission cholinergique dans le cœur (Revington, Potter and McCloskey, 1990; Smith-White, Iismaa and Potter, 2003; Herring *et al.*, 2012). Cependant, le fait que la galanine puisse également cibler les cellules cardiaques, et donc moduler le remodelage cardiaque, n'était pas encore démontré.

La présente étude a permis d'identifier le système galaninergique comme un déterminant clé du remodelage cardiaque dans les phases précoce et tardive. Nos résultats démontrent que parmi les 3 récepteurs de la galanine, GalR2 joue un rôle important lors du remodelage structurel et fonctionnel du myocarde. De plus, dans les cardiomyoblastes, nous

avons observé une augmentation de l'expression de la galanine et de GalR2 en réponse à l'hypoxie. Cette augmentation n'est pas observée pour les récepteurs GalR1 et GalR3.

Les radicaux libres oxygénés jouent un rôle important dans l'initiation des lésions myocardiques après I/R (Hori and Nishida, 2008). Dans le cadre de cette étude, nous avons mis en évidence pour la première fois des activités anti-oxydantes et anti-apoptotiques de la galanine. En effet, nous avons montré que le traitement par la galanine inhibe la formation d' O_2 mitochondrial et de l'apoptose en réponse au stress hypoxique dans les cardiomyoblastes. Ces effets pourraient être associés avec une stimulation de la capacité anti-oxydante enzymatique induite par le peptide. En effet, nous avons récemment démontré que certains peptides endogènes tels que l'apeline peuvent présenter de puissantes propriétés anti-oxydantes (Foussal *et al.*, 2010; Pisarenko *et al.*, 2015). Sur un modèle *in vivo* d'I/R cardiaque chez la souris le traitement par la galanine diminue les lésions tissulaires et préserve l'intégralité ultrastructurelle des mitochondries dans la phase précoce (24h après l'I/R cardiaque). De plus, dans ce même modèle, nous avons confirmé les propriétés anti-oxydantes et anti-apoptotiques de la galanine. Afin d'élucider les mécanismes moléculaires potentiels, nous avons étudié le profil d'expression des facteurs de transcription (FoxO1, FoxO3, Sirt3, Sirt1) qui contrôlent le statut de stress oxydant et métabolique. Parmi ces facteurs, la famille FoxO joue un rôle important dans le contrôle du stress oxydatif et de l'apoptose au niveau cellulaire (Greer and Brunet, 2005). Par des approches *in vitro* et *in vivo*, nous avons identifié un nouveau mécanisme qui pourra être impliqué dans les effets anti-oxydant et anti-apoptotique de la galanine. En effet, nous avons démontré une augmentation de l'expression de FoxO1 après stimulation des cellules cardiaques par la galanine. Par une approche de siRNA, nous avons mis en évidence un nouveau mécanisme de la galanine qui implique la voie FoxO1. Dans un modèle d'I/R cardiaque le traitement des souris par la galanine augmente l'expression de FoxO1 après 24h d'I/R. Ces résultats suggèrent que la galanine peut réguler l'activation de FoxO1 dans les conditions pathologiques. (*Manuscrit en préparation*).

Afin de déterminer le rôle de la galanine dans l'insuffisance cardiaque, nous avons exploré le statut du système galaninergique dans un modèle de constriction transverse de l'aorte (TAC). Dans la phase tardive du remodelage cardiaque, l'accumulation excessive du collagène interstitiel est responsable du développement de la fibrose et de la défaillance cardiaque (Segura, Frazier and Buja, 2014). Au niveau cellulaire, l'activation des fibroblastes est associée à une production massive de collagène et à la sécrétion des facteurs profibrotiques (α SMA, TGF β). Nous avons démontré que le traitement par la galanine diminue la production du collagène induit par le TGF β dans des fibroblastes cardiaques isolés de souris.

De plus, dans un modèle de TAC, nous avons démontré que le traitement chronique par la galanine diminue la fibrose myocardique et améliore la fonction cardiaque altérée par la sténose aortique. (*Manuscrit en préparation*)

En collaborations avec l'équipe de chimistes du Centre de Cardiologie à Moscou, nous avons généré et testé des nouveaux analogues structurels de la galanine: le fragment 1-11 (G1) et le fragment 2-15 (G3). Sur des cellules cardiaques exposées à l'H/R nous avons démontré l'activité inhibitrice puissante des analogues G1 ou G3 contre la formation de ROS mitochondriaux et la mort de cellules par apoptose. Au cours de l'ischémie myocardique aiguë, le manque d'oxygène modifie le métabolisme cellulaire, qui se traduit par l'accumulation de lactate, l'appauvrissement en ATP, la surcharge en $\text{Na}^+ / \text{Ca}^{2+}$ et l'inhibition de la fonction contractile myocardique (Yellon and Hausenloy, 2007; Chen and Zweier, 2014). Dans un modèle d'ischémie *ex-vivo* chez les rats, nous avons pu démontrer que l'administration *i.v.* de G1 ou G3 améliore le statut métabolique du myocarde et le débit cardiaque. En effet, le traitement par G1 ou G3 diminue de manière significative le taux plasmatique de la lactate déshydrogénase et de la créatinine kinase MB. De plus, le traitement avec G1 ou G3 a permis de restaurer les réserves en ATP et en phosphocréatine. Ces données expérimentales indiquent le potentiel thérapeutique des analogues G1 et G3 dans l'atténuation des lésions oxydatives et métaboliques induites par une lésion I/R myocardique. L'ensemble de ces données suggère que le système galaninergique joue un rôle important dans le contrôle de statut métabolique du myocarde au répondeur au stress.

D'autres études sont nécessaires pour définir les mécanismes potentiels de la façon dont la galanine régule le métabolisme cardiaque et le stress oxydant au niveau de la mitochondrie et pour identifier le rôle précis des interactions de la galanine avec le récepteur GalR2 dans ces processus.

CONCLUSIONS

En conclusion, les résultats de cette thèse fournissent la première preuve que le système galaninergique joue un rôle important dans le contrôle du remodelage cardiaque. Dans la phase précoce du remodelage myocardique, la galanine et ses analogues G1 et G3 atténuent la production excessive de ROS mitochondriaux et préservent le statut métabolique dans les modèles *in vitro* (H/R) et *in vivo* (I/R). De plus, nous avons montré qu'une inhibition sélective de la formation de ROS mitochondriaux par des analogues de la galanine est associée à une diminution de la mort cellulaire par l'apoptose, de la nécrose et à l'amélioration de la fonction cardiaque. Ces résultats suggèrent que G1 et G3 peuvent être considérés comme des molécules qui peuvent contre-balancer le stress oxydatif, la perte des cellules cardiaques et les modifications métaboliques lors du remodelage cardiaque.

Dans la phase tardive du remodelage due à une sténose aortique, la galanine prévient l'activation des fibroblastes cardiaques et le développement de la fibrose cardiaque. Ces effets de la galanine sur le remodelage structurel du myocarde ont été associés à l'amélioration de la fonction cardiaque.

Dans la perspective de confirmer le rôle du système galaninergique, nous souhaitons étudier chez la souris les conséquences de la délétion du gène du récepteur à la galanine GalR2 sur le remodelage cardiaque. De plus, le développement de souris galanine KO spécifique dans le cœur nous permettra d'étudier plus précisément le rôle de ce peptide dans un contexte physiopathologique.

BIBLIOGRAPHIE

- Abbott, S. B. G. and Pilowsky, P. M. (2009) 'Galanin microinjection into rostral ventrolateral medulla of the rat is hypotensive and attenuates sympathetic chemoreflex', *American Journal of Physiology - Regulatory, Integrative and Comparative Physiology*, 296(4). Available at: <http://ajpregu.physiology.org/content/296/4/R1019> (Accessed: 3 July 2017).
- Adams, A. C., Clapham, J. C., Wynick, D. and Speakman, J. R. (2008) 'Feeding behaviour in galanin knockout mice supports a role of galanin in fat intake and preference', *Journal of Neuroendocrinology*, 20(2), pp. 199–206. doi: 10.1111/j.1365-2826.2007.01638.x.
- Adeghate, E. and Ponery, A. S. (2001) 'Large Reduction in the Number of Galanin-Immunoreactive Cells in Pancreatic Islets of Diabetic Rats', *Journal of Neuroendocrinology*. Blackwell Science, Ltd, 13(8), pp. 706–710. doi: 10.1046/j.1365-2826.2001.00682.x.
- Ahrén, B. (1990) 'Effects of galanin and calcitonin gene-related peptide on insulin and glucagon secretion in man.', *Acta endocrinologica*. European Society of Endocrinology, 123(6), pp. 591–7. doi: 10.1530/ACTA.0.1230591.
- Ahrén, B., Arkhammar, P., Berggren, P. O. and Nilsson, T. (1986) 'Galanin inhibits glucose-stimulated insulin release by a mechanism involving hyperpolarization and lowering of cytoplasmic free Ca²⁺ concentration', *Biochemical and Biophysical Research Communications*, 140(3), pp. 1059–1063. doi: 10.1016/0006-291X(86)90742-4.
- Ambrosy, A. P., Fonarow, G. C., Butler, J., Chioncel, O., Greene, S. J., Vaduganathan, M., Nodari, S., Lam, C. S. P., Sato, N., Shah, A. N. and Gheorghiade, M. (2014) 'The Global Health and Economic Burden of Hospitalizations for Heart Failure', *Journal of the American College of Cardiology*, 63(12), pp. 1123–1133. doi: 10.1016/j.jacc.2013.11.053.
- AMIRANOFF, B., SERVIN, A. L., ROUYER-FESSARD, C., COUVINEAU, A., TATEMOTO, K. and LABURTHE, M. (1987) 'Galanin Receptors in a Hamster Pancreatic ?-Cell Tumor: Identification and Molecular Characterization', *Endocrinology*, 121(1), pp. 284–289. doi: 10.1210/endo-121-1-284.
- Anversa, P., Beghi, C., Kikkawa, Y. and Olivetti, G. (1986) 'Myocardial infarction in rats. Infarct size, myocyte hypertrophy, and capillary growth', *Circulation Research*, 58(1), pp. 26–37. doi: 10.1161/01.RES.58.1.26.
- Azevedo, P. S., Polegato, B. F., Minicucci, M. F., Paiva, S. A. R. and Zornoff, L. A. M. (2016) 'Cardiac Remodeling: Concepts, Clinical Impact, Pathophysiological Mechanisms and Pharmacologic Treatment', *Arquivos Brasileiros de Cardiologia*. doi: 10.5935/abc.20160005.
- Bailey, K. R. and Crawley, J. N. (2009) 'Galanin and Receptors', in *Encyclopedia of Neuroscience*, pp. 491–498. doi: 10.1016/B978-008045046-9.01441-8.
- Banerjee, R., Henson, B. S., Russo, N., Tsodikov, A. and D'Silva, N. J. (2011) 'Rap1 mediates galanin receptor 2-induced proliferation and survival in squamous cell carcinoma', *Cellular Signalling*, 23(7), pp. 1110–1118. doi: 10.1016/j.cellsig.2011.02.002.
- Barreda-Gómez, G., Lombardero, L., Giralt, M. T., Manuel, I. and Rodríguez-Puertas, R. (2015) 'Effects of galanin subchronic treatment on memory and muscarinic receptors', *Neuroscience*, 293, pp. 23–34. doi: 10.1016/j.neuroscience.2015.02.039.

Barreto, S. G., Bazargan, M., Zotti, M., Hussey, D. J., Sukacheva, O. A., Peiris, H., Leong, M., Keating, D. J., Schloithe, A. C., Carati, C. J., Smith, C., Toouli, J. and Saccone, G. T. P. (2011) 'Galanin receptor 3 - a potential target for acute pancreatitis therapy', *Neurogastroenterology & Motility*, 23(3), pp. e141–e151. doi: 10.1111/j.1365-2982.2010.01662.x.

Bauer, F. E., Zintel, A., Kenny, M. J., Calder, D., Ghatei, M. A. and Bloom, S. R. (1989) 'Inhibitory effect of galanin on postprandial gastrointestinal motility and gut hormone release in humans.', *Gastroenterology*, 97(2), pp. 260–264. Available at: <http://www.ncbi.nlm.nih.gov/pubmed/2472997> (Accessed: 22 June 2017).

Benya, R. V., Matkowskyj, K. A., Danilkovich, A., Marrero, J., Savkovic, S. D. and Hecht, G. (2000) 'Galanin-1 receptor up-regulation mediates the excess colonic fluid production caused by infection with enteric pathogens.', *Nature Medicine*, 6(9), pp. 1048–1051. doi: 10.1038/79563.

Berger, A., Lang, R., Moritz, K., Santic, R., Hermann, A., Sperl, W. and Kofler, B. (2004) 'Galanin Receptor Subtype GalR2 Mediates Apoptosis in SH-SY5Y Neuroblastoma Cells', *Endocrinology*, 145(2), pp. 500–507. doi: 10.1210/en.2003-0649.

Berger, A., Santic, R., Almer, D., Hauser-Kronberger, C., Huemer, M., Humpel, C., Stockhammer, G., Sperl, W. and Kofler, B. (2003) 'Galanin and galanin receptors in human gliomas', *Acta Neuropathologica*. Springer-Verlag, 105(6), pp. 555–560. doi: 10.1007/s00401-003-0680-7.

Berger, A., Santic, R., Hauser-Kronberger, C., Schilling, F. H., Kogner, P., Ratschek, M., Gamper, A., Jones, N., Sperl, W. and Kofler, B. (2005) 'Galanin and galanin receptors in human cancers', *Neuropeptides*, 39(3), pp. 353–359. doi: 10.1016/j.npep.2004.12.016.

Berger, A., Tuechler, C., Almer, D., Kogner, P., Ratschek, M., Kerbl, R., Iismaa, T. P., Jones, N., Sperl, W. and Kofler, B. (2002) 'Elevated Expression of Galanin Receptors in Childhood Neuroblastic Tumors', *Neuroendocrinology*. Karger Publishers, 75(2), pp. 130–138. doi: 10.1159/000048229.

Bhandari, M., Kawamoto, M., Thomas, A. C., Barreto, S. G., Schloithe, A. C., Carati, C. J., Toouli, J. and Saccone, G. T. P. (2011) 'Galanin Receptor Antagonist M35 but Not M40 or C7 Ameliorates Cerulein-Induced Acute Pancreatitis in Mice', *Pancreatology*, 10(6), pp. 682–688. doi: 10.1159/000314603.

Braunwald, E. (2013) 'Heart failure', *JACC: Heart Failure*, pp. 1–20. doi: 10.1016/j.jchf.2012.10.002.

Brooke-Smith, M. E., Carati, C. J., Bhandari, M., Toouli, J. and Saccone, G. T. P. (2008) 'Galanin in the Regulation of Pancreatic Vascular Perfusion', *Pancreas*, 36(3), pp. 267–273. doi: 10.1097/MPA.0b013e31815ac561.

Burazin, T. C. and Gundlach, A. L. (1998) 'Inducible galanin and GalR2 receptor system in motor neuron injury and regeneration', *Journal of Neurochemistry*, 71(2), pp. 879–882. Available at: <http://www.ncbi.nlm.nih.gov/pubmed/9681481%5Cnhttp://onlinelibrary.wiley.com/store/10.1046/j.1471-4159.1998.71020879.x/asset/j.1471-4159.1998.71020879.x.pdf?v=1&t=h3gi222e&s=0bab79b5b80e914844a2324058e3cdc482c4bd4a>.

Burchfield, J. S., Xie, M. and Hill, J. A. (2013) ‘Pathological ventricular remodeling: Mechanisms: Part 1 of 2’, *Circulation*, 128(4), pp. 388–400. doi: 10.1161/CIRCULATIONAHA.113.001878.

Burgevin, M. C., Loquet, I., Quarteronnet, D. and Habert-Ortoli, E. (1995) ‘Cloning, pharmacological characterization, and anatomical distribution of a rat cDNA encoding for a galanin receptor’, *Journal of Molecular Neuroscience*, 6(1), pp. 33–41. doi: 10.1007/BF02736757.

Celi, F., Bini, V., Papi, F., Santilli, E., Ferretti, A., Mencacci, M., Berioli, M. G., De Giorgi, G. and Falorni, A. (2005) ‘Circulating acylated and total ghrelin and galanin in children with insulin-treated type 1 diabetes: Relationship to insulin therapy, metabolic control and pubertal development’, *Clinical Endocrinology*, 63(2), pp. 139–145. doi: 10.1111/j.1365-2265.2005.02313.x.

Chatterjee, K. (2012) ‘Pathophysiology of Systolic and Diastolic Heart Failure’, *Medical Clinics of North America*, 96(5), pp. 891–899. doi: 10.1016/j.mcna.2012.07.001.

Chatterjee, K. and Massie, B. (2007) ‘Systolic and Diastolic Heart Failure: Differences and Similarities’, *Journal of Cardiac Failure*, pp. 569–576. doi: 10.1016/j.cardfail.2007.04.006.

Chen, Y.-R. and Zweier, J. L. (2014) ‘Cardiac mitochondria and reactive oxygen species generation.’, *Circulation research*. NIH Public Access, 114(3), pp. 524–37. doi: 10.1161/CIRCRESAHA.114.300559.

Cheng, S. and Yuan, C.-G. (2007) ‘Differential effect of galanin on proliferation of PC12 and B104 cells’, *NeuroReport*, 18(13), pp. 1379–1383. doi: 10.1097/WNR.0b013e3282c489cc.

Circu, M. L. and Aw, T. Y. (2010) ‘Reactive oxygen species, cellular redox systems, and apoptosis.’, *Free radical biology & medicine*. NIH Public Access, 48(6), pp. 749–62. doi: 10.1016/j.freeradbiomed.2009.12.022.

CLEUTJENS, J., KANDALA, J., GUARDA, E., GUNTAKA, R. and WEBER, K. (1995) ‘Regulation of collagen degradation in the rat myocardium after infarction’, *Journal of Molecular and Cellular Cardiology*, 27(6), pp. 1281–1292. doi: 10.1016/S0022-2828(05)82390-9.

Coelho, E. ., Ferrari, M. F. ., Maximino, J. ., Chadi, G. and Fior-Chadi, D. . (2004) ‘Decreases in the expression of CGRP and galanin mRNA in central and peripheral neurons related to the control of blood pressure following experimental hypertension in rats’, *Brain Research Bulletin*, 64(1), pp. 59–66. doi: 10.1016/j.brainresbull.2004.05.003.

Cohn, J. N., Ferrari, R. and Sharpe, N. (2000) ‘Cardiac remodeling--concepts and clinical implications: a consensus paper from an international forum on cardiac remodeling. Behalf of an International Forum on Cardiac Remodeling’, *Journal of the American College of Cardiology*, 35(3), pp. 569–582. doi: 10.1161/01.CIR.0000155257.33485.6D.

Dallos, A., Kiss, M., Polyanka, H., Dobozy, A., Kemeny, L. and Husz, S. (2006) ‘Galanin receptor expression in cultured human keratinocytes and in normal human skin’, *Journal of the Peripheral Nervous System*, 11(2), pp. 156–164. doi: 10.1111/j.1085-9489.2006.00081.x.

Díaz-Cabiale, Z., Narváez, J. A., Finnman, U. B., Bellido, I., Ogren, S. O. and Fuxé, K. (2000) ‘Galanin-(1-16) modulates 5-HT1A receptors in the ventral limbic cortex of the rat.’, *Neuroreport*, 11(3), pp. 515–9. Available at: <http://www.ncbi.nlm.nih.gov/pubmed/10718306>

(Accessed: 3 July 2017).

Díaz-Cabiale, Z., Parrado, C., Narváez, M., Millón, C., Puigcerver, A., Fuxé, K. and Narváez, J. A. (2010) ‘Neurochemical modulation of central cardiovascular control: the integrative role of galanin.’, *EXS*, 102, pp. 113–31. Available at: <http://www.ncbi.nlm.nih.gov/pubmed/21299065> (Accessed: 3 July 2017).

Díaz-Cabiale, Z., Parrado, C., Vela, C., Razani, H., Coveñas, R., Fuxé, K. and Narváez, J. A. (2005) ‘Role of galanin and galanin(1–15) on central cardiovascular control’, *Neuropeptides*, 39(3), pp. 185–190. doi: 10.1016/j.npep.2004.12.009.

Dickstein, K., Cohen-Solal, A., Filippatos, G., McMurray, J. J. V., Ponikowski, P., Poole-Wilson, P. A., Strømberg, A., Van Veldhuisen, D. J., Atar, D., Hoes, A. W., Keren, A., Mebazaa, A., Nieminen, M., Priori, S. G., Swedberg, K., Vahanian, A., Camm, J., De Caterina, R., Dean, V., Funck-Brentano, C., Hellmans, I., Kristensen, S. D., McGregor, K., Sechtem, U., Silber, S., Tendera, M., Widimsky, P., Zamorano, J. L., Auricchio, A., Bax, J., Böhm, M., Corrao, U., Della Bella, P., Elliott, P. M., Follath, F., Gheorghiade, M., Hasin, Y., Hernborg, A., Jaarsma, T., Komajda, M., Kornowski, R., Piepoli, M., Prendergast, B., Tavazzi, L., Vachiery, J. L., Verheugt, F. W. A. and Zannad, F. (2008) ‘ESC Guidelines for the diagnosis and treatment of acute and chronic heart failure 2008’, *European Heart Journal*, 29(19), pp. 2388–2442. doi: 10.1093/eurheartj/ehn309.

Doenst, T., Nguyen, T. D. and Abel, E. D. (2013) ‘Cardiac metabolism in heart failure: implications beyond ATP production.’, *Circulation research*. NIH Public Access, 113(6), pp. 709–24. doi: 10.1161/CIRCRESAHA.113.300376.

Dunning, B. E. and Ahrén, B. (1992) ‘Reduced Pancreatic Content of the Inhibitory Neurotransmitter Galanin in Genetically Obese , Hyperinsulinemic Mice’, *Pancreas*, 7(2), pp. 233–239. Available at: http://journals.lww.com/pancreasjournal/abstract/1992/03000/reduced_pancreatic_content_of_the_inhibitory.16.aspx (Accessed: 22 June 2017).

Elliott-Hunt, C. R., Holmes, F. E., Hartley, D. M., Perez, S., Mufson, E. J. and Wynick, D. (2011) ‘Endogenous galanin protects mouse hippocampal neurons against amyloid toxicity in vitro via activation of galanin receptor-2.’, *Journal of Alzheimer’s disease : JAD*, 25(3), pp. 455–62. doi: 10.3233/JAD-2011-110011.

Elliott-Hunt, C. R., Marsh, B., Bacon, A., Pope, R., Vanderplank, P. and Wynick, D. (2004) ‘Galanin acts as a neuroprotective factor to the hippocampus’, *Proceedings of the National Academy of Sciences*, 101(14), pp. 5105–5110. doi: 10.1073/pnas.0304823101.

Elliott-Hunt, C. R., Pope, R. J. P., Vanderplank, P. and Wynick, D. (2007) ‘Activation of the galanin receptor?2 (GalR2) protects the hippocampus from neuronal damage’, *Journal of Neurochemistry*, 100(3), pp. 780–789. doi: 10.1111/j.1471-4159.2006.04239.x.

Evans, H. F. and Shine, J. (1991) ‘Human galanin: Molecular cloning reveals a unique structure’, *Endocrinology*, 129(3), pp. 1682–1684. doi: 10.1210/endo-129-3-1682.

Fang, P., Bo, P., Shi, M., Yu, M. and Zhang, Z. (2013) ‘Circulating galanin levels are increased in patients with gestational diabetes mellitus’, *Clinical Biochemistry*, 46(9), pp. 831–833. doi: 10.1016/j.clinbiochem.2012.12.013.

Fang, P., Shi, M., Guo, L., He, B., Wang, Q., Yu, M., Bo, P. and Zhang, Z. (2014) ‘Effect of

endogenous galanin on glucose transporter 4 expression in cardiac muscle of type 2 diabetic rats', *Peptides*, 62, pp. 159–163. doi: 10.1016/j.peptides.2014.10.001.

Fang, P., Yu, M., Gu, X., Shi, M., Zhu, Y., Zhang, Z. and Bo, P. (2017) 'Low levels of plasma galanin in obese subjects with hypertension', *Journal of Endocrinological Investigation*, 40(1), pp. 63–68. doi: 10.1007/s40618-016-0529-2.

Fathi, Z., Battaglino, P. M., Iben, L. G., Li, H., Baker, E., Zhang, D., McGovern, R., Mahle, C. D., Sutherland, G. R., Iismaa, T. P., Dickinson, K. E. . and Antal Zimanyi, I. (1998) 'Molecular characterization, pharmacological properties and chromosomal localization of the human GALR2 galanin receptor', *Molecular Brain Research*, 58(1), pp. 156–169. doi: 10.1016/S0169-328X(98)00116-8.

Fathi, Z., Cunningham, A. M., Iben, L. G., Battaglino, P. B., Ward, S. A., Nichol, K. A., Pine, K. A., Wang, J., Goldstein, M. E., Iismaa, T. P. and Zimanyi, I. A. (1997) 'Cloning, pharmacological characterization and distribution of a novel galanin receptor', *Molecular Brain Research*, 51(1), pp. 49–59. doi: 10.1016/S0169-328X(97)00210-6.

Faure-Virelizier, C., Croix, D., Bouret, S., Prévot, V., Reig, S., Beauvillain, J. C. and Mitchell, V. (1998) 'Effects of estrous cyclicity on the expression of the galanin receptor Gal-R1 in the rat preoptic area: A comparison with the male', *Endocrinology*, 139(10), pp. 4127–4139.

Filippatos, G., Ang, E., Gidea, C., Dincer, E., Wang, R. and Uhal, B. D. (2004) 'Fas induces apoptosis in human coronary artery endothelial cells in vitro.', *BMC cell biology*. BioMed Central, 5, p. 6. doi: 10.1186/1471-2121-5-6.

FISONE, G., LANGEL, ulo, CARLQUIST, M., BERGMAN, T., CONSOLO, S., HOKFELT, T., UNDEN, A., ANDELL, S. and BARTFAI, T. (1989) 'Galanin receptor and its ligands in the rat hippocampus', *European Journal of Biochemistry*. Blackwell Publishing Ltd, 181(1), pp. 269–276. doi: 10.1111/j.1432-1033.1989.tb14721.x.

Flatters, S. J. L., Fox, A. J. and Dickenson, A. H. (2002) 'Nerve injury induces plasticity that results in spinal inhibitory effects of galanin', *Pain*, 98(3), pp. 249–258. doi: 10.1016/S0304-3959(02)00180-X.

Flatters, S. J. L., Fox, A. J. and Dickenson, A. H. (2003) 'In vivo and in vitro effects of peripheral galanin on nociceptive transmission in naive and neuropathic states.', *Neuroscience*, 116(4), pp. 1005–12. Available at: <http://www.ncbi.nlm.nih.gov/pubmed/12617941> (Accessed: 22 June 2017).

Flynn, S. P. and White, H. S. (2015) 'Regulation of glucose and insulin release following acute and repeated treatment with the synthetic galanin analog NAX-5055.', *Neuropeptides*. NIH Public Access, 50, pp. 35–42. doi: 10.1016/j.npep.2015.01.001.

Foussal, C., Lairez, O., Calise, D., Pathak, A., Guilbeau-Frugier, C., Valet, P., Parini, A. and Kunduzova, O. (2010) 'Activation of catalase by apelin prevents oxidative stress-linked cardiac hypertrophy', *FEBS Letters*, 584(11), pp. 2363–2370. doi: 10.1016/j.febslet.2010.04.025.

Gaballa, M. A. and Goldman, S. (2002) 'Ventricular remodeling in heart failure', *J Card Fail*, 8(6 Suppl), pp. S476-85. doi: 10.1054/jcaf.2002.129270S107191640200492X [pii].

Gabet, A., Juilli  re, Y., Lamarche-Vadel, A., Vernay, M. and Oli  , V. (2015) 'National trends

in rate of patients hospitalized for heart failure and heart failure mortality in France, 2000–2012’, *European Journal of Heart Failure*, 17(6), pp. 583–590. doi: 10.1002/ejhf.284.

Gajarsa, J. J. and Kloner, R. A. (2011) ‘Left ventricular remodeling in the post-infarction heart: A review of cellular, molecular mechanisms, and therapeutic modalities’, *Heart Failure Reviews*, 16(1), pp. 13–21. doi: 10.1007/s10741-010-9181-7.

Genet, M., Lee, L. C., Baillargeon, B., Guccione, J. M. and Kuhl, E. (2016) ‘Modeling Pathologies of Diastolic and Systolic Heart Failure’, *Annals of Biomedical Engineering*, 44(1), pp. 112–127. doi: 10.1007/s10439-015-1351-2.

Gilbey, S. G., Stephenson, J., O’halloran, D. J., Burrin, J. M. and Bloom, S. R. (1989) ‘High-Dose Porcine Galanin Infusion and Effect on Intravenous Glucose Tolerance in Humans’, *Diabetes*, 38(9). Available at: <http://diabetes.diabetesjournals.org/content/38/9/1114.short> (Accessed: 22 June 2017).

Gjesdal, O., Bluemke, D. A. and Lima, J. A. (2011) ‘Cardiac remodeling at the population level--risk factors, screening, and outcomes.’, *Nature reviews. Cardiology*, 8(12), pp. 673–85. doi: 10.1038/nrccardio.2011.154.

Go, A. S., Mozaffarian, D., Roger, V. L., Benjamin, E. J., Berry, J. D., Blaha, M. J., Dai, S., Ford, E. S., Fox, C. S., Franco, S., Fullerton, H. J., Gillespie, C., Hailpern, S. M., Heit, J. A., Howard, V. J., Huffman, M. D., Judd, S. E., Kissela, B. M., Kittner, S. J., Lackland, D. T., Lichtman, J. H., Lisabeth, L. D., Mackey, R. H., Magid, D. J., Marcus, G. M., Marelli, A., Matchar, D. B., McGuire, D. K., Mohler, E. R., Moy, C. S., Mussolino, M. E., Neumar, R. W., Nichol, G., Pandey, D. K., Paynter, N. P., Reeves, M. J., Sorlie, P. D., Stein, J., Towfighi, A., Turan, T. N., Virani, S. S., Wong, N. D., Woo, D. and Turner, M. B. (2014) ‘Heart Disease and Stroke Statistics - 2014 Update: A report from the American Heart Association’, *Circulation*, 129(3), pp. e28–e292. doi: 10.1161/01.cir.0000441139.02102.80.

Goldsmith, E. C., Hoffman, A., Morales, M. O., Potts, J. D., Price, R. L., McFadden, A., Rice, M. and Borg, T. K. (2004) ‘Organization of fibroblasts in the heart’, *Developmental Dynamics*, 230(4), pp. 787–794. doi: 10.1002/dvdy.20095.

Gorbatyuk, O. and Hökfelt, T. (1998) ‘Effect of inhibition of glucose and fat metabolism on galanin-R1 receptor mRNA levels in the rat hypothalamic paraventricular and supraoptic nuclei.’, *Neuroreport*, 9(16), pp. 3565–9. Available at: <http://www.ncbi.nlm.nih.gov/pubmed/9858361>.

Gottsch, M. L., Zeng, H., Hohmann, J. G., Weinshenker, D., Clifton, D. K. and Steiner, R. A. (2005) ‘Phenotypic Analysis of Mice Deficient in the Type 2 Galanin Receptor (GALR2)’, *Molecular and Cellular Biology*, 25(11), pp. 4804–4811. doi: 10.1128/MCB.25.11.4804-4811.2005.

Greer, E. L. and Brunet, A. (2005) ‘FOXO transcription factors at the interface between longevity and tumor suppression’, *Oncogene*, 24(50), pp. 7410–7425. doi: 10.1038/sj.onc.1209086.

Grieve, D. and Shah, A. M. (2003) ‘Oxidative stress in heart failure More than just damage’, *European Heart Journal*. Oxford University Press, 24(24), pp. 2161–2163. doi: 10.1016/j.ehj.2003.10.015.

Guha, K. and McDonagh, T. (2013) ‘Heart Failure Epidemiology: European Perspective’,

Current Cardiology Reviews, 9(Mi), pp. 123–127. doi: 10.2174/1573403X11309020005.

Gundlach, A. L. (2002) ‘Galanin/GALP and galanin receptors: Role in central control of feeding, body weight/obesity and reproduction?’, *European Journal of Pharmacology*, 440(2–3), pp. 255–268. doi: 10.1016/S0014-2999(02)01433-4.

Guo, L., Shi, M., Zhang, L., Li, G., Zhang, L., Shao, H., Fang, P., Ma, Y., Li, J., Shi, Q. and Sui, Y. (2011) ‘Galanin antagonist increases insulin resistance by reducing glucose transporter 4 effect in adipocytes of rats’, *General and Comparative Endocrinology*, 173(1), pp. 159–163. doi: 10.1016/j.ygcn.2011.05.011.

Habecker, B. A., Gritman, K. R., Willison, B. D. and Winkle, D. M. Van (2005) ‘Myocardial infarction stimulates galanin expression in cardiac sympathetic neurons’, *Neuropeptides*, 39(2), pp. 89–95. doi: 10.1016/j.npep.2004.11.003.

Habert-Ortoli, E., Amiranoff, B., Loquet, I., Laburthe, M. and Mayaux, J. F. (1994) ‘Molecular cloning of a functional human galanin receptor.’, *Proceedings of the National Academy of Sciences of the United States of America*, 91(October), pp. 9780–9783.

Habert-Ortoli, E., Amiranoff, B., Loquet, I., Laburthe, M. and Mayaux, J.-F. (1994) ‘Molecular cloning of a functional human galanin receptor (Bowes melanoma cei line/guanine nucleotide binding protein-coupled receptor/cAMP)’, *Neurobiology*, 91, pp. 9780–9783. Available at: <https://www.ncbi.nlm.nih.gov/pmc/articles/PMC44900/pdf/pnas01143-0125.pdf> (Accessed: 10 May 2017).

Hammond, P. J., Smith, D. M., Akinsanya, K. O., Mufti, W. A., Wynick, D. and Bloom, S. R. (1996) ‘Signalling Pathways Mediating Secretory and Mitogenic Responses to Galanin and Pituitary Adenylate Cyclase-Activating Polypeptide in the 235-1 Clonal Rat Lactotroph Cell Line’, *Journal of Neuroendocrinology*. Blackwell Science Ltd., 8(6), pp. 457–464. doi: 10.1046/j.1365-2826.1996.04747.x.

Hao, J. X. (1999) ‘Intrathecal galanin alleviates allodynia-like behaviour in rats after partial peripheral nerve injury’, *European Journal of Neuroscience*. Blackwell Science Ltd, 11(2), pp. 427–432. doi: 10.1046/j.1460-9568.1999.00447.x.

He, B., Shi, M., Zhang, L., Li, G., Zhang, L., Shao, H., Li, J., Fang, P., Ma, Y., Shi, Q. and Sui, Y. (2011) ‘Beneficial effect of galanin on insulin sensitivity in muscle of type 2 diabetic rats’, *Physiology & Behavior*, 103(3–4), pp. 284–289. doi: 10.1016/j.physbeh.2011.02.023.

Henson, B. S., Neubig, R. R., Jang, I., Ogawa, T., Zhang, Z., Carey, T. E. and D’Silva, N. J. (2005) ‘Galanin receptor 1 has anti-proliferative effects in oral squamous cell carcinoma.’, *The Journal of biological chemistry*. American Society for Biochemistry and Molecular Biology, 280(24), pp. 22564–71. doi: 10.1074/jbc.M414589200.

Herring, N., Cranley, J., Lokale, M. N., Li, D., Shanks, J., Alston, E. N., Girard, B. M., Carter, E., Parsons, R. L., Habecker, B. A. and Paterson, D. J. (2012) ‘The cardiac sympathetic co-transmitter galanin reduces acetylcholine release and vagal bradycardia: Implications for neural control of cardiac excitability’, *Journal of Molecular and Cellular Cardiology*, 52(3), pp. 667–676. doi: 10.1016/j.jmcc.2011.11.016.

Hochman, J. S. and Bulkley, B. H. (1982) ‘Expansion of acute myocardial infarction: an experimental study.’, *Circulation*, 65(7), pp. 1446–50. Available at: <http://www.ncbi.nlm.nih.gov/pubmed/7074800> (Accessed: 18 July 2017).

Hökfelt, T. and Tatsumoto, K. (2008) 'Galanin - 25 Years with a multitalented neuropeptide', *Cellular and Molecular Life Sciences*, pp. 1793–1795. doi: 10.1007/s00018-008-8152-9.

Hori, M. and Nishida, K. (2008) 'Oxidative stress and left ventricular remodelling after myocardial infarction', *Cardiovascular Research*, 81(3), pp. 457–464. doi: 10.1093/cvr/cvn335.

Howard, G., Peng, L. and Hyde, J. F. (1997) 'An estrogen receptor binding site within the human galanin gene.', *Endocrinology*, 138, pp. 4649–4656. doi: 10.1210/endo.138.11.5507.

Hulting, A. L., Land, T., Berthold, M., Langel, U., Hökfelt, T. and Bartfai, T. (1993) 'Galanin receptors from human pituitary tumors assayed with human galanin as ligand.', *Brain research*, 625(1), pp. 173–6. Available at: <http://www.ncbi.nlm.nih.gov/pubmed/7694774> (Accessed: 30 June 2017).

Iismaa, T. P., Fathi, Z., Hort, Y. J., Iben, L. G., Dutton, J. L., Baker, E., Sutherland, G. R. and Shine, J. (1998) 'Structural organization and chromosomal localization of three human galanin receptor genes', *Ann NY Acad Sci*, 863, pp. 56–63.

Jacoby, A. S., Webb, G. C., Liu, M. L., Kofler, B., Hort, Y. J., Fathi, Z., Bottema, C. D. K., Shine, J. and Iismaa, T. P. (1997) 'Structural Organization of the Mouse and Human GALR1 Galanin Receptor Genes (GalnrandGALNR) and Chromosomal Localization of the Mouse Gene', *Genomics*, 45(3), pp. 496–508. doi: 10.1006/geno.1997.4960.

Ji, R. R., Zhang, X., Zhang, Q., Dagerlind, A., Nilsson, S., Wiesenfeld-Hallin, Z. and Hökfelt, T. (1995) 'Central and peripheral expression of galanin in response to inflammation.', *Neuroscience*, 68(2), pp. 563–76. Available at: <http://www.ncbi.nlm.nih.gov/pubmed/7477966> (Accessed: 18 July 2017).

Jiang, L., Shi, M., Guo, L., He, B., Li, G., Zhang, L., Zhang, L. and Shao, H. (2009) 'Effect of M35, a neuropeptide galanin antagonist on glucose uptake translated by glucose transporter 4 in trained rat skeletal muscle', *Neuroscience Letters*, 467(2), pp. 178–181. doi: 10.1016/j.neulet.2009.10.034.

Jureus, A., Cunningham, M. J., McClain, M. E., Clifton, D. K. and Steiner, R. A. (2000) 'Galanin-Like Peptide (GALP) Is a Target for Regulation by Leptin in the Hypothalamus of the Rat', *Endocrinology*. Oxford University Press, 141(7), pp. 2703–2706. doi: 10.1210/endo.141.7.7669.

Kameda, K. (2003) 'Correlation of oxidative stress with activity of matrix metalloproteinase in patients with coronary artery disease Possible role for left ventricular remodelling', *European Heart Journal*, 24(24), pp. 2180–2185. doi: 10.1016/j.ehj.2003.09.022.

Kanazawa, T., Iwashita, T., Kommareddi, P., Nair, T., Misawa, K., Misawa, Y., Ueda, Y., Tono, T. and Carey, T. E. (2007) 'Galanin and galanin receptor type 1 suppress proliferation in squamous carcinoma cells: activation of the extracellular signal regulated kinase pathway and induction of cyclin-dependent kinase inhibitors', *Oncogene*, 26(39), pp. 5762–5771. doi: 10.1038/sj.onc.1210384.

Kanazawa, T., Kommareddi, P. K., Iwashita, T., Kumar, B., Misawa, K., Misawa, Y., Jang, I., Nair, T. S., Iino, Y. and Carey, T. E. (2009) 'Galanin Receptor Subtype 2 Suppresses Cell Proliferation and Induces Apoptosis in p53 Mutant Head and Neck Cancer Cells', *Clinical Cancer Research*, 15(7), pp. 2222–2230. doi: 10.1158/1078-0432.CCR-08-2443.

- Kang, P. M. and Izumo, S. (2003) 'Apoptosis in heart: basic mechanisms and implications in cardiovascular diseases.', *Trends in molecular medicine*, 9(4), pp. 177–82. Available at: <http://www.ncbi.nlm.nih.gov/pubmed/12727144> (Accessed: 18 July 2017).
- Kashimura, J., Shimosegawa, T., Kikuchi, Y., Yoshida, K., Koizumi, M., Mochizuki, T., Yanaihara, N. and Toyota, T. (1994) 'Effects of galanin on amylase secretion from dispersed rat pancreatic acini.', *Pancreas*, 9(2), pp. 258–62. Available at: <http://www.ncbi.nlm.nih.gov/pubmed/7514793> (Accessed: 22 June 2017).
- Katz, A. (2011) *Physiology of the heart, Journal of cardiology. Supplement.* doi: 10.1136/bmj.2.4883.346.
- Kehr, J., Yoshitake, T., Wang, F. H., Wynick, D., Holmberg, K., Lendahl, U., Bartfai, T., Yamaguchi, M., Hökfelt, T. and Ögren, S. O. (2001) 'Microdialysis in freely moving mice: determination of acetylcholine, serotonin and noradrenaline release in galanin transgenic mice.', *Journal of neuroscience methods*, 109(1), pp. 71–80. Available at: <http://www.ncbi.nlm.nih.gov/pubmed/11489302> (Accessed: 19 September 2017).
- Kemp, C. D. and Conte, J. V. (2012) 'The pathophysiology of heart failure', *Cardiovascular Pathology*, pp. 365–371. doi: 10.1016/j.carpath.2011.11.007.
- Kenchaiah, S. and Pfeffer, M. A. (2004) 'Cardiac remodeling in systemic hypertension', *Medical Clinics of North America*, pp. 115–130. doi: 10.1016/S0025-7125(03)00168-8.
- Kerr, B. J., Cafferty, W. B., Gupta, Y. K., Bacon, A., Wynick, D., McMahon, S. B. and Thompson, S. W. (2000) 'Galanin knockout mice reveal nociceptive deficits following peripheral nerve injury.', *The European journal of neuroscience*, 12(3), pp. 793–802. Available at: <http://www.ncbi.nlm.nih.gov/pubmed/10762308> (Accessed: 22 June 2017).
- Kerr, J. F. R. (1971) 'Shrinkage necrosis: A distinct mode of cellular death', *The Journal of Pathology*, 105(1), pp. 13–20. doi: 10.1002/path.1711050103.
- Kerr, N., Holmes, F. E., Hobson, S.-A., Vanderplank, P., Leard, A., Balthasar, N. and Wynick, D. (2015) 'The generation of knock-in mice expressing fluorescently tagged galanin receptors 1 and 2.', *Molecular and cellular neurosciences*. Elsevier, 68, pp. 258–71. doi: 10.1016/j.mcn.2015.08.006.
- Kim, A. and Park, T. (2010) 'Diet-induced obesity regulates the galanin-mediated signaling cascade in the adipose tissue of mice', *Molecular Nutrition & Food Research*, 54(9), pp. 1361–1370. doi: 10.1002/mnfr.200900317.
- King, M., Kingery, J. and Casey, B. (2012) 'Diagnosis and evaluation of heart failure', *American Family Physician*, 85(12), pp. 1161–1168.
- Klabunde, R. E. (2004) *Cardiovascular Physiology Concepts*, Lippincott Williams & Wilkins. doi: citeulike-article-id:2086320.
- KOCIC, I. (1998) 'Pharmacology: The Influence of the Neuropeptide Galanin on the Contractility and the Effective Refractory Period of Guinea-pig Heart Papillary Muscle Under Normoxic and Hypoxic Conditions', *Journal of Pharmacy and Pharmacology*. Blackwell Publishing Ltd, 50(12), pp. 1361–1364. doi: 10.1111/j.2042-7158.1998.tb03360.x.
- Kofler, B., Liu, M. L., Jacoby, A. S., Shine, J. and Iismaa, T. P. (1996) 'Molecular cloning and characterisation of the mouse preprogalanin gene.', *Gene*, 182(1–2), pp. 71–5. Available

at: <http://www.ncbi.nlm.nih.gov/pubmed/8982069> (Accessed: 18 July 2017).

Kolakowski, L. F., O'Neill, G. P., Howard, a D., Broussard, S. R., Sullivan, K. a, Feighner, S. D., Sawzdargo, M., Nguyen, T., Kargman, S., Shiao, L. L., Hreniuk, D. L., Tan, C. P., Evans, J., Abramovitz, M., Chateauneuf, a, Coulombe, N., Ng, G., Johnson, M. P., Tharian, a, Khoshbouei, H., George, S. R., Smith, R. G. and O'Dowd, B. F. (1998) 'Molecular characterization and expression of cloned human galanin receptors GALR2 and GALR3.', *Journal of neurochemistry*, 71(6), pp. 2239–51. doi: 10.1046/j.1471-4159.1998.71062239.x.

Konstam, M. A., Kramer, D. G., Patel, A. R., Maron, M. S. and Udelson, J. E. (2011) 'Left ventricular remodeling in heart failure: Current concepts in clinical significance and assessment', *JACC: Cardiovascular Imaging*, 4(1), pp. 98–108. doi: 10.1016/j.jcmg.2010.10.008.

Krum, H. and Abraham, W. T. (2009) 'Heart failure', *The Lancet*, 373(9667), pp. 941–955. doi: 10.1016/S0140-6736(09)60236-1.

Lagny-Pourmir, I., Lorinet, A. M., Yanaiharat, N. and Laburthe, M. (no date) 'Structural Requirements for Galanin Interaction With Receptors From Pancreatic Beta Cells and From Brain Tissue of the Rat', *Peptides*, 10, pp. 757–761. Available at: http://ac.els-cdn.com/0196978189901095/1-s2.0-0196978189901095-main.pdf?_tid=2b60c264-5d6b-11e7-8823-00000aacb360&acdnat=1498810234_5982c98bf39e53ee17cb2d5890823f8b (Accessed: 30 June 2017).

Landry, M., Aman, K. and Hökfelt, T. (1998) 'Galanin-R1 receptor in anterior and mid-hypothalamus: distribution and regulation.', *The Journal of comparative neurology*, 399(3), pp. 321–40. Available at: <http://www.ncbi.nlm.nih.gov/pubmed/9733081> (Accessed: 22 June 2017).

Lang, R., Berger, A., Hermann, A. and Kofler, B. (2001) 'Biphasic response to human galanin of extracellular acidification in human Bowes melanoma cells', *European Journal of Pharmacology*, 423(2–3), pp. 135–141. doi: 10.1016/S0014-2999(01)01135-9.

Lang, R., Gundlach, A. L., Holmes, F. E., Hobson, S. A., Wynick, D., Hokfelt, T. and Kofler, B. (2015) 'Physiology, Signaling, and Pharmacology of Galanin Peptides and Receptors: Three Decades of Emerging Diversity', *Pharmacological Reviews*, 67, pp. 118–175. Available at: http://www.academia.edu/13651117/Physiology_signaling_and_pharmacology_of_galanin_peptides_and_receptors_three_decades_of_emerging_diversity (Accessed: 22 June 2017).

Lawrence, C. and Fraley, G. S. (2011) 'Galanin-like peptide (GALP) is a hypothalamic regulator of energy homeostasis and reproduction.', *Frontiers in neuroendocrinology*. NIH Public Access, 32(1), pp. 1–9. doi: 10.1016/j.yfrne.2010.06.001.

Legakis, I., Mantzouridis, T. and Mountokalakis, T. (2005) 'Positive Correlation of Galanin With Glucose in Type 2 Diabetes', *Diabetes Care*, 28(3). Available at: <http://care.diabetesjournals.org/content/28/3/759.short> (Accessed: 22 June 2017).

Lew, W. Y., Chen, Z. Y., Guth, B. and Covell, J. W. (1985) 'Mechanisms of augmented segment shortening in nonischemic areas during acute ischemia of the canine left ventricle.', *Circulation research*, 56(3), pp. 351–8. doi: 10.1161/01.RES.56.3.351.

Lindskog, S. and Ahren, B. (1987) 'Galanin: effects on basal and stimulated insulin and

glucagon secretion in the mouse.', *Acta physiologica Scandinavica*, 129(3), pp. 305–309. doi: 10.1111/j.1748-1716.1987.tb08073.x.

Lindskog, S., Dunning, B. E., Martensson, H., Ar'Rajab, A., Taborsky, G. J. J. and Ahrén, B. (1990) 'Galanin of the homologous species inhibits insulin secretion in the rat and in the pig', *Acta. Physiol. Scand.* Blackwell Publishing Ltd, 129(4), pp. 591–596. doi: 10.1111/j.1748-1716.1990.tb08963.x.

Linzbach, A. J. (1960) 'Heart failure from the point of view of quantitative anatomy', *Am J Cardiol*, 5(3), pp. 370–382. doi: 10.1016/0002-9149(60)90084-9.

Liu, H.-X. and Hökfelt, T. (2000) 'Effect of intrathecal galanin and its putative antagonist M35 on pain 1 behavior in a neuropathic pain model', *Brain Research*, 886, pp. 67–72. Available at: www.elsevier.com (Accessed: 22 June 2017).

Liu, H.-X. and Hökfelt, T. (2002) 'The participation of galanin in pain processing at the spinal level', *Trends in Pharmacological Sciences*, 23(10), pp. 468–474. doi: 10.1016/S0165-6147(02)02074-6.

Liu, H. X., Brumovsky, P., Schmidt, R., Brown, W., Payza, K., Hodzic, L., Pou, C., Godbout, C. and Hökfelt, T. (2001) 'Receptor subtype-specific pronociceptive and analgesic actions of galanin in the spinal cord: selective actions via GalR1 and GalR2 receptors.', *Proceedings of the National Academy of Sciences of the United States of America*. National Academy of Sciences, 98(17), pp. 9960–4. doi: 10.1073/pnas.161293598.

Lu, X., Ross, B., Sanchez-Alavez, M., Zorrilla, E. P. and Bartfai, T. (2008) 'Phenotypic analysis of GalR2 knockout mice in anxiety- and depression-related behavioral tests.', *Neuropeptides*. NIH Public Access, 42(4), pp. 387–97. doi: 10.1016/j.npep.2008.04.009.

Mahns, D. A. and Courtice, G. P. (1996) 'Effect of three galanin antagonists on the pressor response to galanin in the Cane toad, *Bufo marinus*', *Regulatory Peptides*, 67(3), pp. 163–168. doi: 10.1016/S0167-0115(96)00133-4.

Mahoney, S.-A., Hosking, R., Farrant, S., Holmes, F. E., Jacoby, A. S., Shine, J., Iismaa, T. P., Scott, M. K., Schmidt, R. and Wynick, D. (2003) 'The Second Galanin Receptor GalR2 Plays a Key Role in Neurite Outgrowth from Adult Sensory Neurons', *Journal of Neuroscience*, 23(2). Available at: <http://www.jneurosci.org/content/23/2/416.short> (Accessed: 22 June 2017).

Man, P.-S. and Lawrence, C. B. (2008) 'Interleukin-1 Mediates the Anorexic and Febrile Actions of Galanin-Like Peptide', *Endocrinology*. Academic Press, New York, 149(11), pp. 5791–5802. doi: 10.1210/en.2008-0252.

Manabe, T., Okada, Y., Sawai, H., Funahashi, H., Yamamoto, M., Hayakawa, T. and Yoshimura, T. (2003) 'Effect of galanin on plasma glucose, insulin and pancreatic glucagon in dogs.', *The Journal of international medical research*. SAGE PublicationsSage UK: London, England, 31(2), pp. 126–32. doi: 10.1177/147323000303100209.

Massey, P. V., Warburton, E. C., Wynick, D., Brown, M. W. and Bashir, Z. I. (2003) 'Galanin regulates spatial memory but not visual recognition memory or synaptic plasticity in perirhinal cortex.', *Neuropharmacology*, 44(1), pp. 40–8. Available at: <http://www.ncbi.nlm.nih.gov/pubmed/12559120> (Accessed: 19 September 2017).

Mazarati, A. M. (2004) 'Galanin and galanin receptors in epilepsy', *Neuropeptides*, 38(6), pp.

331–343. doi: 10.1016/j.npep.2004.07.006.

McDONALD, M. P., GLEASON, T. C., ROBINSON, J. K. and CRAWLEY, J. N. (1998) ‘Galanin Inhibits Performance on Rodent Memory Tasks’, *Annals of the New York Academy of Sciences*. Blackwell Publishing Ltd, 863(1 GALANIN), pp. 305–322. doi: 10.1111/j.1749-6632.1998.tb10704.x.

McDONALD, T. J., DUPRE, J., GREENBERG, G. R., TEPPERMAN, F., BROOKS, B., TATEMOTO, K. and MUTT, V. (1986) ‘The Effect of Galanin on Canine Plasma Glucose and Gastroenteropancreatic Hormone Responses to Oral Nutrients and Intravenous Arginine*’, *Endocrinology*. Oxford University Press, 119(5), pp. 2340–2345. doi: 10.1210/endo-119-5-2340.

McDonald, T. J., Dupre, J., Tatemoto, K., Greenberg, G. R., Radziuk, J. and Mutt, V. (1985) ‘Galanin Inhibits Insulin Secretion and Induces Hyperglycemia in Dogs’, *Diabetes*, 34(2). Available at: <http://diabetes.diabetesjournals.org/content/34/2/192.short> (Accessed: 22 June 2017).

McMurray, J. J. (2000) ‘HEART FAILURE: Epidemiology, aetiology, and prognosis of heart failure’, *Heart*, 83(5), pp. 596–602. doi: 10.1136/heart.83.5.596.

McMurray, J. J. V (2010) ‘Systolic heart failure’, *New England Journal of Medicine*, 362(3), pp. 228–238. doi: 10.1056/NEJMc1002215.

McMurray J JV, Adamopoulos S, Anker SD, Auricchio A, Böhm M, Dickstein K, et al (2012) ‘ESC Guideline for the diagnosis and treatment of acute and chronic heart failure 2012’, *Eur Heart J*, p. 33: 1791.

Meister, B., Cortés, R., Villar, M. J., Schalling, M. and Hökfelt, T. (1990) ‘Peptides and transmitter enzymes in hypothalamic magnocellular neurons after administration of hyperosmotic stimuli: comparison between messenger RNA and peptide/protein levels.’, *Cell and tissue research*, 260(2), pp. 279–97. Available at: <http://www.ncbi.nlm.nih.gov/pubmed/1694105> (Accessed: 18 July 2017).

Melander, T., Staines, W. A. and Rökaeus, A. (1986) ‘Galanin-like immunoreactivity in hippocampal afferents in the rat, with special reference to cholinergic and noradrenergic inputs’, *Neuroscience*, 19(1), pp. 223–240. doi: 10.1016/0306-4522(86)90017-5.

Merchenthaler, I., López, F. J. and Negro-Vilar, A. (1993) ‘Anatomy and physiology of central galanin-containing pathways’, *Progress in Neurobiology*, pp. 711–769. doi: 10.1016/0301-0082(93)90012-H.

Misawa, K., Ueda, Y., Kanazawa, T., Misawa, Y., Jang, I., Brenner, J. C., Ogawa, T., Takebayashi, S., Grenman, R. A., Herman, J. G., Mineta, H. and Carey, T. E. (2008) ‘Epigenetic Inactivation of Galanin Receptor 1 in Head and Neck Cancer’, *Clinical Cancer Research*, 14(23), pp. 7604–7613. doi: 10.1158/1078-0432.CCR-07-4673.

Nadir, A. M., Beadle, R. and Lim, H. S. (2014) ‘Kussmaul physiology in patients with heart failure’, *Circulation: Heart Failure*, 7(3), pp. 440–447. doi: 10.1161/CIRCHEARTFAILURE.113.000830.

Nagayoshi, K., Ueki, T., Tashiro, K., Mizuuchi, Y., Manabe, T., Araki, H., Oda, Y., Kuhara, S. and Tanaka, M. (2014) ‘Galanin plays an important role in cancer invasiveness and is associated with poor prognosis in stage II colorectal cancer’, *Oncology Reports*, 33(2), pp.

539–46. doi: 10.3892/or.2014.3660.

Nergiz, S., Altinkaya, Ö. S., Küçük, M., Yüksel, H., Sezer, S. D., Kurt Ömürlü, İ. and Odabaşı, A. R. (2014) ‘Circulating galanin and IL-6 concentrations in gestational diabetes mellitus’, *Gynecological Endocrinology*. Taylor & Francis, 30(3), pp. 236–240. doi: 10.3109/09513590.2013.871519.

Nicholl, J., Kofler, B., Sutherland, G. R., Shine, J. and Iismaa, T. P. (1995) *Assignment of the Gene Encoding Human Galanin Receptor (GALNR) to 18q23 by in Situ Hybridization, Genomics*. doi: 10.1006/geno.1995.1292.

Nyhan, D. and Blanck, T. J. J. (2006) ‘Cardiac Physiology’, in *Foundations of Anesthesia*, pp. 473–484. doi: 10.1016/B978-0-323-03707-5.50045-0.

O’Donnell, D., Ahmad, S., Wahlestedt, C. and Walker, P. (1999) ‘Expression of the novel galanin receptor subtype GALR2 in the adult rat CNS: distinct distribution from GALR1.’, *The Journal of comparative neurology*, 409(3), pp. 469–81. Available at: <http://www.ncbi.nlm.nih.gov/pubmed/10379831> (Accessed: 22 June 2017).

O’Meara, G., Coumis, U., Ma, S. Y., Kehr, J., Mahoney, S., Bacon, A., Allen, S. J., Holmes, F., Kahl, U., Wang, F. H., Kearns, I. R., Ove-Ogren, S., Dawbarn, D., Mufson, E. J., Davies, C., Dawson, G. and Wynick, D. (2000) ‘Galanin regulates the postnatal survival of a subset of basal forebrain cholinergic neurons.’, *Proceedings of the National Academy of Sciences of the United States of America*. National Academy of Sciences, 97(21), pp. 11569–74. doi: 10.1073/pnas.210254597.

Olivetti, G., Capasso, J. M., Meggs, L. G., Sonnenblick, E. H. and Anversa, P. (1991) ‘Cellular basis of chronic ventricular remodeling after myocardial infarction in rats.’, *Circulation research*, 68, pp. 856–869. doi: 10.1161/01.RES.68.3.856.

Oosterom-Calò, R., Van Ballegooijen, A. J., Terwee, C. B., Te Velde, S. J., Brouwer, I. A., Jaarsma, T. and Brug, J. (2012) ‘Determinants of heart failure self-care: A systematic literature review’, *Heart Failure Reviews*, pp. 367–385. doi: 10.1007/s10741-011-9292-9.

Opie, L. H., Commerford, P. J., Gersh, B. J. and Pfeffer, M. A. (2006) ‘Controversies in ventricular remodelling’, *Lancet*, pp. 356–367. doi: 10.1016/S0140-6736(06)68074-4.

Oppenheimer, G. M. (2010) ‘Framingham Heart Study: The First 20 Years’, *Progress in Cardiovascular Diseases*, 53(1), pp. 55–61. doi: 10.1016/j.pcad.2010.03.003.

Pang, L., Hashemi, T., Lee, H. J., Maguire, M., Graziano, M. P., Bayne, M., Hawes, B., Wong, G. and Wang, S. (1998) ‘The mouse GalR2 galanin receptor: genomic organization, cDNA cloning, and functional characterization.’, *Journal of neurochemistry*, 71(6), pp. 2252–9. Available at: <http://www.ncbi.nlm.nih.gov/pubmed/9832122> (Accessed: 22 June 2017).

Parker, E. M., Izzarelli, D. G., Nowak, H. P., Mahle, C. D., Iben, L. G., Wang, J. and Goldstein, M. E. (1995) ‘Cloning and characterization of the rat GALR1 galanin receptor from Rin14B insulinoma cells’, *Molecular Brain Research*, 34(2), pp. 179–189. doi: 10.1016/0169-328X(95)00159-P.

Parsons, R. L., Neel, D. S., Konopka, L. M. and McKeon, T. W. (1989) ‘The presence and possible role of a galanin-like peptide in the mudpuppy heart’, *Neuroscience*, 29(3), pp. 749–759. doi: 10.1016/0306-4522(89)90146-2.

Perel, Y., Amrein, L., Dobremez, E., Rivel, J., Daniel, J. Y. and Landry, M. (2002a) 'Galanin and galanin receptor expression in neuroblastic tumours: correlation with their differentiation status', *British Journal of Cancer*, 86(1), pp. 117–122. doi: 10.1038/sj.bjc.6600019.

Perel, Y., Amrein, L., Dobremez, E., Rivel, J., Daniel, J. Y. and Landry, M. (2002b) 'Galanin and galanin receptor expression in neuroblastic tumours: correlation with their differentiation status.', *British journal of cancer*. Nature Publishing Group, 86(1), pp. 117–22. doi: 10.1038/sj.bjc.6600019.

Pfeffer, M. A. and Braunwald, E. (1990) 'Ventricular remodeling after myocardial infarction. Experimental observations and clinical implications', *Circulation*, 81(4), pp. 1161–1172. doi: 10.1161/01.CIR.81.4.1161.

Pirondi, S., Fernandez, M., Schmidt, R., Hokfelt, T., Giardino, L. and Calza, L. (2005) 'The galanin-R2 agonist AR-M1896 reduces glutamate toxicity in primary neural hippocampal cells', *Journal of Neurochemistry*. Blackwell Science Ltd, 95(3), pp. 821–833. doi: 10.1111/j.1471-4159.2005.03437.x.

Pisarenko, O., Shulzhenko, V., Studneva, I., Pelogeykina, Y., Timoshin, A., Anesia, R., Valet, P., Parini, A. and Kunduzova, O. (2015) 'Structural apelin analogues: mitochondrial ROS inhibition and cardiometabolic protection in myocardial ischaemia reperfusion injury', *British Journal of Pharmacology*, 172(12), pp. 2933–2945. doi: 10.1111/bph.13038.

Ponikowski, P., Voors, A. A., Anker, S. D., Bueno, H., Cleland, J. G. F., Coats, A. J. S., Falk, V., González-Juanatey, J. R., Harjola, V. P., Jankowska, E. A., Jessup, M., Linde, C., Nihoyannopoulos, P., Parisi, J. T., Pieske, B., Riley, J. P., Rosano, G. M. C., Ruilope, L. M., Ruschitzka, F., Rutten, F. H. and Van Der Meer, P. (2016) '2016 ESC Guidelines for the diagnosis and treatment of acute and chronic heart failure', *European Heart Journal*, p. 2129–2200m. doi: 10.1093/eurheartj/ehw128.

Poritsanos, N. J., Mizuno, T. M., Lautatzis, M.-E. and Vrontakis, M. (2009) 'Chronic increase of circulating galanin levels induces obesity and marked alterations in lipid metabolism similar to metabolic syndrome', *International Journal of Obesity*. Nature Publishing Group, 33(12), pp. 1381–1389. doi: 10.1038/ijo.2009.187.

Quattrini, F. M. and Pelliccia, A. (2012) '[Physiological versus pathological left ventricular remodeling in athletes]', *G Ital Cardiol (Rome)*, 13(4), pp. 273–280. doi: 10.1714/1056.11559.

Rauch, I. and Kofler, B. (2010) 'The galanin system in cancer.', *EXS*, 102, pp. 223–41. Available at: <http://www.ncbi.nlm.nih.gov/pubmed/21299072> (Accessed: 30 June 2017).

Revington, M., Potter, E. K. and McCloskey, D. I. (1990) 'Prolonged inhibition of cardiac vagal action following sympathetic stimulation and galanin in anaesthetized cats.', *The Journal of physiology*, 431, pp. 495–503. Available at: <http://www.ncbi.nlm.nih.gov/pubmed/1712845> (Accessed: 3 July 2017).

Richter, D. (1999) *Regulatory peptides and cognate receptors*. Springer Berlin Heidelberg. Available at: [https://books.google.fr/books?id=LRzqCAAAQBAJ&pg=PA289&lpg=PA289&dq=Rossmanith+galanin+1996&source=bl&ots=VYnRbH_fDI&sig=7fX_4MgNWZU6NMzNk6faIjRZUjc&hl=fr&sa=X&ved=0ahUKEwiN_4uAvNHUAhXDjRoKHaT_AdAQ6AEIRTAF#v=onepage&q=Rossmanith galanin 1996&f=false](https://books.google.fr/books?id=LRzqCAAAQBAJ&pg=PA289&lpg=PA289&dq=Rossmanith+galanin+1996&source=bl&ots=VYnRbH_fDI&sig=7fX_4MgNWZU6NMzNk6faIjRZUjc&hl=fr&sa=X&ved=0ahUKEwiN_4uAvNHUAhXDjRoKHaT_AdAQ6AEIRTAF#v=onepage&q=Rossmanith%20galanin%201996&f=false) (Accessed: 22 June 2017).

- Roger, V. L. (2013) 'Epidemiology of heart failure', *Circulation Research*, 113(6), pp. 646–659. doi: 10.1161/CIRCRESAHA.113.300268.
- Saraste, A. (1999) 'Morphologic criteria and detection of apoptosis.', *Herz*, 24(3), pp. 189–95. Available at: <http://www.ncbi.nlm.nih.gov/pubmed/10412642> (Accessed: 18 July 2017).
- Saudubray, T., Saudubray, C., Viboud, C., Jondeau, G., Valleron, A.-J., Flahault, A. and Hanslik, T. (2005) 'Prévalence et prise en charge de l'insuffisance cardiaque en France : enquête nationale auprès des médecins généralistes du réseau Sentinelles', *La Revue de Médecine Interne*, 26(11), pp. 845–850. doi: 10.1016/j.revmed.2005.04.038.
- Schmidhuber, S. M., Santic, R., Tam, C. W., Bauer, J. W., Kofler, B. and Brain, S. D. (2007) 'Galanin-Like Peptides Exert Potent Vasoactive Functions In Vivo', *Journal of Investigative Dermatology*, 127(3), pp. 716–721. doi: 10.1038/sj.jid.5700569.
- Schmidhuber, S. M., Starr, A., Wynick, D., Kofler, B. and Brain, S. D. (2008) 'Targeted Disruption of the Galanin Gene Attenuates Inflammatory Responses in Murine Skin', *Journal of Molecular Neuroscience*, 34(2), pp. 149–155. doi: 10.1007/s12031-007-9015-9.
- Schunkert, H., Broeckel, U., Hense, H. W., Keil, U., Riegger, G. A. and Pajak, A. (1998) 'Left-ventricular dysfunction.', *Lancet (London, England)*. Elsevier, 351(9099), p. 372. doi: 10.1016/S0140-6736(05)78298-2.
- Seger, R. and Krebs, E. G. (1995) 'The MAPK signaling cascade.', *FASEB journal : official publication of the Federation of American Societies for Experimental Biology*, 9(9), pp. 726–35. Available at: <http://www.ncbi.nlm.nih.gov/pubmed/7601337> (Accessed: 30 June 2017).
- Segura, A. M., Frazier, O. H. and Buja, L. M. (2014) 'Fibrosis and heart failure', *Heart Failure Reviews*, 19(2), pp. 173–185. doi: 10.1007/s10741-012-9365-4.
- Serdahl, S. a (2008) 'Heart failure: managing systolic dysfunction.', *Rn*, 71(6), p. 24–9; quiz 30. Available at: <http://www.ncbi.nlm.nih.gov/pubmed/18686917>.
- Sethi, T. and Rozengurt, E. (1991) 'Multiple Neuropeptides Stimulate Clonal Growth of Small Cell Lung Cancer: Effects of Bradykinin, Vasopressin, Cholecystokinin, Galanin, and Neurotensin', *Cancer Research*, 51(13). Available at: <http://cancerres.aacrjournals.org/content/51/13/3621.short> (Accessed: 30 June 2017).
- Seufferlein, T. and Rozengurt, E. (1996) 'Galanin, neurotensin, and phorbol esters rapidly stimulate activation of mitogen-activated protein kinase in small cell lung cancer cells.', *Cancer research*, 56(24), pp. 5758–64. Available at: <http://www.ncbi.nlm.nih.gov/pubmed/8971188> (Accessed: 30 June 2017).
- Shadiack, A. M. and Zigmond, R. E. (1998) 'Galanin induced in sympathetic neurons after axotomy is anterogradely transported toward regenerating nerve endings.', *Neuropeptides*, 32(3), pp. 257–64. Available at: <http://www.ncbi.nlm.nih.gov/pubmed/10189060> (Accessed: 18 July 2017).
- Sheeran, F. L. and Pepe, S. (2006) 'Energy deficiency in the failing heart: Linking increased reactive oxygen species and disruption of oxidative phosphorylation rate', *Biochimica et Biophysica Acta (BBA) - Bioenergetics*, 1757(5–6), pp. 543–552. doi: 10.1016/j.bbabiobio.2006.03.008.
- Shen, P. J., Larm, J. A. and Gundlach, A. L. (2003) 'Expression and plasticity of galanin

systems in cortical neurons, oligodendrocyte progenitors and proliferative zones in normal brain and after spreading depression', *European Journal of Neuroscience*. Blackwell Science, Ltd, 18(6), pp. 1362–1376. doi: 10.1046/j.1460-9568.2003.02860.x.

Sherin, J. E., Elmquist, J. K., Torrealba, F. and Saper, C. B. (1998) 'Innervation of Histaminergic Tuberomammillary Neurons by GABAergic and Galaninergic Neurons in the Ventrolateral Preoptic Nucleus of the Rat', *Journal of Neuroscience*, 18(12). Available at: <http://www.jneurosci.org/content/18/12/4705.short> (Accessed: 22 June 2017).

Smith-White, M. A., Iismaa, T. P. and Potter, E. K. (2003) 'Galanin and neuropeptide Y reduce cholinergic transmission in the heart of the anaesthetised mouse', *British Journal of Pharmacology*, 140(1), pp. 170–178. doi: 10.1038/sj.bjp.0705404.

Smith, K. E., Forray, C., Walker, M. W., Jones, K. A., Tamm, J. A., Bard, J., Branchek, T. A., Linemeyer, D. L. and Gerald, C. (1997) 'Expression cloning of a rat hypothalamic galanin receptor coupled to phosphoinositide turnover', *Journal of Biological Chemistry*, 272(39), pp. 24612–24616. doi: 10.1074/jbc.272.39.24612.

Smith, K. E., Walker, M. W., Artymyshyn, R., Bard, J., Borowsky, B., Tamm, J. A., Yao, W. J., Vaysse, P. J., Branchek, T. A., Gerald, C. and Jones, K. A. (1998) 'Cloned human and rat galanin GALR3 receptors. Pharmacology and activation of G-protein inwardly rectifying K⁺ channels.', *The Journal of biological chemistry*, 273(36), pp. 23321–6. Available at: <http://www.ncbi.nlm.nih.gov/pubmed/9722565> (Accessed: 22 June 2017).

Sprague, A. H. and Khalil, R. A. (2009) 'Inflammatory cytokines in vascular dysfunction and vascular disease.', *Biochemical pharmacology*. NIH Public Access, 78(6), pp. 539–52. doi: 10.1016/j.bcp.2009.04.029.

Steininger, T. L., Gong, H., McGinty, D. and Szymusiak, R. (2001) 'Subregional organization of preoptic area/anterior hypothalamic projections to arousal-related monoaminergic cell groups.', *The Journal of comparative neurology*, 429(4), pp. 638–53. Available at: <http://www.ncbi.nlm.nih.gov/pubmed/11135241> (Accessed: 22 June 2017).

Sten Shi, T.-J., Zhang, X., Holmberg, K., Xu, Z.-Q. D. and Hökfelt, T. (1997) 'Expression and regulation of galanin-R2 receptors in rat primary sensory neurons: effect of axotomy and inflammation', *Neuroscience Letters*, 237(2), pp. 57–60. doi: 10.1016/S0304-3940(97)00805-7.

Stevenson, L., Allen, W. L., Turkington, R., Jithesh, P. V., Proutski, I., Stewart, G., Lenz, H.-J., Van Schaeybroeck, S., Longley, D. B. and Johnston, P. G. (2012) 'Identification of galanin and its receptor GalR1 as novel determinants of resistance to chemotherapy and potential biomarkers in colorectal cancer.', *Clinical cancer research: an official journal of the American Association for Cancer Research*. Europe PMC Funders, 18(19), pp. 5412–26. doi: 10.1158/1078-0432.CCR-12-1780.

Sugamura, K., Keaney, J. F. and Jr. (2011) 'Reactive oxygen species in cardiovascular disease.', *Free radical biology & medicine*. NIH Public Access, 51(5), pp. 978–92. doi: 10.1016/j.freeradbiomed.2011.05.004.

Sugimoto, T., Seki, N., Shimizu, S., Kikkawa, N., Tsukada, J., Shimada, H., Sasaki, K., Hanazawa, T., Okamoto, Y. and Hata, A. (2009) 'The galanin signaling cascade is a candidate pathway regulating oncogenesis in human squamous cell carcinoma', *Genes, Chromosomes and Cancer*, 48(2), pp. 132–142. doi: 10.1002/gcc.20626.

- Sutton, M. G. and Sharpe, N. (2000) 'Left ventricular remodeling after myocardial infarction: pathophysiology and therapy.', *Circulation*, 101(25), pp. 2981–8. doi: 10.1161/01.cir.101.25.2981.
- Talero, E., Sánchez-Fidalgo, S., Calvo, J. R. and Motilva, V. (2007) 'Chronic administration of galanin attenuates the TNBS-induced colitis in rats', *Regulatory Peptides*, 141(1–3), pp. 96–104. doi: 10.1016/j.regpep.2006.12.029.
- Talero, E., Sánchez-Fidalgo, S., Ramón Calvo, J. and Motilva, V. (2006) 'Galanin in the trinitrobenzene sulfonic acid rat model of experimental colitis', *International Immunopharmacology*, 6(9), pp. 1404–1412. doi: 10.1016/j.intimp.2006.04.016.
- Tatemoto, K., Rökaeus, Å., Jörnvall, H., McDonald, T. J. and Mutt, V. (1983) 'Galanin - a novel biologically active peptide from porcine intestine', *FEBS Letters*, 164(1), pp. 124–128. doi: 10.1016/0014-5793(83)80033-7.
- Taverne, Y. J. H. J., Bogers, A. J. J. C., Duncker, D. J. and Merkus, D. (2013) 'Reactive oxygen species and the cardiovascular system.', *Oxidative medicine and cellular longevity*. Hindawi, 2013, p. 862423. doi: 10.1155/2013/862423.
- Tiyyagura, S. R. and Pinney, S. P. (2006) 'Left ventricular remodeling after myocardial infarction: past, present, and future.', *The Mount Sinai journal of medicine, New York*, 73(6), pp. 840–51. doi: 10.1016/S0895-7061(00)01113-4.
- Tofighi, R., Barde, S., Palkovits, M., Höög, A., Hökfelt, T., Ceccatelli, S. and Hulting, A.-L. (2012) 'Galanin and its three receptors in human pituitary adenoma.', *Neuropeptides*. Churchill Livingstone, 46(5), pp. 195–201. doi: 10.1016/j.npep.2012.07.003.
- Tsutsui, H., Kinugawa, S. and Matsushima, S. (2011) 'Oxidative stress and heart failure', *AJP: Heart and Circulatory Physiology*, 301(6), pp. H2181–H2190. doi: 10.1152/ajpheart.00554.2011.
- Tuechler, C., Hametner, R., Jones, N., Jones, R., Iismaa, T. P., Sperl, W. and Kofler, B. (1998) 'Galanin and galanin receptor expression in neuroblastoma.', *Annals of the New York Academy of Sciences*, 863, pp. 438–41. Available at: <http://www.ncbi.nlm.nih.gov/pubmed/9928194> (Accessed: 30 June 2017).
- Tuppin, P., Cuerq, A., De Peretti, C., Fagot-Campagna, A., Danchin, N., Juilliére, Y., Alla, F., Allemand, H., Bauters, C., Drici, M. D., Hagège, A., Jondeau, G., Jourdain, P., Leizorovicz, A. and Paccaud, F. (2013) 'First hospitalization for heart failure in France in 2009: Patient characteristics and 30-day follow-up', *Archives of Cardiovascular Diseases*, 106(11), pp. 570–585. doi: 10.1016/j.acvd.2013.08.002.
- Udelson, J. E. (2011) 'Heart Failure With Preserved Ejection Fraction', *Circulation*, 124(21). Available at: <http://circ.ahajournals.org/content/124/21/e540> (Accessed: 18 July 2017).
- Ulman, L. G., Moriarty, M., Potter, E. K. and McCloskey, D. I. (1993) 'Galanin antagonist effects on cardiac vagal inhibitory actions of sympathetic stimulation in anaesthetized cats and dogs.', *The Journal of physiology*. Wiley-Blackwell, 464, pp. 491–9. Available at: <http://www.ncbi.nlm.nih.gov/pubmed/7693918> (Accessed: 3 July 2017).
- Vrontakis, M. E., Peden, L. M., Duckworth, M. L. and Friesen, H. G. (1987) 'Isolation and characterization of a complementary DNA (galanin) clone from estrogen-induced pituitary tumor messenger RNA.', *Journal of Biological Chemistry*, 262(35), pp. 16755–16758.

Wang, S., Hashemi, T., Fried, S., Clemons, A. L. and Hawes, B. E. (1998) 'Differential intracellular signaling of the GalR1 and GalR2 galanin receptor subtypes', *Biochemistry*, 37(19), pp. 6711–6717. doi: 10.1021/bi9728405.

Wang, S., He, C., Hashemi, T. and Bayne, M. (1997) 'Cloning and expressional characterization of a novel galanin receptor. Identification of different pharmacophores within galanin for the three galanin receptor subtypes.', *The Journal of biological chemistry*, 272(51), pp. 31949–52. Available at: <http://www.ncbi.nlm.nih.gov/pubmed/9405385> (Accessed: 22 June 2017).

Wilcken, D. E. L. (2015) 'Physiology of the normal heart', *Surgery (United Kingdom)*, 33(2), pp. 43–46. doi: 10.1016/j.mpsur.2014.11.001.

Wittau, N., Grosse, R., Kalkbrenner, F., Gohla, A., Schultz, G. and Gudermann, T. (2000) 'The galanin receptor type 2 initiates multiple signaling pathways in small cell lung cancer cells by coupling to Gq, Gi and G12 proteins', *Oncogene*, 19(37), pp. 4199–4209. doi: 10.1038/sj.onc.1203777.

Wrenn, C. C. and Crawley, J. N. (2001) 'Pharmacological evidence supporting a role for galanin in cognition and affect', *Progress in Neuro-Psychopharmacology and Biological Psychiatry*, 25(1), pp. 283–299. doi: 10.1016/S0278-5846(00)00156-1.

WYNICK, D., SMALL, C. J., BLOOM, S. R. and PACHNIS, V. (1998) 'Targeted Disruption of the Murine Galanin Gene a', *Annals of the New York Academy of Sciences*. Blackwell Publishing Ltd, 863(1 GALANIN), pp. 22–47. doi: 10.1111/j.1749-6632.1998.tb10681.x.

Xu, X.-J., Wiesenfeld-Hallin, Z., Fisone, G., Bartfai, T. and Hökfelt, T. H. (1990) 'The N-terminal 1-16, but not C-terminal 17-29, galanin fragment affects the flexor reflex in Rats', *European Journal of Pharmacology*, 182, pp. 137–141. Available at: http://ac.els-cdn.com/001429999090502W/1-s2.0-001429999090502W-main.pdf?_tid=1aa05d86-5fe1-11e7-a720-00000aacb35d&acdnat=1499080788_b60e8f2d85bae0488e448e2cd3b61cc2 (Accessed: 3 July 2017).

Xu, X. J., Farkas-Szallasi, T., Lundberg, J. M., Hökfelt, T., Wiesenfeld-Hallin, Z. and Szallasi, A. (1997) 'Effects of the capsaicin analogue resiniferatoxin on spinal nociceptive mechanisms in the rat: behavioral, electrophysiological and in situ hybridization studies.', *Brain research*, 752(1–2), pp. 52–60. Available at: <http://www.ncbi.nlm.nih.gov/pubmed/9106440> (Accessed: 3 July 2017).

Xu, Z.-Q. ., Zhang, X., Pieribone, V. ., Grillner, S. and Hökfelt, T. (1998) 'Galanin–5-hydroxytryptamine interactions: electrophysiological, immunohistochemical and in situ hybridization studies on rat dorsal raphe neurons with a note on galanin R1 and R2 receptors', *Neuroscience*, 87(1), pp. 79–94. doi: 10.1016/S0306-4522(98)00151-1.

Xu, Z. Q., Shi, T. J., Landry, M. and Hökfelt, T. (1996) 'Evidence for galanin receptors in primary sensory neurones and effect of axotomy and inflammation.', *NeuroReport*, 8(1), pp. 237–242.

Yellon, D. M. and Hausenloy, D. J. (2007) 'Myocardial Reperfusion Injury', *New England Journal of Medicine*. Massachusetts Medical Society , 357(11), pp. 1121–1135. doi: 10.1056/NEJMra071667.

Yuzefpolskaya, M., Weinberg, C. and Kukin, M. (2010) 'Advances in systolic heart failure',

F1000 medicine reports, 2(6023), pp. 1439–43. doi: 10.3410/M2-31.

Zannad, F., McMurray, J. J. V., Krum, H., van Veldhuisen, D. J., Swedberg, K., Shi, H., Vincent, J., Pocock, S. J. and Pitt, B. (2011) ‘Eplerenone in Patients with Systolic Heart Failure and Mild Symptoms’, *New England Journal of Medicine*. Massachusetts Medical Society , 364(1), pp. 11–21. doi: 10.1056/NEJMoa1009492.

Zhang, Z., Fang, P., He, B., Guo, L., Runesson, J., Langel, Ü., Shi, M., Zhu, Y., Bo, P., Langel, ??lo, Shi, M., Zhu, Y. and Bo, P. (2016) ‘Central Administration of Galanin Receptor 1 Agonist Boosted Insulin Sensitivity in Adipose Cells of Diabetic Rats’, *Journal of Diabetes Research*. Hindawi Publishing Corporation, 2016, p. 9095648. doi: 10.1155/2016/9095648.

Zhang, Z., Gu, C., Fang, P., Shi, M., Wang, Y., Peng, Y., Bo, P. and Zhu, Y. (2014) ‘Endogenous galanin as a novel biomarker to predict gestational diabetes mellitus’, *Peptides*, 54, pp. 186–189. doi: 10.1016/j.peptides.2014.01.024.

Zhu, Y., Bo, P., Zhang, Z., Fang, P., Guo, L., He, B. and Shi, M. (2017) ‘Cellular Physiology and Biochemistry Cellular Physiology and Biochemistry Akt2-Dependent Beneficial Effect of Galanin on Insulin-Induced Glucose Uptake in Adipocytes of Diabetic Rats’, *Cell Physiol Biochem*, 41, pp. 1777–1787. doi: 10.1159/000471870.

Zorrilla, E. P., Brennan, M., Sabino, V., Lu, X. and Bartfai, T. (2007) ‘Galanin type 1 receptor knockout mice show altered responses to high-fat diet and glucose challenge’, *Physiology and Behavior*, 91(5), pp. 479–485. doi: 10.1016/j.physbeh.2006.11.011.

Zuily, S., Jourdain, P., Decup, D., Agrinier, N., Loiret, J., Groshens, S., Funck, F., Bellorini, M., Juilliére, Y. and Alla, F. (2010) ‘Impact of heart failure management unit on heart failure-related readmission rate and mortality’, *Archives of Cardiovascular Diseases*, 103(2), pp. 90–96. doi: 10.1016/j.acvd.2009.12.006.

ANNEXES

Manuscrit 1: Inhibition of PIKfyve prevents myocardial apoptosis and hypertrophy through activation of SIRT3 in obese mice.

Manuscrit 2: Apelin-13 administration protects against ischaemia/reperfusion-mediated apoptosis through the FoxO1 pathway in high-fat diet-induced obesity.

Manuscrit 3: Apelin regulates FoxO3 translocation to mediate cardioprotective responses to myocardial injury and obesity.

Inhibition of PIKfyve prevents myocardial apoptosis and hypertrophy through activation of SIRT3 in obese mice

Helene Tronchere^{1,2,†}, Mathieu Cinato^{1,2,†}, Andrei Timotin^{1,2}, Laurie Guitou^{1,2}, Camille Villedieu³, Helene Thibault³, Delphine Baetz³, Bernard Payrastre^{1,2}, Philippe Valet^{1,2}, Angelo Parini^{1,2}, Oksana Kunduzova^{1,2}  & Frederic Boal^{1,2,*} 

Abstract

PIKfyve is an evolutionarily conserved lipid kinase that regulates pleiotropic cellular functions. Here, we identify PIKfyve as a key regulator of cardiometabolic status and mitochondrial integrity in chronic diet-induced obesity. *In vitro*, we show that PIKfyve is critical for the control of mitochondrial fragmentation and hypertrophic and apoptotic responses to stress. We also provide evidence that inactivation of PIKfyve by the selective inhibitor STA suppresses excessive mitochondrial ROS production and apoptosis through a SIRT3-dependent pathway in cardiomyoblasts. In addition, we report that chronic STA treatment improves cardiometabolic profile in a mouse model of cardiomyopathy linked to obesity. We provide evidence that PIKfyve inhibition reverses obesity-induced cardiac mitochondrial damage and apoptosis by activating SIRT3. Furthermore, treatment of obese mice with STA improves left ventricular function and attenuates cardiac hypertrophy. In contrast, STA is not able to reduce isoproterenol-induced cardiac hypertrophy in SIRT3.KO mice. Altogether, these results unravel a novel role for PIKfyve in obesity-associated cardiomyopathy and provide a promising therapeutic strategy to combat cardiometabolic complications in obesity.

Keywords apoptosis; cardiac hypertrophy; mitochondria; PIKfyve; SIRT3

Subject Categories Cardiovascular System; Metabolism

DOI 10.1525/ emmm.201607096 | Received 21 September 2016 | Revised 14

March 2017 | Accepted 15 March 2017 | Published online 10 April 2017

EMBO Mol Med (2017) 9: 770–785

Introduction

Global increase in rates of obesity-associated cardiovascular complications poses a major challenge to overall population health (Battiprolu *et al.*, 2012). Obesity has been linked to a spectrum of

changes in metabolic status and cardiac phenotype with reduced contractility, left ventricular hypertrophy and heart failure (Battiprolu *et al.*, 2012). Given the limited capacity of the heart for regeneration, the progression of these abnormalities in obese patients poses a major threat. However, the specific mechanisms through which obesity triggers the decline of cardiac function remain unclear. A fragile balance between survival and death exists in cardiac cells undergoing pathologic stress, and activation of apoptotic machinery leads to premature cell death and heart failure progression (Barouch *et al.*, 2006). This loss of cardiomyocytes may be secondary to mitochondrial dysfunction caused by chronic exposure to reactive oxygen species (ROS) in obese conditions (Bournat & Brown, 2010; Tsutsui *et al.*, 2011). However, to date, effective therapeutic tools that control both metabolic and cardiac abnormalities in obese patients are elusive.

The evolutionarily conserved lipid kinase PIKfyve that synthesizes PI5P and PI(3,5)P₂ has been implicated in a diverse range of cellular processes, including cell proliferation, migration, tyrosine kinase receptor signaling, and membrane trafficking (Shisheva, 2008). PIKfyve is ubiquitously expressed in mammals, including in cardiac tissue (Ikonomov *et al.*, 2013), and the total knockout is embryonic lethal in mice (Ikonomov *et al.*, 2011). It contains a FYVE domain which binds to PI3P on endosomes and is responsible for its intracellular localization (Sbrissa *et al.*, 2002b). Expression of a PIKfyve dominant negative mutant (Ikonomov *et al.*, 2001), epigenetic or pharmacological inhibition of PIKfyve (Jefferies *et al.*, 2008) induces the formation of enlarged endosomal vacuoles, indicating its critical role in the maintenance of the endo-lysosomal membrane homeostasis. Recently, a new potent and highly selective PIKfyve inhibitor has been characterized, shedding light on a new role for PIKfyve in inflammation and autoimmune diseases (Cai *et al.*, 2013). Indeed, this inhibitor, known as apilimod or STA-5326 (referred to STA throughout this study), shows great potency to reduce the production of pro-inflammatory cytokines and TLR signaling in dendritic cells and monocytes. STA has been tested in patients with

1 INSERM U1048 I2MC, Toulouse, Cedex 4, France

2 Université Paul Sabatier, Toulouse, France

3 CarMeN Laboratory, Inserm U1060, Univ-Lyon, Université Claude Bernard Lyon 1, Bron, France

*Corresponding author. Tel: +33 531224117; E-mail: frederic.boal@inserm.fr

†These authors contributed equally to this work

rheumatoid arthritis (Krausz *et al*, 2012), psoriasis (Wada *et al*, 2012), and Crohn's disease (Billich, 2007). To date, there are no reports concerning the effects of STA on cardiac and metabolic disorders.

In this study, we unravel a critical role of PIKfyve in the regulation of cardiometabolic status in obesity-induced phenotype. We provide evidence that chronic inhibition of PIKfyve by STA attenuates obesity-related cardiometabolic phenotype by reducing mitochondrial oxidative stress and apoptosis through the deacetylase SIRT3. Therefore, these data pave the way to new promising therapeutic strategies to prevent cardiometabolic complications in obesity.

Results

STA treatment attenuates hypertrophic response and mitochondrial ROS production in cardiomyoblasts

Oxidative and metabolic stresses are key factors in the pathogenesis of obesity-related diseases (Bournat & Brown, 2010; Tsutsui *et al*, 2011). To investigate whether PIKfyve activity is affected in conditions of metabolic or oxidative stress, we measured PI5P levels in H9C2 cells subjected to hypoxia-induced oxidative stress or 2-deoxy-D-glucose (2DG)-induced metabolic stress. We found a ~fivefold increase in PI5P levels in H9C2 cells in response to hypoxic (Fig 1A) or 2DG stimulations (Fig 1B) as measured by mass assay. This PI5P synthesis was totally abrogated by the selective PIKfyve inhibitor STA, providing the first evidence that stress-induced cellular responses are linked to PIKfyve activity. Interestingly, we found that basal levels of PI5P are refractory to STA treatment in cardiomyoblasts.

Cardiac hypertrophy is a potent predictor of cardiovascular risk in obesity (Battiprolu *et al*, 2012). To examine the potential role of the lipid kinase PIKfyve in hypertrophic responses to stress, we evaluated the effects of its pharmacological inhibition by STA on hypoxia-induced hypertrophy in cardiomyoblasts. As shown in Fig 1C, STA treatment of H9C2 cells induced the formation of enlarged vacuoles, a hallmark of PIKfyve inhibition (Ikonomov *et al*, 2001; Jefferies *et al*, 2008). As described by Dupuis-Coronas *et al* (2011) and others (Jefferies *et al*, 2008) in various cell types, the formation of these endosomal vacuoles did not impede H9C2 cell viability (Fig EV1A), even at high concentration. Strikingly, STA treatment abrogated hypoxia-induced hypertrophic responses as

shown by measuring the cell surface (Fig 1C) and quantification of the hypertrophic marker β -MHC (Fig 1D). Cell hypertrophy is closely linked to ROS production by mitochondria, a major site for ROS production (Sawyer *et al*, 2002); therefore, we next investigated whether PIKfyve inhibition affects hypoxia-induced mitochondrial ROS production. Remarkably, H9C2 cells treated with STA presented a reduced level of mitochondrial O_2^- (Fig 1E, MitoSOX) and H_2O_2 (Fig 1E, MitoPY1) in response to hypoxic stress. Moreover, PIKfyve inhibition by STA attenuated 2DG-induced mitochondrial ROS production in H9C2 cells (Fig 1F). In order to confirm STA specificity toward PIKfyve, we resorted to siRNA-mediated silencing of PIKfyve in H9C2 cells. Silencing efficiency was monitored by qRT-PCR (Fig EV1B). Notably, we found that PIKfyve silencing prevented hypoxia-induced ROS production to the same extent as STA treatment (Fig EV1C). Interestingly, we demonstrated that in cells depleted for PIKfyve, STA has no further effect on hypoxia-induced ROS generation, validating PIKfyve as the target for the anti-oxidant properties of STA.

PIKfyve inhibition prevents stress-induced cell apoptosis and mitochondrial structural damage

Mitochondrial damage and excessive ROS production may result in activation of apoptotic cascades and cell death (Tsutsui *et al*, 2011). As shown in Fig 2, in response to hypoxia, STA treatment of H9C2 cells attenuated apoptosis as shown by TUNEL staining (Fig 2A) and cleavage of caspase 3, a bona fide marker of apoptotic cascade activation (Fig 2B). Importantly, STA-dependent anti-apoptotic activity was confirmed in conditions of metabolic stress induced by 2DG (Fig 2C and D).

One of the hallmarks of apoptosis is the fragmentation of the mitochondrial network (Youle & Karbowski, 2005). Therefore, we next examined whether inhibition of PIKfyve could affect stress-induced mitochondrial fragmentation. While control cells harbored a typical elongated and interconnected mitochondrial network, both hypoxia (Fig 2E) and 2DG (Fig 2F) resulted in mitochondrial fragmentation. Strikingly, PIKfyve inhibition by STA prevented mitochondrial fragmentation induced by both oxidative (Fig 2E) and metabolic stresses (Fig 2F) suggesting STA-dependent preservation of mitochondrial integrity. Notably, depletion of PIKfyve by siRNA recapitulated STA effect on the preservation of mitochondrial structures upon hypoxic stress (Fig EV1D).

Mitochondrial fragmentation is mediated by recruitment of the small cytosolic GTPase dynamin-related protein 1 (Drp1) at the

Figure 1. Inhibition of PIKfyve by STA reduces cardiomyoblast hypertrophic response and mitochondrial ROS production.

- A Rat H9C2 cardiomyoblasts were subjected to hypoxia (H) or kept in normoxia (N) in the presence of STA or vehicle only (DMSO). PI5P levels were measured by mass assay to address PIKfyve activation (left panel). Quantification of PI5P from independent experiments is shown on the right panels ($n = 3\text{--}5$).
- B Same as in (A) but cells were exposed to 2DG-induced metabolic stress.
- C H9C2 cells were subjected to hypoxia (H) to induce cell hypertrophy or kept in normoxia (N) in the presence of STA or vehicle only (DMSO). Phase contrast images are shown (left panel). Scale bar is 25 μm . Cell surface was quantified from 239 to 279 cells across three independent experiments.
- D qRT-PCR quantification of the expression level of the hypertrophic marker β -MHC from three to six independent experiments.
- E, F H9C2 cells were exposed to oxidative- (E) or 2DG-induced metabolic (F) stress as indicated and mitochondrial O_2^- production or mitochondrial H_2O_2 were assessed using the MitoSOX Red fluorescent probe and MitoPY1 probe, respectively (left panels). Scale bar is 10 μm . Quantifications are shown on the right panels ($n = 16\text{--}81$).

Data information: Data are presented as mean \pm SEM. Two-way ANOVA followed by Bonferroni's *post hoc* test: *** $P < 0.001$, ** $P < 0.01$, and * $P < 0.05$ between indicated conditions. The exact P -values are specified in Appendix Table S1.

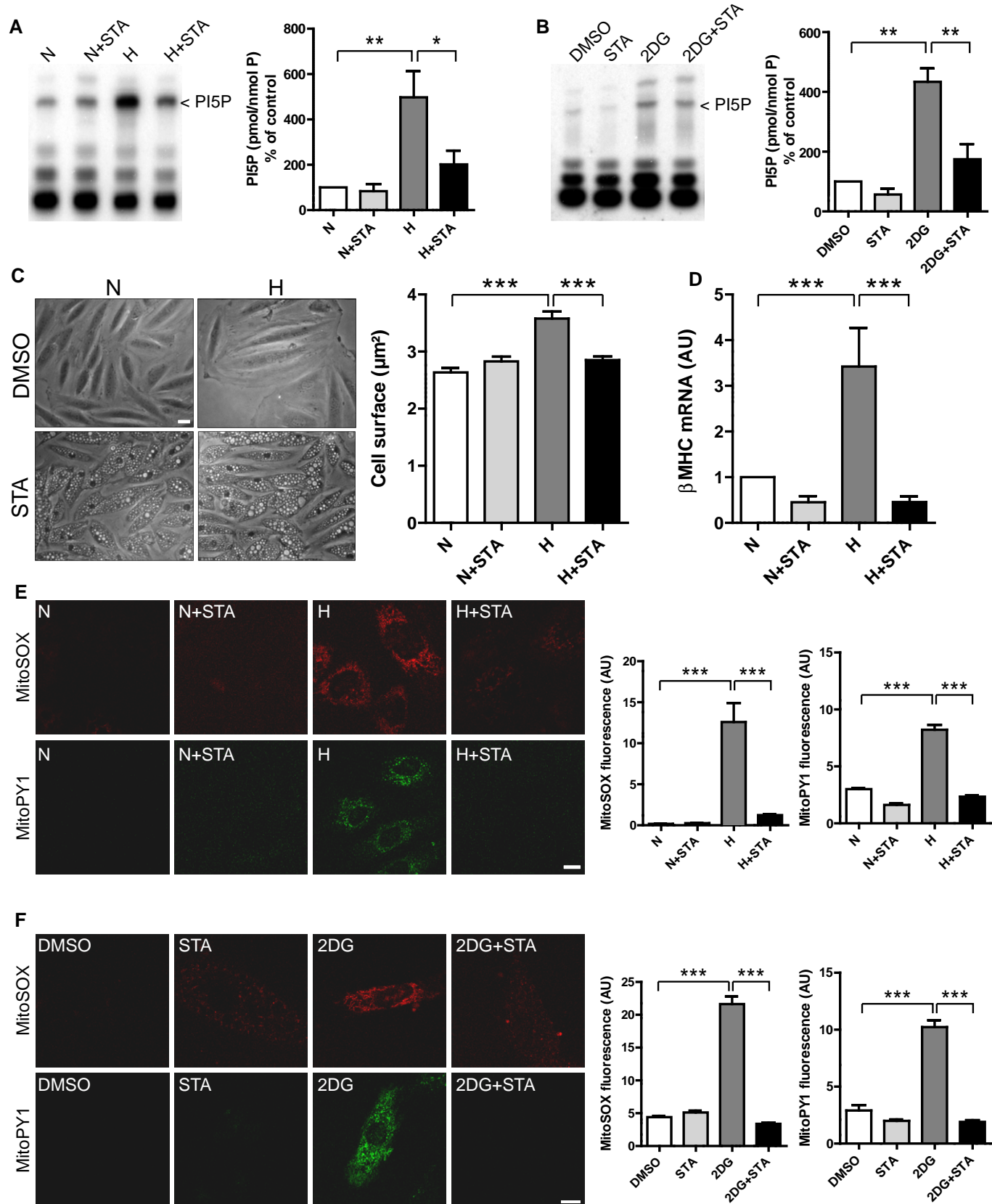


Figure 1.

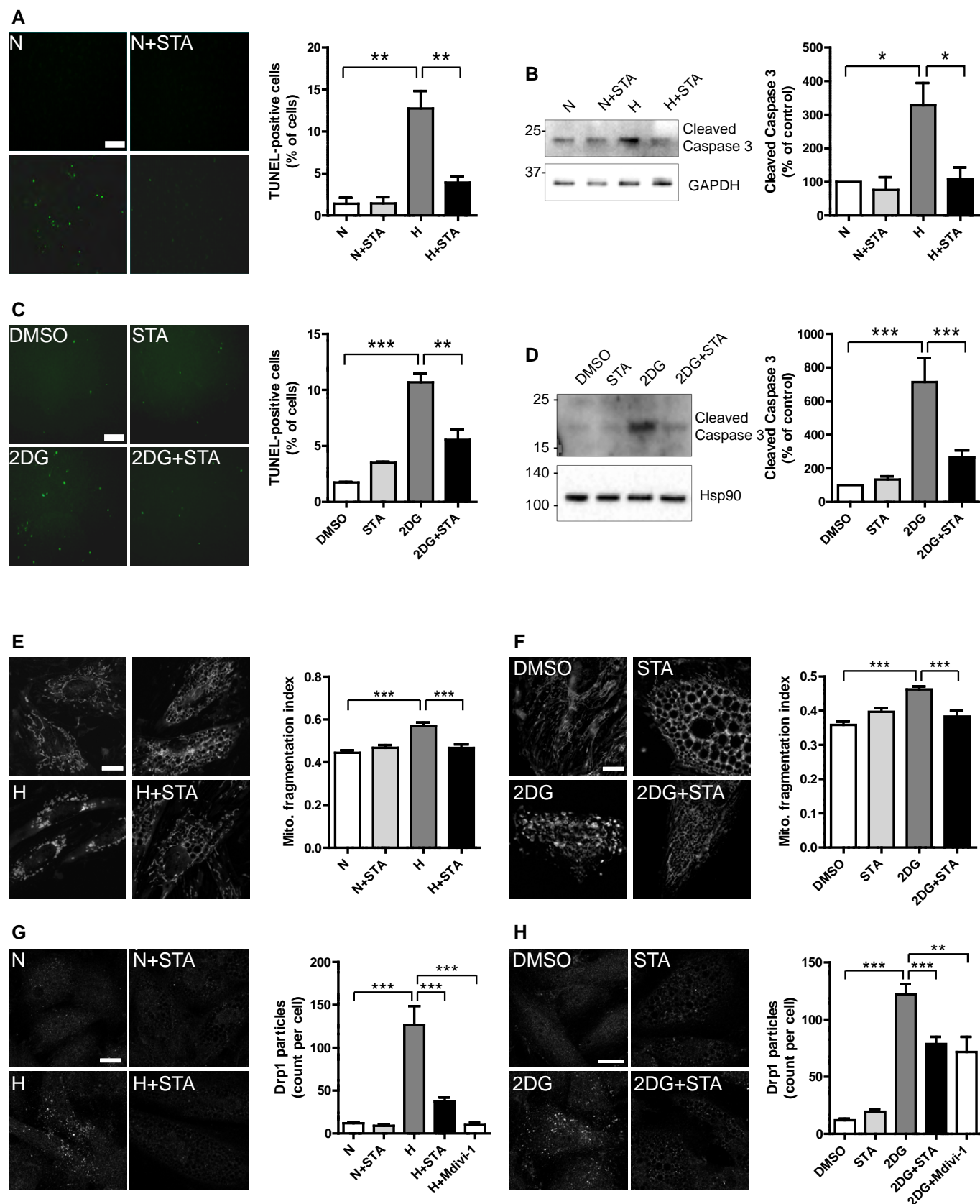


Figure 2.

Figure 2. STA treatment prevents cardiomyoblast apoptotic cell death and preserves mitochondrial structures.

- A TUNEL staining of apoptotic H9C2 cells treated as indicated (left panel). Scale bar is 50 μ m. Right panel shows quantification of apoptotic cells from three to four independent experiments.
- B Cell lysates from H9C2 cells treated as in (A) were probed with the indicated antibodies (left panel). Quantification of caspase 3 cleavage is shown on the right panel from three to four independent experiments.
- C TUNEL staining of apoptotic cells treated with 2-deoxy-D-glucose (2DG) in the presence or not of STA. Quantification is shown on the right panel from three to four independent experiments. Scale bar is 50 μ m.
- D Western blot of H9C2 cells treated as in (C). Results are from four independent experiments.
- E, F H9C2 cells were treated as indicated, and live-stained with MitoTracker Red to assess mitochondrial structures (left panels). Scale bar is 10 μ m. Mitochondrial fragmentation was quantified on thresholded images using a dedicated ImageJ plugin. Quantification of mitochondrial fragmentation is shown on the right panels ($n = 10–51$).
- G, H Self-assembly of Drp1 at mitochondrial fission sites was monitored by immunofluorescence on treated cells (left panels). Scale bar is 10 μ m. Quantification of the number of Drp1 punctae per cell is shown on the right panels ($n = 33–114$).

Data information: Data are presented as mean \pm SEM. Two-way ANOVA followed by Bonferroni's *post hoc* test: *** $P < 0.001$, ** $P < 0.01$, and * $P < 0.05$ between indicated conditions.

Source data are available online for this figure.

active fission site on the surface of mitochondria, which can be followed by immunofluorescence (Frank *et al*, 2001; Smirnova *et al*, 2001). As shown in Fig 2G and H, both oxidative (Fig 2G) and metabolic (Fig 2H) stresses induced the self-assembly of Drp1 in H9C2 cells. In these conditions, STA treatment reduced Drp1 assembly, to the same extent as the Drp1-specific inhibitor Mdivi-1 (Fig 2G and H). siRNA-mediated depletion of PIKfyve also led to the reduction in Drp1 self-assembly induced by hypoxia (Fig EV1E), demonstrating the implication of PIKfyve in the control of mitochondrial dynamics.

PIKfyve induces mitochondrial ROS production and apoptosis through a SIRT3-dependent pathway

In cardiac myocytes, the high density of mitochondria reflects the high energy demand needed to maintain contractile functions. Therefore, in order to maintain the redox cellular status and optimize the bioenergetic efficiency of the heart, the functioning of mitochondria is in turn tightly regulated. The NAD⁺-dependent lysine deacetylase SIRT3 has recently emerged as a key regulator of mitochondrial functions, through the control of the oxidative and metabolic status, mitochondrial dynamics, and apoptosis (Huang *et al*, 2010; McDonnell *et al*, 2015). SIRT3 is a nuclear-encoded protein and therefore needs to be translocated into the mitochondrial matrix to deacetylate its targets (Schwer *et al*, 2002). In order to test whether PIKfyve affects cardiac SIRT3, we first localized endogenous SIRT3 in H9C2 cells subjected to oxidative stress in the presence of STA. In control cells, SIRT3 was found mainly cytosolic (Fig 3A). Interestingly, a strong translocation of SIRT3 to the mitochondria was induced by STA treatment independently of stress stimuli (Fig 3A and B). This mitochondrial enrichment was confirmed biochemically by isolating mitochondria from control or STA-treated cells (Fig 3C and D). Importantly, the localization of the nuclear SIRT1 was not altered by STA treatment (Fig 3E), suggesting a specificity toward SIRT3. In order to confirm the results obtained with the pharmacological inhibition of PIKfyve, we examined SIRT3 localization in H9C2 cells silenced for PIKfyve expression using siRNA. As shown in Fig 3F, knockdown of PIKfyve in H9C2 cells resulted in a strong translocation of SIRT3 to the mitochondrion without changes in SIRT1 localization.

Next, in order to determine whether SIRT3 is involved in PIKfyve regulation of mitochondrial ROS generation and apoptosis, we resorted to its silencing using specific siRNA. Knockdown efficiency was confirmed by qRT-PCR (Fig EV2). We hypothesized that SIRT3 depletion may result in the loss of STA-induced anti-oxidant and anti-apoptotic activities. As shown in Fig 4, in conditions of metabolic stress, SIRT3 silencing totally prevented STA effects on mitochondrial ROS production (Fig 4A and B) and cell apoptosis (Fig 4C and D). These results point to an unprecedented role of PIKfyve in the control of mitochondrial ROS production, cell hypertrophy, and apoptosis through the control of SIRT3 pathway.

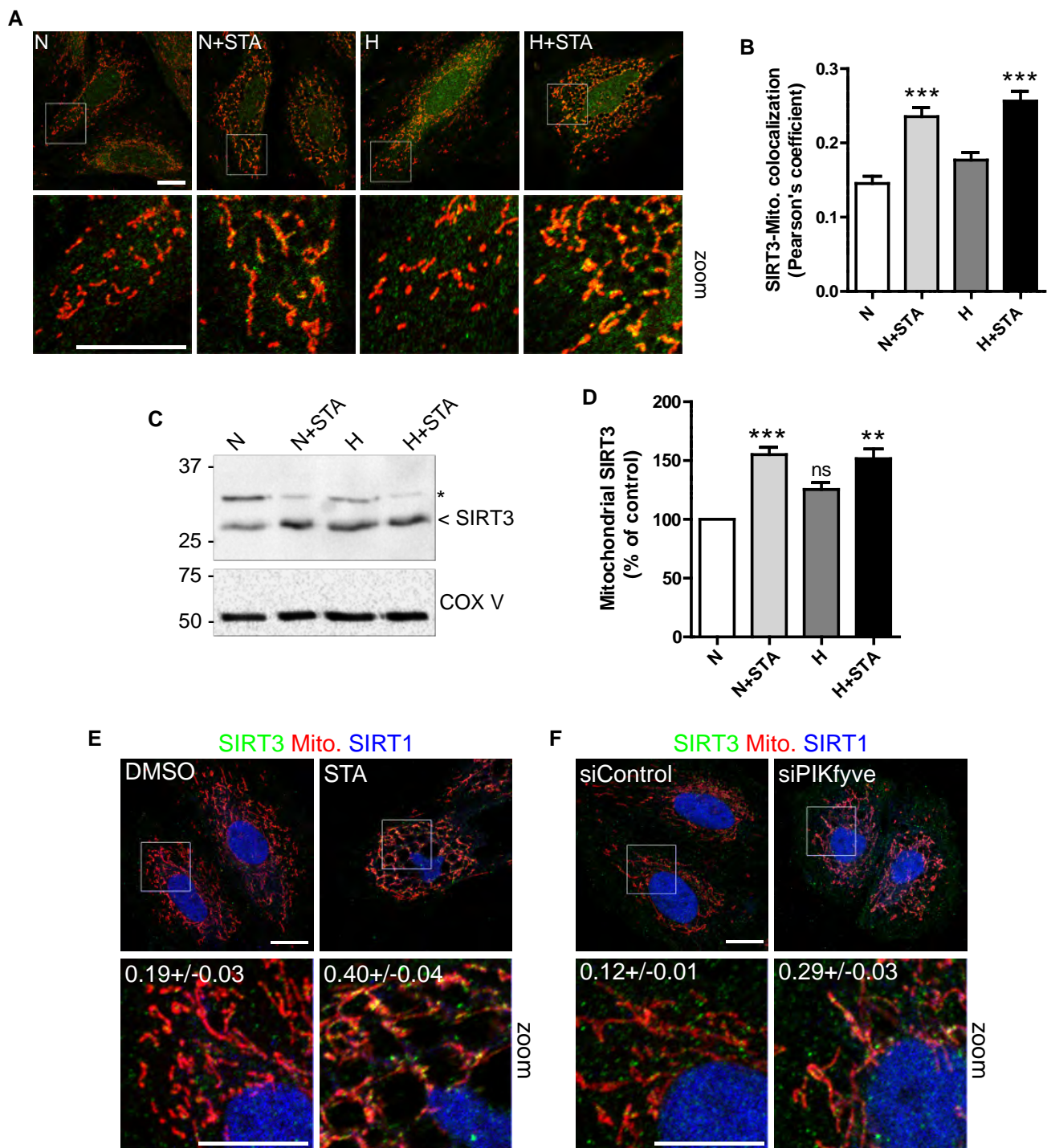
STA treatment reduces cardiac hypertrophy and improves cardiac function in a mouse model of diet-induced obesity

Considering the *in vitro* effects of STA on cellular responses to oxidative and metabolic stresses, we next examined whether PIKfyve inhibition could improve cardiometabolic phenotype in a mouse model of chronic high fat diet (HFD)-induced obesity. As shown in Table 1, the exposure of mice to HFD for 12 months resulted in the development of glucose intolerance, insulin resistance, and morphometric changes as compared with normal diet (ND) fed mice. Echocardiographic analysis revealed ventricular dysfunction characterized by the decreased ejection fraction (EF) and fractional shortening (FS) and cardiac hypertrophy as shown by elevated LVPWd and IVSTd in HFD-fed mice as compared to ND-fed mice (Fig 5A–E). Analysis of heart weight-to-body weight ratio (HW/BW, Fig 5F), cardiac myocyte cross-sectional area (Fig 5G),

Table 1. Metabolic parameters of mice under ND or HFD feeding.

Parameters	ND	HFD
Body weight (g)	42.8 \pm 2.1	51.7 \pm 1.8**
Fat mass (%)	9.6 \pm 0.8	19.6 \pm 2.2***
Glucose (mmol/l)	10.2 \pm 0.4	12.8 \pm 0.8**
IGTT AUCglucose	38,310 \pm 842	45,722 \pm 4,161*

Body weight, fat mass, plasma glucose, area under the curve of intraperitoneal glucose tolerance test (IGTT AUCglucose) were evaluated in male C57BL/6J mice after 12 months HFD or ND feeding. $n = 6–14$ per group. Data are means \pm SEM; Student's *t*-test, * $P < 0.05$, ** $P < 0.01$, and *** $P < 0.001$ versus ND-fed group.

**Figure 3.** PIKfyve inhibition induces SIRT3 translocation to the mitochondria.

A H9C2 cells were treated as indicated, mitochondria were live-stained with MitoTracker Red (in red), and the cells were fixed and stained for endogenous SIRT3 (in green) and imaged by confocal microscopy. Scale bar is 10 μ m.

B Quantification of the colocalization between SIRT3 and mitochondria in treated cells from (A). Data are presented as mean \pm SEM. Two-way ANOVA followed by Bonferroni's *post hoc* test: *** P < 0.001 as compared with control (n = 69–91).

C Mitochondria were isolated from H9C2 cells treated as indicated and blotted for SIRT3 and COX V as a control. Asterisk indicates non-specific band.

D Quantification of SIRT3 enrichment in mitochondria from (C). Data are presented as mean \pm SEM. Two-way ANOVA followed by Bonferroni's *post hoc* test: ** P < 0.01 and *** P < 0.001 as compared with control (n = 3). ns, non-significant.

E H9C2 cells were treated with STA as indicated, fixed and stained for endogenous SIRT3 (in green), SIRT1 (in blue). Mitochondria were live-stained with MitoTracker Red (in red). Scale bar is 10 μ m. Pearson's coefficients are indicated in the zoomed boxes as mean \pm SEM from three to four independent experiments.

F H9C2 cells were transfected with a control siRNA (siControl) or with a siRNA targeting PIKfyve (siPIKfyve), fixed and stained as in (E). Scale bar is 10 μ m.

Source data are available online for this figure.

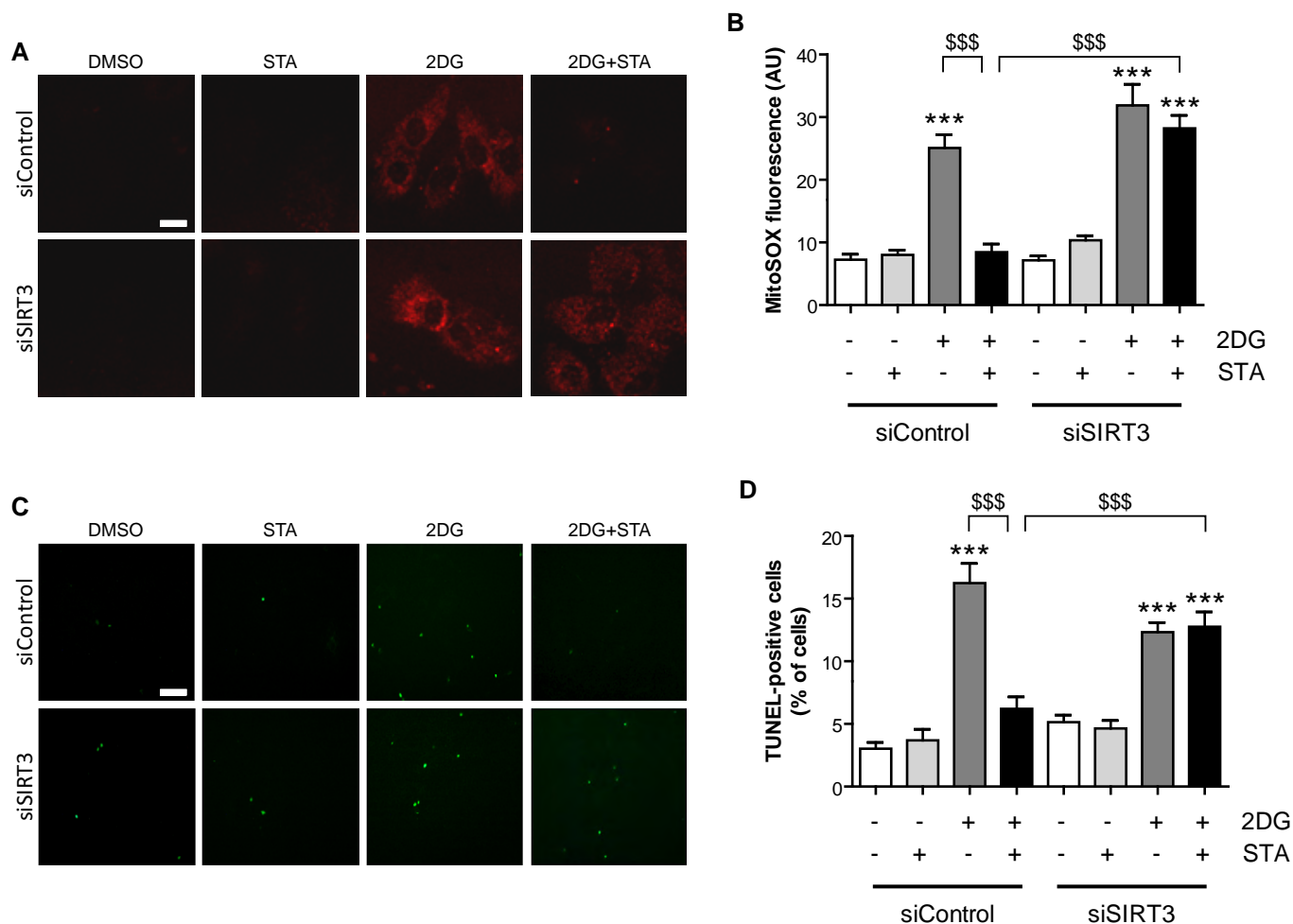


Figure 4. Endogenous SIRT3 is required for STA anti-oxidant and anti-apoptotic properties.

A H9C2 cells were transfected with a control siRNA (siControl) or with a siRNA targeting SIRT3 (siSIRT3), and cells were treated as indicated. Mitochondrial O₂⁻ production was assessed using the MitoSOX Red fluorescent probe. Scale bar is 10 μm.

B Quantification from (A) (*n* = 75–157).

C TUNEL staining of apoptotic cells treated as in (A). Scale bar is 50 μm.

D Quantification of apoptotic cells from (C) (*n* = 4–7).

Data information: Data are presented as mean ± SEM. One-way ANOVA followed by Bonferroni's *post hoc* test: ****P* < 0.001 as compared with control cells; \$\$\$*P* < 0.001 between indicated conditions.

and myocardial expression of hypertrophic markers β-MHC (Fig 5H) and BNP (Fig 5I) confirmed the induction of cardiac hypertrophy in HFD-fed mice as compared to ND-fed mice. In HFD-fed mice, PIKfyve inhibition prevented obesity-induced impairments in cardiac function and structure. Indeed, in HFD-fed mice, chronic treatment with STA improved cardiac function as shown by the increased EF and FS (Fig 5A–C). Compared to vehicle-treated HFD-fed mice, STA treatment reduced cardiac hypertrophy as shown by the decrease in the LVPWd and IVSTd (Fig 5D and E, respectively), HW/BW ratio (Fig 5F), cardiomyocyte cross-sectional area (Fig 5G), and myocardial expression of β-MHC and BNP (Fig 5H and I). Importantly, STA-dependent preservation of cardiac function was accompanied by a reduction in myocardial fibrosis as compared to vehicle-treated HFD-fed mice (Fig 5J). Moreover, STA treatment,

leading to reduced myocardial PI5P level (Fig EV3A), improved glucose tolerance as compared to vehicle-treated mice (Fig EV3B and C) without significant changes in body weight (44.8 g ± 3.3 in control versus 51.7 g ± 2.8 in STA-treated mice). In the same line, we found that STA did not change the amount of perigonadal adipose tissue (2.27% ± 0.16 in vehicle-treated mice versus 2.20% ± 0.11 in STA-treated mice, expressed as % of body weight), suggesting that STA treatment had no major effect on fat depot in obese mice. In addition, anti-glycemic activity of STA was associated with reduced levels of plasma triglycerides and myocardial content of lipid peroxide (LPO), an oxidative stress marker (Fig EV3D and E).

STA has been initially described for its anti-inflammatory properties (Cai *et al.*, 2013). In cardiac tissue from HFD-fed mice, STA

treatment did not significantly affect myocardial expression level of key inflammatory factors including IL-1 β , IL-12, IL-23, IL-6, TNF- α , and MCP1 (Fig EV4A). Moreover, no changes were detected in plasma IL-6 and TNF- α in STA-treated mice (Fig EV4B). This suggests that the cardioprotective effects of STA in cardiomyopathy linked to obesity are not due to its systemic anti-inflammatory properties.

PIKfyve inhibition prevents obesity-induced oxidative stress, cardiac apoptosis, and mitochondrial damage

Based on our *in vitro* data, we next asked whether PIKfyve inhibition was able to affect obesity-induced oxidative stress and cardiac apoptosis. Chronic consumption of HFD resulted in enhanced production of mitochondrial ROS (Fig 6A and B) and

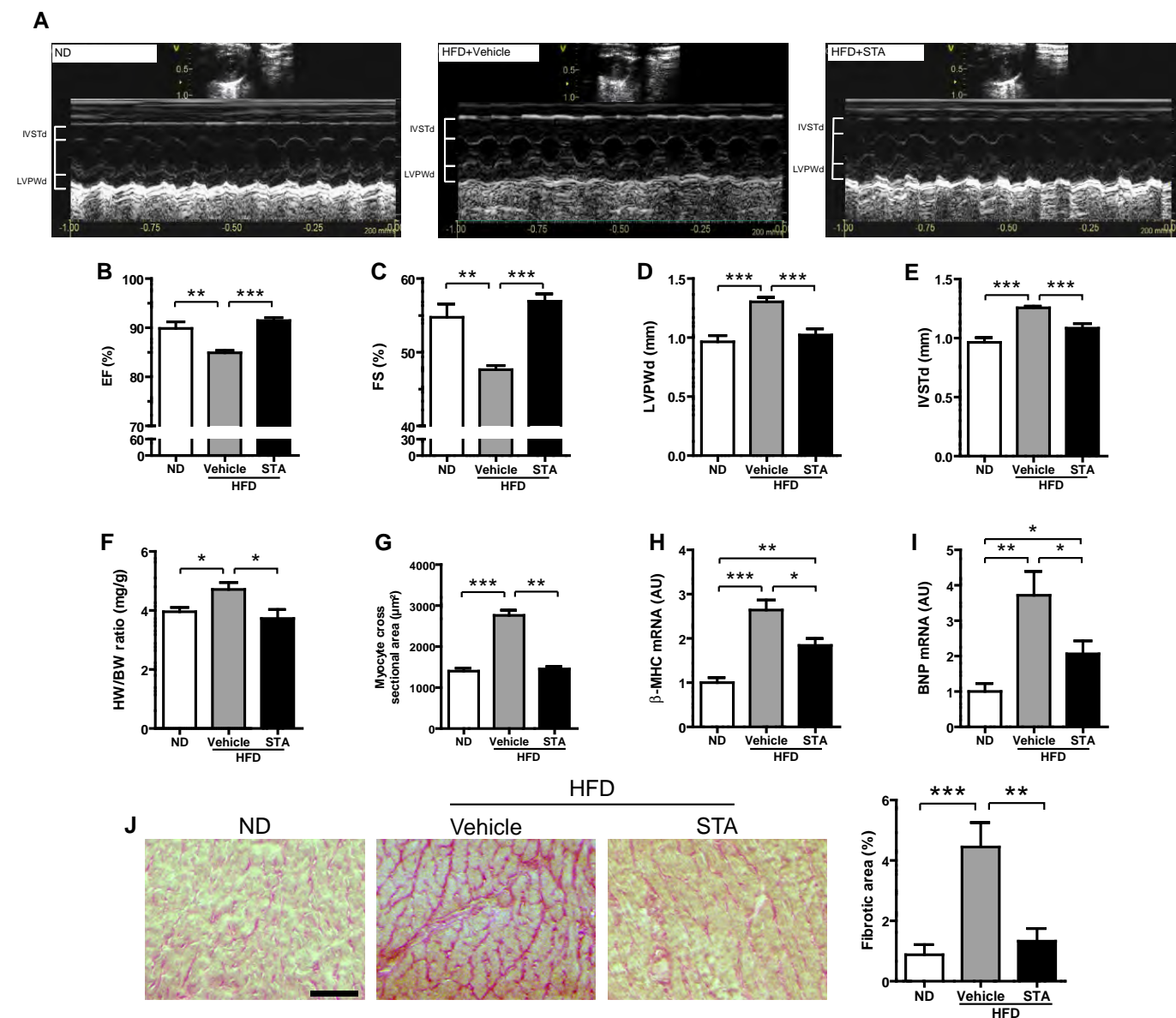


Figure 5. PIKfyve inhibition reduces cardiac hypertrophy and improves cardiac function *in vivo*.

- A Representative 2D-Mode echocardiographic images of non-obese (ND) or obese (HFD) mice treated intraperitoneally with STA or vehicle only (Vehicle).
- B–E Echocardiographic measures of ejection fraction (EF, B), fractional shortening (FS, C), left ventricular posterior wall thickness at end diastole (LVPWd, D) and interventricular septum thickness at end diastole (IVSTd, E) of ND or HFD vehicle- or STA-treated mice.
- F Quantification of the heart weight-to-body weight ratio (HW/BW).
- G Quantification of myocyte cross-sectional area from heart cryosections.
- H, I Expression levels of β -MHC (H) and BNP (I) were measured by qRT-PCR from cardiac tissues.
- J Cardiac fibrosis was quantified on heart cryosections stained with Sirius red. Scale bar is 100 μ m.

Data information: Data are presented as mean \pm SEM. Student's t-test, * P < 0.05; ** P < 0.01 *** P < 0.001 between indicated conditions, n = 4–8 mice per group.

activation of apoptosis (Fig 6C and E). Importantly, PIKfyve inhibition culminated in the reduction in mitochondrial O₂⁻ levels (Fig 6A and B) in HFD-fed mice. As compared to vehicle-treated mice, myocardial levels of apoptosis (Fig 6C and D) and pro-apoptotic factor Bax (Fig 6E) were significantly lower in STA-treated HFD-fed mice. Electron microscopy analysis of mitochondrial integrity in cardiac tissue from HFD-fed mice revealed ultrastructural changes including decreased mitochondrial size and fragmented rounded interfibrillar mitochondria (Fig 7A and B), a typical hallmark of cardiac injury (Ong *et al.*, 2010). In contrast, treatment of HFD-fed mice with STA preserved mitochondrial size and prevented mitochondrial damage as compared to vehicle-treated HFD-fed mice (Fig 7A and B). Defects in mitochondrial architecture are hallmarks for respiratory chain damage and ROS production. Therefore, we analyzed the expression profile of key complexes of the mitochondrial respiratory chain (OXPHOS complexes). Strikingly, in conditions of PIKfyve inhibition, we found an increased expression of mitochondrial-encoded genes in complexes I, II, III, IV, and V in cardiac tissue (Fig 7C and D) suggesting an improved respiratory efficiency.

PIKfyve inactivation drives cardiac SIRT3 pathways in obesity-related cardiometabolic phenotype

We next studied the activation status of SIRT3 in STA-treated mice. It has been recently shown that phosphorylation of SIRT3 on

Ser/Thr residues led to increased enzymatic activity in mitochondria (Liu *et al.*, 2015). Therefore, we performed immunoprecipitation of endogenous SIRT3 in heart extracts from control or STA-treated mice followed by immunoblot of phosphorylated proteins on serine residues. As shown in Fig 8A, STA treatment increased significantly the amount of phosphorylated SIRT3. Moreover, we investigated the acetylation status of two mitochondrial targets of SIRT3 involved in redox homeostasis, the superoxide dismutase 2 (SOD2) (Tao *et al.*, 2010) and the isocitrate dehydrogenase 2 (IDH2) (Yu *et al.*, 2012). STA treatment significantly reduced the amount of acetylated cardiac IDH2 (Fig 8B) and SOD2 (Fig 8C). Altogether, these data suggest that PIKfyve inhibition led to increased SIRT3 activity in hearts from obese mice.

STA loses its anti-hypertrophic properties in SIRT3.KO mice

In order to confirm the implication of SIRT3 in the anti-hypertrophic effects of STA, we evaluated the effects of PIKfyve inhibition in SIRT3.KO mice treated with isoproterenol (ISO) to induce cardiac hypertrophy (Fig 9A and B). As shown in Fig 9B and C, treatment with STA significantly prevented ISO-induced cardiac hypertrophy as measured by decreased IVSTd and cardiomyocyte cross-sectional area as compared to vehicle-treated WT mice. In contrast, STA-mediated effects on cardiac hypertrophy were totally abrogated in SIRT3.KO mice (Fig 9B and C) suggesting that SIRT3 is required for the anti-hypertrophic activity of STA.

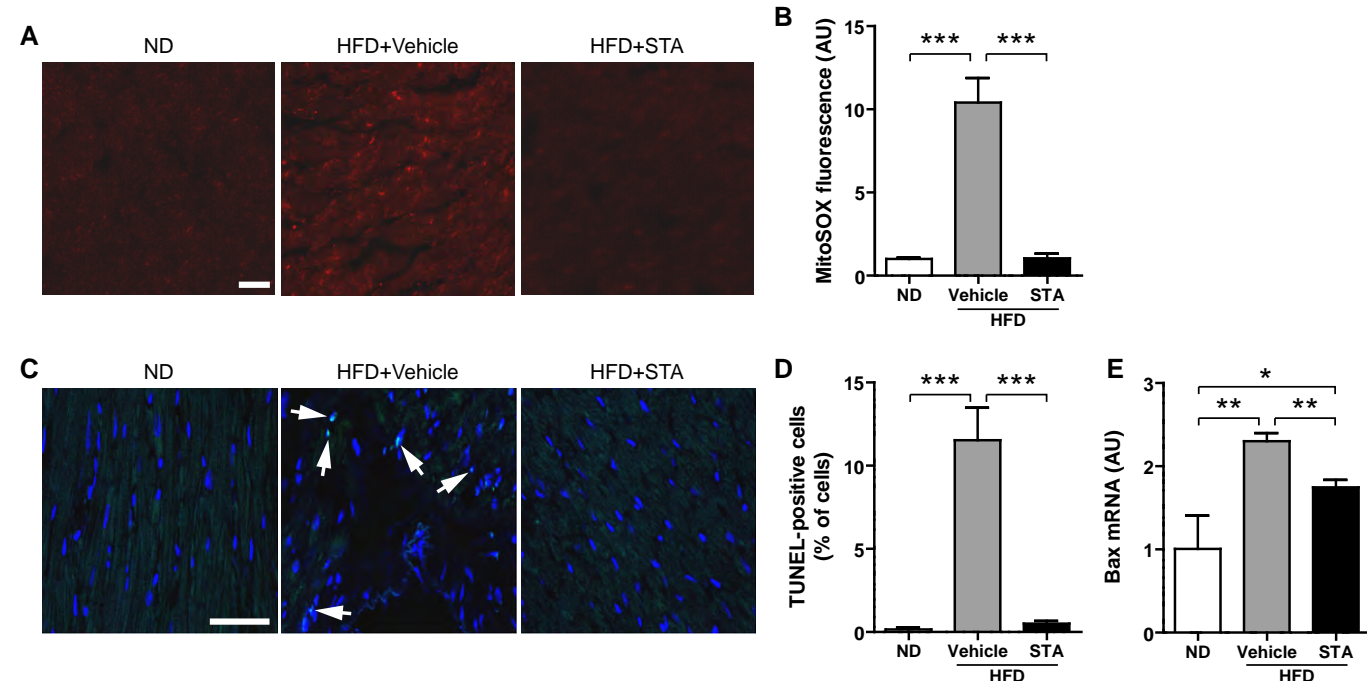


Figure 6. Inhibition of PIKfyve decreases cardiac oxidative stress and apoptosis induced by obesity.

A Mitochondria-derived O₂⁻ production was measured on heart cryosections using MitoSOX Red by confocal microscopy. Scale bar is 50 μm.

B Quantification of MitoSOX fluorescence from (A).

C TUNEL staining of heart cryosections showing apoptotic cells (arrows). The nuclei are stained in blue with DAPI. Scale bar is 50 μm.

D Quantification from (C).

E Bax expression level was measured by qRT-PCR from heart tissues.

Data information: Data are presented as mean ± SEM. Student's t-test, *P < 0.05; **P < 0.01 ***P < 0.001 between indicated conditions, n = 3–6 mice per group.

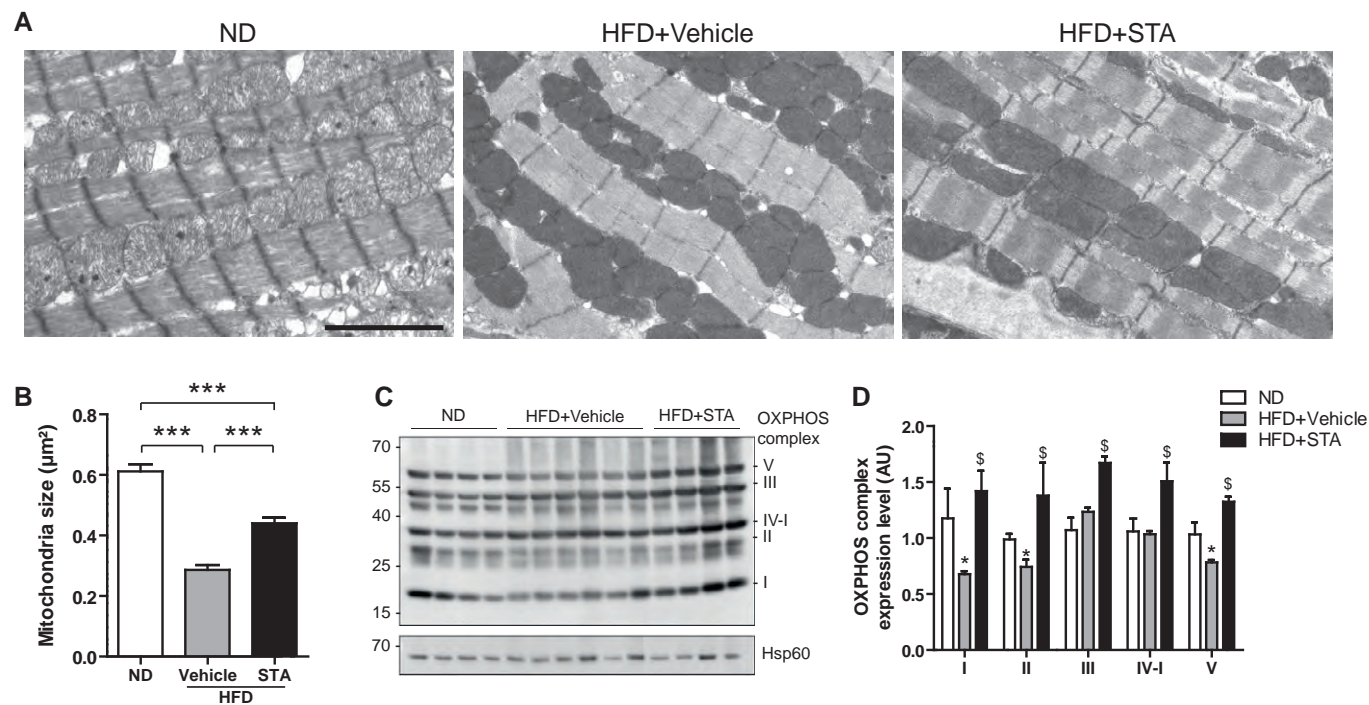


Figure 7. Chronic STA treatment reduces mitochondrial damages in obese mice.

A Electron micrographs showing preservation of myocardial mitochondrial structure in HFD STA-treated mice. Scale bar is 1 μm .

B Quantification of mitochondria size from (A). Data are presented as mean \pm SEM. Student's t-test, *** $P < 0.001$ between indicated conditions, $n = 4$ –6 mice per group.

C Expression of several OXPHOS complexes was measured by Western blot on heart lysates.

D Quantification of OXPHOS complexes expression from (C). Data are presented as mean \pm SEM. Student's t-test, * $P < 0.05$ as compared with ND, \$ $P < 0.05$ as compared with HFD+Vehicle. $n = 3$ –6 mice per group.

Source data are available online for this figure.

Finally, in order to investigate whether PIKfyve inhibition affects cardiac SIRT3 protein content in mitochondria under hypertrophic stimulation, we examined the level of mitochondrial SIRT3 in control or ISO-treated mice hearts. As shown in Fig 9D, ISO treatment induced a reduction in mitochondrial level of SIRT3, most likely due to mitochondrial damage induced by ISO (Bloom & Cancilla, 1969). Strikingly, STA treatment induced a strong accumulation of SIRT3 in the mitochondria (Fig 9D). Taken together, these results indicate that PIKfyve inhibition reduces cardiac hypertrophy through mitochondrial SIRT3 activation.

Discussion

Obesity is closely associated with cardiovascular and metabolic complications (Battiprolu *et al*, 2012). Increasing evidence suggests that abnormal mitochondrial ROS production and mitochondrial defects are at the center of the pathophysiology of the failing heart and metabolic disorders (Bournat & Brown, 2010; Tsutsui *et al*, 2011). The loss of mitochondrial integrity inevitably disturbs cell functions, sensitizes cells to stress and may trigger cell death, with potentially dramatic irreversible pathological consequences. In the present study, we unravel a critical role for the phosphoinositide kinase PIKfyve in the control of stress-induced mitochondrial

damage, ROS generation, apoptosis, and ventricular dysfunction in obesity-induced phenotype. Long-term HFD-induced obesity increases the heart workload, causes left ventricular hypertrophy, and impairs cardiac function (Battiprolu *et al*, 2012; Fuentes-Antrias *et al*, 2015). Our *in vitro* results demonstrate that inhibition of PIKfyve attenuated stress-induced hypertrophic responses in cardiomyoblasts. In addition, in a mouse model of obesity-induced phenotype, we show that chronic treatment with STA decreased ventricular hypertrophy, a major predictor of cardiovascular events, and improves left ventricular contractility, suggesting a tight association between myocardial PIKfyve activity and cardiac function in the setting of obesity.

Obesity is associated with metabolic disorders leading to the installation of type 2 diabetes (Battiprolu *et al*, 2012). The present study is the first report that demonstrates the efficacy of pharmacological inhibition of PIKfyve on glycemic status in obesity-induced type 2 diabetes. If the total knockout of PIKfyve in mice is lethal at embryonic stage (Ikonomov *et al*, 2011), the generation of tissue-specific PIKfyve knockout mice has given some insights in the *in vivo* functions of the lipid kinase. Indeed, muscle-specific PIKfyve knockout mice are glucose intolerant and insulin resistant (Ikonomov *et al*, 2013). The key difference between the genetic and pharmacological inactivation of PIKfyve is that in KO mice, the protein is totally absent, preventing both the kinase activity and any

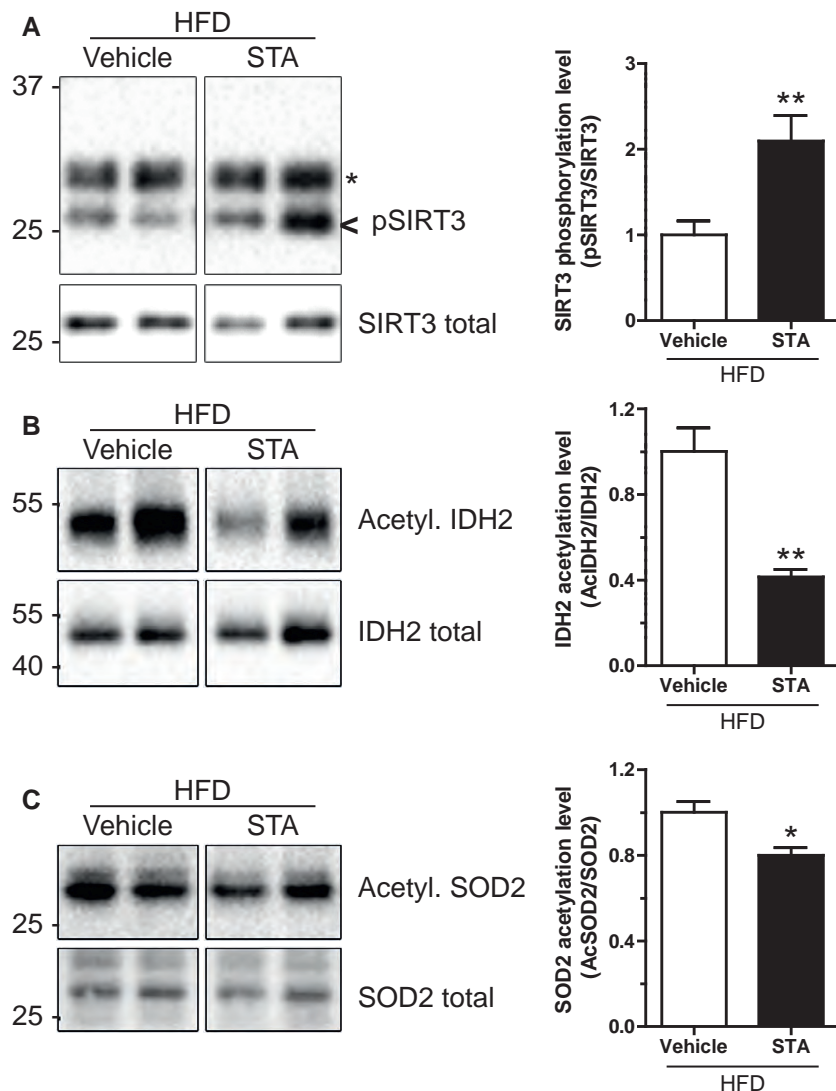


Figure 8. SIRT3 is activated in hearts from STA-treated mice.

A Heart lysates from vehicle- or STA-treated obese mice were immunoprecipitated using an anti-SIRT3 antibody. Bound proteins were immunoblotted with an anti-phospho-serine antibody to reveal the phosphorylated SIRT3 (pSIRT3). As a loading control, total homogenates were probed with an anti-SIRT3 antibody (SIRT3 total). Asterisk indicates antibody light chains. Quantification is shown on the right panel.

B, C Same as in (A) but lysates were immunoprecipitated with an anti-acetyl-lysine antibody and immunoblotted for IDH2 (B) and SOD2 (C). Quantifications are shown on the right panels.

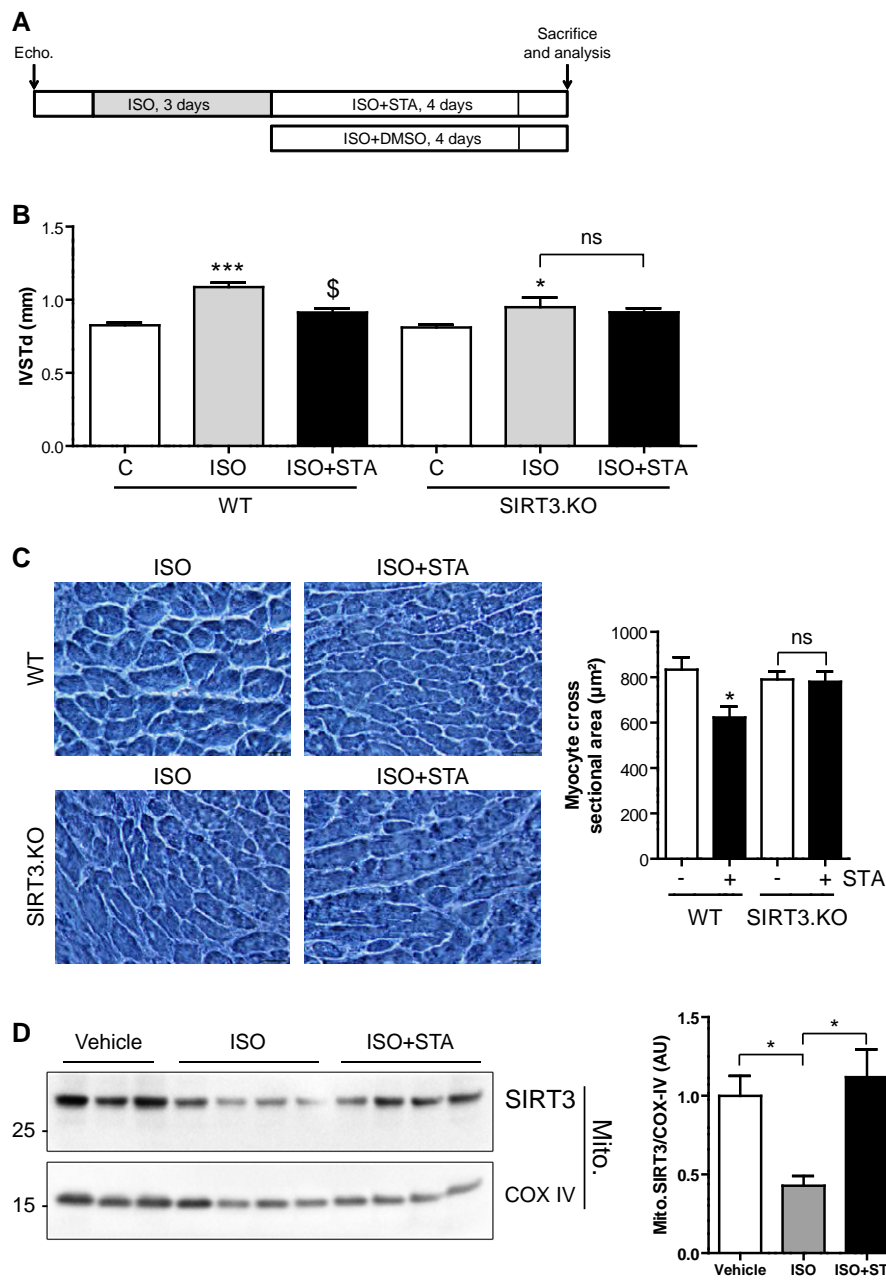
Data information: Data are presented as mean \pm SEM. Student's *t*-test, **P* < 0.05; ***P* < 0.01, *n* = 3–8 mice per group.

Source data are available online for this figure.

scaffolding/docking function of PIKfyve. The use of pharmacological inhibitors allows a more detailed dissection of these two characteristics.

Our study provides the first evidence that PIKfyve controls the structural mitochondrial integrity and ROS production in cardiac cells through a SIRT3-dependent pathway. One might hypothesize that PIKfyve could be found on mitochondria to play such a role. However, PIKfyve is a cytosolic protein localized on endosomes through its FYVE domain (Sbrissa *et al.*, 2002b). One might speculate that some lipid transfer may occur, allowing PIKfyve lipid products PI5P and/or PI(3,5)P₂ to be accumulated in mitochondrial

membranes. The capacity of phospholipids to alter membrane dynamics is widely recognized (van Meer *et al.*, 2008), and interestingly, membrane fluidity has been shown to be a key factor in the respiratory chain efficiency (Waczulikova *et al.*, 2007). Although a direct transfer between two distant lipid bilayers is very unlikely, there are examples of lipid exchange through protein carriers between two organelles, for example endoplasmic reticulum to Golgi apparatus (Moser von Filseck *et al.*, 2015) or to plasma membrane (Stefan *et al.*, 2013). Such a transfer mechanism could exist between the endosomal system and the mitochondria. Further work is needed to explore these possibilities and to

**Figure 9.** STA loses its anti-hypertrophic properties in SIRT3.KO mice.

- A Schematic of the protocol used. WT or SIRT3.KO mice received isoproterenol (ISO) for 3 days followed by injections of ISO+STA or ISO+DMSO for 4 days. Echocardiography analysis was performed at the beginning and at the end of the protocol to compare the groups.
- B IVTd was measured in WT and SIRT3.KO mice treated with ISO or ISO+STA as indicated. Data are presented as mean \pm SEM. Student's t-test, * $P < 0.05$; *** $P < 0.001$ as compared with control (C, before treatment) and $\$P < 0.05$ as compared with ISO, from three to nine mice per group. ns, non-significant.
- C Hematoxylin–eosin staining of heart cryosections from WT or SIRT3.KO mice after ISO or ISO+STA acute treatment and quantification of myocyte cross-sectional area. Scale bar is 25 μm . Data are presented as mean \pm SEM. Student's t-test, * $P < 0.05$ as compared with ISO-treated group, from three to four mice per group. ns, non-significant.
- D SIRT3 is enriched in mitochondria after STA treatment. Mitochondria were isolated from mice cardiac tissue treated as indicated, and blotted for SIRT3. COX IV was used as a loading control. Right panel shows quantification of mitochondrial SIRT3 normalized against COX IV. Data are presented as mean \pm SEM. Student's t-test, * $P < 0.05$ between indicated conditions ($n = 3$ –4 mice per group).

Source data are available online for this figure.

examine mitochondrial dynamics in the context of obesity-induced cardiomyopathy. Alternatively, we could not exclude that PIKfyve effects on mitochondria involve its protein kinase activity. Indeed,

it has been suggested that PIKfyve is able to phosphorylate several protein substrates (Ikonomov *et al*, 2003), although the regulation of this protein kinase activity remains poorly documented. It is

tempting to speculate that PIKfyve directly phosphorylates SIRT3 to control the redox status of the cell. However, given the fact that PIKfyve inhibition by STA increased SIRT3 phosphorylation and that only activating phosphorylations have been described for SIRT3 (Liu *et al.*, 2015), one has to admit that PIKfyve controls SIRT3 activity through a different mechanism. One possibility would be that PIKfyve phosphorylates SIRT3 on a different site through an inhibitory phosphorylation. In any case, our results clearly demonstrate that PIKfyve is activated upon metabolic and oxidative stresses, adding new activation pathways to the already described osmotic shock (Sbrissa *et al.*, 2002a). Taken together, these observations clearly identify PIKfyve as a stress sensor which is able to orchestrate the cell response.

A line of evidence suggests that obesity-induced cardiac dysfunction is linked to excessive mitochondrial ROS production, oxidative stress, and massive loss of cardiac cells (Sawyer *et al.*, 2002; Battiprolu *et al.*, 2012; Aurigemma *et al.*, 2013). Both *in vitro* and *in vivo*, we show here that STA was able to reduce mitochondrial ROS generation, oxidative stress, and apoptosis. Interestingly, anti-hypertrophic activity of STA was associated with activation of SIRT3 pathways in the heart. SIRT3 has been shown to be a negative regulator of cardiac hypertrophy (Sundaresan *et al.*, 2009), ROS production (Qiu *et al.*, 2010), apoptotic cell death (Sundaresan *et al.*, 2008), metabolism (Alfarano *et al.*, 2014), and aging (McDonnell *et al.*, 2015). Our data suggest the existence of a novel PIKfyve-dependent regulatory pathway that impinges on key processes of mitochondrial biogenesis. This is supported by the following evidences: First, PIKfyve inhibition increases myocardial phosphorylation level of SIRT3; second, PIKfyve inhibition decreases mitochondrial ROS production; third, PIKfyve inhibition is able to increase OXPHOS components in cardiac tissue; and fourth, PIKfyve inactivation causes an increase in mitochondrial size in the heart.

Despite its fundamental role, little is known on how SIRT3 is translocated into the mitochondrial matrix (Schwer *et al.*, 2002). Here, we show that PIKfyve inhibition induced the translocation of SIRT3 to the mitochondria, independently of stress. We postulate that such a regulation would prime the cell for a quick response under stress and ultimately protecting it from ROS overproduction and cell death. In that regard, deciphering the molecular mechanisms involved in STA-dependent SIRT3 translocation and activation would help to better understand the regulation of SIRT3, and would pave the way to new therapies for diseases associated with SIRT3 deficiency.

With the increasing prevalence of obesity-associated metabolic and cardiovascular disorders, our study places the lipid kinase PIKfyve in the context of cardiometabolic diseases and highlights the therapeutic potential of PIKfyve pharmacological inhibition to limit mitochondrial damage and to improve cardiometabolic phenotype in obese patients.

Materials and Methods

Reagents and antibodies

Antibodies used in this study are the following: anti-GAPDH (sc-32233), anti-HSP90 (sc-13119), anti-Drp1 (H-300), and anti-caspase 3 (sc-7148) from SantaCruz Biotechnology; anti-phospho-serine

(4A4) from Millipore; anti-OXPHOS/COX (MS604/G2594) from Mitoscience; and anti-acetylated-lysine (9441S), anti-SIRT3 (D22A3), anti-SIRT1 (1F3), anti-COX IV (4844), and anti-cleaved caspase 3 (9661) from Cell Signaling Technology. All antibodies were used at 1:1,000 for immunoblot and 1:100 for immunofluorescence. Fluorescent Alexa-coupled secondary antibodies (used at 1:300) and DAPI were from Life Technologies. HRP-coupled secondary antibodies (used at 1:3,000) were from Cell Signaling Technology. STA-5326 was purchased from Axon MedChem and was referred to as STA throughout this study. All other chemicals were from Sigma-Aldrich unless otherwise stated.

Molecular biology

siRNA against SIRT3 were from Eurogentec and as follows: 5'-GCGU UGUGAAACCCGACAU-3' and 5'-AUGUCGGGUUUCACAACGC-3'. siRNA Universal negative control was from Sigma. siRNA against PIKfyve were from Sigma and as follows: 5'-GUUGUCAAUGGCUU GUUU-3' and 5'-AAACAAAGCCAUUGACAAAC-3'. Primers for qRT-PCR used in this study are as detailed in Table EV1.

Quantitative RT-PCR analysis

Total RNAs were isolated from cultured mouse cardiac fibroblasts using the RNeasy mini kit (Qiagen). Total RNAs (300 ng) were reverse transcribed using Superscript II reverse transcriptase (Invitrogen) in the presence of a random hexamers. Real-time quantitative PCR was performed as previously described (Alfarano *et al.*, 2014). The expression of target mRNA was normalized to GAPDH mRNA expression.

Evaluation of apoptosis and ROS production

Apoptosis level was assessed as before (Boal *et al.*, 2016) using the DeadEnd Fluorometric TUNEL system according to manufacturer's instructions (Promega). Mitochondrial O₂⁻ and H₂O₂ were measured using MitoSOX Red indicator (Life Technologies) and MitoPY1 (Sigma-Aldrich) as described (Boal *et al.*, 2015b). Mitochondrial superoxide levels on heart cryosections were assessed as described elsewhere (Sun *et al.*, 2013).

Quantification of PIKfyve product PI5P

Quantification of the PI5P level was performed using a mass assay as described before (Morris *et al.*, 2000) with slight modifications (Dupuis-Coronas *et al.*, 2011).

Animal studies, experimental protocol, and metabolic measurements

The investigation conforms to the Guide for the Care and Use of Laboratory Animals published by the US National Institutes of Health (NIH Publication No. 85-23, revised 1985) and was performed in accordance with the recommendations of the French Accreditation of the Laboratory Animal Care (approved by the local Centre National de la Recherche Scientifique ethics committee). Two-month-old wild-type male C57BL6/J mice purchased from Janvier Labs were fed a high fat diet (HFD, 45% fat) for 12 months.

Animals were randomly divided into two groups ($n = 8$ each). Mice then received for 17 consecutive days intraperitoneal injections of STA (2 mg/kg/day) or vehicle (DMSO), corresponding to a final DMSO concentration of 50% diluted in PBS. The dose of STA was selected on the basis of our preliminary animal studies. The efficiency of PIKfyve inhibition was monitored by the quantification of cardiac PI5P (Fig EV4A). Plasma glucose (Accu-check, Roche Diagnostics) was measured in fasted state. LPO (lipid peroxide) quantification was done as described before (Foussal *et al.*, 2010) using an ELISA-based kit (Cayman). Triglycerides were quantified using enzymatic assay (TG enzymatic PAP150, Biomerieux). Plasma insulin was measured using an ELISA-based kit (Mercodia). Plasma IL-6 and TNF- α were quantified using ELISA kit (eBiosciences). Mice genetically invalidated for SIRT3 and their controls have been described previously and display no significant phenotype under basal conditions (Bochaton *et al.*, 2015). In order to induce cardiac hypertrophy, WT or SIRT3.KO mice ($n = 9$ per group) were intraperitoneally treated with ISO (15 mg/kg/day) for 3 days. Mice were then randomly segregated into two groups and treated for 4 days with either ISO+DMSO or ISO+STA (2 mg/kg/day).

Echocardiographic studies

Blinded echocardiography was performed as described (Pchejetski *et al.*, 2012) on isoflurane-anesthetized mice using a Vivid7 imaging system (General Electric Healthcare) equipped with a 14-MHz sectorial probe. Two-dimensional images were recorded in parasternal long- and short-axis projections, with guided M-mode recordings at the midventricular level in both views. Left ventricular (LV) dimensions and wall thickness were measured in at least five beats from each projection and averaged. Fractional shortening and ejection fraction were calculated from the two-dimensional images.

Morphology

Ultrastructural studies of cardiac tissue by electron microscopy were done as before (Boal *et al.*, 2015b). Briefly, cardiac tissues were fixed in cold 2.5% glutaraldehyde/1% paraformaldehyde, post-fixed in 2% osmium tetroxide, embedded in resin, and sectioned. Hematoxylin–eosin and Sirius red stainings of heart cryosections were done according to standard methods. The extent of cardiac fibrosis was quantified using ImageJ software (Pchejetski *et al.*, 2012). Quantification of myocyte cross-sectional area was performed as described (Foussal *et al.*, 2010).

Cell culture, transfection, and treatments

The rat embryonic cardiomyoblastic cell line H9C2 (ATCC) was cultured in DMEM medium (Life Technologies) supplemented with 10% FBS and 1% penicillin–streptomycin in a 37°C, 5% CO₂ incubator. siRNA transfection was performed with Lipofectamine RNAiMAX (Life Technologies) according to manufacturer's instructions. For hypoxic treatment, cells were pretreated for 30 min with STA (100 nM) or DMSO (vehicle only) and then subjected to normoxia (5% CO₂; 21% O₂, balance N₂) or hypoxia in a hypoxic chamber (5% CO₂, 1% O₂, balance N₂) for 2 h (for ROS measurement) or 16 h (for apoptosis). To assess cell hypertrophy, the medium was replaced and cells were further incubated for 24 h in

normoxic conditions (reoxygenation) in the continuous presence of STA or DMSO. To induce metabolic stress, the cells were treated with 2-deoxy-D-glucose (2DG, 50 mM) in complete medium for 4 h (for ROS production) or 24 h for apoptosis. Cell viability was assessed using MTT colorimetric assay.

Immunofluorescence, determination of mitochondrial fragmentation, and cell size measurement

Immunofluorescence was performed as previously described (Boal *et al.*, 2015a). For determination of mitochondrial fragmentation, H9C2 cells were live-stained with MitoTracker Red CMXRos (Life Technologies) at 200 nM for 15 min at 37°C. Fixed cells were then imaged by widefield microscopy. Mitochondrial fragmentation was measured using a dedicated ImageJ plugin as described (Dagda *et al.*, 2009). For cell size measurement, three fields of view were randomly selected per conditions and cell surface was quantified using ImageJ.

Isolation of mitochondria from H9C2 cells

Cells were extensively washed in ice-cold PBS, scraped in HB (20 mM HEPES, 270 mM sucrose, protease/phosphatase inhibitor cocktails from Biotools, pH 7.4), and disrupted by 10 strokes through a 27-gauge needle. Cell debris were pelleted by centrifugation (10 min 400 g 4°C). The supernatant was further spun 25 min 10,000 g 4°C. The resulting pellet corresponding to the isolated mitochondria was solubilized in RIPA buffer (50 mM Tris–HCl (pH 7.5), 150 mM NaCl, 0.1% SDS, 0.5% DOC, 1% Triton X-100, 1 mM EDTA, and protease/phosphatase inhibitor cocktails).

Isolation of mitochondria from mice heart

Mitochondria were isolated from mouse hearts essentially as described (Fazal *et al.*, 2017).

Protein extraction, immunoprecipitation, and Western blotting

Proteins from cardiac tissues and H9C2 cells were extracted using RIPA buffer and quantified using the Bio-Rad Protein Assay (Bio-Rad). For immunoprecipitation, lysates (500 µg proteins) were incubated overnight at 4°C with 5 µl of the specific antibody bound to Protein G Sepharose 4 Fast Flow (GE Healthcare). After extensive washes, bound proteins were eluted in Laemmli sample buffer (50 mM Tris–HCl (pH 6.8), 2% SDS, 6% glycerol, 0.2 mM DTT, and 0.02% bromophenol blue) and denatured at 70°C for 15 min. Proteins were resolved by SDS–PAGE and Western blotting. Immunoreactive bands were detected by chemiluminescence with the Clarity Western ECL Substrate (Bio-Rad) on a ChemiDoc MP Acquisition system (Bio-Rad).

Statistical analysis

Data are expressed as mean ± SEM. Statistical comparison between two groups was performed by Student's *t*-test, while comparison of multiple groups was performed by one- or two-way ANOVA followed by a Bonferroni's *post hoc* test when appropriate using GraphPad Prism version 5.00 (GraphPad Software, Inc.).

The paper explained

Problem

Obesity is a growing health issue in modern societies and is associated with cardiovascular diseases, metabolic complication, and cardiac dysfunction. Increasing evidences suggest that mitochondrial defects are central to the pathophysiology of the failing heart and metabolic disorders. However, the specific mechanisms remain unclear, and the clinical management of this multifactorial disease requires a multidisciplinary approach and new therapeutic strategies.

Results

Here, we show that the lipid kinase PIKfyve is critical for stress-induced mitochondrial damage in myocardium. Pharmacological inhibition of the kinase by STA-5326 reduces mitochondrial ROS production and apoptosis through the deacetylase SIRT3. Moreover, chronic PIKfyve inhibition reduces ventricular hypertrophy and improves cardiac function in morbidly obese mice.

Impact

Our study reveals the importance of PIKfyve inhibition in the treatment of cardiomyopathy in obese mice and propose new therapeutic avenue to improve cardiometabolic phenotype in obese patients.

Expanded View for this article is available online.

Acknowledgements

This project was supported by grants from Région Midi-Pyrénées (HT, MC, and FB) and Fondation Lefoulon-Delalande (FB), MEDEA Erasmus Mundus Program (MC and AT). We are grateful to Sophie Legonidec and Anexplo platform for mice phenotyping. We thank Claire Vinel, Gwendoline Astre, and Simon Deleruyelle for technical assistance. We are grateful to Jean-Emanuel Sarry (CRCT, Toulouse) for the anti-SOD2 and IDH2 antibodies and Hélène Authier (IRD, Toulouse) for IL-12 and IL-23 primers. We thank Franck Desmoulin for his help in statistical analysis and Olivier Lairez for echocardiography analysis.

Author contributions

FB, OK, and HT conceived and designed the experiments and analyzed the data. FB, MC, AT, LG, HT, and OK performed the experiments. HTh, CV, and DB performed the experiments on the SIRT3.KO mice. BP, PV, and AP assisted in the development of the project. FB, HT, and OK co-wrote the manuscript.

Conflict of interest

The authors declare that they have no conflict of interest.

References

- Alfarano C, Foussal C, Lairez O, Calise D, Attane C, Anesia R, Daviaud D, Wanecq E, Parini A, Valet P et al (2014) Transition from metabolic adaptation to maladaptation of the heart in obesity: role of apelin. *Int J Obes* 39: 312–320
- Aurigemma GP, de Simone G, Fitzgibbons TP (2013) Cardiac remodeling in obesity. *Circ Cardiovasc Imaging* 6: 142–152
- Barouch LA, Gao D, Chen L, Miller KL, Xu W, Phan AC, Kittleson MM, Minhas KM, Berkowitz DE, Wei C et al (2006) Cardiac myocyte apoptosis is associated with increased DNA damage and decreased survival in murine models of obesity. *Circ Res* 98: 119–124
- Battiprolu PK, Lopez-Crisosto C, Wang ZV, Nemchenko A, Lavandero S, Hill JA (2012) Diabetic cardiomyopathy and metabolic remodeling of the heart. *Life Sci* 92: 609–615
- Billich A (2007) Drug evaluation: apilimod, an oral IL-12/IL-23 inhibitor for the treatment of autoimmune diseases and common variable immunodeficiency. *IDrugs* 10: 53–59
- Bloom S, Cancilla PA (1969) Myocytolysis and mitochondrial calcification in rat myocardium after low doses of isoproterenol. *Am J Pathol* 54: 373–391
- Boal F, Mansour R, Gayral M, Saland E, Chicanne G, Xuereb JM, Marcellin M, Burlet-Schiltz O, Sansonetti PJ, Payrastre B et al (2015a) TOM1 is a PISP effector involved in the regulation of endosomal maturation. *J Cell Sci* 128: 815–827
- Boal F, Roumegoux J, Alfarano C, Timotin A, Calise D, Anesia R, Drougard A, Knauf C, Lagente C, Roncalli J et al (2015b) Apelin regulates FoxO3 translocation to mediate cardioprotective responses to myocardial injury and obesity. *Sci Rep* 5: 16104
- Boal F, Timotin A, Roumegoux J, Alfarano C, Calise D, Anesia R, Parini A, Valet P, Tronchere H, Kunduzova O (2016) Apelin-13 administration protects against ischaemia/reperfusion-mediated apoptosis through the FoxO1 pathway in high-fat diet-induced obesity. *Br J Pharmacol* 173: 1850–1863
- Bochaton T, Crola-Da-Silva C, Pillot B, Villedieu C, Ferreras L, Alam MR, Thibault H, Strina M, Gharib A, Ovize M et al (2015) Inhibition of myocardial reperfusion injury by ischemic postconditioning requires sirtuin 3-mediated deacetylation of cyclophilin D. *J Mol Cell Cardiol* 84: 61–69
- Bournat JC, Brown CW (2010) Mitochondrial dysfunction in obesity. *Curr Opin Endocrinol Diabetes Obes* 17: 446–452
- Cai X, Xu Y, Cheung AK, Tomlinson RC, Alcazar-Roman A, Murphy L, Billich A, Zhang B, Feng Y, Klumpp M et al (2013) PIKfyve, a class III PI kinase, is the target of the small molecular IL-12/IL-23 inhibitor apilimod and a player in Toll-like receptor signaling. *Chem Biol* 20: 912–921
- Dagda RK, Cherra SJ III, Kulich SM, Tandon A, Park D, Chu CT (2009) Loss of PINK1 function promotes mitophagy through effects on oxidative stress and mitochondrial fission. *J Biol Chem* 284: 13843–13855
- Dupuis-Coronas S, Lagarrigue F, Ramel D, Chicanne G, Saland E, Gaits-Iacovoni F, Payrastre B, Tronchere H (2011) The nucleophosmin-anaplastic lymphoma kinase oncogene interacts, activates, and uses the kinase PIKfyve to increase invasiveness. *J Biol Chem* 286: 32105–32114
- Fazal L, Laudette M, Paula-Gomes S, Pons S, Conte C, Tortosa F, Sicard P, Sainte-Marie Y, Bisserier M, Lairez O et al (2017) The multifunctional mitochondrial epac1 controls myocardial cell death. *Circ Res* 120: 645–657
- Foussal C, Lairez O, Calise D, Pathak A, Guilbeau-Frugier C, Valet P, Parini A, Kunduzova O (2010) Activation of catalase by apelin prevents oxidative stress-linked cardiac hypertrophy. *FEBS Lett* 584: 2363–2370
- Frank S, Gaume B, Bergmann-Leitner ES, Leitner WW, Robert EG, Catez F, Smith CL, Youle RJ (2001) The role of dynamin-related protein 1, a mediator of mitochondrial fission, in apoptosis. *Dev Cell* 1: 515–525
- Fuentes-Antras J, Picatoste B, Gomez-Hernandez A, Egido J, Tunon J, Lorenzo O (2015) Updating experimental models of diabetic cardiomyopathy. *J Diabetes Res* 2015: 656795
- Huang JY, Hirschey MD, Shimazu T, Ho L, Verdin E (2010) Mitochondrial sirtuins. *Biochim Biophys Acta* 1804: 1645–1651
- Ikonomov OC, Sbrissa D, Shisheva A (2001) Mammalian cell morphology and endocytic membrane homeostasis require enzymatically active phosphoinositide 5-kinase PIKfyve. *J Biol Chem* 276: 26141–26147
- Ikonomov OC, Sbrissa D, Mlak K, Deeb R, Fligger J, Soans A, Finley RL Jr, Shisheva A (2003) Active PIKfyve associates with and promotes the membrane attachment of the late endosome-to-trans-Golgi network transport factor Rab9 effector p40. *J Biol Chem* 278: 50863–50871

- Ikonomov OC, Sbrissa D, Delvecchio K, Xie Y, Jin JP, Rappolee D, Shisheva A (2011) The phosphoinositide kinase PIKfyve is vital in early embryonic development: preimplantation lethality of PIKfyve^{-/-} embryos but normality of PIKfyve^{+/-} mice. *J Biol Chem* 286: 13404–13413
- Ikonomov OC, Sbrissa D, Delvecchio K, Feng HZ, Cartee GD, Jin JP, Shisheva A (2013) Muscle-specific PIKfyve gene disruption causes glucose intolerance, insulin resistance, adiposity, and hyperinsulinemia but not muscle fiber-type switching. *Am J Physiol Endocrinol Metab* 305: E119–E131
- Jefferies HB, Cooke FT, Jat P, Boucheron C, Koizumi T, Hayakawa M, Kaizawa H, Ohishi T, Workman P, Waterfield MD et al (2008) A selective PIKfyve inhibitor blocks PtdIns(3,5)P₂ production and disrupts endomembrane transport and retroviral budding. *EMBO Rep* 9: 164–170
- Krausz S, Boumans MJ, Gerlag DM, Lufkin J, van Kuijk AW, Bakker A, de Boer M, Lodde BM, Reedquist KA, Jacobson EW et al (2012) Brief report: a phase IIa, randomized, double-blind, placebo-controlled trial of apilimod mesylate, an interleukin-12/interleukin-23 inhibitor, in patients with rheumatoid arthritis. *Arthritis Rheum* 64: 1750–1755
- Liu R, Fan M, Candas D, Qin L, Zhang X, Eldridge A, Zou JX, Zhang T, Juma S, Jin C et al (2015) CDK1-mediated SIRT3 activation enhances mitochondrial function and tumor radioresistance. *Mol Cancer Ther* 14: 2090–2102
- McDonnell E, Peterson BS, Bomze HM, Hirschey MD (2015) SIRT3 regulates progression and development of diseases of aging. *Trends Endocrinol Metab* 26: 486–492
- van Meer G, Voelker DR, Feigenson GW (2008) Membrane lipids: where they are and how they behave. *Nat Rev Mol Cell Biol* 9: 112–124
- Morris JB, Hinchliffe KA, Ciruela A, Letcher AJ, Irvine RF (2000) Thrombin stimulation of platelets causes an increase in phosphatidylinositol 5-phosphate revealed by mass assay. *FEBS Lett* 475: 57–60
- Moser von Filseck J, Vanni S, Mesmin B, Antonny B, Drin G (2015) A phosphatidylinositol-4-phosphate powered exchange mechanism to create a lipid gradient between membranes. *Nat Commun* 6: 6671
- Ong SB, Subrayan S, Lim SY, Yellon DM, Davidson SM, Hausenloy DJ (2010) Inhibiting mitochondrial fission protects the heart against ischemia/reperfusion injury. *Circulation* 121: 2012–2022
- Pchejetski D, Foussal C, Alfarano C, Lairez O, Calise D, Guilbeau-Frugier C, Schaa S, Seguelas MH, Wanecq E, Valet P et al (2012) Apelin prevents cardiac fibroblast activation and collagen production through inhibition of sphingosine kinase 1. *Eur Heart J* 33: 2360–2369
- Qiu X, Brown K, Hirschey MD, Verdin E, Chen D (2010) Calorie restriction reduces oxidative stress by SIRT3-mediated SOD2 activation. *Cell Metab* 12: 662–667
- Sawyer DB, Siwik DA, Xiao L, Pimentel DR, Singh K, Colucci WS (2002) Role of oxidative stress in myocardial hypertrophy and failure. *J Mol Cell Cardiol* 34: 379–388
- Sbrissa D, Ikonomov OC, Deeb R, Shisheva A (2002a) Phosphatidylinositol 5-phosphate biosynthesis is linked to PIKfyve and is involved in osmotic response pathway in mammalian cells. *J Biol Chem* 277: 47276–47284
- Sbrissa D, Ikonomov OC, Shisheva A (2002b) Phosphatidylinositol 3-phosphate-interacting domains in PIKfyve. Binding specificity and role in PIKfyve. Endomembrane localization. *J Biol Chem* 277: 6073–6079
- Schwer B, North BJ, Frye RA, Ott M, Verdin E (2002) The human silent information regulator (Sir)2 homologue hSIRT3 is a mitochondrial nicotinamide adenine dinucleotide-dependent deacetylase. *J Cell Biol* 158: 647–657
- Shisheva A (2008) PIKfyve: partners, significance, debates and paradoxes. *Cell Biol Int* 32: 591–604
- Smirnova E, Griparic L, Shurland DL, van der Bliek AM (2001) Dynamin-related protein Drp1 is required for mitochondrial division in mammalian cells. *Mol Biol Cell* 12: 2245–2256
- Stefan CJ, Manford AG, Emr SD (2013) ER-PM connections: sites of information transfer and inter-organelle communication. *Curr Opin Cell Biol* 25: 434–442
- Sun K, Guo XL, Zhao QD, Jing YY, Kou XR, Xie XQ, Zhou Y, Cai N, Gao L, Zhao X et al (2013) Paradoxical role of autophagy in the dysplastic and tumor-forming stages of hepatocarcinoma development in rats. *Cell Death Dis* 4: e501
- Sundaresan NR, Samant SA, Pillai VB, Rajamohan SB, Gupta MP (2008) SIRT3 is a stress-responsive deacetylase in cardiomyocytes that protects cells from stress-mediated cell death by deacetylation of Ku70. *Mol Cell Biol* 28: 6384–6401
- Sundaresan NR, Gupta M, Kim G, Rajamohan SB, Isbatan A, Gupta MP (2009) Sirt3 blocks the cardiac hypertrophic response by augmenting Foxo3a-dependent antioxidant defense mechanisms in mice. *J Clin Invest* 119: 2758–2771
- Tao R, Coleman MC, Pennington JD, Ozden O, Park SH, Jiang H, Kim HS, Flynn CR, Hill S, Hayes McDonald W et al (2010) Sirt3-mediated deacetylation of evolutionarily conserved lysine 122 regulates MnSOD activity in response to stress. *Mol Cell* 40: 893–904
- Tsutsui H, Kinugawa S, Matsushima S (2011) Oxidative stress and heart failure. *Am J Physiol Heart Circ Physiol* 301: H2181–H2190
- Waczulikova I, Habodaszova D, Cagliniec M, Ferko M, Ulicna O, Mateasik A, Sikurova L, Ziegelhoffer A (2007) Mitochondrial membrane fluidity, potential, and calcium transients in the myocardium from acute diabetic rats. *Can J Physiol Pharmacol* 85: 372–381
- Wada Y, Cardinale I, Khatcherian A, Chu J, Kantor AB, Gottlieb AB, Tatsuta N, Jacobson E, Barsoum J, Krueger JG (2012) Apilimod inhibits the production of IL-12 and IL-23 and reduces dendritic cell infiltration in psoriasis. *PLoS ONE* 7: e35069
- Youle RJ, Karbowski M (2005) Mitochondrial fission in apoptosis. *Nat Rev Mol Cell Biol* 6: 657–663
- Yu W, Dittenhafer-Reed KE, Denu JM (2012) SIRT3 protein deacetylates isocitrate dehydrogenase 2 (IDH2) and regulates mitochondrial redox status. *J Biol Chem* 287: 14078–14086



License: This is an open access article under the terms of the Creative Commons Attribution 4.0 License, which permits use, distribution and reproduction in any medium, provided the original work is properly cited.

RESEARCH PAPER

Apelin-13 administration protects against ischaemia/reperfusion-mediated apoptosis through the FoxO1 pathway in high-fat diet-induced obesity

Correspondence Dr Oksana Kunduzova, National Institute of Health and Medical Research (INSERM) U1048, 1 Av. J Poulhès, 31432 Toulouse, Cedex 4, France. E-mail: oxana.koundouzova@inserm.fr

Received 3 November 2015; **Revised** 2 February 2016; **Accepted** 28 February 2016

Frederic Boal^{1,2*}, Andrei Timotin^{1,2*}, Jessica Roumegoux^{1,2}, Chiara Alfarano^{1,2}, Denis Calise^{2,3}, Rodica Anesia^{1,2}, Angelo Parini^{1,2}, Philippe Valet^{1,2}, Hélène Tronchere^{1,2} and Oksana Kunduzova^{1,2}

¹National Institute of Health and Medical Research (INSERM) U1048, Toulouse, Cedex 4, France, ²University of Toulouse, UPS, Institute of Metabolic and Cardiovascular Diseases, Toulouse, France, and ³US006, Microsurgery Services, Toulouse, Cedex 4, France

*Equally contributing authors.

BACKGROUND AND PURPOSE

Apelin-13, an endogenous ligand for the apelin (APJ) receptor, behaves as a potent modulator of metabolic and cardiovascular disorders. Here, we examined the effects of apelin-13 on myocardial injury in a mouse model combining ischaemia/reperfusion (I/R) and obesity and explored their underlying mechanisms.

EXPERIMENTAL APPROACH

Adult male C57BL/6J mice were fed a normal diet (ND) or high-fat diet (HFD) for 6 months and then subjected to cardiac I/R. The effects of apelin-13 post-treatment on myocardial injury were evaluated in HFD-fed mice after 24 h I/R. Changes in protein abundance, phosphorylation, subcellular localization and mRNA expression were determined in cardiomyoblast cell line H9C2, primary cardiomyocytes and cardiac tissue from ND- and HFD-fed mice. Apoptosis was evaluated by TUNEL staining and caspase-3 activity. Mitochondrial ultrastructure was analysed by electron microscopy.

KEY RESULTS

In HFD-fed mice subjected to cardiac I/R, i.v. administration of apelin-13 significantly reduced infarct size, myocardial apoptosis and mitochondrial damage compared with vehicle-treated animals. In H9C2 cells and primary cardiomyocytes, apelin-13 induced FoxO1 phosphorylation and nuclear exclusion. FoxO1 silencing by siRNA abolished the protective effects of apelin-13 against hypoxia-induced apoptosis and mitochondrial ROS generation. Finally, apelin deficiency in mice fed a HFD resulted in reduced myocardial FoxO1 expression and impaired FoxO1 distribution.

CONCLUSIONS AND IMPLICATIONS

These data reveal apelin as a novel regulator of FoxO1 in cardiac cells and provide evidence for the potential of apelin-13 in prevention of apoptosis and mitochondrial damage in conditions combining I/R injury and obesity.

Abbreviations

FoxO, forkhead box O; HFD, high-fat diet; I/R, ischaemia/reperfusion; MI, myocardial infarction; mtDNA, mitochondrial DNA; HF, heart failure; DCFHDA, dichlorodihydrofluorescein diacetate

Tables of Links

TARGETS	
Other protein targets ^a	Enzymes ^c
Bax	Caspase 3
Bcl-2	COX1
GPCRs^b	Cyclophilin A
Apelin receptor	

LIGANDS	
Adiponectin	H ₂ O ₂
Apelin-13	Leptin

These Tables list key protein targets and ligands in this article which are hyperlinked to corresponding entries in <http://www.guidetopharmacology.org>, the common portal for data from the IUPHAR/BPS Guide to PHARMACOLOGY (Pawson *et al.*, 2014) and are permanently archived in the Concise Guide to PHARMACOLOGY 2015/16 (^{a,b,c}Alexander *et al.*, 2015a,b,c).

Introduction

Myocardial infarction (MI) due to coronary artery disease is a leading cause of death and disability in obese individuals (Rana *et al.*, 2004). Deprivation of oxygen and energy after coronary artery occlusion causes severe damage in the cardiac tissue and mediates cell death. Cardiomyocyte death was originally considered to occur exclusively via necrosis, an uncontrolled disintegration of the cell through rupture of the plasma membrane and subsequent release of intracellular contents into surrounding tissue. However, it is now clear that apoptosis, or programmed cell death, plays a significant role in the failing heart (Kang and Izumo, 2000; Wencker *et al.*, 2003; Konstantinidis *et al.*, 2012). Because of the limited ability of cardiac myocytes to proliferate, low levels of apoptosis can result in profound structural and functional consequences in the myocardium leading to cardiac dysfunction and heart failure (HF) (Mani, 2008). Wencker *et al.* demonstrated that induction of apoptosis in just 0.02% of myocytes is sufficient to cause a lethal cardiomyopathy in mice at 9 weeks of age (Wencker *et al.*, 2003), suggesting that cardiac apoptosis may be an important component of HF pathogenesis. However, in situations combining myocardial damage and obesity, the molecular and cellular mechanisms that govern apoptotic machinery are poorly understood.

The FoxO transcription factor family governs fundamental programmes, including apoptosis, stress resistance and mitochondrial activities (Wang *et al.*, 2014). FoxO transcription factors (FoxO1, FoxO3, FoxO4 and FoxO6) belong to the forkhead family of transcriptional regulators, of which FoxO1 is abundantly expressed in the cardiovascular system (Evans-Anderson *et al.*, 2008; Sengupta *et al.*, 2011). A deficiency of FoxO1 induces embryonic lethality due to impaired vasculogenesis and is important in the aetiology of cardiovascular diseases (Furuyama *et al.*, 2004). Recent studies have demonstrated that FoxO1 is a critical mediator of oxidative stress resistance in cardiac cells (Sengupta *et al.*, 2011). Likewise, defects in FoxO1 specifically in mouse cardiomyocytes lead to increased oxidative damage and decreased myocardial function after acute ischaemia/reperfusion (I/R) or MI (Sengupta *et al.*, 2011). A recent report has provided new *in vivo* evidence of the role of FoxO1 in cardiomyopathy related to metabolic stress (Battiprolu *et al.*, 2012). However, the exact role of FoxO1 in obesity-triggered myocardial

remodelling processes and related mechanisms remains obscure.

Obesity is associated with altered levels of adipose tissue-derived factors, commonly referred to as adipokines (Maury *et al.*, 2007). Dysregulation of adipokines such as leptin and adiponectin contributes to the development of metabolic and cardiovascular disease (Bluher, 2013; Nakamura *et al.*, 2014). Circulating levels of leptin are elevated in obesity, hypertension, chronic HF and MI, while diminished level of adiponectin are found in obese, diabetic and coronary artery disease patients (Nakamura *et al.*, 2014). Changes in adipokine production can affect the balance between apoptosis and survival, and ultimately cell fate decisions. We have previously demonstrated that apelin, a recently described adipokine, plays an important role in the regulation of cardiovascular and metabolic homeostasis (Dray *et al.*, 2008; Pchejetski *et al.*, 2012). Apelin, an endogenous ligand for the GPCR, apelin (APJ) receptor, exerts inotropic activity and increases coronary blood flow by vascular dilation (Klein *et al.*, 2005). Pyr1-1apelin-13 (apelin 13) is the main form circulating in plasma, and it has greater biological activity than apelin-36 or apelin-17, measured as the extracellular acidification rate in cultured cells expressing the apelin receptor (Tatemoto *et al.*, 1998; Zhen *et al.*, 2013). In response to stress, apelin-13 prevents myocardial remodelling and improves cardiac function (Foussal *et al.*, 2010; Pchejetski *et al.*, 2012). The defects in apelin in mice induce age-dependent progressive cardiac dysfunction, which is prevented by apelin infusion (Kuba *et al.*, 2007), suggesting an important role for the apelinergic system in maintaining cardiac performance. In humans, circulating and cardiac levels of apelin are reduced in subjects with acute MI and established coronary artery disease (Weir *et al.*, 2009; Kadoglou *et al.*, 2010; Tycinska *et al.*, 2010), whereas in obese individuals, plasma apelin concentrations are increased (Klein and Davenport, 2005; Dray *et al.*, 2010). The loss of apelin enhances the susceptibility to apoptosis and myocardial injury *ex vivo* and *in vivo* suggesting that apelin plays an important role in cell fate decisions in response to ischaemic stress (Wang *et al.*, 2013). We have previously demonstrated that apelin regulates ROS production during the cardiac remodelling processes. ROS play a dual role in I/R acting as secondary messengers in intracellular signalling cascades, which maintain the cellular 'redox' status; however,

ROS can also trigger irreversible injury leading to cell death. To date, the precise role of apelin ROS-dependent cellular responses to I/R in an obese state remains to be determined.

The results of the present study revealed that apelin-13 prevents myocardial apoptosis, mitochondrial damage and myocardial injury in conditions combining I/R injury and obesity. We demonstrated that apelin-13 is an important regulator of FoxO1 dynamics in cardiac myocytes in response to stress. Furthermore, we showed that apelin counteracted cell apoptosis and ROS generation via the FoxO1 pathway.

Methods

Reagents and antibodies

Antibodies used in this study are as follows: anti-FoxO1 (C29H4) and phospho-FoxO1 (Ser²⁵⁶) antibodies (#9416) from Cell Signalling Technology (Danvers, MA, USA); anti-tubulin from Santa Cruz Biotechnologies (Dallas, TX, USA); anti-β-actin from Sigma (A1978; St Louis, MO, USA). Fluorescent Alexa-coupled secondary antibodies were from Life Technologies (Carlsbad, CA, USA) and HRP-coupled secondary antibodies from Cell Signalling Technologies. DAPI was from Life Technologies. Apelin-13 was purchased from Bachem (Bubendorf, Switzerland) and is referred to as apelin throughout this study. OXPHOS was from Mitosciences (MS604/G2594; Eugene, OR, USA). siRNA against FoxO1 was from Ambion (Foster City, CA, USA). All other chemicals were from Sigma unless otherwise stated.

Animal studies

The investigation conforms to the Guide for the Care and Use of Laboratory Animals published by the US National Institutes of Health (NIH Publication No. 85-23, revised 1985) and was performed in accordance with the recommendations of the French Accreditation of the Laboratory Animal Care (approved by the local Centre National de la Recherche Scientifique Ethics Committee). At 8 weeks,

C57BL/6J mice were fed a high-fat diet (HFD, 45% fat) or normal diet (ND, 4% fat) for 6 months. The metabolic profile of HFD-fed mice is summarized in Table 1. Apelin knock-out (KO) mice were fed with ND as described previously (Alfarano *et al.*, 2014). Animal studies are reported in compliance with the ARRIVE guidelines (Kilkenny *et al.*, 2010; McGrath and Lilley, 2015).

Experimental protocol

A mouse model of I/R was used as previously described (Pchejetski *et al.*, 2007). In brief, the mice were incubated and placed under mechanical ventilation after undergoing general anaesthesia, induced by i.p. injection of ketamine (35 mg·kg⁻¹) and xylazine (5 mg·kg⁻¹). A left parasternotomy was performed to expose hearts, and a 7–0 silk suture (Softsilk; US Surgical, Norwalk, CT, USA) was placed around the left anterior descending coronary artery. A snare was placed on the suture, and regional myocardial ischaemia was produced by tightening the snare. After 45 min of ischaemia, the occlusive snare was released to initiate reperfusion up to 24 h. Sham-operated control mice underwent the same surgical procedures except that the snare was not tightened. Animals were randomly divided into four groups: (i) sham vehicle ($n = 6$); (ii) I/R vehicle ($n = 7$); (iii) sham apelin ($n = 7$); and (iv) I/R apelin ($n = 7$). Apelin-13 (0.1 µg·kg⁻¹) or vehicle (PBS) was injected into the jugular vein at 5 min of reperfusion in a final volume of 100 µL.

Evaluation of apoptosis

The apoptosis level both *in vivo* and *in vitro* was assessed using the DeadEnd Fluorometric TUNEL system according to manufacturer's instructions (Promega, Madison, WI, USA) as described previously (Pchejetski *et al.*, 2012).

Determination of area at risk and infarct size

Determination of area at risk and infarct size was done as described previously (Pchejetski *et al.*, 2012). Briefly, after injection of 1.5% Evans blue into the left ventricular

Table 1

Cardiometabolic profile of ND- and HFD-fed mice

Metabolic parameters	ND	HFD
Body weight (g)	30.2 ± 0.7	48.3 ± 0.4*
Glucose (mM)	8.5 ± 0.6	11.4 ± 0.8*
Insulin (pg·mL ⁻¹)	1364.7 ± 293.2	4053.3 ± 518.4*
Echocardiographic parameters	ND	HFD
IVST, cm	0.08 ± 0.01	0.10 ± 0.01*
LVID, cm	0.37 ± 0.01	0.39 ± 0.01
LVPWT, cm	0.08 ± 0.01	0.10 ± 0.01*
EF, %	79.15 ± 2.73	69.23 ± 0.889*
FS, %	39.43 ± 1.35	33.59 ± 0.63*

Body weight, plasma levels of glucose and insulin, interventricular septum thickness (IVST), left ventricular internal diameter (LVID), left ventricular posterior wall thickness (LVPWT), fractional shortening (FS) and ejection fraction (EF) were measured in mice fed a ND or HFD for 6 months. Data are means ± SEM; $n = 5$ –6 per group.

* $P < 0.05$ versus ND-fed group.

cavity, mice were killed, and the heart was removed. Infarct size was evaluated by triphenyltetrazolium chloride staining and expressed as a percentage of the ischaemic risk area.

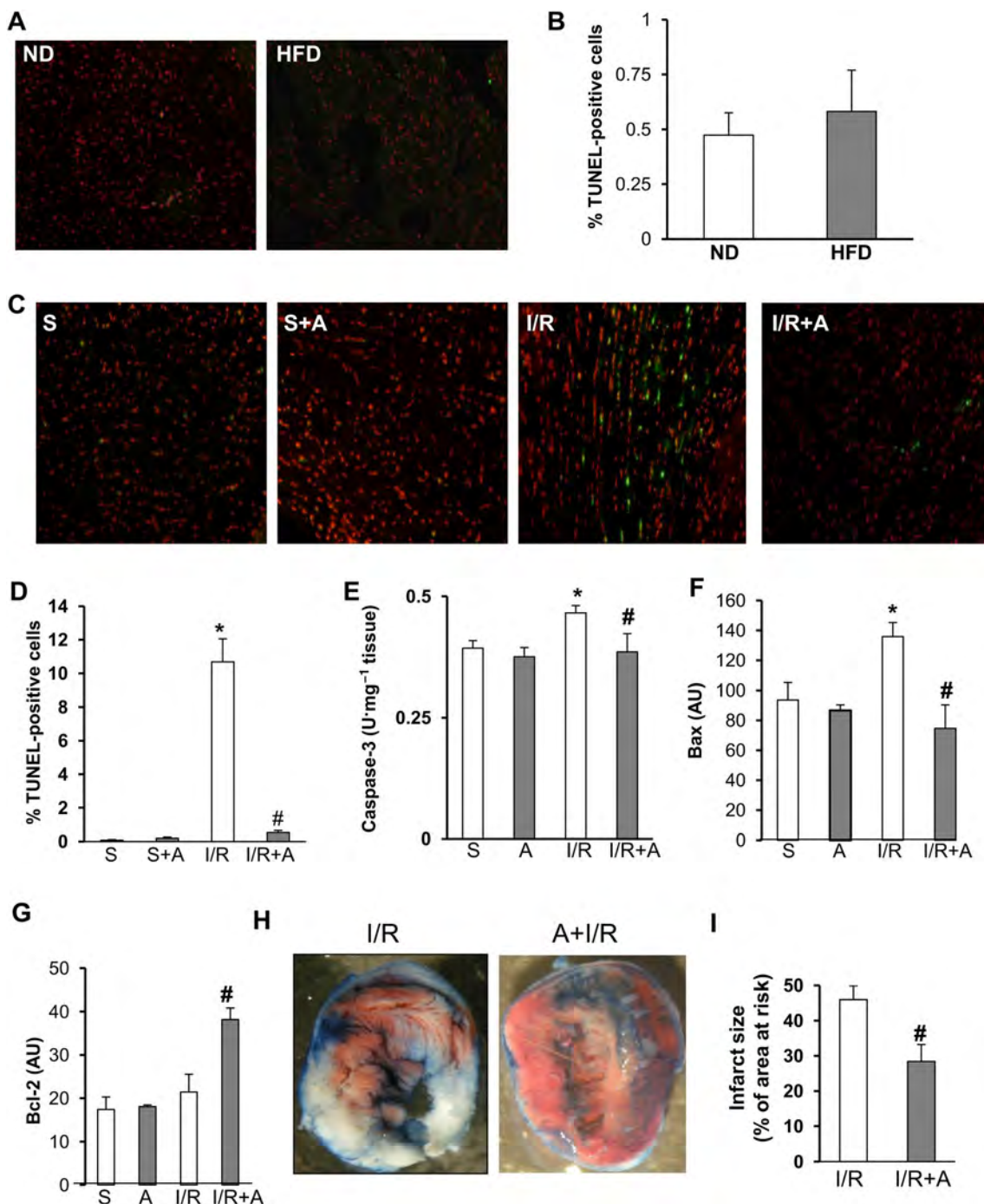


Figure 1

Protection of cardiac tissue by apelin-13 against apoptosis and necrosis in acute phase of myocardial I/R in obese mice. (A) Representative images and (B) quantification of TUNEL positive cells in the heart sections from ND-fed and HFD-fed mice. (C) Representative images of TUNEL analysis of cardiac tissue sections from HFD-fed mice treated with vehicle or apelin-13, A, after 24 h of sham-operation, S, or I/R. (D) Quantification of apoptosis in (C). (E-G), Caspase-3 activity (E), Bax (F) and Bcl-2 (G) expression levels in hearts from HFD-fed mice treated as indicated. (H-I) Representative images of triphenyltetrazolium chloride staining of heart sections from HFD-fed mice treated with vehicle or apelin-13, A, after 24 h of sham-operation, S, or I/R. (I) Quantification of infarct size expressed as % of area at risk. *, P < 0.05 versus S; #, P < 0.05 versus I/R.

glutaraldehyde/1% paraformaldehyde, post-fixed in 2% osmium tetroxide, embedded in resin and sectioned.

Immunolabelling of paraffin sections

Paraformaldehyde-fixed (4%) and paraffin-embedded heart sections were deparaffinized and rehydrated; antigen retrieval was performed using a sodium citrate treatment, followed by permeabilization with 0.2% Triton X-100 for 20 min. After the blocking of non-specific sites with 1% BSA, the primary antibodies were incubated overnight at 4°C. After labelling with appropriate secondary antibodies, the sections were mounted in Vectashield mounting medium including DAPI (Vector Laboratories, Burlingame, CA, USA) and imaged by confocal microscopy.

Echocardiographic studies

Echocardiography was performed in isoflurane-anaesthetized mice using a Vivid7 imaging system (General Electric Healthcare, Toulouse, France) equipped with a 14 MHz sectorial probe. Two-dimensional images were recorded in parasternal long-axis and short-axis projections, with guided

M-mode recordings at the midventricular level in both views. Left ventricular (LV) dimensions and wall thickness were measured in at least three beats from each projection and averaged. Interventricular septum, LV posterior wall thickness and LV internal dimensions at diastole (LVID) were measured. Fractional shortening and ejection fraction were calculated from the two-dimensional images.

Caspase-3 activity and metabolic plasma measurements

Caspase-3 activity was assessed with EnzChek Caspase-3 Assay Kit #1 (Life Technologies) according to the manufacturer's instructions. Insulinemia (Mercodia, Uppsala, Sweden) and glycemia (Accu-check, Roche Diagnostics, Risch-Rotkreuz, Switzerland) were measured in fasted state. Body fat mass composition was determined as described previously (Alfarano *et al.*, 2014).

Primary mice cardiomyocytes preparation, cell culture, transfection and treatments

Adult mice ventricular cardiomyocytes were isolated from adult obese mice and maintained as described previously

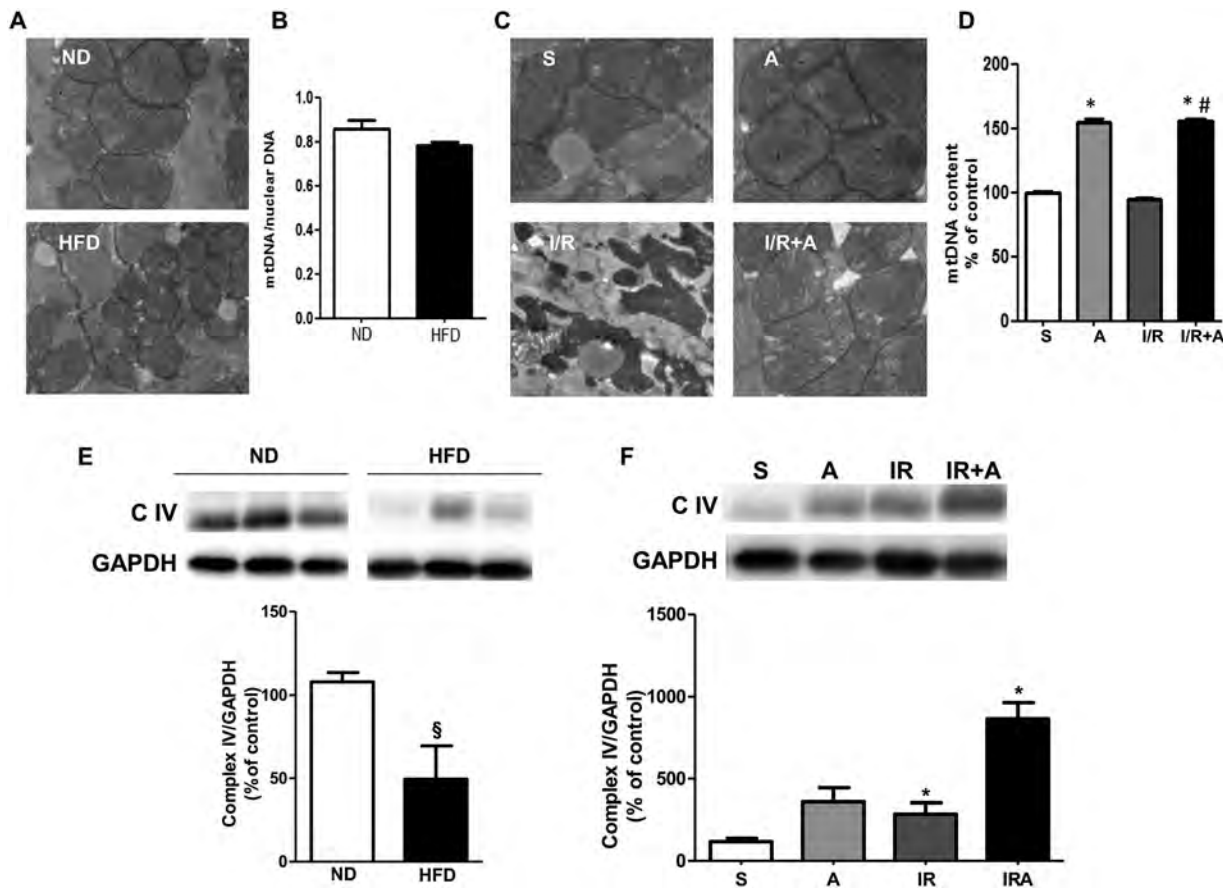


Figure 2

Prevention of mitochondrial damage by apelin-13 in acute phase of myocardial I/R in obese mice. (A) Typical electron micrographs (original magnifications $\times 10000$) from ND- and HFD-fed mice. (B) Quantitative RT-PCR analysis of mtDNA content in hearts from ND- and HFD-fed mice. (C) Scanning electron microscope images (original magnification $\times 10000$) in mice treated with vehicle or apelin-13, A, after 24 h of sham-operation, S, or I/R. (D) Effect of apelin-13 treatment on mtDNA content in hearts from HFD-fed mice subjected to I/R. (E) Western blot analysis of the myocardial OXPHOS complex IV in ND- and HFD-fed mice. (F) Effect of apelin-13 treatment on expression of OXPHOS complex IV in hearts from HFD-fed mice subjected to I/R. *, P < 0.05 versus S; #, P < 0.05 versus I/R; §, P < 0.05 versus ND.

(Alfarano *et al.*, 2014). The rat embryonic cardiomyoblastic cell line H9C2 was cultured in MEM (Gibco 41090-028, ThermoFischer Scientific, Waltham, MA, USA) supplemented with 10% FBS and 1% penicillin–streptomycin in a 37°C, 5% CO₂ incubator. siRNA transfection was performed with Lipofectamine RNAiMAX (Life Technologies) according to manufacturer's instructions. Cells were pretreated for 15 min with apelin (10⁻⁷–10⁻⁹ mol·L⁻¹) and then subjected to normoxia (5% CO₂; 21% O₂, balance N₂) or hypoxia for 2 h in a hypoxic chamber (5% CO₂, 1% O₂, balance N₂). To measure cell apoptosis induced by hypoxia, the cells were left for 16 h in hypoxic conditions.

Hydrogen peroxide and superoxide production

Global ROS production in cells was assessed as described previously (Bianchi *et al.*, 2005; Pchelatski *et al.*, 2007) using the

oxidation of H₂DCFDA (Life Technologies) to DCF (dichlorodihydrofluorescein). Mitochondrial O₂[−] and H₂O₂ production in cells was measured by MitoSOX (Life Technologies) and MitoPY1 (Sigma-Aldrich, St Louis, MO, USA) at 1 μM (on H9C2 cells) or 5 μM (on cardiomyocytes) for 30 min following live-cell imaging on a confocal microscope equipped with an incubation chamber with temperature control and CO₂ enrichment.

Western blotting

Immunoblot analyses were carried out on clarified lysates of cardiac tissues or cells quantified using the BCA (bicinchoninic acid) protein assay (Thermo Scientific; Thermo Fisher Scientific Waltham, MA, USA) and denatured in Laemmli sample buffer (Sigma-Aldrich, St Louis, MO, USA). Proteins were separated by SDS-PAGE, before western blotting on nitrocellulose membranes using the Trans-Blot Turbo Transfer System

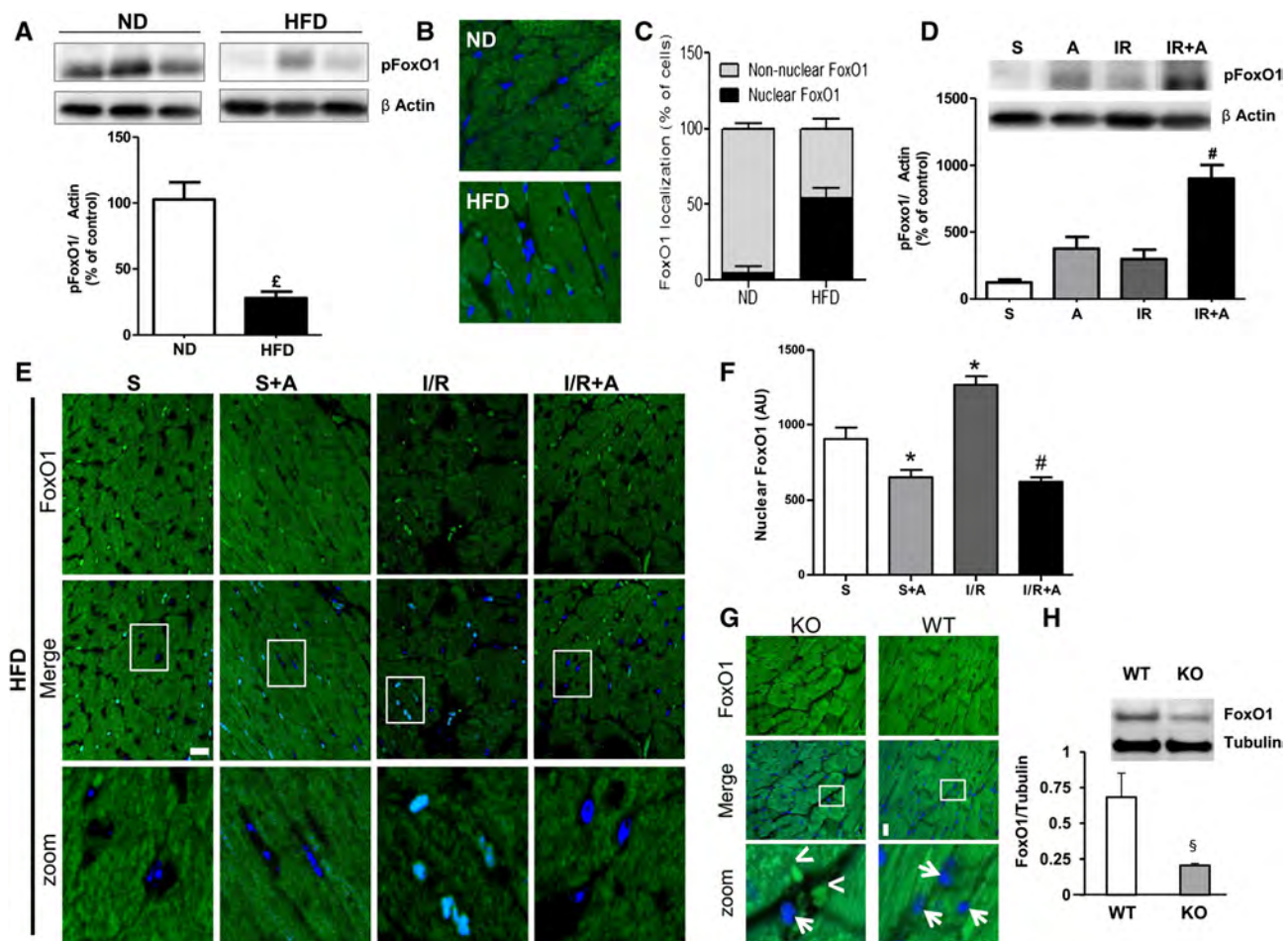


Figure 3

Apelin-dependent myocardial FoxO1 activation in cardiac tissue from obese mice subjected to cardiac I/R. (A) Myocardial phosphorylation pattern of FoxO1 in ND- and HFD-fed mice. (B) Representative images for nuclear and cytoplasmic localization of FoxO1 in ND- and HFD-fed mice. (C) Whole-tissue quantification of nuclear and cytoplasmic distribution of FoxO1 in ND- and HFD-fed mice. (D) Effect of apelin-13 treatment on FoxO1 phosphorylation in cardiac tissue from HFD-fed mice subjected to I/R. (E) Effect of apelin-13 treatment on subcellular localization of FoxO1 in cardiac sections from HFD-fed mice treated with vehicle or apelin-13, A, after 24 h of sham, S, or I/R operations. (F) Quantification of FoxO1 nuclear translocation was carried out by measuring the mean fluorescence intensity of nuclear FoxO1 in HFD-fed mice. (G) FoxO1 immunostaining (in green) on heart sections from HFD-fed WT or apelin KO mice. Nuclei were stained with DAPI (in blue). Bar is 20 μm. Arrows point to nuclei devoid of FoxO1, whereas arrowheads point to nuclear staining. (H) FoxO1 protein expression levels in hearts from WT or apelin KO mice. *, P < 0.05 versus S; £, P < 0.05 versus ND; #, P < 0.05 versus IR; §, P < 0.05 versus WT.

(Bio-Rad, Hercules, CA, USA). Immunoreactive bands were detected by chemiluminescence with the Clarity Western ECL Substrate (Bio-Rad) on a ChemiDoc MP Acquisition System (Bio-Rad).

Immunofluorescence

Immunofluorescence was performed essentially as previously described (Boal *et al.*, 2010). Briefly, cells grown on glass coverslips were PFA(paraformaldehyde)-fixed and permeabilized using TritonX-100 before incubation with primary and secondary antibodies, mounted in Mowiol and imaged using confocal microscopy on a Zeiss LSM780 microscope. For nuclear FoxO quantification, the fluorescence intensity of FoxO1 protein in the nucleus was quantified and normalized against the fluorescence intensity within the total cell.

Real-time RT-PCR analysis

Total RNAs were isolated from cultured mouse cardiac fibroblasts using the RNeasy mini kit (Qiagen, Hilden, Germany). Total RNAs (300 ng) were reverse transcribed using SuperScript II reverse transcriptase (Invitrogen, Carlsbad, CA, USA)

in the presence of random hexamers. Real-time quantitative PCR was performed as previously described (Alfarano *et al.*, 2014). The expression levels of Bax and Bcl2 were normalized to GAPDH mRNA expression. The sequences of the primers used are as follow and given in the 5'-3' orientation: FoxO1, sense GCGGGCTGGAAGAATTCAAT, antisense GTTCCTTCATTCTGCACTCGAAATA; GAPDH, sense TGCA CCACCAACTGCTTAGC, antisense GGCATGGACTGTGG TCATGAG; Bax, sense CGGCAATTGGAGATGAAC, antisense GTCCACGTCAGCAATCATCCT; Bcl-2, sense TCCCGATTCAATT GCAAGTTGTA, antisense GCAACCACACCATCGATCTTC. For mitochondrial DNA (mtDNA) analysis, the content of mtDNA was calculated using real-time quantitative PCR by measuring the threshold cycle ratio of a mitochondrial-encoded gene (COX1) and a nuclear-encoded gene (cyclophilin A) as previously described (Attane *et al.*, 2012).

Statistical analysis

Data are expressed as mean \pm SEM. Comparison between two groups was performed by Student's *t*-test, while comparison

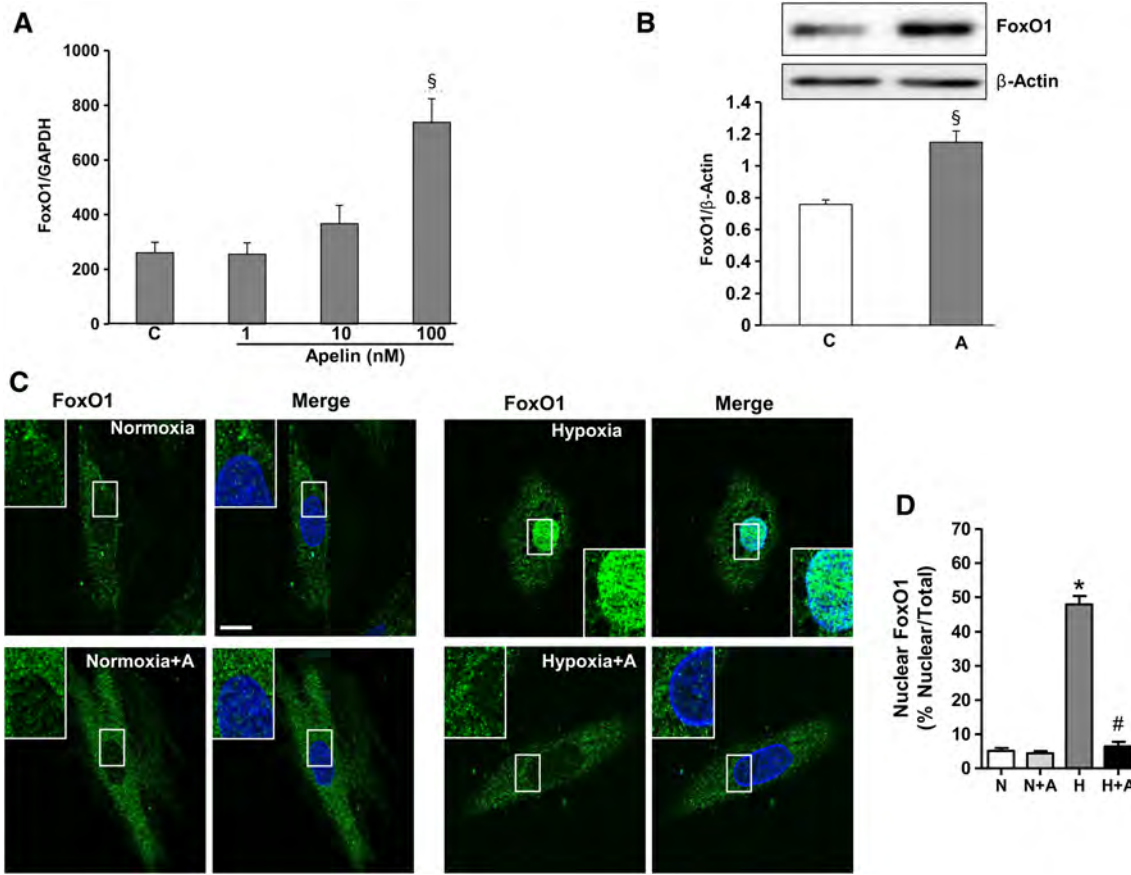


Figure 4

FoxO1 activity is regulated by apelin in H9C2 cardiomyoblasts. (A) Dose-dependent effect of apelin-13 on FoxO1 expression levels was assessed by quantitative RT-PCR in H9C2 cardiomyoblasts treated or not with apelin (1–100 nM) for 24 h. (B) H9C2 cells were treated with apelin (A, 100 nM), and cell lysates were probed with anti-FoxO1 and anti- β actin antibodies. FoxO1 protein expression levels were quantified by densitometry and normalized against β actin. (C) Representative confocal images of H9C2 cells pretreated or not with apelin for 15 min (A, 100 nM), submitted to hypoxia, H, or normoxia, N, for 2 h and stained for FoxO1 antibody. FoxO1 proteins are shown in green; nuclei were stained with DAPI (in blue). Bar is 10 μ m. (D) Quantification of FoxO1 nuclear translocation is expressed as the fluorescence intensity in the nucleus normalized to the total fluorescence intensity in the cell. *, $P < 0.05$ versus N; #, $P < 0.05$ versus H; §, $P < 0.05$ versus C.

of multiple groups was performed by one-way ANOVA followed by a Bonferroni's *post hoc* test using GraphPad PRISM version 5.00 (GraphPad Software, Inc, La Jolla, CA, USA.). Statistical significance was defined as $P < 0.05$. The data and statistical analysis comply with the recommendations on experimental design and analysis in pharmacology (Curtis *et al.*, 2015).

Results

Protection of cardiac tissue by apelin-13 against apoptosis and mitochondrial injury in acute phase of myocardial I/R in obese state

To evaluate the impact of obesity on cardiometabolic parameters, male C57BL/6J mice were fed a ND (4% fat) or HFD (45% fat) for 6 months. As shown in Table 1, in comparison with ND-fed mice, HFD-fed animals had increased body

weight, plasma glucose and insulin levels. Echocardiographic analysis revealed an increased interventricular septum, LV posterior wall and decreased EF and FS in HFD-fed mice as compared with ND-fed animals, suggesting that chronic exposure to a HFD induces cardiac dysfunction.

We next examined the effect of obesity on myocardial apoptosis in cardiac tissue stained using the TUNEL assay. As shown in Figure 1A and B, no differences were observed in the number of apoptotic nuclei between ND- and HFD-fed mice. However, cardiac I/R resulted in increased apoptosis, activation of caspase-3 and deregulation of pro-apoptotic proteins in HFD-fed mice (Figure 1C–F). Importantly, apelin-13 administration at 5 min of reperfusion significantly reduced the number of TUNEL positive cells, myocardial caspase-3 activity and expression of Bax as compared with vehicle-treated mice after 24 h I/R (Figure 1C–F). In contrast, Bcl-2 expression level, an anti-apoptotic protein, was increased in apelin-treated I/R hearts from HFD-fed mice (Figure 1G).

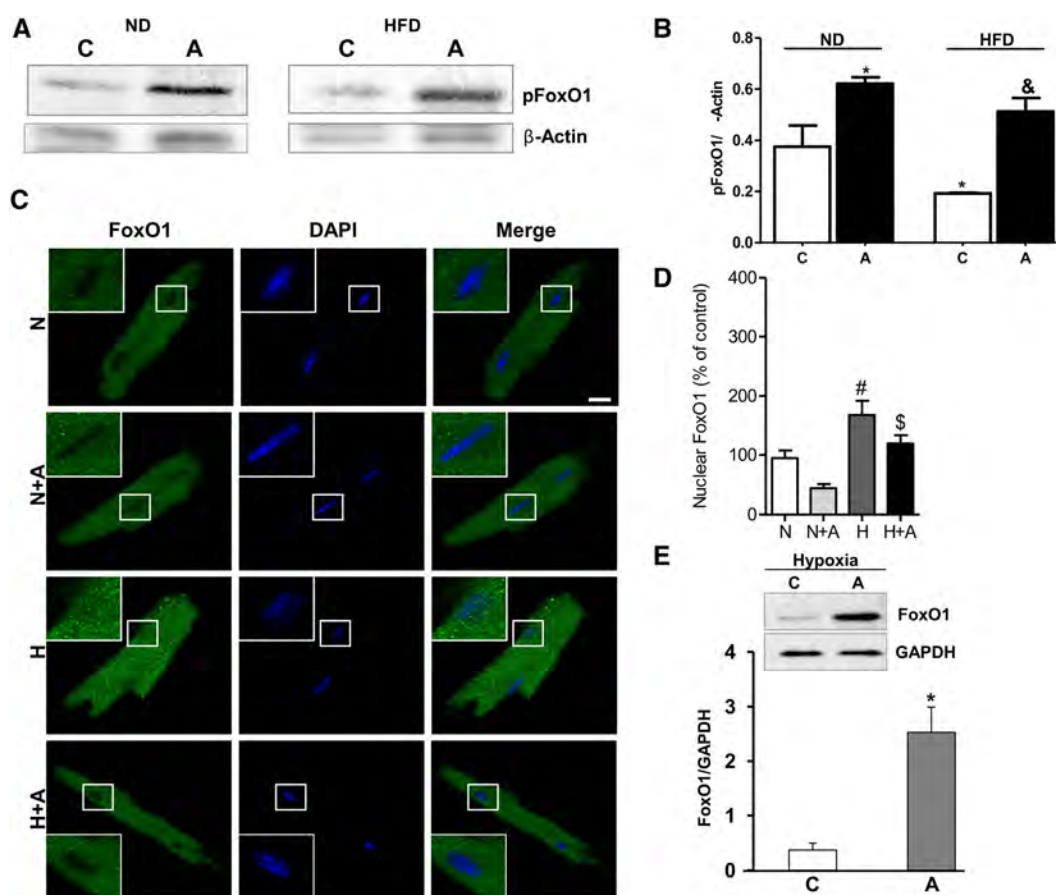


Figure 5

Apelin-dependent regulation of FoxO1 activity in cardiomyocytes isolated from HFD-fed mice under hypoxia. (A) Representative western blot images of FoxO1 phosphorylation pattern in cardiomyocytes isolated from ND- and HFD-fed mice. (B) Quantification of FoxO1 phosphorylation in cardiomyocytes isolated from ND- and HFD-fed mice and treated with apelin. *, $P < 0.05$ versus C (ND); &, $P < 0.05$ versus C (HFD). (C) Representative confocal images of cardiomyocytes isolated from HFD-fed mice stimulated with apelin for 15 min (A, 100 nM) under hypoxia, H, or normoxia, N,. Nuclei were stained with DAPI (in blue) and FoxO1 (in green). Bar is 20 μ m. (D) Quantification of FoxO1 nuclear translocation is expressed as the fluorescence intensity in the nucleus normalized against the total fluorescence intensity in the cell. (E) Effect of apelin on FoxO1 protein expression levels was assessed by western blot analysis in cardiomyocytes treated with apelin (100 nM) for 24 h. FoxO1 protein expression levels were quantified by densitometry. *, $P < 0.05$ versus C; #, $P < 0.05$ versus N; \$, $P < 0.05$ versus H.

Apelin-dependent prevention of apoptosis in HFD-fed mice after I/R was accompanied by a reduction in infarct size as compared with vehicle-treated animals (Figure 1H and I). Electron microscopy examination of cardiac tissue from ND- and HFD-fed mice revealed the presence of numerous lipid

droplets with a higher proportion of smaller mitochondria (Figure 2A) without changes in mtDNA content (Figure 2B) in obese mice. As shown in Figure 2C, myocardial I/R in HFD-fed mice induced mitochondrial damage, including swelling and structural disruption. Administration of apelin-

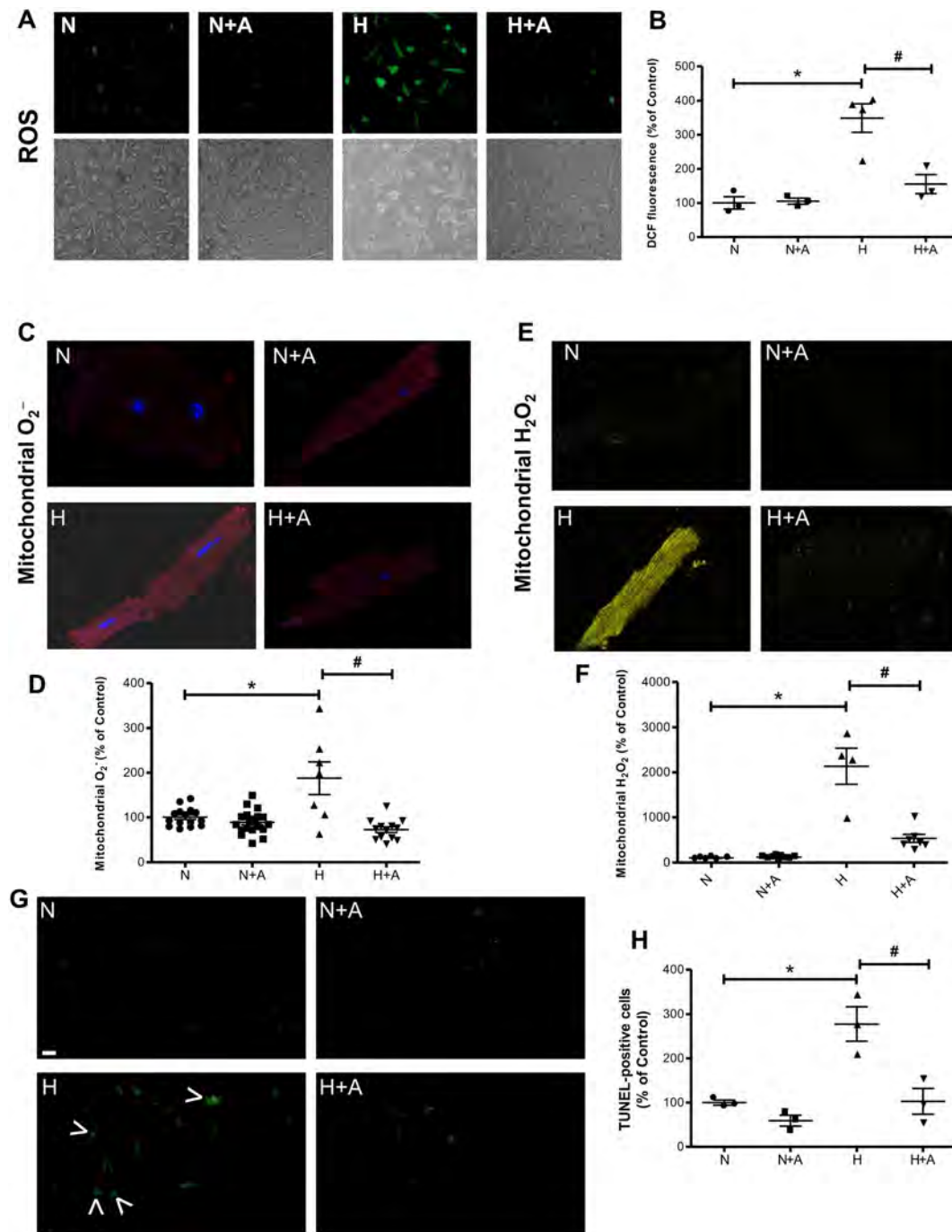


Figure 6

Apelin-13 treatment attenuates hypoxia-induced apoptosis and ROS overproduction in cardiomyocytes isolated from HFD-fed mice. Primary cardiomyocytes isolated from HFD-fed mice were treated with apelin (A, 100 nM) for 15 min. Representative images and quantification of intracellular ROS (A and B), mitochondrial O₂⁻ (C and D) and H₂O₂ (E and F) levels measured by the fluorescent probes DCFDA, MitoSOX Red or MitoPY1 respectively. (G) Apoptosis was measured by TUNEL. Arrowheads highlight TUNEL-positive cells. Bar is 20 μm. (H) Quantification of % of apoptotic TUNEL-positive cells.* P < 0.05 versus N; # P < 0.05 versus H.

13 prevented I/R-induced mitochondrial damage (Figure 2C) and stimulated mtDNA content (Figure 2D) as compared with vehicle-treated HFD-fed mice. In addition, we found that chronic HFD consumption resulted in a decrease in OXPHOS complex IV, the terminal enzyme in the mitochondrial respiratory chain (Figure 2E), and treatment of HFD-fed mice with apelin significantly increased cytochrome c oxidase expression in response to cardiac I/R (Figure 2F).

Attenuation of FoxO1 nuclear translocation by apelin-13 in relation to HFD status

Given the importance of FoxO1 transcription factor for governing apoptosis, mitochondrial activity and metabolism, we next examined the effect of apelin on the myocardial activation status of FoxO1 in response to obesity and I/R injury. Activation of FoxO1 was examined by

monitoring the phosphorylation of FoxO1 proteins at Ser²⁵⁶ and nucleocytoplasmic distribution in cardiac tissue. Compared with the control ND group, HFD-fed mice exhibited decreased levels of FoxO1 phosphorylation in whole heart tissue extracts (3a) and increased nuclear localization of FoxO1 (Figure 3B and C). In response to I/R injury, apelin stimulated FoxO1 phosphorylation in whole cell extracts from HFD-fed mouse hearts (Figure 3D) and prevented its nuclear translocation in cardiac tissue (Figure 3E and F). To confirm the role of apelin in FoxO1 dynamics in cardiac tissue, we finally examined its localization in left ventricles from apelin KO obese mice. As shown in Figure 3G, apelin-deficient mice displayed a FoxO1 nuclear targeting phenotype, as compared with wild-type (WT) mice. Analysis of the confocal images revealed a significant decrease in the fluorescence intensity of FoxO1 (Figure 3G) in apelin KO mice as compared with WT

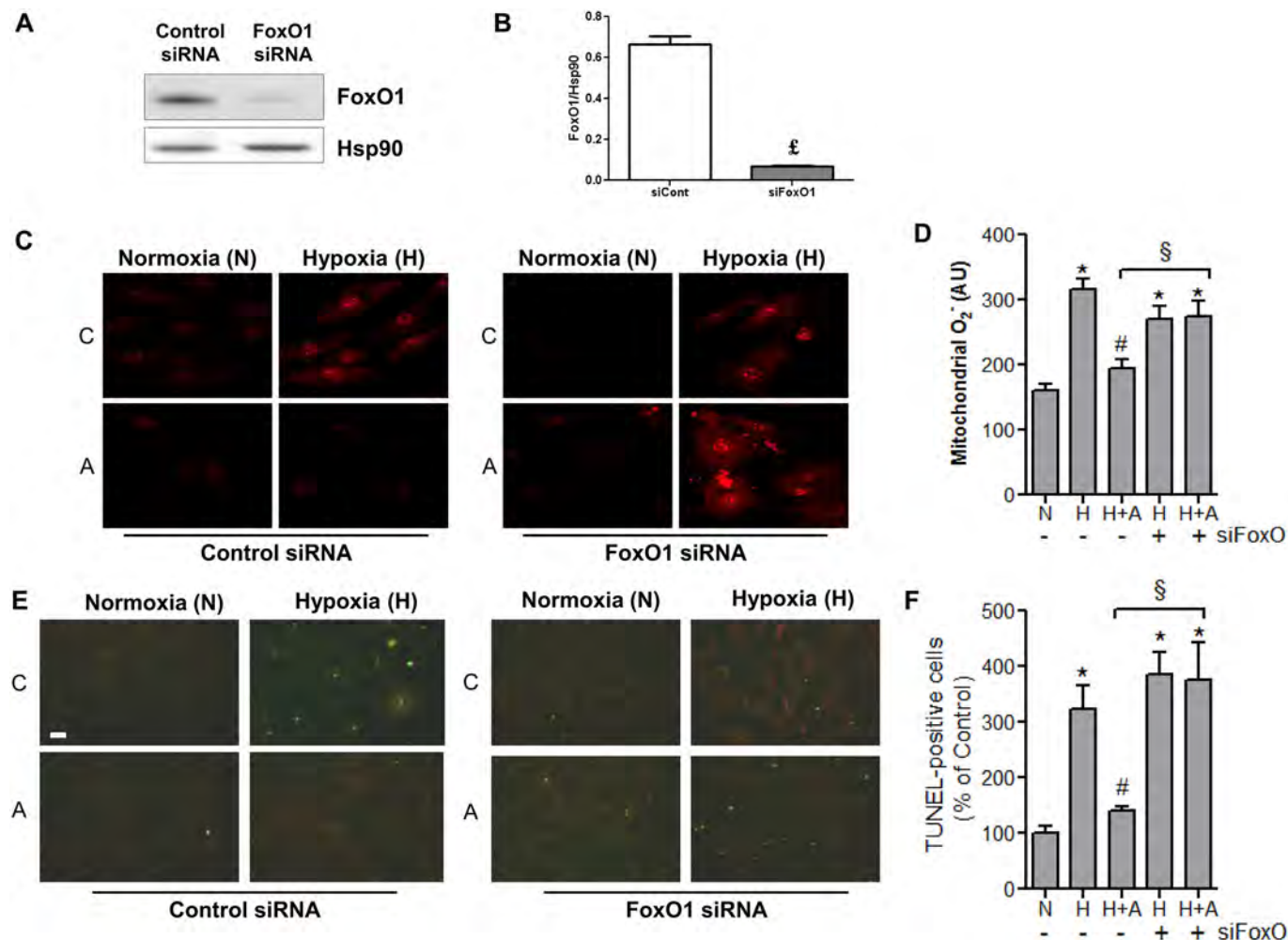


Figure 7

Apelin-13 treatment regulates cell apoptosis and mitochondrial ROS production through a FoxO1 pathway. (A and B) Quantification of FoxO1 protein expression levels in H9C2 transfected with scramble control siRNA (siRNA Control) or FoxO1 siRNA; £, P < 0.05 versus si RNA Control. (C and D) Representative images and quantification of transfected H9C2 cells treated or not, C, with apelin (A, 100 nM for 15 min) under hypoxia, H, or normoxia, N, for 2 h. Mitochondrial ROS production was measured by MitoSOX Red fluorescence (in red). (E and F) Analysis of TUNEL-positive H9C2 cells transfected with siRNA Control or FoxO1 siRNA and treated as in (C–D) Bar is 20 µm. *, P < 0.05 versus N; #, P < 0.001 versus H; §, P < 0.05 between indicated conditions.

animals. In addition, myocardial FoxO1 expression level, as assessed by Western blot, was down-regulated in apelin KO mice as compared with WT (Figure 3H).

Cardiac cell expression and trafficking of FoxO1 are regulated by apelin-13

The regulation of expression and trafficking of FoxO factors are critical for the transcriptional control of cell death and mitochondrial function in response to cellular stress (Ullman *et al.*, 1997; Wang *et al.*, 2014). We next examined whether apelin-13 can regulate FoxO1 in cardiac cells under normoxia and hypoxia. As shown in Figure 4A, treatment of H9C2 cardiomyoblast cells with apelin induced a dose-dependent increase in FoxO1 mRNA levels under normoxia as detected by quantitative RT-PCR. Western blot analysis confirmed the increased expression of FoxO1 proteins induced by apelin in H9C2 cells (Figure 4B). As shown in Figure 4C and D, exposure of H9C2 cells to hypoxia (1% O₂) for 2 h resulted in noticeable nuclear translocation of FoxO1, as compared with the uniform cytosolic distribution in normoxic cardiomyoblasts. Quantitative analysis of FoxO1 subcellular localization in H9C2 cells revealed that apelin not only maintained FoxO1 in the cytoplasm but also significantly prevented its hypoxia-induced nuclear retention (Figure 4D).

Examination of phosphorylation pattern of FoxO1 expression in cardiomyocytes isolated from ND- and HFD-fed mice indicated that apelin increased FoxO1 phosphorylation in both obese and non-obese conditions (Figure 5A and B). Analysis of subcellular localization of FoxO1 in isolated cardiomyocytes from HFD-fed mice demonstrated that in response to hypoxia, FoxO1 translocated massively in the nuclei, as demonstrated in Figure 5C and quantified in Figure 5D. Treatment of cardiomyocytes with apelin-13 inhibited hypoxia-induced nuclear translocation of FoxO1 (Figure 5C and D). As shown in Figure 5E, cardiomyocyte protein levels of FoxO1 were decreased under hypoxia, whereas treatment of cells with apelin significantly increased FoxO1 protein expression in response to hypoxia.

Apelin-13 reduces hypoxia-induced mitochondrial ROS and apoptosis through a FoxO1 pathway

FoxO1 coordinates the transcriptional programme of cardiomyocyte survival upon induction of oxidative stress (Wang Y *et al.*, 2014). We next examined whether FoxO1 is involved in apelin-dependent effects on mitochondrial ROS generation and apoptosis. Analysis of mitochondria-specific ROS generation in response to hypoxia in cardiomyocytes isolated from HFD-fed mice demonstrated that apelin treatment attenuated hypoxia-induced intracellular ROS production (Figure 6A and B) measured by DCFDA. At the level of mitochondria, we found that apelin significantly reduced superoxide (O₂) (Figure 6C and D) and H₂O₂ (Figure 6E and F) levels, measured by MitoSOX and MitoPY1 respectively. Moreover, the apoptosis of cardiomyocytes induced by hypoxia was markedly decreased by apelin treatment (Figure 6G and H).

In order to elucidate the molecular mechanisms underlying apelin-mediated protection of cells from apoptosis and ROS overproduction, we transfected H9C2 cells with FoxO1 siRNA. As shown in Figure 7A and B, siRNA knockdown of

FoxO1 specifically inhibited its expression by 85% in H9C2 cells. Importantly, we found that silencing of FoxO1 abolished the ability of apelin to attenuate hypoxia-induced mitochondrial O₂⁻ production (Figure 7C and D). In addition, FoxO1 knockdown drastically inhibited apelin-mediated anti-apoptotic activity in response to hypoxia (Figure 7E and F). Taken together, these data suggest that FoxO1 is a crucial target for apelin in the control of oxidative stress and cardiac cell apoptosis.

Discussion and conclusions

The FoxO1 transcription factor orchestrates a number of cellular processes involved in cell fate decisions in a cell type- and environment-specific manner, including cell resistance to apoptosis and oxidative stress (Medema *et al.*, 2000; Kops *et al.*, 2002). The present study provides evidence for a novel regulatory mechanism of FoxO1 activation in cardiac cells. The main finding of this work is that apelin-13 regulates myocardial FoxO1 phosphorylation status and nucleocytoplasmic shuttling at the acute phase of cardiac I/R injury in obese mice. Moreover, we demonstrated that apelin promotes cardiomyocyte survival and counteracts excessive mitochondria-derived ROS formation through the FoxO1 pathway. Using a mouse model combining obesity and I/R injury, we showed that a reduction in apoptosis and mitochondrial damage by apelin-13 post-reperfusion treatment is associated with increased levels of phosphorylated FoxO1 protein and the prevention of FoxO1 nuclear translocation in injured cardiac tissue. Finally, we showed that apelin gene-deficient mice exposed to HFD display impaired FoxO1 expression and trafficking with nuclear translocation in cardiac tissue. These results point to a novel mechanism of FoxO1-shuttling system in cardiac cells and provide *in vitro* and *in vivo* evidence for the therapeutic potential of apelin-13 to limit I/R-induced myocardial apoptosis and mitochondrial damage in obese subjects.

There is accumulating evidence that subcellular localization of FoxO transcription factors is critical for various cellular functions (Kowluru and Matti, 2012; Ponugoti *et al.*, 2012). The translocation of FoxO transcriptional factors is regulated by multiple mechanisms, including the inhibition of nuclear import and promotion of nuclear export (Wang *et al.*, 2014). The shuttling of proteins between the nucleus and cytoplasm is a highly regulated process and requires accessory factors (Ullman *et al.*, 1997). At present, the molecular mechanisms of FoxO1 regulation in cardiac cells remain obscure. In the present study, we demonstrated that subcellular distribution of FoxO1 may be modulated by apelin in cardiomyocytes. Analysis of cardiac cells by confocal laser scanning microscopy showed that obesity promoted the translocation of FoxO1 into the nucleus in cardiomyocytes. Phosphorylation modification is a critical mechanism to regulate the nuclear/cytoplasmic shuttling of FoxOs and their transcriptional activity (Zhao *et al.*, 2011). Here, we demonstrated a significant decrease in FoxO1 phosphorylation at Ser²⁵⁶ in cardiac tissue from HFD-fed mice. These data are in line with a recent report showing FoxO1 dephosphorylation in whole cell extracts from HFD-fed mouse hearts (Battiprolu *et al.*, 2012). In response to hypoxia, we observed FoxO1

translocation into the nucleus in cardiomyocytes isolated from HFD-fed mice. Our findings are consistent with results reported by recent studies showing that FoxO1 is mainly localized in the nucleus under hypoxic conditions in a variety of cell lines (Battiprolu *et al.*, 2012; Awad *et al.*, 2014). Analysis of subcellular localization of FoxO1 revealed that apelin-13 promotes the retention of FoxO1 in the cytoplasm by preventing its nuclear translocation in response to oxygen deprivation. Furthermore, we found that apelin prevents hypoxia-induced FoxO1 dephosphorylation in cardiac myocytes. In a mouse model of cardiac injury induced by I/R, we showed that an injection of apelin at the early phase of reperfusion stimulates the phosphorylation of FoxO1 proteins and inhibits its nuclear import confirming apelin-dependent regulation of myocardial FoxO1 status. Consistent with these data, we revealed cardiac nuclear translocation of FoxO1 in apelin KO mice, providing strong evidence for a key role of apelin in the control of nucleocytoplasmic distribution of FoxO1 in the heart.

FoxO transcription factors sense cellular stress and govern fundamental processes including cell death and ROS production. Because the heart is constantly adapting to different stresses, FoxOs appear to play an extremely important role in cardiac physiology and pathophysiology. In mice, FoxO1 deficiency specifically in cardiomyocytes results in increased myocardial cell death, reduced cardiac performance and increased scar formation following myocardial ischaemia (Sengupta *et al.*, 2011). Increased cardiac I/R injury in mice with cardiac FoxO deficiency is accompanied by reduced expression of antioxidants, DNA repair enzymes and anti-apoptotic genes (Sengupta *et al.*, 2011). In our study, we demonstrated for the first time that activation of FoxO1 by apelin prevents hypoxia-induced mitochondrial O₂⁻ and H₂O₂ generation in cultured cardiomyoblasts exposed to hypoxia. Given the importance of the FoxO family in the regulation of oxidative stress, FoxO1 may be an important indicator of mitochondrial oxidative stress in cardiac cells. This notion is corroborated by the recent study demonstrating that FoxO3 is an early biomarker of oxidative stress in conditions of metabolic stress (Raju *et al.*, 2013). However, ROS might play a dual role acting as secondary messengers in intracellular signalling cascades and as highly reactive molecules causing irreversible oxidative damage to mtDNA, proteins and lipids (Braunersreuther *et al.* 2012). Excessive mitochondrial ROS production triggers activation of cellular apoptotic programmes leading to cell death (Wang, 2001). Limiting mitochondrial ROS production by apelin may be particularly important in cardiac protection against I/R damage. Indeed, we showed that apelin-dependent reduction in hypoxia-induced ROS production is associated with inhibition of apoptotic cell death in response to oxygen deprivation. Importantly, silencing of FoxO1 by siRNA in cardiomyoblasts attenuated apelin-mediated anti-apoptotic and mitochondrial ROS reduction activities, suggesting that apelin may control cell fate decisions through FoxO1 pathways. One of the major limitations of our *in vitro* models is their inability to fully mimic the *in vivo* conditions. In order to adopt the *in vivo* experiments and protocol treatment that more closely approximate the clinical situation, we have examined the effects of apelin-13 post-treatment on myocardial damage and oxidative stress in HFD-fed mice subjected to I/R.

Our results suggest that apelin administration after 5 min of reperfusion reduced myocardial apoptosis and oxidative stress in conditions combining obesity and cardiac I/R injury. Moreover, apelin-13 post-treatment decreased myocardial expression of pro-apoptotic protein Bax and increased the level of anti-apoptotic Bcl-2 leading to reduced myocardial cell death. In addition, we found apelin-dependent attenuation of I/R-induced mitochondrial damage and increased mtDNA content in the myocardium, suggesting an accelerated mitochondrial biogenesis in the context of a well-preserved mitochondrial ultrastructure after apelin administration. Regulators of mitochondrial activity play an important role in coordinating cellular adaptation to stress (Ferber *et al.*, 2011). Further studies are required to determine whether the protection provided by apelin on acute I/R injury could improve cardiac function in the late phase of the reperfusion period. Together, these studies reveal a major role for apelin in the regulation of myocardial FoxO1 activation and offer a new treatment option for cardiac I/R injury in obese subjects.

Acknowledgements

This work was supported by grants from the National Institute of Health and Medical Research (INSERM), Fondation Lefoulon-Delalande, Fondation de France, Région Midi-Pyrénées and Fondation pour la Recherche Médicale (FRM) and ERASMUS MUNDUS MEDEA project.

Author contributions

P.V., A.P. and O.K. conceived and designed the study. F.B. and J.R. performed *in vivo* experiments. F.B., H.T., A.T. and O.K. performed *in vitro* experiments. D.C. performed microsurgery procedures on mice. J.R. and R.A. performed and analysed quantitative RT-PCR. C.A. and J.R. performed histomorphological analysis. F.B., H.T. and O.K. wrote the manuscript.

Conflict of interest

The authors declare no conflicts of interest.

Declaration of transparency and scientific rigour

This Declaration acknowledges that this paper adheres to the principles for transparent reporting and scientific rigour of preclinical research recommended by funding agencies, publishers and other organizations engaged with supporting research.

References

- Alexander SPH, Kelly E, Marrion N, Peters JA, Benson HE, Faccenda E *et al.* (2015a). The Concise Guide to PHARMACOLOGY 2015/16: Overview. Br J Pharmacol 172: 5729–5143.

- Alexander SPH, Davenport AP, Kelly E, Marrion N, Peters JA, Benson HE *et al.* (2015b). The Concise Guide to PHARMACOLOGY 2015/16: G protein-coupled receptors. *Br J Pharmacol* 172: 5744–5869.
- Alexander SPH, Fabbro D, Kelly E, Marrion N, Peters JA, Benson HE *et al.* (2015c). The Concise Guide to PHARMACOLOGY 2015/16: Enzymes. *Br J Pharmacol* 172: 6024–6109.
- Alfarano C, Foussal C, Lairez O, Calise D, Attané C, Anesia R *et al.* (2014). Transition from metabolic adaptation to maladaptation of the heart in obesity: role of apelin. *Int J Obes (Lond)* 39: 312–320.
- Attané C, Foussal C, Le Gonidec S, Benani A, Daviaud D, Wanecq E *et al.* (2012). Apelin treatment increases complete Fatty Acid oxidation, mitochondrial oxidative capacity, and biogenesis in muscle of insulin-resistant mice. *Diabetes* 61: 310–320.
- Awad H, Nolette N, Hinton M, Dakshinamurti S (2014). AMPK and FoxO1 regulate catalase expression in hypoxic pulmonary arterial smooth muscle. *Pediatr Pulmonol* 49: 885–897.
- Battiprolu P, Hojajev B, Jiang N, Wang ZV, Luo X, Iglesias M *et al.* (2012). Metabolic stress-induced activation of FoxO1 triggers diabetic cardiomyopathy in mice. *J Clin Invest* 122: 1109–1118.
- Bianchi P, Kunduzova O, Masini E, Cambon C, Bani D, Raimondi L *et al.* (2005). Oxidative stress by monoamine oxidase mediates receptor-independent cardiomyocyte apoptosis by serotonin and postischemic myocardial injury. *Circulation* 112: 3297–3305.
- Bluher M (2013). Adipose tissue dysfunction contributes to obesity related metabolic diseases. *Best Pract Res Clin Endocrinol Metab* 27: 163–177.
- Boal F, Guetzyan L, Sessions RB, Zeghouf M, Spooner RA, Lord JM *et al.* (2010). LG186: An inhibitor of GBF1 function that causes Golgi disassembly in human and canine cells. *Traffic* 11: 1537–1551.
- Braunersreuther V, Mach F, Montecucco F (2012). Reactive oxygen-induced cardiac intracellular pathways during ischemia and reperfusion. *Curr Signal Transduct Ther* 7: 89–95.
- Curtis MJ, Bond RA, Spina D, Ahluwalia A, Alexander SPA, Giembycz MA *et al.* (2015). Experimental design and analysis and their reporting: new guidance for publication in BJP. *Br J Pharmacol* 172: 3461–3471.
- Dray C, Debard C, Jager J, Disse E, Daviaud D, Martin P *et al.* (2010). Apelin and APJ regulation in adipose tissue and skeletal muscle of type 2 diabetic mice and humans. *Am J Physiol Endocrinol Metab* 298: E1161–E1169.
- Dray C, Knauf C, Daviaud D, Waget A, Boucher J, Buléon M *et al.* (2008). Apelin stimulates glucose utilization in normal and obese insulin-resistant mice. *Cell Metab* 8: 437–445.
- Evans-Anderson H, Alfieri C, Yutzy E (2008). Regulation of cardiomyocyte proliferation and myocardial growth during development by FOXO transcription factors. *Circ Res* 102: 686–694.
- Ferber E, Peck B, Delpuech O, Bell GP, East P, Schulze A *et al.* (2011). FOXO3a regulates reactive oxygen metabolism by inhibiting mitochondrial gene expression. *Cell Death Differ* 19: 968–979.
- Foussal C, Lairez O, Calise D, Pathak A, Guilbeau-Frugier C, Valet P *et al.* (2010). Activation of catalase by apelin prevents oxidative stress-linked cardiac hypertrophy. *FEBS Lett* 584: 2363–2370.
- Furuyama T, Kitayama K, Shimoda Y, Ogawa M, Sone K, Yoshida-Araki K *et al.* (2004). Abnormal angiogenesis in Foxo1 (Fkhr)-deficient mice. *J Biol Chem* 279: 34741–34749.
- Kadoglou N, Lampropoulos S, Kapelouzou A, Gkrontopoulos A, Theofiliannakos EK, Fotiadis G *et al.* (2010). Serum levels of apelin and ghrelin in patients with acute coronary syndromes and established coronary artery disease—KOZANI STUDY. *Transl Res* 155: 238–246.
- Kang P, Izumo S (2000). Apoptosis and heart failure a critical review of the literature. *Circ Res* 86: 1107–1113.
- Kilkenny C, Browne W, Cuthill IC, Emerson M, Altman DG (2010). Animal research: Reporting in vivo experiments: the ARRIVE guidelines. *Br J Pharmacol* 160: 1577–1579.
- Kleinz MJ, Davenport AP (2005). Emerging roles of apelin in biology and medicine. *Pharmacol Ther* 107: 198–211.
- Kleinz MJ, Skepper JN, Davenport AP (2005). Immunocytochemical localisation of the apelin receptor, APJ, to human cardiomyocytes, vascular smooth muscle and endothelial cells. *Regul Pept* 126: 233–240.
- Konstantinidis K, Whelan R, Kitsis R (2012). Mechanisms of cell death in heart disease. *Arterioscler Thromb Vasc Biol* 32: 1552–1562.
- Kops G, Dansen T, Polderman P, Saarloos I, Wirtz K, Coffer P *et al.* (2002). Forkhead transcription factor FOXO3a protects quiescent cells from oxidative stress. *Nature* 419: 316–321.
- Kowluru A, Matti A (2012). Hyperactivation of protein phosphatase 2A in models of glucolipotoxicity and diabetes: potential mechanisms and functional consequences. *Biochem Pharmacol* 84: 591–597.
- Kuba K, Zhang L, Imai Y, Arab S, Chen M, Maekawa Y *et al.* (2007). Impaired heart contractility in Apelin gene-deficient mice associated with aging and pressure overload. *Circ Res* 101: e32–e42.
- Mani K (2008). Programmed cell death in cardiac myocytes: strategies to maximize post-ischemic salvage. *Heart Fail Rev* 13: 193–209.
- Maury E, Ehala-Aleksejev K, Guiot Y, Detry R, Vandenhooft A, Brichard S (2007). Adipokines oversecreted by omental adipose tissue in human obesity. *Am J Physiol Endocrinol Metab* 293: E656–E665.
- McGrath JC, Lilley E (2015). Implementing guidelines on reporting research using animals (ARRIVE etc.): new requirements for publication in BJP. *Br J Pharmacol* 172: 3189–3193.
- Medema R, Kops G, Bos J, Burgener B (2000). AFX-like Forkhead transcription factors mediate cell-cycle regulation by Ras and PKB through p27kip1. *Nature* 404: 782–787.
- Nakamura K, Fuster J, Walsh K (2014). Adipokines: a link between obesity and cardiovascular disease. *J Cardiol* 63: 250–259.
- Pawson AJ, Sharman JL, Benson HE, Faccenda E, Alexander SP, Buneman OP *et al.* (2014). The IUPHAR/BPS guide to PHARMACOLOGY: an expert-driven knowledge base of drug targets and their ligands. *Nucleic Acids Res* 42: D1098–D1106.
- Pchejetski D, Foussal C, Alfarano C, Lairez O, Calise D, Guilbeau-Frugier C *et al.* (2012). Apelin prevents cardiac fibroblast activation and collagen production through inhibition of sphingosine kinase 1. *Eur Heart J* 33: 2360–2369.
- Pchejetski D, Kunduzova O, Dayon A, Calise D, Seguelas MH, Leducq N *et al.* (2007). Oxidative stress-dependent sphingosine kinase-1 inhibition mediates monoamine oxidase A-associated cardiac cell apoptosis. *Circ Res* 100: 41–49.
- Ponugoti B, Dong G, Graves D (2012). Role of forkhead transcription factors in diabetes-induced oxidative stress. *Exp Diabetes Res* 2012: 939751.
- Rana J, Mukamal K, Morgan J, Muller J, Mittleman M (2004). Obesity and the risk of death after acute myocardial infarction. *Am Heart J* 147: 841–846.

- Raju I, Kannan K, Abraham E (2013). FoxO3a Serves as a Biomarker of Oxidative Stress in Human Lens Epithelial Cells under Conditions of Hyperglycemia. *PLoS One* 8: e67126.
- Sengupta A, Molkentin J, Paik J, DePinho R, Yutzey K (2011). FoxO transcription factors promote cardiomyocyte survival upon induction of oxidative stress. *J Biol Chem* 286: 7468–7478.
- Tatemoto K, Hosoya M, Habata Y, Fujii R, Kakegawa T, Zou M *et al.* (1998). Isolation and characterization of a novel endogenous peptide ligand for the human APJ receptor. *Biochem Biophys Res Commun* 251: 471–476.
- Tycinska A, Sobkowicz B, Mroczko B, Sawicki R, Musial W, Dobrzycki S *et al.* (2010). The value of apelin-36 and brain natriuretic peptide measurements in patients with first ST-elevation myocardial infarction. *Clin Chim Acta* 411: 2014–2018.
- Ullman K, Powers M, Forbes D (1997). Nuclear export receptors: from importin to exportin. *Cell* 90: 967–970.
- Wang W, McKinnie S, Patel V, Haddad G, Wang Z, Zhabayev P *et al.* (2013). Loss of apelin exacerbates myocardial infarction adverse remodeling and ischemia-reperfusion injury: therapeutic potential of synthetic apelin analogues. *J Am Heart Assoc* 2: e000249.
- Wang X (2001). The expanding role of mitochondria in apoptosis. *Genes Dev* 15: 2922–2933.
- Wang Y, Zhou Y, Graves D (2014). FOXO transcription factors: their clinical significance and regulation. *Biomed Res Int* 2014; Article ID 925350, 13 pages.
- Weir R, Chong K, Dalzell J, Petrie C, Murphy C, Steedman T *et al.* (2009). Plasma apelin concentration is depressed following acute myocardial infarction in man. *Eur J Heart Fail* 11: 551–558.
- Wencker D, Chandra M, Nguyen K, Miao W, Garantziotis S, Factor SM *et al.* (2003). A mechanistic role for cardiac myocyte apoptosis in heart failure. *J Clin Invest* 111: 1497–1504.
- Zhao Y, Wang Y, Zhu WG (2011). Applications of post-translational modifications of FoxO family proteins in biological functions. *J Mol Cell Biol* 3: 276–282.
- Zhen EY, Higgs RE, Gutierrez AJ (2013). Pyroglutamyl apelin-13 identified as the major apelin isoform in human plasma. *Anal Biochem* 442: 1–9.

SCIENTIFIC REPORTS



OPEN

Apelin regulates FoxO3 translocation to mediate cardioprotective responses to myocardial injury and obesity

Received: 22 April 2015

Accepted: 25 September 2015

Published: 06 November 2015

Frederic Boal^{1,2,*}, Jessica Roumegoux^{1,2,*}, Chiara Alfarano^{1,2}, Andrei Timotin^{1,2}, Denis Calise^{2,3}, Rodica Anesia^{1,2}, Anne Drougard^{1,2}, Claude Knauf^{4,2}, Christine Lagente⁴, Jerome Roncalli⁴, Franck Desmoulin^{1,2}, Helene Tronchere^{1,2}, Philippe Valet^{1,2}, Angelo Parini^{1,2} & Oksana Kunduzova^{1,2}

The increasing incidence of obesity accentuates the importance of identifying mechanisms and optimal therapeutic strategies for patients with heart failure (HF) in relation to obesity status. Here, we investigated the association between plasma level of apelin, an adipocyte-derived factor, and clinicopathological features of obese and non-obese patients with HF. We further explored potential regulatory mechanisms of cardiac cell fate responses in conditions combining myocardial injury and obesity. In a prospective, cross-sectional study involving patients with HF we show that obese patients ($BMI \geq 30\text{ kg/m}^2$) have higher left ventricular ejection fraction (LVEF) and greater levels of plasma apelin ($p < 0.005$) than non-obese patients ($< 30\text{ kg/m}^2$), independently of ischemic etiology. In a mouse model combining ischemia-reperfusion (I/R) injury and high-fat diet (HFD)-induced obesity, we identify apelin as a novel regulator of FoxO3 trafficking in cardiomyocytes. Confocal microscopy analysis of cardiac cells revealed that apelin prevents nuclear translocation of FoxO3 in response to oxygen deprivation through a PI3K pathway. These findings uncover apelin as a novel regulator of FoxO3 nucleocytoplasmic trafficking in cardiac cells in response to stress and provide insight into its potential clinical relevance in obese patients with HF.

Cardiovascular disease and obesity are common, interrelated health problems in industrialized societies. In the general population, obesity is considered to be a risk factor in the development of heart failure and is traditionally regarded to impact negatively on the outcome of myocardial ischemia. However, despite the evidence for a higher prevalence of obesity in myocardial ischemia patients, a number of recent publications suggested that obesity in humans with ischemic heart disease is associated with reduced morbidity and mortality, the so-called “obesity paradox”^{1–3}. The mechanism underlying this paradox is complex and remains unclear.

Many lines of evidence suggest that mitochondrial dysfunction, including mitochondrial loss and the production of reactive oxygen species (ROS) may be important in the development and progression of heart failure^{4,5}. Excessive generation of ROS in the heart can directly lead to increased necrosis and apoptosis of cardiomyocytes which subsequently induce cardiac dysfunction^{6,7}. The mitochondria are both the primary sources of ROS and the primary targets of ROS damage under pathological conditions including myocardial ischemia/reperfusion (I/R)⁸. The central role of mitochondria-derived ROS in the

¹National Institute of Health and Medical Research (INSERM) U1048, Toulouse, Cedex 4, France. ²University of Toulouse, UPS, Institute of Metabolic and Cardiovascular Diseases, Toulouse, France. ³US006, Microsurgery Services, Toulouse, Cedex 4, France. ⁴Department of cardiology, Toulouse University Hospital, Toulouse, Cedex 9, France. ^{*}These authors contributed equally to this work. Correspondence and requests for materials should be addressed to O.K. (email: Oxana.Koundouzova@inserm.fr)

obesity-related processes and cardiac I/R-induced damage has been shown recently^{9,10}. However, the mechanisms through which mitochondrial ROS may regulate cell fate decisions in response to stress remain poorly defined.

The forkhead box O (FoxO) family of transcription factors plays a fundamental role in the regulation of mitochondrial activity and cellular responses to oxidative stress. In mammals, the FoxO family comprises four isoforms (FoxO1, FoxO3, FoxO4, and FoxO6) characterized by an overlapping expression during development and in adulthood. FoxO acts as transcriptional activators governing a variety of vital cellular processes including cell survival, apoptosis, metabolism, DNA repair and resistance to oxidative stress. A number of studies point toward a role for FoxO3 in maintaining cardiovascular and metabolic homeostasis^{11,12}. Although the existing data are controversial, there is some evidence that FoxO3 regulates life/death decisions in response to cellular stressors. In cardiac microvascular endothelial cells FoxO3 leads to ROS accumulation, and in parallel, induces the disturbance of Bcl-2 family proteins which results in activation of apoptosis¹³. In contrast, in cardiomyocytes, knockdown of endogenous FoxO3 sensitizes cells to undergo apoptosis, whereas enforced expression of FoxO3 inhibits apoptosis¹⁴. Additional work in animal models of age-dependent oxidative stress responses demonstrated that up-regulation of FoxO3 in the heart and adipose tissue is associated with activation of cellular anti-oxidant systems¹⁵. Trafficking of FoxO between the nucleus and the cytoplasm plays a decisive role in stress-related regulation of cell death/cell survival. Shuttling in and out of the nucleus not only provides a mechanism to control signal-dependent access of proteins to nuclear targets, but also contributes to regulate the activity of proteins in the cytoplasm¹⁶. Given the fundamental role of FoxO3 in cardiovascular and metabolic homeostasis, the function and fine-tuned regulation of its subcellular distribution is critical for the future development of specific and effective cardioprotective therapeutics in clinical situations combining obesity and myocardial damage.

The adipose tissue acts as an endocrine organ, and plays a substantial role in the pathogenesis of cardiovascular and metabolic diseases¹⁷. Altered levels of adipocyte-derived factors or “adipokines”, may be particularly related with heart disease^{17,18}. We have previously demonstrated that apelin, a recently described adipokine, plays an important role in the regulation of cardiovascular and metabolic homeostasis^{19,20}. Apelin, an endogenous ligand for the G-protein-coupled receptor APJ, exerts strong inotropic activity and increases coronary blood flow by vascular dilation²¹. In response to pathological stress, apelin-APJ axis regulates myocardial remodeling and cardiac function^{20,22}. The loss of apelin impairs I/R remodeling and exacerbates myocardial I/R injury *ex vivo* and *in vivo*²³. Apelin-deficient mice develop age-related progressive cardiac dysfunction which is prevented by apelin infusion²⁴, suggesting an important role of apelinergic system in maintaining cardiac performance. In humans, circulating and cardiac levels of apelin are reduced in patients with acute myocardial infarction and established coronary artery disease^{25–27}. In explanted human hearts, the primary ischemic injury is associated with the loss of apelin in various compartments confirming an important role of apelin in human heart failure²³. By contrast, in obese subjects, plasma apelin concentrations are increased^{28,29}. However, the role of apelin in conditions combining myocardial infarction and obesity remains to be determined.

Materials and Methods

Reagents and antibodies. Antibodies used in this study are: anti-FoxO3 (75D8) from Cell Signalling Laboratories, anti-tubulin from SantaCruz Biotechnologies; anti-beta-actin from Sigma (A1978). Fluorescent Alexa-coupled secondary antibodies were from Life Technologies and HRP-coupled secondary antibodies from Cell Signaling Technologies. DAPI was from Life Technologies. Apelin-13 was purchased from Bachem and was referred to as apelin throughout this study. All other chemicals were from Sigma unless otherwise stated. siRNA against FoxO3 were from Eurogentec and were as follows: 5'-GGAUAGGGCGACAGAAC-3' and 5'-GUUGCUGUCGCCCUUAUCC-3'. The dominant-negative mutant FoxO3-TM plasmid was kindly provided by Dr A. Dejean (Physiopathology Center of Toulouse-Purpan, Toulouse, France) and was as described³⁰.

Primary mice cardiomyocytes preparation, cell culture, transfection and treatments. Adult mice ventricular cardiomyocytes were isolated from adult obese mice and maintained as described³¹. The rat embryonic cardiomyoblastic cell line H9C2 was cultured in MEM medium (Gibco 41090-028) supplemented with 10% FBS and 1% penicillin-streptomycin in a 37°C, 5% CO₂ incubator. siRNA transfection was performed with Lipofectamine RNAiMAX (Life Technologies) according to manufacturer's instructions. H9C2 cells were transfected using JetPrime (Polyplus Transfection) according to manufacturer's instructions. For transfection studies, FoxO3-TM was co-transfected with peGFP-C1 at a ratio of 80:20 to identify transfected cells. Cells were pretreated for 15 minutes with apelin (10⁻⁷ M) and then subjected to normoxia (5% CO₂; 21% O₂, balance N₂) or hypoxia for 2 hours in a hypoxic chamber (5% CO₂, 1% O₂, balance N₂). The dose of apelin was chosen on the basis of our previous *in vitro* studies^{20,22}. To measure cell apoptosis induced by hypoxia, the cells were left for 16 hours in hypoxic conditions.

Evaluation of apoptosis. Apoptosis level both *in vivo* and *in vitro* was assessed using the DeadEnd Fluorometric TUNEL system according to manufacturer's instructions (Promega) as described before²⁰.

	ND	HFD
Body weight (g)	28.5 ± 0.6	47.5 ± 0.4***
Fat mass (%)	14.1 ± 0.9	38.8 ± 1.2***
Glycemia (mM)	8.0 ± 0.2	10.9 ± 0.8***
Insulinemia (pg/ml)	1545.7 ± 293.2	3753.3 ± 591.8**

Table 1. Metabolic parameters of mice under ND or HFD feeding. Male C57BL/6J mice were fed ND or HFD for 20 weeks. Body weight, fat mass, and plasma parameters were measured at the end of week 4. Data are means ± sem; n = 8 per group. **p < 0.01 and ***p < 0.001 vs ND-fed group.

Hydrogen peroxyde and superoxide production. Mitochondrial O₂⁻ and H₂O₂ production in cells was measured by MitoSOX (Life Technologies) and MitoPY1 (Sigma-Aldrich) at 1 μM (on H9C2 cells) or 5 μM (on cardiomyocytes) for 30 min following live-cell imaging on a confocal microscope equipped with an incubation chamber with temperature control and CO₂ enrichment. H₂O₂ level in hearts were measured by amperometry as described³² and LPO (lipid hydroperoxyde) quantification was done as described before²².

Caspase-3, plasmatic troponin I and metabolic measurements. Caspase-3 activity was assessed with EnzChek Caspase-3 Assay Kit #1 (Life Technologies) according to the manufacturer's instructions. Plasmatic Troponin-I (Life Diagnostics) were quantified using specific ELISA kits according to the manufacturers' instructions. Insulinemia (Mercodia) and glycemia (Accu-check, Roche Diagnostics) were measured in fasted state. Body fat mass composition was determined as described before³¹.

Animal studies. The investigation conforms to the Guide for the Care and Use of Laboratory Animals published by the US National Institutes of Health (NIH Publication No. 85-23, revised 1985) and was performed in accordance with the recommendations of the French Accreditation of the Laboratory Animal Care (approved by the local Centre National de la Recherche Scientifique ethics committee). Wild-type male C57BL6/J mice purchased from Janvier Labs or apelin-KO mice (generated as described³¹) were fed a high fat diet (HFD, 45% fat) for 20 weeks, corresponding to the acquisition of an obese and insulin resistant phenotype^{31,32}. The metabolic profile of HFD-fed mice is summarized in Table 1. Apelin KO mice were as described before³¹.

Experimental protocol. A mouse model of ischemia-reperfusion (I/R) was used as previously described³³. In brief, the mice were intubated and placed under mechanical ventilation after undergoing general anesthesia with an intraperitoneal injection of ketamine HCl (35 mg/kg) and xylazine (5 mg/kg). A left parasternotomy was performed to expose hearts, and a 7–0 silk suture (Softsilk) was placed around the left anterior descending coronary artery. A snare was placed on the suture, and regional myocardial ischemia was produced by tightening the snare. After 45 minutes of ischemia, the occlusive snare was released to initiate reperfusion up to 24 hours. Sham-operated control mice underwent the same surgical procedures except that the snare was not tightened. Animals were randomly divided into four groups: (I) sham vehicle (n = 6), (II) ischemia-reperfusion (I/R) vehicle (n = 7), (III) sham apelin (n = 7), and (IV) ischemia-reperfusion apelin (n = 7). Mice received intravenously apelin (0.1 μg/kg) or vehicle (PBS) at 5 min of reperfusion in a final volume of 100 μl. The dose of apelin was selected on the basis of our preliminary animal studies.

Determination of area at risk and infarct size. Determination of area at risk and infarct size was done as described before³³. Briefly, at the end of the infarction protocol, in some animals of each group, the left coronary artery was reoccluded, and 1 mL of 1.5% Evans blue dye was injected into the left ventricular cavity to measure the myocardial ischemic area at risk. The animals were euthanized immediately, and the heart was removed and cut from apex to base in 4 to 5 transverse sections. After incubation in 1% triphenyltetrazolium chloride (TTC) solution in isotonic pH 7.4 phosphate buffer at 37 °C for 20 minutes, the slices were subsequently fixed in 10% formalin solution for 6 hours to assess myocardial tissue viability and determine myocardial infarct size. Evans blue stained area represents non-ischemic tissues, TCC stained zone (red) indicates ischemic but viable tissues while white unstained area represents the necrotic/ischemic tissues. Infarct size was expressed as a percentage of the ischemic risk area.

Immunofluorescence. Immunofluorescence was performed essentially as previously described³⁴. Briefly, cells grown on glass coverslips were PFA-fixed and permeabilized using TritonX-100 before incubation with primary and secondary antibodies, mounted in Mowiol and imaged using confocal microscopy on a Zeiss LSM780 microscope. For nuclear FoxO3 quantification, the fluorescence intensity of FoxO3 proteins in the nucleus was quantified and normalized against the fluorescence intensity within the total cell.

Immunolabeling of heart sections. Paraformaldehyde-fixed (4%) and paraffin embedded heart sections were deparaffinized and rehydrated, antigen retrieval was performed using a sodium citrate treatment. Alternatively, serial cryosections (10 µm) immobilized on Superfrost Plus slides (Thermoscientific) were rehydrated in PBS, fixed in 4% PFA for 10 min. Permeabilization of cardiac tissues was performed with 0.2% Triton X-100 for 20 min. After blocking of non specific sites with 1% BSA, the primary antibodies were incubated o/n at 4°C. After labeling with appropriate secondary antibodies, the sections were mounted in Vectashield mounting medium including DAPI (Vector Laboratories) and imaged by confocal microscopy.

Morphology. Ultrastructural studies of cardiac tissues by electron microscopy were done as before³¹. Briefly, cardiac tissues were fixed in cold 2.5% glutaraldehyde/1% paraformaldehyde, post-fixed in 2% osmium tetroxide, embedded in resin, and sectioned. Cardiac mitochondrial number relative to the section area was determined from electron micrographs as described previously³⁵.

Real-time RT-PCR analysis. Total RNAs were isolated from cultured mouse cardiac fibroblasts using the RNeasy mini kit (Qiagen). Total RNAs (300 ng) were reverse transcribed using Superscript II reverse transcriptase (Invitrogen) in the presence of a random hexamers. Real-time quantitative PCR was performed as previously described³¹. The expression of target mRNA was normalized to GAPDH mRNA expression. The sequences of the primers used are as follow and given in the 5'-3' orientation:

FoxO3, sense GCAAAAGCAGACCTCAAATG, antisense TGAGAGCAGATTGGCAAAGG; GAP DH, sense TGCACCACCAACTGCTTAGC, antisense GGCATGGACTGTGGTCATGAG; Bax, sense CGCGAATTGGAGATGAAC, antisense GTCCACGTCAGCAATCATCCT; Bcl-2, sense TCCCGATTTC ATTGCAAGTTGTA, antisense GCAACCACACCATCGATCTTC; ANP, sense AGAGTGGCAGAGA CAGAAA, antisense AAGGCCAAGACGAGGAAGAAG; IL-6, sense GCCCACCAAGAACGATA GTCA, antisense CAAGAAGGCAACTGGATGGAA. The content of mitochondrial DNA (mtDNA) was calculated using real-time quantitative PCR by measuring the threshold cycle ratio of a mitochondrial encoded gene (COX1) and a nuclear-encoded gene (cyclophilin A) as previously described³⁵.

Population and plasma samples collection. Forty patients, aged 43 to 82 years, with heart failure (HF) were included in this observational study. Patients were recruited from the cardiology department at the Toulouse-Rangueil University hospital, France from May 2013 to January 2014. CHF patients had known stable HF with more than 3 months without any decompensation episodes, irrespective of clinical severity (stage II to IV of NYHA classification) and etiology. Diagnosis of heart failure had been formally established by a cardiologist from clinical observations, heart disease follow-up, transthoracic echocardiography (TTE) for all patients and BNP monitoring. These patients were included during their regular scheduled visit at the hospital. The study was approved by a local ethics committee and included only patients who provided written informed consent. The research protocol conforms to the ethical guidelines of the 1975 Declaration of Helsinki. Patients were stratified according to their obesity status (obesity defined by a BMI $\geq 30 \text{ kg/m}^2$). Thus, 13 were enrolled in the obese group and 27 were enrolled in the non-obese group. Peripheral venous blood from the cohort subjects was collected into EDTA tubes. After centrifugation at 1500 g at 4 °C for 10 min, plasma was separated and stored at –80 °C until assayed.

Statistical analysis. Data are expressed as mean \pm SEM. Comparison between two groups was performed by Student's t-test while comparison of multiple groups was performed by one-way ANOVA followed by a Bonferroni's post hoc test using GraphPad Prism version 5.00 (GraphPad Software, Inc). Statistical significance was defined as $p < 0.05$ unless otherwise stated in figure legends.

For clinical studies, data were presented as mean values \pm SD or when the data failed the D'Agostino-Pearson test for normal distribution as median with 95% confident interval (CI) for continuous variables and as percentage for categorical variables. For categorical variables, a Pearson Chi-square test was used to determine the statistical significance of the association between the variable and obesity status. For continuous variables, a Student's t-test or Mann-Whitney rank sum test when normality test failed was used to determine the statistical significance of the association between the variable and obesity status with a 2-tailed P value determination. Plasma apelin concentrations were analyzed by two-way ANOVA followed by Bonferroni's post-hoc analysis using GraphPad Prism (version 5.0) software (GraphPad Software, San Diego, CA, USA). $P < 0.05$ was considered statistically significant. Logistic regression analysis was performed using Statistical R (version 3.0.1; <http://www.r-project.org>, MASS package version 7.3.37) to analyze the relationship between obesity or ischemic heart failure status and apelin. Two methods were used to select independent variables in the model: enter method, all variables were included without checking; stepwise method, variables were sequentially included, check and possibly remove variables that became non-significant after entering a variable (enter if $P < 0.1$ remove if $P > 0.2$).

Results

Plasma apelin levels and cardiac functions in obese and non-obese patients with HF. Apelin plasma levels are increased in obese individuals^{28,29}, whereas circulating apelin levels are reduced in patients with HF^{25–27}. In order to evaluate whether plasma levels of apelin differ among patients with

	All HF	non-obese HF	obese HF	P
	(N = 40)	(N = 27)	(N = 13)	
Age, y	64 ± 9	63 ± 10	66 ± 7	0.305
Sex, Female, % (F/M)	12 (5/35)	15 (4/23)	8 (1/12)	0.653
BMI	27.6 ± 5.1	24.8 ± 2.6	33.2 ± 4.6.	<0.001
Cardiovascular risk factors				
Hypertensive, % (n)	40 (16)	41 (11)	39 (5)	1.000
T2-Diabetes, % (n)	35 (14)	22 (6)	61 (8)	0.031
Dyslipidemia, % (n)	45 (18)	37 (10)	61 (8)	0.185
Smoking, % (n)	10 (4)	11 (3)	8 (1)	1.000
Heart failure etiology				
Ischemic CM, % (n)	60 (24)	56 (15)	69 (9)	0.503
Valvular CM, % (n)	5 (2)	7 (2)	0 (0)	0.550
Dilated CM, % (n)	35 (14)	37 (10)	31(4)	0.740
Medication				
ACEIs, % (n)	72 (29)	74 (20)	69 (9)	1.000
ARBs, % (n)	15 (6)	11 (3)	23 (3)	0.370
Beta-blockers, % (n)	90 (36)	92 (25)	85 (11)	0.583
Diuretics, % (n)	67 (27)	74 (20)	53 (7)	0.100
Vitamin K antagonists, % (n)	45 (18)	52 (14)	31 (4)	0.312
Antiplatelet agents, % (n)	67 (27)	63 (17)	77 (10)	0.484
Statines, % (n)	65 (26)	59 (16)	77 (10)	0.316
Admission labs				
BNP, pmol/ml	450 [245–957]	614 [326–1487]	214 [127–774]	0.073
Creatinine, µmol/l	101 [96–124]	103 [93–134]	100 [82–143]	0.817
C reactive protein, mg/l	7.8 [3.5–11.6]	8.1 [2.7–13.6]	7.8 [3.3–14.7]	0.858
Na ⁺ mM	138 ± 3	138 ± 3	138 ± 3	0.523
ALT, U/ml	29 [25–36]	26 [19–38]	32 [26–48]	0.311
Admission vitals				
Mean Blood Pressure, mmHg	86 ± 12	83 ± 11	91 ± 12	0.035
Heart rate, Bpm	73 ± 16	75 ± 16	70 ± 17	0.449
Echocardiography				
LVEF, %	31 ± 13	27 ± 10	39 ± 13	0.003
LVEF < 30%, % (n)	42 (17)	52 (14)	23 (3)	0.103
NYHA class				
II, % (n)	60 (24)	55 (15)	69 (9)	0.503
III, % (n)	35 (14)	37 (10)	31(4)	0.740
IV, % (n)	5 (2)	4 (1)	8 (1)	1.000

Table 2. Characteristics of the patients with HF. CHF, cardiac heart failure; BMI, body mass index; CM, cardiomyopathy; ACEIs, angiotensin-converting enzyme inhibitors; ARBs, angiotensin II receptor blockers; BNP, B-type natriuretic peptide concentration; ALT, alanine aminotransferase; LVEF, left ventricular ejection fraction; NYHA class, New York Heart Association functional classification.

HF in relation to obesity status, patients were divided into 2 categories based on BMI: non-obese and obese patients. Demographic and clinical data of these patients are shown in Table 2. The ischemic cardiomyopathy constituted 60% of all causes of HF. The mean apelin concentration was 401 ± 172 pg/ml in the cohort. Plasma levels of apelin were significantly higher in obese than in non-obese HF patients (503 ± 202 and 352 ± 134 pg/ml, $p < 0.005$, respectively). Plasma apelin level measured in obese patients was independent of the ischemic status (Fig. 1A). Indeed, the multivariate analysis of the association of apelin including sex, age, LVEF, T2-diabetes and ischemic HF with obesity gave odds ratio (OR) of 3.95 (95% CI, 1.31–11.94), $p = 0.015$ and 2.82 (95% CI, 1.23–6.47) per 100 pg/ml, $p = 0.014$ by using enter and

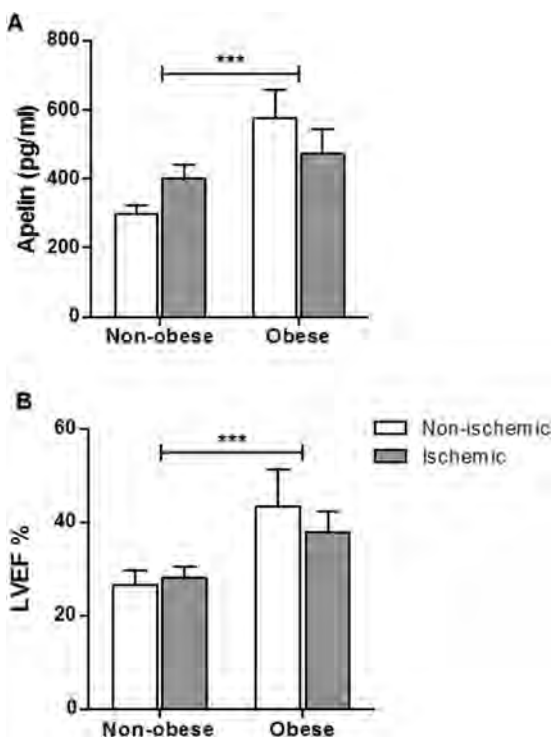


Figure 1. Apelin plasmatic levels and LVEF in patients with HF. (A) Plasma apelin concentrations in obese and non-obese patients. Data are presented as mean \pm SEM. *** $p < 0.005$, two way Anova/Bonferroni's post-test for pair-wise comparison of obese and non-obese patients. $p = 0.946$, two way Anova/Bonferroni's post-test for pair-wise comparison of non-ischemic vs ischemic cardiomyopathy. (B) Left ventricular ejection fraction (LVEF) values in obese and non-obese patients. Data are presented as mean \pm SEM. *** $p < 0.005$, two way Anova/Bonferroni's post-test for pair-wise comparison of obese and non-obese patients. $p = 0.562$, two way Anova /Bonferroni's post-test for pair-wise comparison of non-ischemic vs ischemic HF.

stepwise computing method, respectively whereas association of apelin with ischemic heart failure status remained not significant, $p = 0.566$ (Table 3). Mean LVEF value was significantly higher in obese patients (Fig. 1B). The higher mean LVEF value measured in obese patients was independent of the ischemic heart disease status (Table 3).

Effect of apelin on cardiac apoptosis, infarct size and inflammation in a mouse model combining I/R injury and obesity. Myocardial infarction is the most frequent cause of heart failure³⁶. We next examined physiopathological features and effects of post-treatment with apelin in a mouse model combining I/R injury and HFD-induced obesity. In cardiac tissue from HFD-fed mice subjected to 24h I/R, TUNEL assay revealed a significant increase in apoptotic cells as compared to sham-operated animals (Fig. 2A,B). Myocardial apoptosis was further confirmed by analysis of caspase-3 activation and apoptosis-related proteins. Apelin post-reperfusion treatment of I/R mice reduced caspase-3 activity (Fig. 2C) and expression of Bax (Fig. 2D) as compared to vehicle-treated mice after I/R. Conversely, Bcl-2 expression level, an anti-apoptotic protein, was increased in apelin-treated I/R hearts (Fig. 2E). As compared to vehicle-treated HFD-fed I/R mice, the infarct area was significantly reduced in apelin-treated animals compared to vehicle I/R animals as shown visually and quantitatively in Fig. 2F,G, respectively. Apelin-dependent cardiac protection was accompanied by a reduction in troponin I, a specific indicator of cardiac damage (Fig. 2H), and in ANP level (Fig. 2I). We also evaluated the cardiac expression of inflammatory factors in mice subjected to sham or I/R. Apelin-treated mice had significantly decreased levels of MPO activity (Fig. 2J) and IL-6 level (Fig. 2K) compared with vehicle-treated I/R mice.

Apelin post-treatment prevents mitochondrial damage after I/R injury in HFD-induced obesity. Given the central role for mitochondria in ROS production and cell fate decisions, we next examined mitochondrial ultrastructure, density and DNA content in HFD-fed mice after 24h I/R. Electron microscopy analysis revealed I/R-induced mitochondrial damage including swelling and structural alterations, as compared with sham-operated mice (Fig. 3A). As shown in Fig. 3B, tissue sections from HFD-fed hearts subjected to I/R exhibited a 39% decrease in mitochondrial density as compared to control sham mice. There were no differences in mtDNA content between HFD-fed sham and I/R mice (Fig. 3C). Importantly, plasma concentration of LPO, a marker of oxidative stress (Fig. 3D), and

	OR ^a	95% CI	P	OR ^b	95% CI	P
Association with Obesity						
Apelin per 100 pg/ml	3.95	1.31–11.94	0.015	2.82	1.23–6.47	0.014
Sex, Female = 1	17.20	0.21–1394	0.205	E		
Age per 10 years	1.87	0.54–6.42	0.322	E		
LVEF per 5%	2.46	1.20–5.08	0.014	2.26	1.20–5.08	0.015
Ischemic HF = 1	1.71	0.10–29.54	0.710	E		
T2-Diabetes = 1	32.00	1.60–635	0.024	13.23	1.38–126	0.025
Association with Ischemic HF^c						
Apelin per 100 pg/ml	1.15	0.71–1.86	0.566	E		
Sex, Female = 1	0.18	0.20–10.79	0.179	E		
Age per 10 years	1.74	0.79–3.81	0.166	E		
LVEF per 5%	0.95	0.68–1.32	0.766	E		
Obese = 1	1.47	0.20–10.79	0.706	E		
T2-Diabetes = 1	0.68	0.13–3.46	0.645	E		

Table 3. Multivariate analysis association between plasma apelin level, obesity and ischemic HF. OR, odds ratio; CI, confident interval, LVEF, left ventricular ejection fraction. ^aenter method: all variables were included without checking. P < 0.0005 for the association with obesity; p = 0.3414 for the association with Ischemic HF. ^bstepwise method: variables were sequentially included in the model, variable with p > 0.2 were excluded (E). ^cpopulation was dichotomized according the cardiovascular artery disease status (Ischemic HF, n = 24; without ischemic HF, n = 16 patient).

cardiac H₂O₂ level (Fig. 3E) were markedly increased after I/R in HFD-fed mice as compared to control group. Remarkably, apelin post-reperfusion treatment significantly prevented mitochondrial ultrastructural damage (Fig. 3A,B), increased mtDNA content (Fig. 3C) and reduced myocardial LPO (Fig. 3D) and H₂O₂ (Fig. 3E) levels in HFD conditions after I/R.

Apelin reduces hypoxia-induced mitochondrial ROS and apoptosis through the FoxO3 pathways. In order to evaluate mitochondrial ROS production in conditions combining cardiomyocytes damage and obesity, we measured mitochondria-specific superoxide (O₂[·]) and H₂O₂ generation by MitoSOX and MitoPY1 probes, respectively, in cardiomyocytes isolated from HFD-fed mice under hypoxia. Analysis of mitochondria-specific ROS formation after 2 h of hypoxic stress demonstrated that apelin treatment attenuated hypoxia-induced mitochondria-specific O₂[·] (Fig. 4A,B) and H₂O₂ generation (Fig. 4C,D). Moreover, in cardiomyocytes derived from HFD-fed mice, hypoxia-induced apoptosis was significantly reduced by apelin treatment (Fig. 4E,F).

FoxO3 is known to be critical for the regulation of oxidative stress and apoptosis in cells¹³. Therefore, we investigated if apelin's ability to reduce cell death and oxidative stress in cardiac cells was FoxO3-dependent. Silencing of FoxO3 by siRNA abolished the ability of apelin to attenuate hypoxia-induced mitochondrial O₂[·] production in cardiomyoblasts (Fig. 4G,H). In addition, FoxO3 knockdown drastically blocked apelin-mediated anti-apoptotic activity in response to hypoxia (Fig. 4I,J).

In order to confirm the implication of FoxO3 in apelin's ability to reduce mitochondrial ROS production, we overexpressed the constitutively active FoxO3-TM mutant. As shown in Fig. 5A,B overexpression of FoxO3-TM in H9C2 cells did not result in significant increase in mitochondrial O₂[·] as compared with non-transfected cells (Fig. 5A,B). Strikingly, overexpression of FoxO3-TM abolished the ability of apelin to reduce mitochondrial O₂[·] generation in response to hypoxia (Fig. 5A,B).

FoxO3 nucleocytoplasmic shuttling is regulated by apelin in cardiac cells in response to oxidative stress through a PI3K pathway. The subcellular trafficking of FoxO factors is one of the key aspects to control cell fate decisions³⁷. We next examined the nucleocytoplasmic dynamics of FoxO3 in cardiomyocytes isolated from HFD-fed mice in response to hypoxia. Positive staining with anti-FoxO3 antibodies was identified in cardiomyocytes isolated from HFD-fed mice (Fig. 6A), where FoxO3 was found in the cytoplasm in normoxia (21% O₂). Exposure of cardiomyocytes to hypoxia (1% O₂) for 2 h resulted in predominant nuclear translocation of FoxO3 as demonstrated by the strong colocalization with DAPI (Fig. 6A). Strikingly, apelin treatment completely prevented hypoxia-induced nuclear translocation of FoxO3 (Fig. 6A,B) suggesting that apelin coordinates FoxO3 nucleocytoplasmic trafficking in response to stress.

To elucidate the potential mechanisms of FoxO3 trafficking in response to oxidative stress, we examined whether PI3K/Akt or p38/MAPK are involved in hypoxia-dependent FoxO3 nuclear translocation.

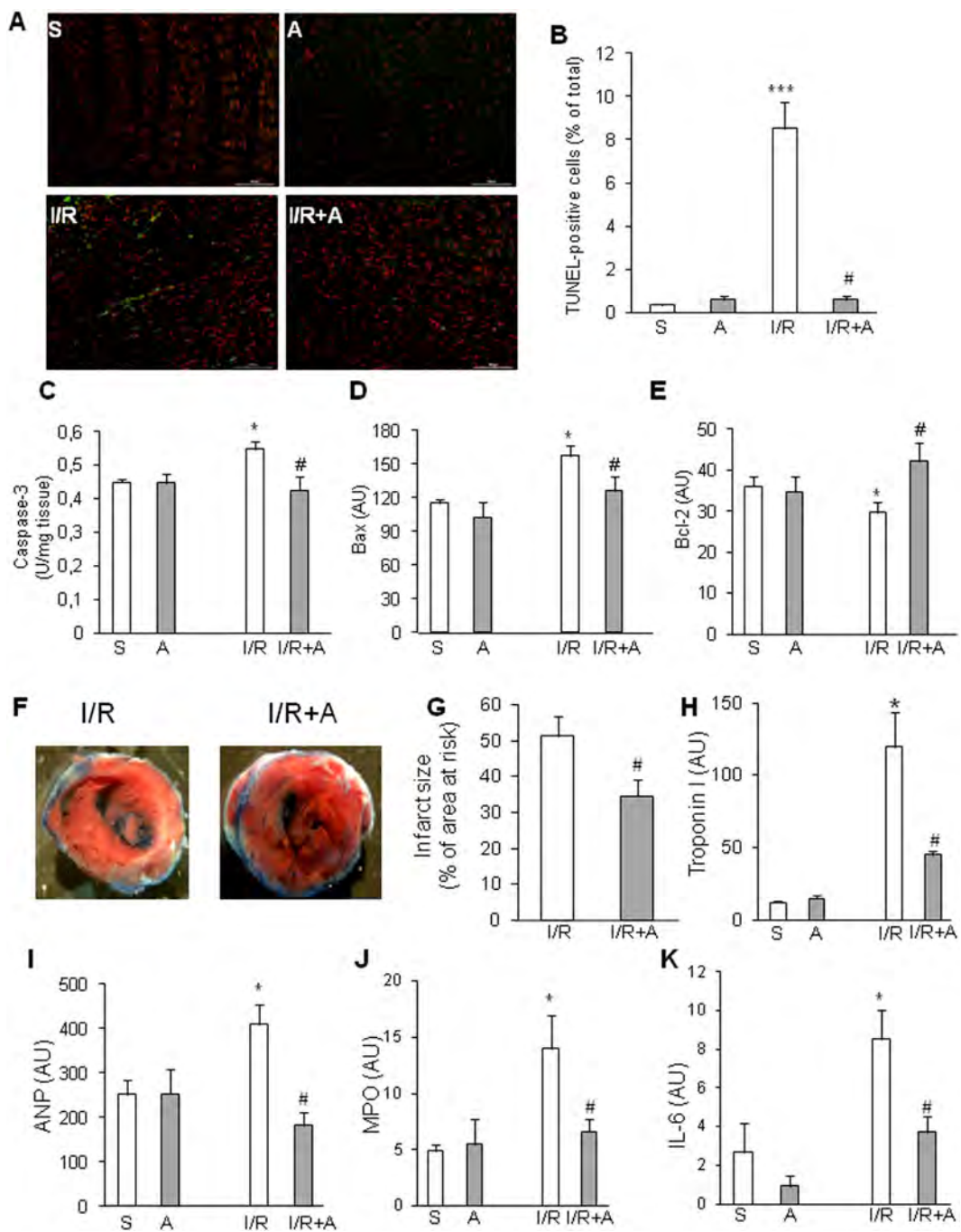


Figure 2. Apelin reduces cell death, infarct size and inflammation in obese mice hearts after I/R surgery. (A) TUNEL staining of heart sections from obese mice treated or not with apelin (A) and sham-operated (S) or subjected to I/R. Apoptotic cells are labeled in green, nuclei are stained in red. (B) Quantification of apoptosis from (A). The percentage of apoptotic cells was quantified for each condition. (C–E) Caspase-3 activity (C), Bax (D) and Bcl-2 (E) expression levels in hearts from obese mice treated as indicated.

* $p < 0.05$ compared with S; # $p < 0.05$ as compared with I/R. (F) Cross-sections of hearts treated as indicated were stained with Evans blue and TTC. (G) Quantification of infarct size expressed as percentage of area at risk. # $p < 0.05$ as compared with I/R. (H–K) Troponin I plasmatic levels (H), ANP expression level (I), MPO activity (J) and IL-6 expression level (K) in hearts of obese mice treated as indicated. *** $p < 0.001$ vs S; * $p < 0.05$ vs S; # $p < 0.05$ vs I/R.

As shown in Fig. 6C in H9C2 cells, we observed the same profile of FoxO3 nuclear translocation as in isolated cardiomyocytes. Inhibition of the PI3K pathway by LY294002 in normoxic H9C2 cells resulted in a selective FoxO3 nuclear accumulation (Fig. 6C and quantified in Fig. 6D). Strikingly, LY294002 treatment

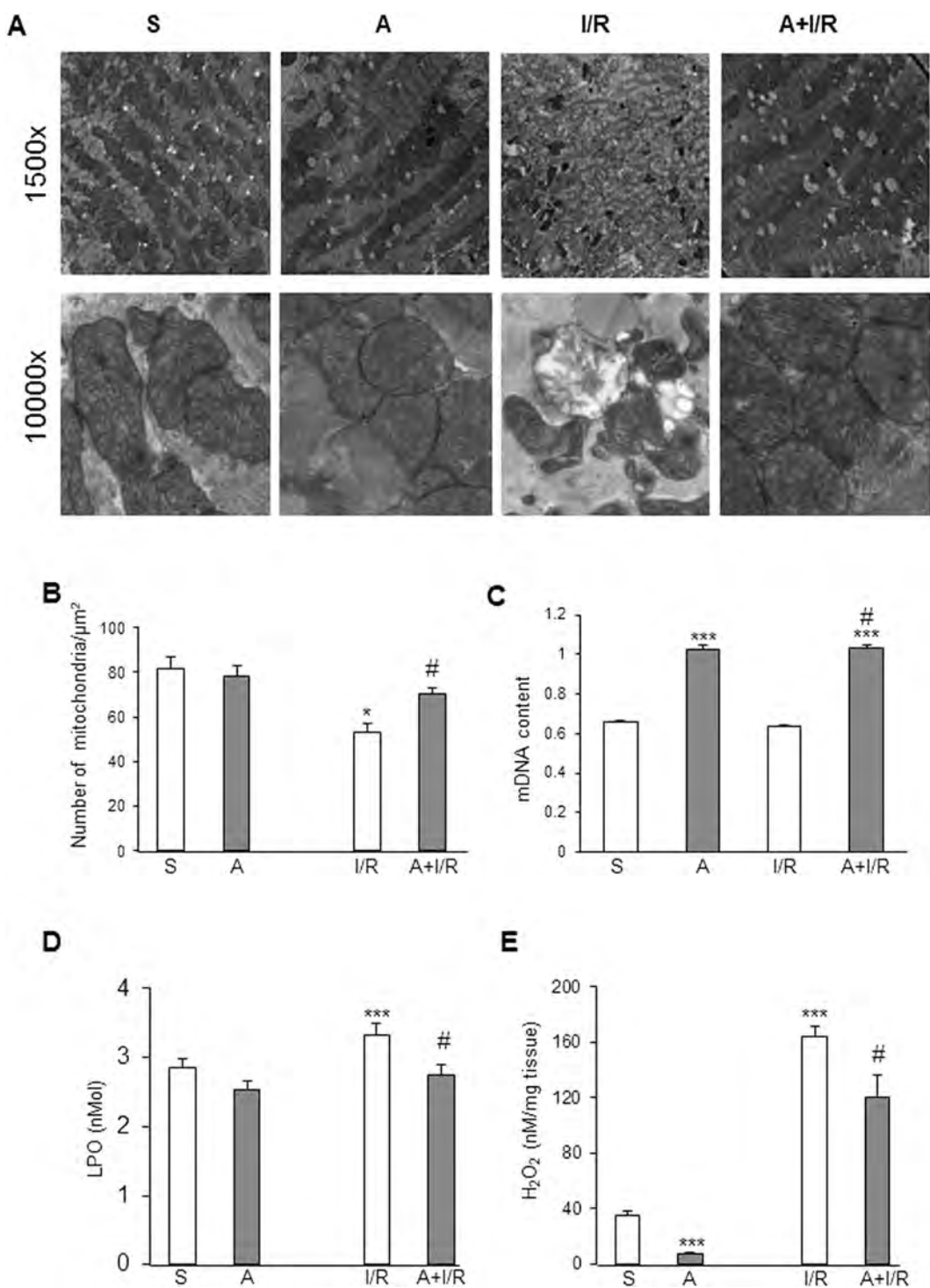


Figure 3. Apelin-treatment protects from mitochondrial damage, H_2O_2 production and lipid peroxidation in obese heart. (A) Typical electron micrographs from sham (S), apelin-treated (A) or animals subjected to I/R are shown at original magnifications x1500 and x10000. (B) Quantitative analysis of mitochondrial density in heart tissues. (C) qRT-PCR analysis of mtDNA content. (D,E), Plasmatic LPO (D) and H_2O_2 levels in cardiac tissues (E) from obese mice treated as indicated. * $p < 0.05$; *** $p < 0.001$ vs S; # $p < 0.05$ vs I/R.

completely abolished apelin effect on hypoxia-induced FoxO3 nuclear localization (Fig. 6C,D). However, inhibition of the p38/MAPK pathway by SB203580 did not abrogate the effect of apelin (Fig. 6C,D). In order to confirm the implication of PI3K/Akt pathway in apelin-dependent FoxO3 nuclear translocation, we resorted to the use of the non-phosphorylatable FoxO3-TM mutant. As shown in Fig. 7, this mutant

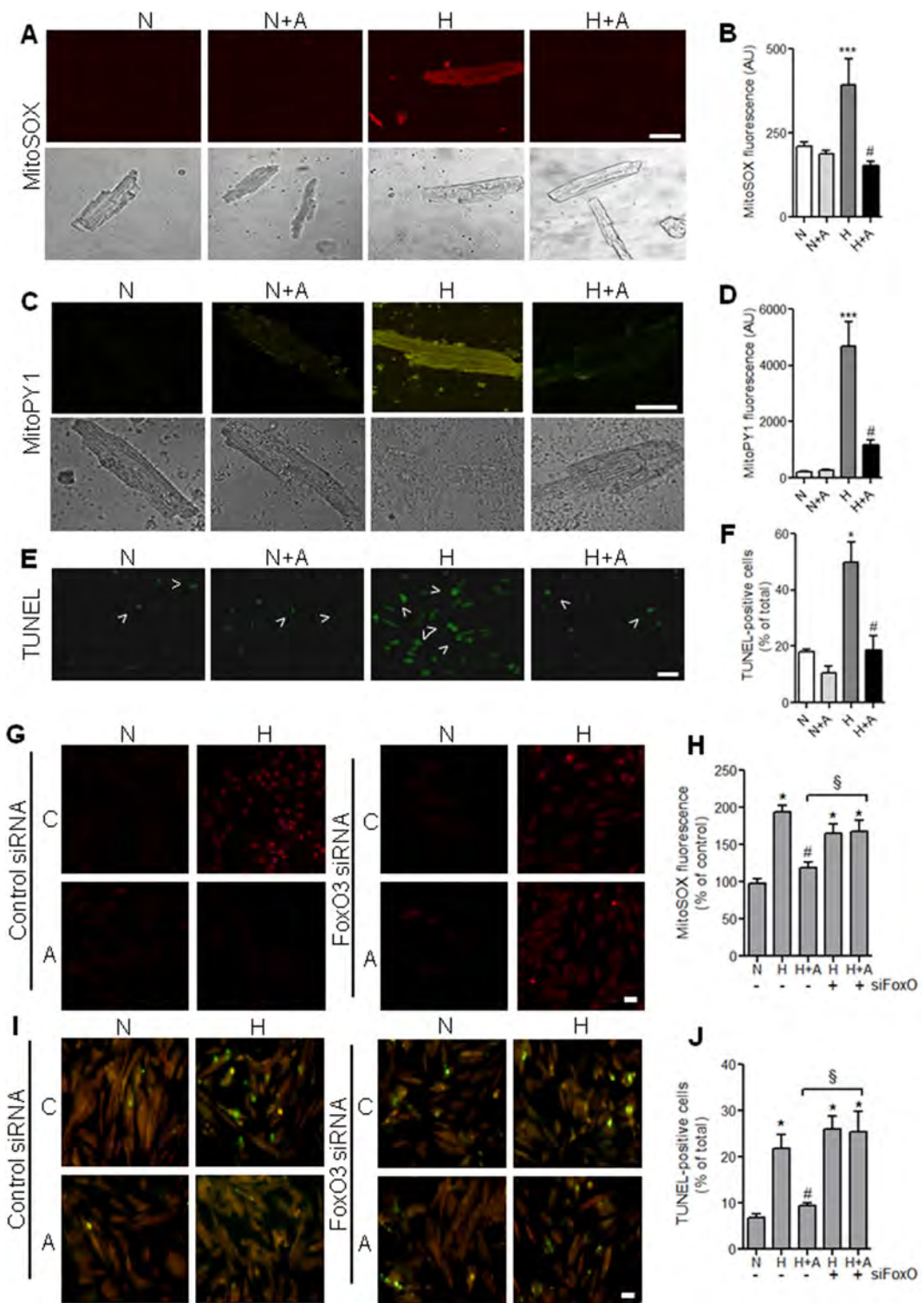


Figure 4. Apelin treatment reduces hypoxia-induced ROS production and apoptosis in cardiomyocytes through the FoxO3 pathway. Primary cardiomyocytes isolated from HFD-fed mice were treated with apelin for 15 minutes and submitted to hypoxia for 2 h. (A–F) Mitochondrial O₂⁻ (A,B) and H₂O₂ (C,D) production were followed using the fluorescent probes MitoSOX Red and MitoPY1 respectively. Apoptosis was measured by TUNEL labeling (E,F). Arrowheads highlight TUNEL-positive cells. Bar is 20 μm in all panels. (G,H) H9C2 cardiomyoblasts were transfected with siRNA targeting FoxO3 or with scramble control siRNA, treated or not (C) with apelin (A, 10⁻⁷M for 15 minutes) and subjected to hypoxia (H) or normoxia (N) for 2 hours. Mitochondrial ROS production was measured by MitoSOX Red fluorescence (in red). (I,J) H9C2 cells were treated as in (G) and apoptotic cells were labeled with TUNEL staining. Bar is 20 μm. *p < 0.05 vs N; ***p < 0.001 vs N; #p < 0.05 vs H; §p < 0.05 between indicated conditions.

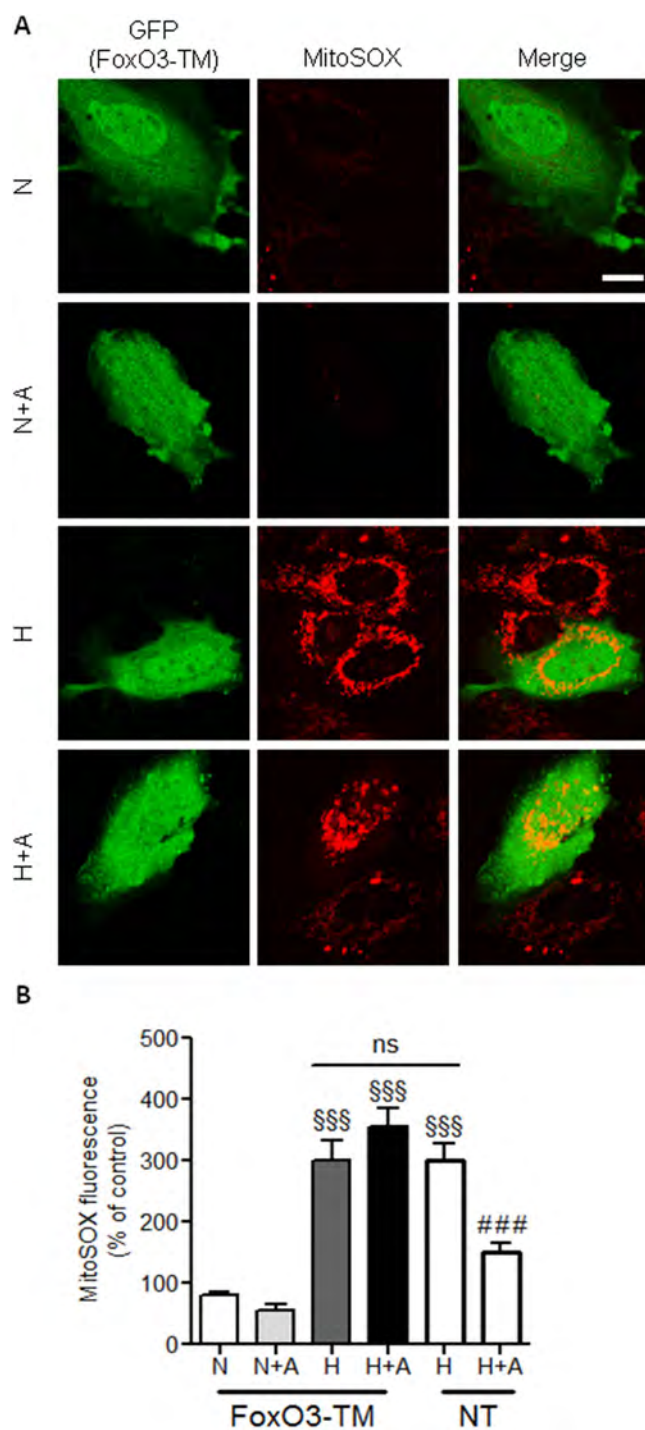


Figure 5. Abbrogation of anti-oxidant effect of apelin by overexpression of FoxO3-TM in H9C2 cells. (A) H9C2 cells were transfected to express GFP (in green) and the dominant negative mutant FoxO3-TM. Cells were submitted to hypoxic conditions (H) or kept in normoxia (N) in the presence or not of apelin (A). Mitochondrial O²⁻ production was measured by confocal microscopy using MitoSOX (in red) in transfected cells and in non-transfected cells (NT) as a control. Bar is 10 μm. (B) Quantification of MitSOX fluorescence per cells from (A). ***p < 0.001 vs N from transfected cells; #***p < 0.001 vs H from NT cells; ns, non significant.

is constitutively localized in the nuclei in H9C2 cells in basal condition. Strikingly, apelin was not able to induce the nuclear exclusion of FoxO3-TM both in normoxia and hypoxia (Fig. 7A,B), confirming that apelin prevents hypoxia-induced FoxO3 nuclear translocation through a PI3K/Akt dependent pathway.

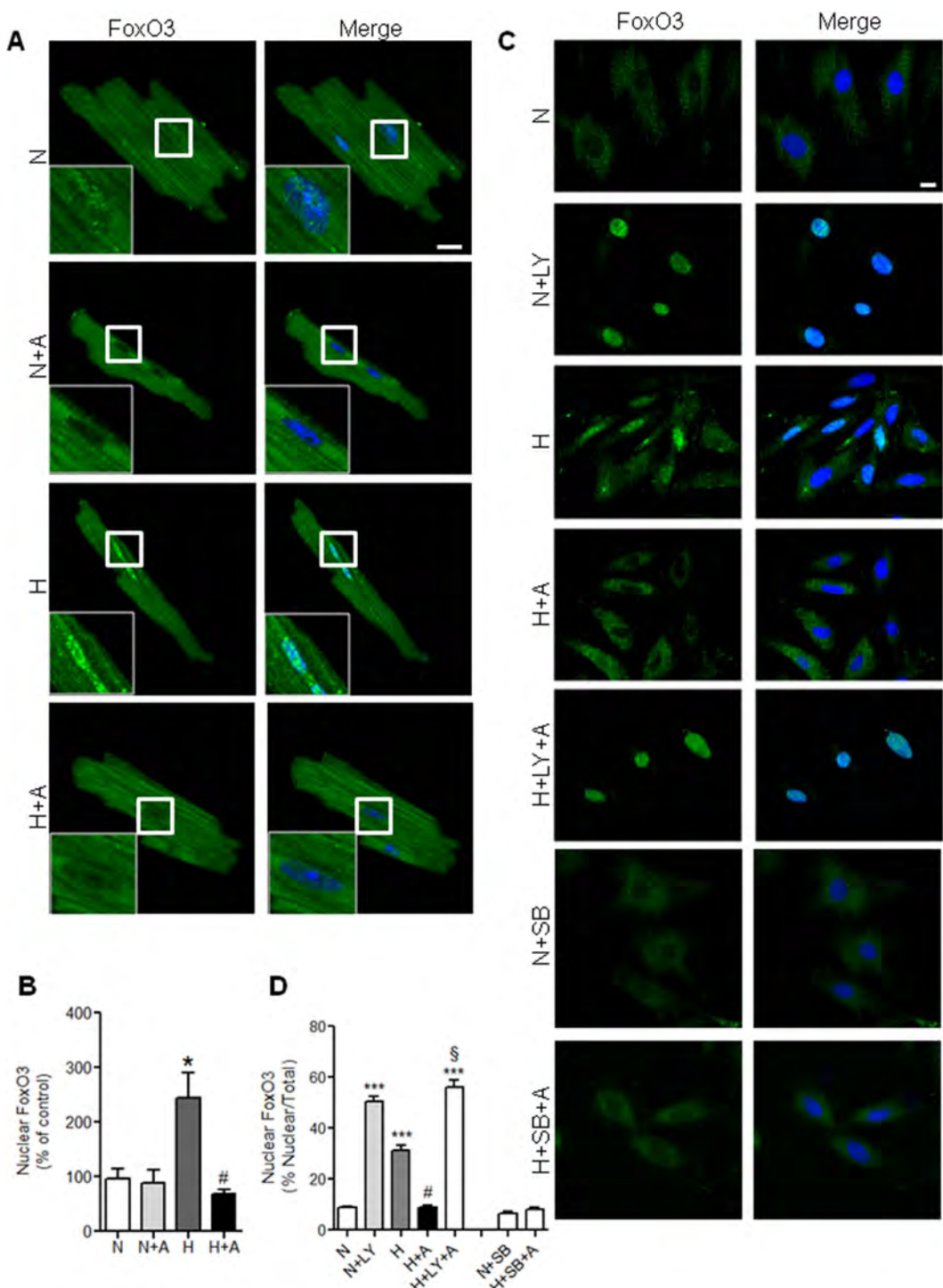


Figure 6. Apelin treatment reverses FoxO3 nuclear translocation induced by hypoxia in cardiac cells through a PI3-K dependent pathway. (A) Representative confocal images of cardiomyocytes isolated from HFD-fed mice stimulated or not by apelin for 15 minutes (A, 10^{-7} M), submitted to hypoxic (H) or normoxic (N) conditions for 2 hours, and stained in green for FoxO3. Nuclei were stained with DAPI (in blue). Bar is $20\mu\text{m}$. (B) Quantification of FoxO3 nuclear translocation from (A,C) H9C2 cells treated with the PI3-K inhibitor LY294002 (LY) or with the p38/MAPK SB203580 (SB) in the presence (A) or absence of apelin, and then submitted to hypoxic conditions (H) or left in normoxia (N) for 2h. Cells were fixed and stained with an anti-FoxO3 antibody (in green), nuclei were stained with DAPI (in blue). Bar is $10\mu\text{m}$. (D) Quantification of FoxO3 nuclear translocation was done as in (B). * $p < 0.05$ vs N; *** $p < 0.001$ vs N; # $p < 0.001$ vs H; § $p < 0.001$ vs H+A.

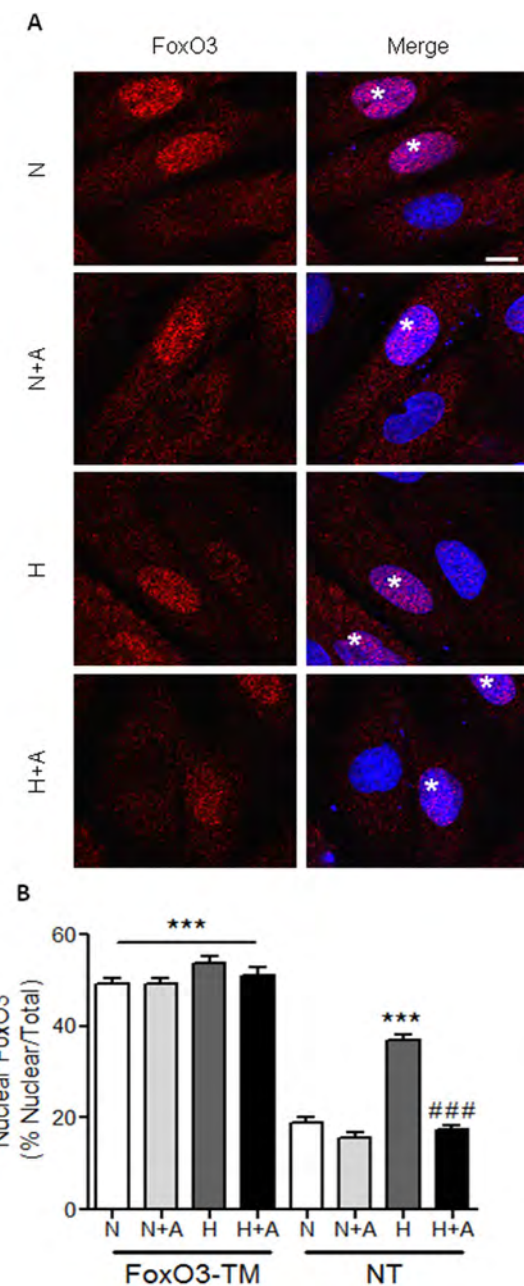


Figure 7. Apelin is not able to induce the nuclear exclusion of FoxO3-TM in H9C2 cells. (A) H9C2 cells overexpressing the dominant negative mutant FoxO3-TM were submitted to hypoxic conditions (H) or kept in normoxia (N) in the presence or not of apelin (A), fixed and stained with an anti-FoxO3 antibody (in red). Nuclei were stained with DAPI (in blue). Imaging parameters were set to easily identify cells overexpressing FoxO3-TM (highlighted by stars in merge pictures). Bar is 10 μm. (B) Quantification of FoxO3 nuclear accumulation in both untransfected cells (NT) and cells expressing FoxO3-TM.

***p < 0.001 vs N from non-transfected cells (NT, endogenous FoxO3); #p < 0.001 vs H from NT cells.

Attenuation of FoxO3 nuclear translocation by apelin in response to I/R injury in obese conditions in mice. Consistent with the *in vitro* results, analysis by confocal microscopy of cardiac tissue from HFD-fed mice subjected to I/R showed an increased nuclear staining for FoxO3 compared to sham-operated mice (Fig. 8A and quantified in Fig. 8B). Strikingly, apelin post-reperfusion treatment prevented FoxO3 nuclear translocation after I/R injury (Fig. 8A,B). To confirm the role of apelin in cardiac FoxO3 regulation, we examined its subcellular localization in left ventricles from apelin KO HFD-fed mice. As shown in Fig. 8C, apelin deficient mice displayed a FoxO3 nuclear targeting phenotype, as compared to WT mice.

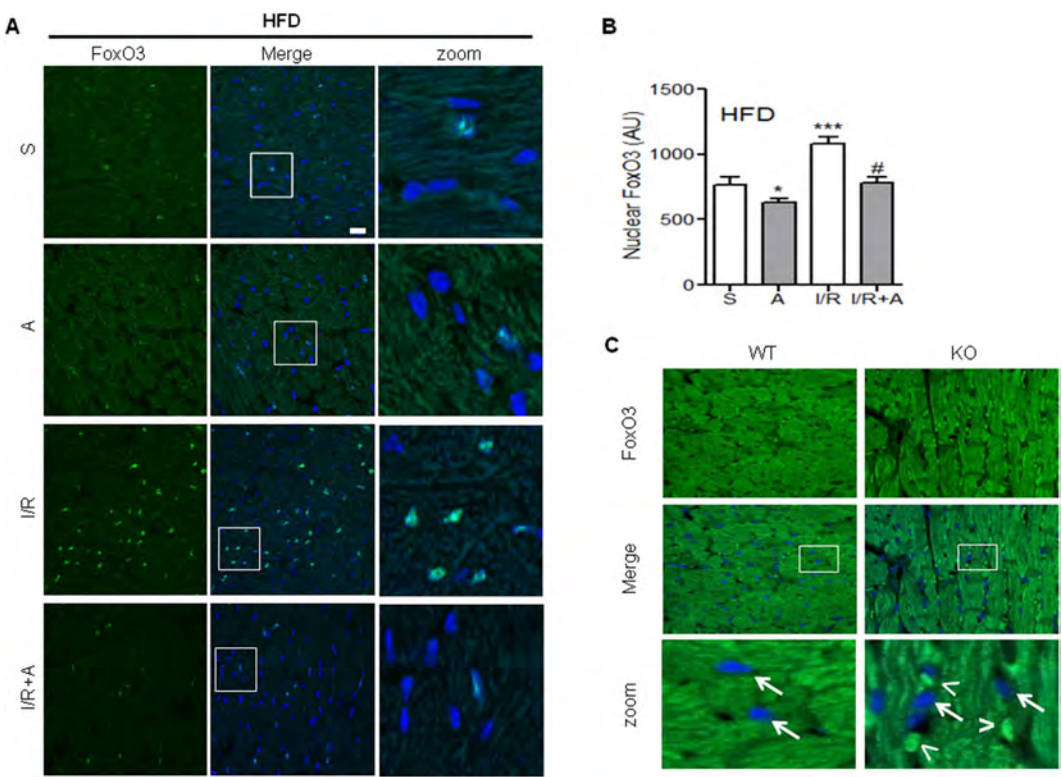


Figure 8. FoxO3 nuclear translocation in mice hearts subjected to I/R is abrogated by post-reperfusion injection of apelin. (A) Heart sections from HFD-fed mice treated or not with apelin (A) and sham-operated (S) or submitted to I/R were immunostained for FoxO3 (in green). Nuclei were stained with DAPI (in blue). Bar is $20\mu\text{m}$. (B) Quantification of FoxO3 nuclear translocation from (A). * $p<0.05$ vs S *** $p<0.001$ vs S; # $p<0.05$ vs I/R. (C) Immunostaining of FoxO3 (in green) on heart sections from HFD-fed WT or apelin KO mice. Nuclei were stained with DAPI (in blue). Arrows point to nuclei devoid of FoxO3, whereas arrowheads point to nuclear staining.

Discussion

In the present work, we provide the first line of evidence that in obese patients with HF greater apelin levels are associated with the higher LVEF independently of ischemic etiology. In addition, using *in vitro* and *in vivo* approaches, we identify apelin as a novel regulator of FoxO3 nucleocytosolic trafficking in cardiomyocytes in conditions combining myocardial injury and obesity. In many cell types, FoxO3 translocates to the nucleus in response to stress where it activates genes directly involved in cell-fate decisions such as apoptosis, survival and oxidative stress status³⁸. Our results suggest that prevention of I/R-induced FoxO3 nuclear translocation by apelin is associated with activation of survival pathways and cardioprotection in obese mice after ischemic injury.

FoxO3 transcription factor orchestrates a number of vital processes involving cell survival, apoptosis, metabolism and stress responses^{39,40}. The evidences that subcellular localization of FoxO transcription factors is critical for fundamental cellular functions have been extensively reported in non-myocyte cells^{16,41}. However, in cardiomyocytes FoxO3 trafficking and regulation remain to be elucidated. In the present study we revealed that FoxO3 translocation is regulated by apelin through a PI3K-dependent mechanism in cardiac cells. Indeed, pharmacological inhibition of PI3K and expression of the non-phosphorylatable FoxO3 mutant resulted in the loss of apelin's ability to control FoxO3 translocation. Analysis of cardiomyocytes isolated from HFD-fed mice demonstrated that hypoxic stress triggers FoxO3 nuclear translocation. These data are consistent with the results reported in recent studies showing that FoxO3 is sensitive to hypoxia, and is mainly localized in the nucleus under conditions of cellular stress in non-myocyte cells^{42,43}. Consistent with the *in vitro* results, nuclear FoxO3 localization was observed in cardiac tissue from I/R mice under HFD conditions. Most importantly, our *in vitro* and *in vivo* results suggest that apelin promotes the retention of FoxO3 in the cytoplasm by preventing its nuclear translocation in response to stress. Indeed, in cardiac cells and mice exposed to stress apelin was able to inhibit nuclear accumulation of FoxO3. Furthermore, we show that in apelin KO mice cardiac FoxO3 is mainly nuclear, suggesting that apelin plays an important role in FoxO3 nucleocytoplasmic distribution in the heart. Together, these data demonstrate that subcellular localization of FoxO3 is an important indicator of cell fate decisions in response to stress. Indeed, FoxO3 nuclear accumulation is associated with activation of cell death cascades and ROS overproduction, whereas, cytoplasmic retention of FoxO3 may reflect

activation of survival-promoting pathways. In mice, FoxO1/FoxO3 deficiency in cardiomyocytes results in increased myocardial cell death, reduced cardiac performance and increased scar formation following myocardial infarction¹². Cardiac I/R injury in mice with cardiac FoxO deficiency is accompanied by reduced expression of antioxidants, DNA repair enzymes and antiapoptotic genes¹². In our study we demonstrated for the first time that inhibition of hypoxia-induced FoxO3 nuclear translocation by apelin is associated with reduced mitochondrial O₂⁻ and H₂O₂ generation *in vitro* and *in vivo* models. Given the importance of FoxO family in the regulation of redox status, FoxO3 subcellular localization may be an important indicator of mitochondrial oxidative stress in cardiac cells. This notion is corroborated by a recent study demonstrating that FoxO3 is an early biomarker of oxidative stress in conditions of metabolic stress⁴⁴. In our *in vitro* experiments we showed that silencing of endogenous FoxO3 or over-expression of FoxO3-TM did not induce ROS production in basal condition. This is in line with a recent report showing that in neonatal cardiomyocytes constitutive activation of FoxO3 did not alter basal level of ROS and apoptosis¹². Importantly, epigenetic inhibition of FoxO3 or expression of the mutant FoxO3 abolished apelin-dependent cell protection from excessive mitochondrial ROS production, suggesting that the apelinergic system plays an important role in cell resistance to stress.

Mitochondrial ROS are highly reactive and can cause irreversible oxidative damage to the mtDNA, proteins and lipids, but are also involved in signaling from the mitochondria to the cytoplasm. Excessive mitochondrial ROS production triggers activation of cellular apoptotic programs leading to cell death⁴⁵. Limiting mitochondrial ROS production by apelin may be particularly important in cardioprotection against I/R damage. Indeed, we show that apelin-dependent reduction in oxidative stress is associated with reduced infarct size, inhibition of apoptotic cell death and inflammation in HFD-fed mice subjected to I/R. Perhaps the most significant finding from our study is that post-treatment with apelin preserves mitochondrial ultrastructural integrity and increases mtDNA content in conditions combining I/R injury and obesity. Structural defects of mitochondria in cardiac tissue is a major determinant of myocardial injury in chronic heart failure and obesity^{4,5,31}. Since mitochondria are major sources for ROS production and energy generation, any structural and functional alterations of mitochondria may lead to impaired mitochondrial biogenesis and oxidative stress. Recently, we have demonstrated that the perturbations in myocardial energy metabolism play a central role in cardiac performance during the transition from adaptation to maladaptation of the heart in obese state³¹. High-energy requiring cells, such as cardiomyocyte, require large quantities of ATP and maintain high mtDNA content⁵. Our data suggest that regulation of mtDNA content and mitochondrial integrity by apelin may play an important role for maintaining cellular bioenergetics and mitochondrial redox processes in response to myocardial I/R.

Regulation of mitochondrial function is an important role of FoxO factors in coordinating cellular adaptation to hypoxia⁴⁶. Moreover, apelin decreased myocardial expression of pro-apoptotic protein Bax and increased expression of anti-apoptotic Bcl-2. Interestingly, inhibition of apoptotic signaling was associated with reduced myocardial markers of oxidative stress suggesting that apelin activates survival pathways conditions combining cardiac I/R injury and obesity. In accordance with *in vivo* evidence, we found that higher levels of plasma apelin are associated with a higher LVEF in obese patients with HF as compared to non-obese patients with HF. Our data are in line with previously reported clinical data demonstrating that obese patients with established cardiovascular disease might have better short- and long-term prognosis, suggesting an “obesity paradox”^{47,48}. In chronic HF, convincing evidence has accumulated from studies including > 30 000 patients over a broad spectrum of disease severity, that being overweight is associated with decreased mortality^{49,50}. Similarly, in patients with acutely compensated heart failure, higher BMI is associated with lower in-hospital mortality⁵¹. Our data suggest that high plasma concentrations of apelin in obese patients with HF are associated with better cardiac performance. However, the sample size of our study is relatively small which may impact on our power to detect more subtle differences between obese and non-obese phenotype. Future studies with larger sample sizes would needed to confirm our findings.

Taken together, these results unravel a novel function of apelin in the regulation of FoxO3 nucleocytoplasmic trafficking and may provide new insights into the mechanistic basis of obesity paradox.

References

- Chase, P.J., Davis, P.G. & Bensimhon, D.R. The obesity paradox in chronic heart failure: what does it mean? *Curr Heart Fail Rep* **11**, 111–117 (2014).
- Clark, A.L., Fonarow, G.C. & Horwitz, T.B. Obesity and the obesity paradox in heart failure. *Prog Cardiovasc Dis* **56**, 409–414 (2014).
- Dierckx, D.B. *et al.* The obesity paradox in non-ST-segment elevation acute coronary syndromes: results from the Can Rapid risk stratification of Unstable angina patients Suppress ADverse outcomes with Early implementation of the American College of Cardiology/American Heart Association Guidelines Quality Improvement Initiative. *Am Heart J* **152**, 140–148 (2006).
- Ajith, T.A. & Jayakumar, T.G. Mitochondria-targeted agents: Future perspectives of mitochondrial pharmaceuticals in cardiovascular diseases. *World J Cardiol* **6**, 1091–1099 (2014).
- Marin-Garcia, J., Ahmedov, A.T. & Moe, G.W. Mitochondria in heart failure: the emerging role of mitochondrial dynamics. *Heart Fail Rev* **18**, 439–456 (2013).
- Andreadou, I., Iliodromitis, E.K., Farmakis, D. & Kremastinos, D.T. To prevent, protect and save the ischemic heart: antioxidants revisited. *Expert Opin Ther Targets* **13**, 945–956 (2009).
- Tsutsui, H., Kinugawa, S. & Matsushima, S. Oxidative stress and heart failure. *Am J Physiol Heart Circ Physiol* **301**, H2181–2190 (2011).

8. Kalogeris, T., Bao, Y. & Korthuis, R.J. Mitochondrial reactive oxygen species: a double edged sword in ischemia/reperfusion vs preconditioning. *Redox Biol* **2**, 702–714 (2014).
9. Bournat, J.C. & Brown, C.W. Mitochondrial dysfunction in obesity. *Curr Opin Endocrinol Diabetes Obes* **17**, 446–452 (2010).
10. Penna, C., Perrelli, M.G. & Pagliaro, P. Mitochondrial pathways, permeability transition pore, and redox signaling in cardioprotection: therapeutic implications. *Antioxid Redox Signal* **18**, 556–599 (2013).
11. Evans-Anderson, H.J., Alfieri, C.M. & Yutzey, K.E. Regulation of cardiomyocyte proliferation and myocardial growth during development by FOXO transcription factors. *Circ Res* **102**, 686–694 (2008).
12. Sengupta, A., Molkentin, J.D., Paik, J.H., DePinho, R.A. & Yutzey, K.E. FoxO transcription factors promote cardiomyocyte survival upon induction of oxidative stress. *J Biol Chem* **286**, 7468–7478 (2011).
13. Zhang, S. et al. FoxO3a modulates hypoxia stress induced oxidative stress and apoptosis in cardiac microvascular endothelial cells. *PLoS One* **8**, e80342 (2013).
14. Lu, D. et al. Transcription factor Foxo3a prevents apoptosis by regulating calcium through the apoptosis repressor with caspase recruitment domain. *J Biol Chem* **288**, 8491–8504 (2013).
15. Ferrara, N. et al. Exercise training promotes SIRT1 activity in aged rats. *Rejuvenation Res* **11**, 139–150 (2008).
16. Ponugoti, B., Dong, G. & Graves, D.T. Role of forkhead transcription factors in diabetes-induced oxidative stress. *Exp Diabetes Res* **2012**, 939751 (2012).
17. Nakamura, K., Fuster, J.J. & Walsh, K. Adipokines: a link between obesity and cardiovascular disease. *J Cardiol* **63**, 250–259 (2014).
18. Bluhm, M. Adipose tissue dysfunction contributes to obesity related metabolic diseases. *Best Pract Res Clin Endocrinol Metab* **27**, 163–177 (2013).
19. Dray, C. et al. Apelin stimulates glucose utilization in normal and obese insulin-resistant mice. *Cell Metab* **8**, 437–445 (2008).
20. Pchelatski, D. et al. Apelin prevents cardiac fibroblast activation and collagen production through inhibition of sphingosine kinase 1. *Eur Heart J* **33**, 2360–2369 (2012).
21. Kleinz, M.J. & Davenport, A.P. Emerging roles of apelin in biology and medicine. *Pharmacol Ther* **107**, 198–211 (2005).
22. Foussal, C. et al. Activation of catalase by apelin prevents oxidative stress-linked cardiac hypertrophy. *FEBS Lett* **584**, 2363–2370 (2010).
23. Wang, W. et al. Loss of Apelin exacerbates myocardial infarction adverse remodeling and ischemia-reperfusion injury: therapeutic potential of synthetic Apelin analogues. *J Am Heart Assoc* **2**, e000249 (2013).
24. Kuba, K. et al. Impaired heart contractility in Apelin gene-deficient mice associated with aging and pressure overload. *Circ Res* **101**, e32–42 (2007).
25. Kadoglou, N.P. et al. Serum levels of apelin and ghrelin in patients with acute coronary syndromes and established coronary artery disease—KOZANI STUDY. *Transl Res* **155**, 238–246 (2010).
26. Tyrcinska, A.M. et al. The value of apelin-36 and brain natriuretic peptide measurements in patients with first ST-elevation myocardial infarction. *Clin Chim Acta* **411**, 2014–2018 (2010).
27. Weir, R.A. et al. Plasma apelin concentration is depressed following acute myocardial infarction in man. *Eur J Heart Fail* **11**, 551–558 (2009).
28. Dray, C. et al. Apelin and APJ regulation in adipose tissue and skeletal muscle of type 2 diabetic mice and humans. *Am J Physiol Endocrinol Metab* **298**, E1161–1169 (2010).
29. Kleinz, M.J., Skepper, J.N. & Davenport, A.P. Immunocytochemical localisation of the apelin receptor, APJ, to human cardiomyocytes, vascular smooth muscle and endothelial cells. *Regul Pept* **126**, 233–240 (2005).
30. Brunet, A. et al. Akt promotes cell survival by phosphorylating and inhibiting a Forkhead transcription factor. *Cell* **96**, 857–868 (1999).
31. Alfarano, C. et al. Transition from metabolic adaptation to maladaptation of the heart in obesity: role of apelin. *Int J Obes* **39**, 312–20 (2015).
32. Drougard, A. et al. Hypothalamic apelin/reactive oxygen species signaling controls hepatic glucose metabolism in the onset of diabetes. *Antioxid Redox Signal* **20**, 557–573 (2013).
33. Pchelatski, D. et al. Oxidative stress-dependent sphingosine kinase-1 inhibition mediates monoamine oxidase A-associated cardiac cell apoptosis. *Circ Res* **100**, 41–49 (2007).
34. Boal, F. et al. LG186: An inhibitor of GBF1 function that causes Golgi disassembly in human and canine cells. *Traffic* **11**, 1537–1551 (2010).
35. Attane, C. et al. Apelin treatment increases complete Fatty Acid oxidation, mitochondrial oxidative capacity, and biogenesis in muscle of insulin-resistant mice. *Diabetes* **61**, 310–320 (2012).
36. Nahrendorf, M., Pittet, M.J. & Swirski, F.K. Monocytes: protagonists of infarct inflammation and repair after myocardial infarction. *Circulation* **121**, 2437–2445 (2010).
37. Van Der Heide, L.P., Hoekman, M.F. & Smidt, M.P. The ins and outs of FoxO shuttling: mechanisms of FoxO translocation and transcriptional regulation. *Biochem J* **380**, 297–309 (2004).
38. Calnan, D.R. & Brunet, A. The FoxO code. *Oncogene* **27**, 2276–2288 (2008).
39. Kops, G.J. et al. Forkhead transcription factor FOXO3a protects quiescent cells from oxidative stress. *Nature* **419**, 316–321 (2002).
40. Medema, R.H., Kops, G.J., Bos, J.L. & Burgering, B.M. AFX-like Forkhead transcription factors mediate cell-cycle regulation by Ras and PKB through p27kip1. *Nature* **404**, 782–787 (2000).
41. Kowluru, A. & Matti, A. Hyperactivation of protein phosphatase 2A in models of glucolipotoxicity and diabetes: potential mechanisms and functional consequences. *Biochem Pharmacol* **84**, 591–597 (2012).
42. Awad, H., Nolette, N., Hinton, M. & Dakshinamurti, S. AMPK and FoxO1 regulate catalase expression in hypoxic pulmonary arterial smooth muscle. *Pediatr Pulmonol* (2013).
43. Battiprolu, P.K. et al. Metabolic stress-induced activation of FoxO1 triggers diabetic cardiomyopathy in mice. *J Clin Invest* **122**, 1109–1118 (2013).
44. Raju, I., Kannan, K. & Abraham, E.C. FoxO3a Serves as a Biomarker of Oxidative Stress in Human Lens Epithelial Cells under Conditions of Hyperglycemia. *PLoS One* **8**, e67126 (2013).
45. Wang, X. The expanding role of mitochondria in apoptosis. *Genes Dev* **15**, 2922–2933 (2001).
46. Ferber, E.C. et al. FOXO3a regulates reactive oxygen metabolism by inhibiting mitochondrial gene expression. *Cell Death Differ* **19**, 968–979 (2011).
47. Arthat, S.M., Lavie, C.J., Milani, R.V. & Ventura, H.O. Obesity and hypertension, heart failure, and coronary heart disease-risk factor, paradox, and recommendations for weight loss. *Ochsner J* **9**, 124–132 (2009).
48. De Schutter, A., Lavie, C.J. & Milani, R.V. The impact of obesity on risk factors and prevalence and prognosis of coronary heart disease—the obesity paradox. *Prog Cardiovasc Dis* **56**, 401–408 (2014).
49. Curtis, J.P. et al. The obesity paradox: body mass index and outcomes in patients with heart failure. *Arch Intern Med* **165**, 55–61 (2005).
50. Horwich, T.B. et al. The relationship between obesity and mortality in patients with heart failure. *J Am Coll Cardiol* **38**, 789–795 (2001).
51. Fonarow, G.C. et al. An obesity paradox in acute heart failure: analysis of body mass index and inhospital mortality for 108,927 patients in the Acute Decompensated Heart Failure National Registry. *Am Heart J* **153**, 74–81 (2007).

Acknowledgements

We thank Dr. A. Dejean (CTPT Toulouse-Purpan) for kindly providing the FoxO3-TM plasmid. This work was supported by grants from the National Institute of Health and Medical Research (INSERM), Fondation Lefoulon-Delalande, Fondation de France, Région Midi-Pyrénées and Fondation pour la Recherche Médicale (FRM).

Author Contributions

F.B., O.K. and J.R. conceived and designed the experiments and analyzed the data. F.B., A.T., H.T., L.G., R.A., F.D., H.T., A.D., C.K., C.L. and O.K. performed the experiments. J.R., P.V. and A.P. assisted in the development of the project. F.B. and O.K. co-wrote the manuscript. All authors reviewed the manuscript.

Additional Information

Competing financial interests: The authors declare no competing financial interests.

How to cite this article: Boal, F. *et al.* Apelin regulates FoxO3 translocation to mediate cardioprotective responses to myocardial injury and obesity. *Sci. Rep.* 5, 16104; doi: 10.1038/srep16104 (2015).



This work is licensed under a Creative Commons Attribution 4.0 International License. The images or other third party material in this article are included in the article's Creative Commons license, unless indicated otherwise in the credit line; if the material is not included under the Creative Commons license, users will need to obtain permission from the license holder to reproduce the material. To view a copy of this license, visit <http://creativecommons.org/licenses/by/4.0/>

BREVET

**Titre: METHODS AND PHARMACEUTICAL COMPOSITIONS FOR THE
TREATMENT OF HEART FAILURE**

Numéro de dépôt : EP17305088.1

Date de dépôt : 27 janvier 2017